Department of Imaging and Applied Physics

Coronary CT Angiography: Radiation Dose Measurements and Image Quality Assessments

Akmal Sabarudin

This thesis is presented for the Degree of
Doctor of Philosophy
of
Curtin University

October 2012

Declaration

To the best of my knowledge and belief this thesis contains no material previously published by any other person except where due acknowledgment has been made.

This thesis contains no material which has been accepted for the award of any other degree or diploma in any university.

Signature: 

Date: Oct 2012

Dedicated to my nephews Zarif Fathi & Ammar Ajwad

Abstract

Prospective ECG-triggering is regarded as one of the most effective approaches for reduction of radiation dose to patients during coronary CT angiography (CCTA). This study was conducted to investigate the diagnostic performance of prospective ECG-triggered CCTA with regard to the image quality and dose reduction, based on a multi-centre research. The research was performed in four stages, with stage 1 investigating the different CT scanning protocols and conventional angiography procedures with corresponding radiation dose measurements; stage 2 focused on the analysis of radiation dose in patients undergoing different generations of multislice CT scanners; stage 3 conducted a survey among medical specialists and radiographers with the aim of obtaining opinions regarding the benefits and difficulties in performing prospective ECG-triggered CCTA; stage 4 analysed image quality and radiation dose in patients undergoing single-source and dual-source 64-slice CT coronary angiography with use of prospective ECG-triggering.

Stage 1 is a pilot study conducted on an anthropomorphic phantom. In this experiment, the radiation dose was compared between the invasive coronary angiography (ICA) and CCTA. These imaging protocols for ICA included the standard angular projection views with different magnifications. These ICA protocols were compared with several CT protocols including prospective and retrospective ECG gating. In addition, tube current modulation was applied in retrospective gating protocol. The radiation dose was also measured at the selected radiosensitive organs including breast and thyroid gland. Although ICA produced lower radiation dose than CCTA, application of modified techniques in both CCTA and ICA is recommended in clinical practice for further radiation dose reduction.

Stage 2 involved a retrospective analysis of radiation dose in patients undergoing prospective ECG-triggered CCTA with different CT generations including single-source 64-slice CT (SSCT), dual-source 64-slice CT (DSCT), dual-source 128-slice CT and 320-slice CT based on several hospitals in Perth, Western Australia and Kuala Lumpur, Malaysia. A total of 164 patients undergoing prospective ECG-triggered CCTA with different types of CT scanners were studied. The analysis showed that the mean effective dose was estimated at 6.8 mSv, 4.2 mSv, 4.1 mSv, and 3.8 mSv, corresponding to 128-slice DSCT, 64-slice DSCT, 64-slice SSCT and 320-slice CT scanners, respectively. A positive relationship was found between effective dose and body mass index (BMI) in this study. Low radiation dose was achieved in prospective ECG-triggered CCTA, regardless of any CT scanner generation. BMI is identified as the major factor that has a direct impact on the effective dose associated with prospective ECG-triggered CCTA.

A well-designed survey was performed in stage 3 among specialists and radiographers from 6 national health institutions in Malaysia in order to explore the opinion concerning the benefits and difficulties in performing prospective ECG triggered CCTA. In total, 53 responses were received (85%), comprising specialists (21%) and radiographers (79%). Across all the respondents, the main benefits of prospective triggering were agreed as: radiation dose reduction, image quality improvement and patients' output increases. On the other hand, the issue of heart rate was agreed by all respondents as a main challenge when performing prospective triggered CCTA. The remaining challenges such as difficulty in obtaining cardiac functional assessments, diagnostic accuracy concerns and data processing management issue have been seen to vary according to the groups of respondents and the scanner type. Radiation dose reduction seems to be the main benefit, which is most agreed upon, while the issue of the heart rate is seen as the main challenge in prospective ECG-triggered CCTA.

Finally, stage 4 is a comparative study consisting of quantitative and qualitative analysis, and it was conducted to investigate the image quality and radiation dose performance between retrospective gated and prospective ECG triggered CCTA with use of 64-slice SSCT and DSCT. The SSCT component was performed in the Royal Perth Hospital, Western Australia, while the DSCT component was conducted in the National heart Institute, Kuala Lumpur, Malaysia. A total of 209 patients who underwent CCTA with suspected coronary artery disease (CAD) scanned with SSCT (n=95) and DSCT (n=114) scanners using prospective ECG-triggering and retrospective ECG-gating protocols. The image was qualitatively assessed by two experienced observers, while quantitative assessment was performed by measuring the image noise, the signal-to-noise ratio (SNR) and the contrast-to-noise ratio (CNR).

A total of 2,087 coronary artery segments were evaluated. Both DSCT and SSCT resulted in good image quality, regardless of prospective or retrospective gating protocols. Although radiation dose calculated between DSCT (6.5 mSv) and SSCT (6.2 mSv) showed no significant difference, the effective dose in prospective triggering was significantly lower than that in retrospective gating protocol. The results indicated that in the retrospective gating protocol, the effective dose with DSCT (18.2 mSv) was also significantly lower than that in SSCT (28.3 mSv). This study confirmed that prospective ECG triggered CCTA reduces radiation dose significantly compared to retrospective ECG-gating CCTA, while maintaining good image quality.

In summary, the results of this project show that coronary CT angiography with prospective ECG-triggering is a reliable diagnostic technique with resultant very low radiation dose, but still maintaining diagnostic images. With widespread use of coronary CT angiography in the diagnosis of coronary artery disease, increased awareness of radiation dose associated with coronary CT angiography is of paramount importance, and application of dose-reduction strategies is highly recommended for routine clinical practice.

Acknowledgements

First of all I would like to thank my supervisor Assoc. Prof. Dr. Zhonghua Sun for all the time he spent with me in the last three years teaching me a lot about preparing manuscripts, editing my manuscripts and not to forget, sharing the most precious experience on CT coronary angiography. The supervision I received during my PhD journey was amazing and I could not make it without his assistance.

I would also like to thank Prof. Ng Kwan-Hoong as my associate supervisor for sharing the idea on the medical physics part including radiation dose calculation, dose measurements and many more in completing my thesis. Furthermore, I would like to thank to Prof. Walter Huda and Gil Stevenson for the useful and interesting academic discussion and the advice throughout the process.

I am extremely grateful to Ministry of Higher Education (Malaysia) and National University of Malaysia (UKM) for the financial support of my PhD study. In addition, I would like to express my thank to invaluable contribution of Melanie Rosenberg, Andrew Bartlett, John Burrage, Neam Fadzin, Dr. Ahmad Khairuddin and all National Heart Institute CT team who put their effort in helping my PhD project.

To my colleagues at Curtin and UKM, I would also like to say thank you for your advice, support and friendship. Additionally, Fatty, Asha, Pijon, Remy and Tee deserve my sincere thanks. Last but not least, I would like to thank my family members for their everlasting love and moral support all these years.

List of publications included as part of this thesis

1. **Sabarudin, A.**, Z. Sun, and K.-H. Ng. 2012. A systematic review of radiation dose associated with different generations of multidetector CT coronary angiography. *J Med Imag Radiat Oncol* 56 (1): 5-17.

2. **Sabarudin, A.**, Z. Sun, and K-H. Ng. 2012. Radiation dose associated with coronary CT angiography and invasive coronary angiography: An experimental study of the effect of dose-saving strategies. *Radiat Prot Dosim* 150 (2): 180-187.

3. **Sabarudin, A.**, Z. Sun, and K-H. Ng. 2013. Coronary CT angiography with prospective ECG-triggering: A systematic review of image quality and radiation dose. *Singapore Med J* 54 (1):15-23

4. **Sabarudin, A.**, Z. Sun, and K-H. Ng. 2012. Radiation dose in coronary CT angiography associated with prospective ECG-triggering technique: comparisons with different CT generations. *Radiat Prot Dosim (Epub ahead of print)*

5. **Sabarudin, A.**, Z. Sun, and A.K. Md Yusof. 2012. Coronary CT angiography with single-source and dual-source CT: Comparison of image quality and radiation dose between prospective ECG-triggering and retrospective ECG-gating protocols. *Int J Cadiol (Epub ahead of print)*

6. **Sabarudin, A.**, Z. Sun, and K-H. Ng. 2012. A survey study exploring local specialists and radiographers' perceptions of the benefits and challenges in relation to prospective ECG-triggered coronary CT angiography. *Journal of Medical Imaging and Health Informatics (In press)*

List of additional publications relevant to the thesis but not forming part of it

1. **Sabarudin,A.**, A.K. Md Yusof, M.F. Tay, K-H. Ng, Z. Sun. 2013. Dual source CT coronary angiography: effectiveness of radiation dose reduction with low tube voltage. *Radiat Prot Dosim* 153(4):441-447.

This paper is attached to the thesis in the **Appendix A**

Statement the candidate's contribution to the PhD project

Of all the publications included as part of the thesis, I am the lead author who is responsible for developing the research topics, designing the experiments, and writing up the manuscripts. I was the principal investigator of these studies under the guidance of my supervisor and through collaboration with clinical colleagues from both Australia and Malaysia. Through the entire course of my PhD, I developed the methodology, conducted the experiments, collected patients' data and wrote these papers myself,

List of conferences

International conferences

1. **Sabarudin, A.**, Z. Sun, K-H. Ng. '*Multislice CT coronary angiography: a systematic review of radiation dose associated with different multislice CT scanners'* at the 8th South-East Asian Congress of Medical Physics, Biophysics, and Biomedical Engineering, Bandung, Indonesia (10-13th December 2010). Oral presentation

2. **Sabarudin, A.**, Z. Sun, K-H. Ng. '*A comparison of dose reduction between routine and dose saving protocols in CT angiography examinations: a pilot study*' at the 8th South-East Asian Congress of Medical Physics, Biophysics, and Biomedical Engineering (SEACOMP), Bandung, Indonesia (10-13th December 2010). Oral presentation

National conferences

1. **Sabarudin, A.**, Z. Sun, K-H. Ng. '*Radiation dose measurements in angiography protocols: a pilot study*' at the 8th Annual Scientific Meeting of Medical Imaging and Radiation Therapist Conference (ASMMIRT), Adelaide, Australia (14-17th April 2011). Oral presentation

2. **Sabarudin, A.**, Z. Sun, K-H. Ng. '*Radiation dose associated with coronary CT angiography and invasive coronary angiography: An experimental study of the effect of dose-saving strategies'* at the Radiation 2012 conference, Lucas Height, NSW, Australia (15-17th February 2012). Oral presentation

Contents

CHAPTER 1: INTRODUCTION AND LITERATURE REVIEW

1.1 Coronary artery anatomy

1.1.1 Normal anatomy-Right coronary artery

The two coronary arteries are the first vessels to branch off the ascending aorta and supply oxygenated blood to the myocardium. The right coronary artery (RCA) arises from the right coronary sinus inferior to the origin of the left coronary artery (LCA). After its origin from the aorta, the RCA passes to the right and posterior to the pulmonary artery and then emerges from under the right atrial appendage to travel in the right anterior atrioventricular (AV) groove. The RCA gives off small branches that supply the right atrium. In about 50% of the cases, the conus artery is the first branch of the RCA (Figure 1-1). The conus artery can also arise directly from the aorta. The conus branch always courses anteriorly to supply the pulmonary outflow tract. The posterior interventricular branch follows the posterior interventricular sulcus and supplies the walls of the two ventricles with oxygenated blood. The right marginal branch in the coronary sulcus carries oxygenated blood to the myocardium of the right ventricle. The distal RCA starts just after the acute marginal branch passes horizontally along the diaphragmatic surface of the heart, which gives rise to the right posterior descending artery (PDA) that adjoins the middle cardiac vein and runs anteriorly in the posterior interventricular sulcus (Figure 1-2). The coronary artery that gives rise to the PDA and posterolateral branch is referred to as the 'dominant' artery, with the RCA being dominant in approximately 70% of cases. If it is RCA dominant, the RCA continues beyond the crux in the left atrioventricular sulcus where it terminates into the posterior left ventricular branch (PLB) (Kini, Bis, and Weaver 2007).

1.1.2 Normal anatomy-Left coronary anatomy

The LCA normally arises from the left coronary sinus as the left main artery (LMA). The LMA coronary artery is a short branch (5–10 mm), and it courses for a variable distance before giving rise to the left anterior descending (LAD) and left circumflex (LCx) (Figure 1-2). In some cases, the LMA trifurcates into the LAD, LCx, and the ramus intermedius artery. The ramus intermedius artery itself has different types of branching. The ramus intermedius can be distributed as a diagonal branch or as an obtuse marginal branch depending on whether it supplies the anterior or the lateral wall, respectively.

The LAD artery passes behind the pulmonary trunk and moves forward between the pulmonary trunk and the left arterial appendage to the anterior interventricular sulcus, along

the ventricular septum. The LAD artery has branches called “septal perforators” which supply the anterior ventricular septum. These septal branches have wide variations in number, size and distribution. A first distribution contains large, located more vertical and sometimes divided into a number of secondary branches that split throughout the septum. In certain condition, septal perforator could be found parallel to the LAD. A collateral channel also can be created between two septal branches which originate from the LAD and the PDA of the right coronary artery.

Figure 1-1: The multi-planar reformation (MPR) images of right coronary artery inclusive of RCA (a-b) and PDA (c-d).

Figure 1-2: The multi-planar reformation (MPR) images of left coronary artery inclusive of LAD (a-b), diagonal artery (c), LCx (d) and OM (e-f).

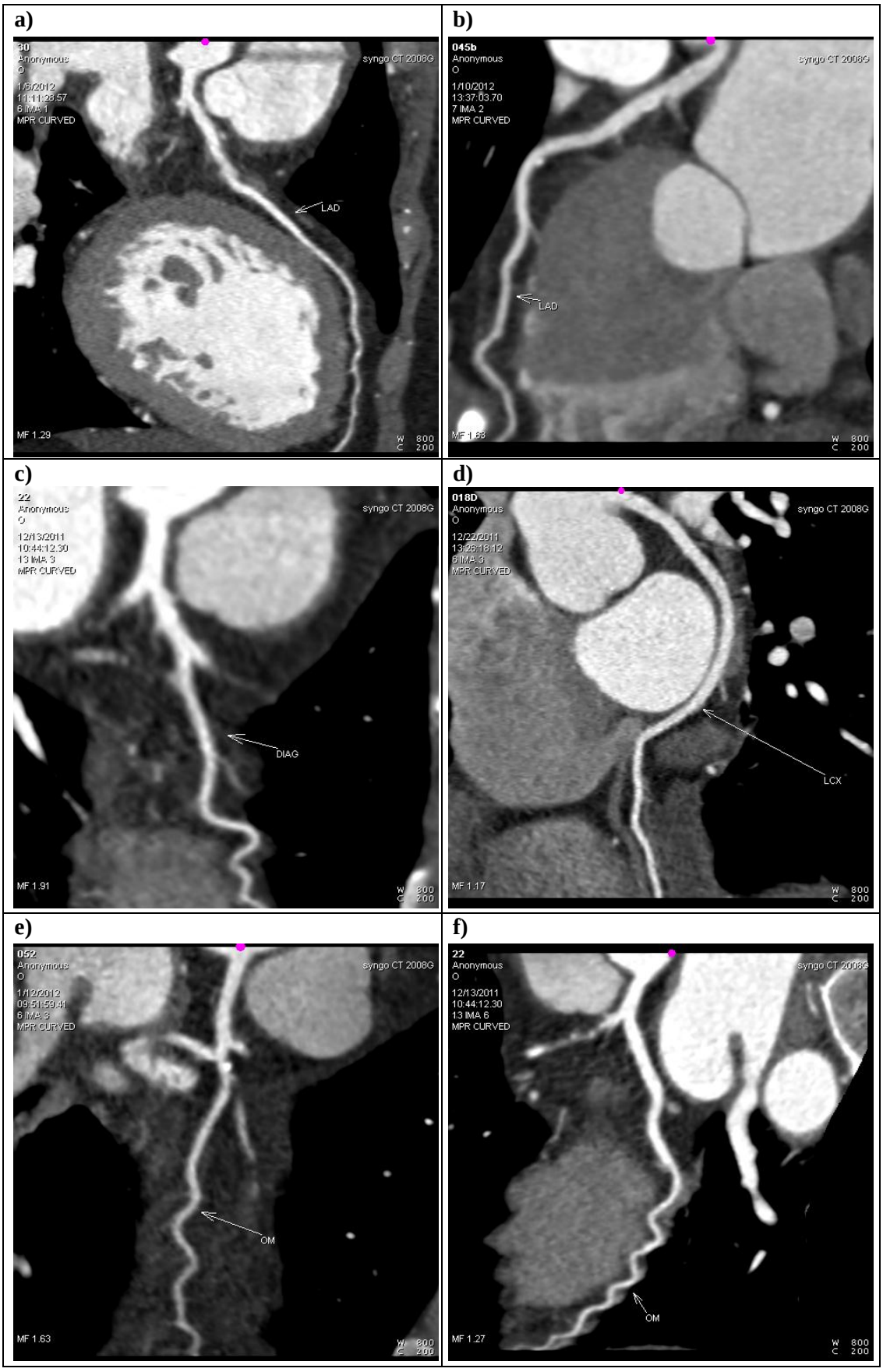

LAD also has diagonal arteries that course over and supply the anterior wall of the left ventricle (Kini, Bis, and Weaver 2007). A wide variation in number and size of diagonal branches exist with all originating from the LAD and passing over the anterolateral aspect of the heart. The diagonals and septal perforators are numbered sequentially from proximal to distal as D1, D2, S1 and S2 (van Ooijen et al. 2004).

The LCx runs in the posterior AV groove analogous to the course of the RCA on the opposite side. The LCx angles posteriorly from the bifurcation to pass below the left atrial appendage towards AV groove. The major branches of the LCx consist of obtuse marginals (OM) (Figure 1-2). OM branches supply the lateral wall of the left ventricle (LV) and they are numbered sequentially from proximal to distal as OM1, OM2 and OM3. Sometimes, LCx gives rise to one or two left arterial circumflex branches which supply the lateral and posterior aspect of the left atrium (Kini, Bis, and Weaver 2007).

1.1.3 Normal anatomy-Coronary dominance

The artery that supplies the PDA and the posterolateral branch determines the coronary dominance. If the PDA and PLB arise from the RCA, then the system is said to be right dominant (80–85% of cases). In this instance, the RCA supplies the inferoseptal and inferior segments of the left ventricle (Cerqueira et al. 2002). On the other hand, if the PDA and PLB arise from the LCx artery, then the system is said to be left dominant (15–20% of cases). In this instance, the LCA supplies the inferoseptal and inferior segments of the left ventricle. However, in about 5% of cases, the PDA comes from the RCA and the PLB comes from the LCx artery in which is called co-dominant (Kini, Bis, and Weaver 2007).

1.1.4 Coronary artery anomalies

Anomalies of the coronary arteries may be found incidentally in 0.3%–1% of healthy individuals (Angelini, Velasco, and Flamm 2002). For several decades, premorbid diagnosis of coronary artery anomalies has been made with invasive coronary angiography. The coronary artery anomalies are classified into anomalies of origin, anomalies of course, and anomalies of termination. Coronary artery anomalies may also be classified as either haemodynamically significant or insignificant. Haemodynamically significant anomalies of the coronary arteries are characterized by abnormalities of myocardial perfusion, which lead to an increased risk of myocardial ischemia or sudden death (Reagan, Boxt, and Katz 1994). These anomalies include an anomalous origin of either the LCA or the RCA from the pulmonary artery, an anomalous course between the pulmonary artery and the aorta

(interarterial) of either the RCA arising from the left sinus of Valsalva or the LCA arising from the right sinus of Valsalva.

1.1.5 Coronary artery disease

Coronary artery disease (CAD) is a common cardiovascular disease that is responsible for the leading cause of death in advanced countries and its prevalence is increasing in developing countries. Early detection and diagnosis plays an important role in patient management. Traditionally, this is achieved with use of invasive coronary angiography; however, it is associated with procedure-related complications. Since multislice computed tomography (MSCT) has been introduced, coronary CT angiography (CCTA) has been widely used as a non-invasive technique to detect CAD in cardiac imaging (Brenner and Hall 2007; Naghavi et al. 2006). CAD results from the deposition of atheroma in the artery which supplies blood to the heart muscle. As the plaque accumulates in the coronary arteries, blood supply to the heart muscle is decreased which results in ischemia, a local and temporary impairment of circulatory and myocardial damage as an infarction (an area of ischemic necrosis). The plaque accumulation in the vessel lumens is characterised into two categories; stable plaque and unstable plaque. Generally, stable atherosclerotic plaques, which tend to be asymptomatic, are rich in extracellular matrix and smooth muscle cells, while, unstable plaques are rich in macrophage and foam cells and the extracellular matrix separating the lesion from the arterial lumen (also known as the fibrous cap) is usually weak and prone to rupture (Ross 1999).

Plaque accumulation can be classified as soft and hard plaques. Soft plaque is normally referred to lipid or cholesterol deposition in the vessels whereas hard plaque is normally referred to calcium deposition in the vessels and it equally results in blood flow obstruction. Atherosclerotic calcification is an organized, regulated process similar to bone formation that occurs only when other aspects of atherosclerosis are also present. Although calcification is found more frequently in advanced lesions, it may also occur in a small number of populations in earlier lesions, which appear in the second and third decades of life. Histopathological investigation has shown that plaques with microscopic evidence of mineralization are larger and associated with larger coronary arteries than plaques or arteries without calcification (Wexler et al. 1996). The relation of arterial calcification to the probability of plaque rupture is unknown. Although the amount of coronary calcium correlates with the amount of atherosclerosis in different individuals and to a lesser extent in segments of the coronary tree in the same individuals, it is not known if the quantity of calcification tracks the quantity of atherosclerosis over time in the same individuals (Ross

1999). Further research is needed to better elucidate the relation of calcification to the pathogenesis of both atherosclerosis and plaque rupture.

Major complications of CAD include angina pectoris, myocardial infarction and subsequent myocardial necrosis if the patient survives from heart attack. CAD is responsible for over 30% of all annual death in the United States and is the single most frequent cause of death in both men and women (Mace and Kowalczyk 2004). Most cases on autopsy demonstrate significant widespread atherosclerotic disease of the coronary arteries. As mentioned earlier, the exact aetiology of plaque formation is unknown. However, risk factors for CAD are well known which include tobacco use, diets with content high in fats and calories, nutrition with low in phytochemicals and fibre, also poor physical fitness (Wexler et al. 1996).

Medical treatment for CAD may include vasodilators or antithrombotic/anticoagulant drugs to improve cardiovascular circulation and use of beta-blockers to decrease the risk of further injury to myocardium. Percutaneous transluminal coronary angioplasty (PTCA) which uses balloon or stent placement would be considered as a treatment option in order to open up the occluded coronary lumen that is caused by soft plaques. However, it depends on the degree and location of the occlusion (Mace and Kowalczyk 2004). In addition, percutaneous transluminal coronary rotational atherectomy (PTCRA) is an option for calcified lesions (Khoury et al. 1996). Alternatively, CAD could be treated surgically with coronary artery bypass grafts (CABG).

1.2 Imaging modalities in the diagnosis of coronary artery disease

With the advancement in imaging technology, there are a number of imaging modalities that can be used in cardiac imaging. These modalities range from invasive to non-invasive and from ionizing to non-ionizing radiation approaches which are available to be used depending on the availability and most importantly the sensitivity and specificity of the imaging modalities. There are several imaging modalities available for the diagnosis of CAD including conventional angiography, CCTA, magnetic resonance imaging (MRI), ultrasound and nuclear medicine.

1.2.1 Conventional coronary angiography

Coronary angiography is regarded as the "gold standard" and most accurate method for evaluating and defining CAD especially in quantifying lumen stenosis of the coronary arteries (Arbab-Zadeh et al. 2010). Coronary angiography is used to identify the exact location and severity of CAD. A catheterization procedure is required in the assessment of the coronary arteries. Specifically, coronary catheterization is a visually interpreted procedure which is performed to identify occlusion, stenosis, restenosis, thrombosis or aneurysmal enlargement of the coronary artery lumens, heart chamber size, heart muscle contraction performance and some aspects of heart valve function. Important internal measurements associated with ventricular ejection fraction can be accurately performed during the procedure. The most common indication for coronary angiography is coronary atherosclerosis, which leads to coronary stenosis or occlusion (Rees et al. 2004).

1.2.1.1 Coronary angiography views

A complex three-dimensional pattern of coronary artery branches need to be visualised clearly in different angles. Therefore, a series of angiographic views are generated and named according to the x-ray image intensifier position in order to obtain a complete picture of the coronary anatomy. The names are completely different from the normal radiological nomenclature as they are given corresponding to the position of the beam passing through the patients. For example, a left anterior oblique 60° with 40° caudal view means that position of the image intensifier on the left side of the patient with 60° angulation relating to the degree of displacement of the image intensifier from the vertical position. The additional caudal angulation of 40° refers to tilting the image intensifier towards patient's feet. The tube is usually angulated in two planes which are left or right oblique and in caudal or cranial tilting. It is a standard procedure to perform a series of 8-10 views for left coronary arteries and 3-5 views for right coronary arteries (Table 1-1). Some additional views or multiple

views are also required for a full clinical interpretation of the disease in some patients (Rees et al. 2004).

Table 1-1: Visualisation of coronary artery structures based on different angiographic views (Rees et al. 2004)

Angiographic views	**Anatomical Structures**
AP 0°	LMA, LAD, D2, LCx
RAO 30°	LMA, LAD, S, D1, D2, LCx
LAO 60°	LMA, LAD, S, D1, D2, LCx
Left lateral 90°	LMA, LAD, D1, D2, LCx
RAO 30°/30° cranial	LMA, LAD, S, D2
RAO 30°/30° caudal	LMA, LAD, S, D1, D2, LCx
LAO 50°/20° cranial	LMA, LAD, S, D1, D2, LCx
LAO 50°/30° caudal	LMA, LAD, LCx
AP 30° caudal	LAD, S, D1, D2, LCx
AP 40° cranial	LMA, LAD, S, D2, LCx
LAO 45°	RCA, RV, PLB, PDA
AP 30° cranial	RCA, PLB, PDA
RAO 30°	RCA, RV, PDA
AP 0°	RCA, RV, PLB, PDA
Right lateral 90°	RCA, RV, PLB, PDA

*AP= anterior-posterior; RAO= right anterior oblique; LAO= left anterior oblique; LMA= left main artery; LAD= left anterior descending artery; S=septal artery; D1=first diagonal artery; D2= second diagonal artery; LCx= left circumflex artery; RCA= right coronary artery; RV= right ventricular branch; PLB= posterior lateral branch; PDA= posterior descending artery

1.2.1.2 Risks and limitations

Coronary angiography is regarded as a safe procedure even it is an invasive approach. One of the earlier studies by Adams et al. in 1973 was carried out to report the complications of

coronary angiography. The study showed that mortality rate of coronary angiography was 0.44% in a cohort of 55,640 cases. However, in 1975, the mortality rate was dropped to 0.17% in a study consisting of 35,500 patients conducted by the same research group (Abrams and Adams 1975). The mortality rate was decreased gradually by years when the Registry of the Society for cardiac angiography carried out an observation on participating hospitals in the United States between 1978 and 1981 and reported that the life time risk of coronary angiography was only 0.13% (Kennedy 1982). Furthermore, the Society also reported that other cardiovascular risks decreased gradually including myocardial infarction (0.09%), stroke (0.07%) and vascular complications (0.50%). The statistics data also showed that the risk of angiography increased with the severity of the disease. The highest mortality rate (0.86%) was identified in patients with left main artery disease which was assumed to have the highest mortality risk (Kennedy 1982). However, the current rate of complications for diagnostic coronary angiography is assumed to be less than 1% (Rees et al. 2004).

1.2.2 Coronary magnetic resonance angiography

Coronary angiography by MRI has long been a goal for bringing MRI to the forefront of application in diagnosis of CAD. Although many non-invasive tests are commonly used for the diagnosis of CAD, conventional angiography is still considered as the most reliable method for assessment of the coronary vessels (Tsapaki et al. 2009). However, the coronary magnetic resonance angiography (MRA) was introduced due to its non-ionizing radiation approach and also does not require the use of iodinated contrast media which is potentially nephrotoxic (Danias 2004). Furthermore, coronary MRA can be obtained in any direction and plane, without any restriction to the angulation of the images. Finally, coronary MRA can easily be combined with a comprehensive evaluation of the anatomy and function of the left ventricle and assessment of myocardial viability, thus meeting all the requirements of a comprehensive cardiac examination.

1.2.2.1 Imaging principles

When time-of-flight MRA techniques were introduced, two-dimensional (2D) breath hold angiography was applied to the coronary arteries (Danias 2004). The used of conventional black blood techniques (spin echo) with electrocardiographic gating (ECG) was introduced earlier in 2D imaging technique. However, this technique was insufficient to determine coronary stenosis. Then, a white blood sequence (gradient echo), which acquires the image data with ECG-gating in multiple segments (segmented k-space) in many cardiac cycles was introduced. In this sequence, a 2D image with resolution of 1.9 × 0.9 mm could be completed in 16 consecutive cardiac cycles with breath hold in order to minimize respiratory

motion. The data was acquired at approximately 100 ms with cardiac motionless at a mid-diastolic phase. In addition to the advantage of least motion (diastasis), mid-diastolic phase also presents with maximum blood flow in the coronary arteries. Multiple sections were obtained with consecutive breath holds in order to depict the entire coronary tree within a total of 10 to 15 breath holds. However, the inconsistency in depth variability between a series of breath holds lead to discontinuities of the coronary vessels which mimic a stenosis. These techniques, although promising and have an excellent in-plane resolution, depend on experienced user placement of slices to cover the coronary arteries and suffer from poor through-plane resolution. Nevertheless, early reports of the sensitivity and specificity of 2D coronary MRA were encouraging (Manning, Li, and Edelman 1993; Danias 2004).

Since then, a three-dimensional (3D) technique has been introduced in clinical practice to overcome the limitations of the 2D approaches. Compared to multislice 2D-breath hold approaches, 3D imaging takes advantage of the enhanced signal-to-noise ratio (SNR) and the post-processing benefits of thin adjacent slices. Spatial resolution in free-breathing 3D coronary MRA is only restricted by SNR and not the physiological limits of a sustained breath hold (Botnar et al. 1999). A 3D acquisition also offers volume imaging data with continuity between image sections. An impediment of 3D technique, however, is the prolonged scanning time, which might be problematic in patients, or diaphragmatic drifts associated with prolonged breath holds (Botnar et al. 1999; Danias 2004; Taylor et al. 1997).

The MRA technique has been improved with an ultra-fast 3D interleaved gradient echo planar technique (TFE-EPI) to overcome the long scanning time problem by using a combination of a 3D segmented k-space ultra-fast echo time (TFE) with an echo planar imaging (EPI) technique (McKinnon 1993). This approach takes advantage of the short echo time (TE) of TFE techniques and also shortens acquisition window of EPI techniques. Since fewer radio frequency (RF) excitations are needed per shot, higher excitation flip angles can be used and the steady-state magnetization is expected to be increased with respect to TFE scans. Compared to 2D breath hold multislice approaches, where adjacent slices are acquired at different time points within the cardiac cycle (Slavin, Riederer, and Ehman 1998), all slices of the 3D volume are acquired simultaneously at the same time point. Therefore miss-registration problems between adjacent slices due to bulk cardiac motion may be further minimized. Signal voids due to rapid blood flow or cardiac motion are expected to be reduced because of the shorter TE compared to pure EPI techniques and residual respiratory motion artefacts could be minimized because of the shorter acquisition window duration than in TFE scans (Botnar et al. 1999).

In coronary MRA, the magnitude of signal loss correlates with the degree of stenosis visualised on angiographic images. Nevertheless, with the latest bright blood technique, the false positive and false negative results of coronary disease may still occur. For instance, a slow blood flow distal to a stenosis may represent as complete signal loss, although the vessel is patent. In addition, bright blood technique is not sensitive to the direction of blood flow, whereas a total occlusion with adequate collateral circulation may represent as adequate signal, even in the vessel lumen distal to the stenosis. Data from more than 30 studies based on single centre experiences have been published to date regarding the ability of coronary MRA to identify atherosclerotic stenosis (Bunce and Pennell 1999; Danias 2004). These studies used both 2D and 3D MRI imaging techniques with breath hold and free breathing approaches with navigator monitoring of the diaphragmatic motion applied for suppression of the respiratory motion. As a result, there is considerable heterogeneity in the reported sensitivities and specificities, which to a greater extent depend on the different technical procedures, evaluation of different patient groups, methods used for data analysis and the various experiences of the individual centres.

Over the past few years most of the cardiac MRI centres use 3D coronary MRA technique, since it increases SNR and allows reconstruction in any orientation compared to 2D technique. With the technical advancements and better patient selection, the accuracy of coronary MRA for the detection of significant coronary stenosis seems to be improving over the last few years (Danias 2004). Moreover, with developments in the magnetic field (from 1.5 T to 3.0 T), coronary MRA has become more accurate and is increasingly used in cardiac imaging. Imaging coronary artery with 3.0 T MRA potentially increases SNR, which in turn increases spatial resolution and shortens the imaging acquisition time (Bi et al. 2005). In fact, various studies have shown that SNR is improved by approximately 50% at 3.0 T over 1.5 T with similar sequences and parameters (Bi et al. 2005; Sommer et al. 2005). In addition, there are a few ongoing studies on coronary MRA with the latest magnetic field 7.0 T MRI.

1.2.2.2 Diagnostic accuracy

A few studies have reported the diagnostic accuracy of the whole heart coronary MRA with specificity, diagnostic accuracy and positive predictive value being 92.1%, 91.1% and 52.0%, respectively (Kim et al. 2006; Danias 2004; Sakuma et al. 2005). Sakuma et al. (2005) in their prospective study using whole heart coronary MRA reported that the sensitivity and specificity of the 3D coronary MRA were 82% and 91%, for detecting significant stenosis respectively (Sakuma et al. 2005). Kim et al. (2001) conducted a prospective multicentre study using 3D coronary MRA with the targeted volume acquisition technique, in which the sensitivity, specificity, accuracy and the negative predictive value for

patients with disease of the left main artery or three vessel disease were 100%, 85%, 87% and 81%, respectively (Kim et al. 2001).

1.2.3.2 Limitations

Coronary MRA faces several challenges. Firstly, the coronary arteries themselves are a moving target, subject to continuous movement due to cardiac contraction and respiration. Moreover, the coronary tree is complicated in terms of anatomical details with three-dimensional structure, which moves towards the cardiac apex and rotates in counter-clockwise direction at the same time during ventricular contraction. However, during the diastolic period, it follows an opposite trajectory. In addition, the heart (and the coronary arteries) follows the diaphragmatic displacement during free breathing; moves cranially during inspiration and caudally during expiration. The displacement of the heart could vary widely depending on the depth of inspiration (Hofman, Wickline, and Lorenz 1998). Another limitation of coronary MRA is the limited spatial resolution of MR imaging, which is less than 1.0 mm in z-axis direction. This is inferior to that of multislice CT angiography, which is between 0.4-0.5 mm. This limits the visualisation of distal coronary arteries and branches during coronary MRA.

1.2.3 Echocardiography

Since the technology in cardiac imaging has been developed, more and more imaging modalities were introduced to clinical practice in order to detect and diagnose coronary artery disease. Cardiovascular ultrasound or echocardiography is one of those techniques which are increasingly used nowadays in cardiac imaging. Cardiovascular ultrasound has progressed immensely from scan of A-mode images deriving from a thin ultrasound beam, to graphic displays of M-mode echocardiography, and to 2D and 3D examinations, assisting physicians with real-time images of the heart in motion (Pandian et al. 1994). Doppler techniques are now routinely used in assessing haemodynamic and blood flow to the cardiovascular system. Cardiac ultrasound has evolved as an important diagnostic tool in the contemporary cardiology. Nevertheless, the heart is a complex 3D organ that has been displayed anatomically and functionally in only 2D views at any given time. Advances in ultrasound instrumentation supported by computer technology have led to dynamic 3D echocardiography, thus introducing a new era in cardiovascular imaging.

1.2.3.1 Imaging principles

The rationale to develop 3D echocardiography is the awareness of the limitations of current imaging modalities, and the desire to exploit the potential ultrasound methods in order to

improve the diagnostic performance of echocardiography. Three-dimensional echocardiography could complement current echocardiography techniques by providing realistic 3D images of cardiac anatomy and pathology in projections that cannot be obtained with 2D images; by offering quantitative data more accurate than those that are currently available; and additional quantitative information and functional indices (Kisslo et al. 2000).

Colour Doppler displays 2D spatial maps of flow jets and makes evaluation of flow abnormalities easier. Trans-oesophageal echocardiography yields new orientations of viewing the heart and provides high resolution 2D images. However, the 3D heart is only projected in a 2D format by all these modalities. From a multitude of 2D images, clinicians must make an effort to visualise the heart in its original form by a mental 3D reconstruction process. This is not always easily achieved or accurately demonstrated. For instance, in a heart with vegetation or a flail mitral valve, perceptions on the attachment sites of vegetation, or the precise portion of the valve that is flail, could be erroneous despite viewing 2D images in multiplanar reconstructions. Furthermore, it is difficult to determine the spatial relationship of pathology to adjacent structures. Therefore, 3D imaging is the solution to overcome those problems. With 3D imaging method, it could allow visualization of the true nature of cardiac abnormalities in a clinically useful manner; provide better understanding of the topographical aspects of pathology, and define the spatial relationship of structures more reliably (Pandian et al. 1994).

The 3D echocardiography could demonstrate lesions such as an atrial septal defect very well. The precise location of the defect, its relation to adjacent valves, vena cava, and pulmonary veins, are also easily located. In addition, measurements of the size, length of pathological lesions, volume and function of cardiac chambers which may influence management decisions can be obtained. Traditionally, left ventricular chamber volume is calculated from a single plane or biplane 2D images with the use of equations that require a number of assumptions with regard to the 3D geometry of the ventricle. The ability to reconstruct the chamber in all its dimensions and slice it three-dimensionally could aid in measuring left ventricular volume and ejection fraction accurately without any geometric assumptions. This could be especially helpful in ventricles with distorted shape. For estimation of right ventricular volume, no reliable method using 2D techniques has emerged recently. This problem may be solved with 3D imaging (Pandian et al. 1994; Pandian and Vannan 1993).

1.2.3.2 Diagnostic accuracy

A systematic review showed that the diagnostic accuracy of echocardiography for cardiac disease was also moderate, with the mean sensitivity and specificity of 83% (95% CI 73% to

90%) and 72% (95% CI 53% to 85%), respectively (Janda et al. 2011). Moreover, another technique on echocardiography using stress test (exercise versus *dobutamine*) with the same purpose for the diagnosis of CAD, resulted in mean sensitivity and specificity of 84% and 82% on exercise echocardiography (15 studies); and 80% and 84% with *dobutamine* echocardiography (28 studies), respectively (Bax, Van der Wall, and De Roos 2005).

1.2.3.3 Limitations

Several limitations exist in 3D echocardiography imaging. Firstly, the real-time 3D range resolution is 2 mm, whereas the lateral resolution is 3 mm at a depth of 7 cm. This indicates a planar resolution inferior to that with conventional phased-array scanners. In a circular matrix array, however, the transmitted and received beams are symmetrically circular, steered, and focused in two dimensions instead of one dimension, like in a conventional linear array. A focus on all dimensions, therefore, results in the significant improvement in volumetric resolution over conventional 2D imaging arrays. Thus, a real-time 3D imaging from a circular aperture transducer provides better volume resolution throughout the field of view than conventional 2D echocardiography, although the planar resolution is slightly low (Pandian et al. 1994). The clinical significance of these differences in resolution needs to be tested. Secondly, system sensitivity is still limited to some extent. The definition of the endocardia borders is a crucial issue in quantitative echocardiography, and the determination of right ventricular volume requires saline contrast enhancement to adequately locate right ventricular endocardium for the purpose of measurement. Thirdly, the frame rate of echocardiography is 22 frames/seconds. This relatively slow frame rate may provide sufficient samples at slow heart rates but could be quite problematic for the determination of volumes in small children and infants or in adults with high heart rates. Lastly, the pyramidal scan may not always be adequate to acquire an entire volume of the enlarged heart or left ventricle (Kisslo et al. 2000).

1.2.4 Cardiac radionuclide imaging

Advancements in radionuclide imaging have brought about significant developments in the non-invasive evaluation of cardiovascular disease. Radionuclide imaging demonstrates cardiac functional changes and is more sensitive than other imaging modalities for the detection and diagnosis of various cardiovascular abnormalities. Radionuclide imaging techniques include single-photon emission computed tomography (SPECT), positron emission tomography (PET), and integrated imaging modalities such as SPECT/CT and PET/CT or PET/MRI.

1.2.4.1 Imaging principles

SPECT is composed of conventional scintigraphy and computed tomography technique which presents 3D and functional information about the patient's anatomy in more detail and in higher contrast when a radioactive substance is simultaneously included in the procedure. The scintillation of SPECT consists of one or more cameras in a classic SPECT system that obtains multiple two dimensional planer projection images around the patient. It is used to assess the myocardial viability and left ventricular function.

The imaging principle of SPECT is very similar to conventional nuclear medicine planar imaging using gamma camera. However, it is able to provide true 3D information. This is not only presented as cross-sectional slices of the patient, but also can be freely reformatted or manipulated at any orientations. The basic technique requires intravenous injection of a gamma-emitting radioisotope, which is a simple soluble dissolved ion, such as a radioisotope of gallium (III) for disease detection (Elhendy, Bax, and Poldermans 2002). However, in most of the SPECT examinations, a marker radioisotope is attached to a specific ligand to create a radio-ligand, which is of interest for its chemical binding properties to certain types of tissues. This bond allows the combination of ligand and radioisotope to be carried and bound to a place of interest in the body, which then allows the ligand concentration to be seen by a gamma-camera.

Myocardial perfusion imaging (MPI) is a form of functional cardiac imaging, and is used for the diagnosis of ischemic heart disease. The underlying principle is that under conditions of stress, diseased myocardium receives less blood flow than normal myocardium. MPI is one of the several types of cardiac stress tests. A cardiac-specific radiopharmaceutical is administered, such as Tc-99m-*tetrofosmin* and Tc-*sestamibi*. Then, the heart rate is elevated to induce myocardial stress, either by exercise or pharmacologically with *adenosine*, *dobutamine*, or *dipyridamole* (Elhendy, Bax, and Poldermans 2002).

SPECT imaging performed after stress reveals the distribution of the radiopharmaceutical, and therefore assessing the relative blood flow to the different regions of the myocardium. Diagnosis is made by comparing images acquired during stress to a further set of images obtained at rest. As the radionuclide redistributes slowly, the series of images (during stress and rest situations) may not possible to be performed on the same day, hence a second attendance is required 1–7 days later. The rest images are normally acquired at two hours post-stress. However, if stress imaging is normal, it is unnecessary to perform rest imaging, as it will be normal too; thus, stress imaging is always performed first (Elhendy, Bax, and Poldermans 2002).

PET is a nuclear medicine imaging technique that produces a 3D image of functional processes in the body. Unlike SPECT, PET scan needs a radioactive material called positron which produces two gamma rays moving in opposite directions. The system detects pairs of gamma rays emitted indirectly by a positron-emitting radionuclide (tracer), which is introduced into the body on a biologically active molecule. Three-dimensional images of the tracer concentration within the body are then processed and reconstructed by computer analysis. In modern scanners, three dimensional imaging is often accomplished with the aid of a CT X-ray scan performed on the patient during the same session, in the same machine.

If the biologically active molecule chosen for PET is 18F-FDG (*fluorodeoxyglucose*), an analogue of glucose, the concentrations of tracer imaged then give rise to tissue metabolic activity, in terms of regional glucose uptake. Use of this tracer to explore the possibility of cancer metastasis results in the most common type of PET scan in routine clinical practice (90% of current scans). However, many other radiotracers are increasingly used in PET scans to image the tissue concentration of many other types of molecules of interest (Elhendy, Bax, and Poldermans 2002).

Combined or integrated PET/CT represents a recently developed technique that provides both anatomical and functional information, thus, maximising the diagnostic performance of the individual imaging modality. Multislice CT provides excellent anatomical details, while PET offers superior physiological information of the body organs, thus combining these two techniques in a single gantry system improves diagnostic value and allows accurate assessment of disease extent.

1.2.4.2 Diagnostic accuracy

Myocardial perfusion imaging with SPECT is a widely established method for non-invasive evaluation of coronary artery stenosis (Hachamovitch 2003). In fact, the sensitivity of SPECT for detecting CAD is consistently beyond 70%. However, some studies have reported that the sensitivity of SPECT was within the range of 85-90% (Di Carli and Hachamovitch 2006; Slomka et al. 2008). PET has also contributed significantly to the diagnosis of coronary artery disease. With regard to the assessment of CAD, the diagnostic accuracy of myocardial perfusion by PET has been reported to be superior to SPECT (Santana et al. 2007; Donati et al. 2011). PET with rest-stress myocardial perfusion is also known as an accurate imaging modality for investigating and managing patients with CAD (Donati et al. 2011). Moreover, the combined modality of PET/CT further increases the diagnostic accuracy in CAD (Di Carli and Hachamovitch 2006; Slomka et al. 2008; Santana et al. 2007; Donati et al. 2011; van der Vaart et al. 2008).

A systematic review of sensitivity, specificity and the accuracy of SPECT, PET and PET/CT in the detection of CAD showed that PET demonstrated the highest sensitivity, specificity and the accuracy at 91%, 89% and 89%, respectively (Al Moudi, Sun, and Lenzo 2011). Whereas PET/CT had 85%, 83% and 88% while SPECT was found to have 82%, 76% and 83% corresponding to sensitivity, specificity and accuracy. With the moderate results of sensitivity, specificity and accuracy in detecting CAD, therefore, this analysis indicates that SPECT has not reached the diagnostic accuracy to be considered as a reliable technique for assessment of CAD. Several studies also showed that the mean sensitivity and specificity of SPECT was 86% and 74% for the detection of CAD. However, the lower specificity of SPECT may be due to referral bias which is introduced by including patients with normal SPECT studies, only those with a high suspicion for CAD are referred for coronary angiography (Underwood et al. 2004).

1.2.4.3 Limitations

SPECT scanning can be time-consuming. It can take hours or days for the radiotracers to accumulate in some parts of the body under investigation and imaging may take up to several hours to complete though in some cases, newer equipment is available that can substantially shorten the procedure time (Mettler and Guiberteau 1998; Strauss and Griffeth 1994). In addition to the limitation of time-consuming, it is essential that no patient movement is required during the scan time. Movements can cause significant degradation of the reconstructed images, although movement compensation reconstruction techniques can help solve the problem to some extent. In addition, a highly uneven distribution of radiopharmaceutical also has the potential to cause artifacts. A very intense area of activity can cause extensive streaking of the images and obscure adjacent areas of activity.

Limitations to the widespread use of PET arise from the high costs of cyclotrons needed to produce the short-lived radionuclides for PET scanning and the need for specially adapted on-site chemical synthesis apparatus to produce the radiopharmaceuticals after radioisotope preparation. Furthermore, the radioactive material used in PET/CT has shorter half-life. Since the half-life of 18F-FDG is about two hours, the prepared dose of a radiopharmaceutical bearing this radionuclide will undergo multiple half-lives of decay during the working day (Mettler and Guiberteau 1998). This necessitates frequent recalibration of the remaining dose and careful planning with respect to patient scheduling.

1.3 Coronary CT angiography

1.3.1 Technical aspects-spatial resolution

Spatial resolution is determined as the ability to visualize small structures in the scanned volume. A voxel is the volume element that is represented by a 2D pixel in the axis of *x*- and *y*-plane. The third dimension is the *z*-axis which represents a voxel height. Image reconstructions with a smaller field of view can substantially decrease the pixel size in the axial planes (Kroft, de Roos and Geleijns 2007), however, the spatial resolution of coronary CT angiography depends on the resolution at the z-axis, which is determined by the slice thickenss. With current MSCT scanners, volume data with thinner slice thickness (0.5-0.6 mm) can be easily acquired with high resolution, thus, partial volume artefacts can be eliminated.

Many cardiac structures, especially the coronary arteries and the cardiac valves including the valve flaps, represent small and complex 3D structures that require very high and submillimeter isotropic spatial resolution with longitudinal resolution close or equal to in-plane resolution (0.4-0.6 mm). The lumen diameter of the main segments of the coronary artery tree ranges from 3-5 mm in the main segments to about 1 mm in the distal segments. With early type of MSCT scanners such as 4-slice CT, the image quality is poor and limited due to limited spatial resolution (0.6 x 0.6 x 1.0 mm), and the non-assessable coronary segments could be as high as more than 20% in 4-slice studies (Dirksen et al. 2005; Giesler et al. 2002; Hong et al. 2001; Nieman et al. 2002). With the introduction of 16-slice (0.5 x 0.5 x 0.6 mm) and development of 64-slice CT, acquisition of isotropic volume data is made available, especially with 64-slice CT (0.4 x 0.4 x 0.4 mm), thus detection of main and side coronary artery branches is significantly improved when compared to earlier types of MSCT scanners (Dewey et al. 2004; Hoffmann, Lessick, et al. 2006; Kantarci et al. 2006; Leschka et al. 2009; Mollet et al. 2005; Pugliese et al. 2006).

1.3.2 Technical aspects-temporal resolution

Temporal resolution is the ability to resolve fast-moving objects in the displayed CT image (Geleijns et al. 2006). Temporal resolution remains a major challenge in coronary CT angiography since the heart is a fast-moving organ during CT scans. Limitations in temporal resolution are strongly related to the visualisation of coronary artery anatomical details. The temporal resolution of MSCT scanners is mainly determined by the speed of gantry rotation. As it is possible to accurately reconstruct images using data acquired from a 180 degree rotation rather than the full 360 degree rotation, the temporal resolution is equal to half the

gantry rotation speed (e.g. 250 ms for 500-ms rotation time, and 200 ms for 400-ms rotation time).

A temporal resolution of about 250 ms is estimated to be appropriate for motion free imaging in the diastolic phase up to a heart rate of about 60 bpm, about 200 ms up to a heart rate of 70 bpm, and approximately 150 ms for clinically usual heart rates up to 90 bp. It can be expected that a temporal resolution of about 100 ms is sufficient for imaging the heart during the diastolic or end-systolic phase also at high heart rates. The temporal resolution for 4-slice CT is 250 ms, and this is further reduced to 165 ms for 16- and 64-slice CT, and to 83 ms for dual source CT (Flohr 2003; Flohr, Küttner, et al. 2003; Flohr, McCollough, et al. 2006)

1.3.3 Artefacts

Image artefacts can be defined as any inconsistency between the reconstructed Hounsfield values in the image and the true attenuation coefficients of the object in such a way that these discrepancies are clinically significant or relevant as judged by the radiologist (Hsieh 2003). Imaging coronary arteries using CT angiography requires high spatial resolution, high temporal resolution, good low-contrast resolution, intravascular contrast enhancement and a short scanning time. Image artefacts always associated with the limitations of either temporal resolution, or noise and the reconstruction algorithm in the scanner system. Images artefacts are mainly demonstrated as blooming, streaks, partial volume and motion artefacts. All these artefacts can arise from technical, operator, and patient errors (Barrett and Keat 2004).

Stair-step artefact is the most common artefact that occurs in CCTA. Stair-step artefact is also known as slab artefact which is attributable to cardiac pulsation often degrading image quality. Stair-step artefact occurs especially in patients with high heart rates, heart rate variability, and the presence of irregular or ectopic heart beats such as premature ventricular contractions and atrial fibrillation during image acquisition. It can be best recognized in a sagittal or coronal view. Therefore, beta-blockers should be used to reduce the heart rate prior to the scan. Reducing this artefact is achieved by reconstructing the dataset at different phases of the cardiac cycle. In general, reconstructions for CCTA are performed in mid-diastole to late diastole (60%–70% of the R-R interval). However, because the duration of diastole decreases as the heart rate increases, an end-systolic phase reconstruction at 25%–35% of the R-R interval might be considered for image processing (Barrett and Keat 2004).

1.3.4 CT scanner developments

CT scanner has rapidly evolved from single slice to multislice CT which started from 4-slice systems in 1998 to the latest 256-slice and 320-slice CT systems. With smaller detector element size and faster gantry rotation speed, spatial and temporal resolutions of the 64- or more MSCT scanners have enabled coronary artery imaging a feasible and reliable clinical test. The technological advancements from 16- to 64-slice systems progressed in a relatively uniform fashion with improved longitudinal (z-axis) volume coverage, decreased gantry rotation time, and smaller detector elements (Paul et al. 2003; Ropers et al. 2003). With the ability to acquire volume data, technological improvements in CT scanning also enables generation of 3D image processing such as multiplanar reformation (MPR), maximum intensity projection (MIP), surface-shaded display, and volume-rendering techniques, and these reconstructed visualisations have become an important component of medical imaging visualization in daily practice (Sun, Choo, and Ng 2012).

1.3.4.1 Single-slice CT

Parallel fan beams of radiation are produced by the X-ray tubes with the earlier successive generations of CT scanners. This resulted in very slow image acquisition since no movement occurred along the axis of the patient during each of the projections. Axial scanning requires long examination times because of the interscan delays necessary to move the table incrementally from one scan position to the next and unwind the cable, thus it is prone to misregistration or loss of anatomical details due to potential movement of the relevant anatomical structures between two scans (by patient breathing, motion or swallowing). Besides, only a few slices are scanned during maximum contrast enhancement when the contrast medium is used. These problems may be overcome if the scan speed is increased and interscan delay is eliminated. The development of spiral CT possesses these features which help to overcome the above problems.

The introduction of spiral CT in the late 1980s represented a fundamental evolutionary step in the development and continuing refinement of CT imaging techniques (Ciernak 2011). In 1989, spiral CT became available as a mode for continuous volume scanning (Ciernak 2011). With spiral CT, the patient table is continuously moved and translated through the gantry while scan data are acquired simultaneously. A prerequisite for spiral CT scanning is the introduction of slip-ring technology, which eliminates the need to rewind the cable after each rotation and enables continuous data acquisition during multiple rotations. The purpose of slip-ring is to allow the x-ray tube and detectors to rotate continuously so that a volume data of the region of interest, rather than a single slice can be acquired very quickly in a single

breath hold. Spiral CT scanning does not suffer from the danger of misregistration or loss of anatomic details. Images could be reconstructed at any position along the patient longitudinal axis, and overlapping image reconstruction could be generated (normally 50% overlap) to improve longitudinal resolution. Acquisition of volume data has become the very basis for applications such as CT angiography (Goldman 2008).

1.3.4.2 4-slice CT

In 1998, a 4-slice CT scanner was introduced by several manufacturers representing an obvious quantum leap in clinical performance (Costello 1996; Taguchi and Aradate 1998). Four detector 'rows' corresponding to the 4 simultaneously collected slices fed data into four parallel data 'channels', so that these 4-slice scanners were said to possess four data channels. These 4-slice scanners, however, were quite flexible with regard to how detector rows could be configured; groups of detector elements in the z-direction could be electronically linked to function as a single, longer detector, thus providing much flexibility in the slice thickness of the four acquired slices (Flohr et al. 2005; McCollough and Zink 1999). Fundamental advantages of MSCT include substantially shorter acquisition times, retrospective creation of thinner or thicker sections from the same raw data, and improved three-dimensional rendering with diminished helical artefacts (Costello 1996).

For example, the SOMATOM Volume Zoom with a 500 ms gantry rotation time and the simultaneous acquisition of 4 slices offers an eight-fold increase of performance compared to previous 1 second, single-slice scanning. Obviously, such a significant improvement opens up a new area in spiral CT improving all existing applications and allowing the realization of new clinical applications. The key issue is correspondingly increased volume coverage per unit time at high axial resolution and subsequent improved temporal resolution (Costello 1996).

Four-slice scanners are the basic system for CCTA examination. With only 250 ms of temporal resolution from a gantry rotation of 500 ms CCTA with use of 4-slice CT requires longer longitudinal scan to cover the entire cardiac chamber and coronary arteries, thus, this may result in long breath hold between 30 and 40 seconds which lead to breathing and motion artefacts (Haberl et al. 2005).

1.3.4.3 16-slice CT

The installation of 16-slice CT scanners in 2002 provides 16 detector channels enabling simultaneously acquisition of 16 slices per gantry rotation (Goldman 2008). In addition to simultaneously acquiring up to 16 slices, the detector arrays associated with 16-slice

scanners were redesigned to allow thinner slices to be obtained as well. Note that in all of the models, the innermost 16 detector elements along the z-axis are half the size of the outermost elements, allowing the simultaneous acquisition of 16 thin slices (from 0.5 mm to 0.75 mm thick, depending on the model and manufacturer). When the inner detectors were used to acquire submillimeter slices, the total acquired z-axis length and therefore the total width of the x-ray beam ranged from 8 mm for the Toshiba model to 12 mm for the Philips and Siemens scanners. Alternatively, the inner 16 elements could be linked in pairs for the acquisition of 16 thicker slices (Lewis, Keat, and Edyvean 2006).

Sixteen-slice scanners have a slightly better spatial resolution and faster gantry rotation (420 ms) than that in 4-slice CT (Kopp et al. 2002). The major advantage of 16-slice scanners over 4-slice CT is the longer z-axis coverage (16 × 0.75 mm vs 4 × 1.0 mm), resulting in significantly shorter breath hold and less motion artefacts (Achenbach et al. 2005; Gibbons et al. 1997; Kuettner, Beck, and Drosch 2005). The rotational speed of 16-slice scanners is only marginally faster, and adaptive multi-cycle reconstructions, which require a high number of detectors, often cannot be applied because of heart rate variations. As a consequence of these factors, image quality with the 16-slice scanner is significantly improved, reducing the number of coronary segments with poor image quality (Achenbach et al. 2005; Flohr, Schoepf, et al. 2003; Garcia, Lessick, and Hoffmann 2006; Gibbons et al. 1997; Kuettner, Beck, and Drosch 2005).

Coronary CT angiography became more clinically practical with retrospective electrocardiogram (ECG) gating to capture cardiac motion plus the z-axis coverage from 16-detector row scanners (Kalender et al. 1990). However, cardiac motion and stair-step artefacts are the main challenge in this system. Therefore, there are few steps suggested to overcome those problems, which include increasing the number of detector elements and the volume coverage along the z-axis of detector block. Moreover, increase in the sensitivity of detector material and application of iterative image reconstruction algorithms represents another approach to improve cardiac image quality (Klingenbeck-Regn et al. 1999; Liang and Kruger 1996). During 2003 and 2004, manufacturers introduced different types of MSCT models with less than 16-slice scanners, but most commonly the introduction of more than 16-slice scanners represented the main direction for improving MSCT systems (Goldman 2008).

1.3.4.4 64-slice CT

The 64-slice CT was first introduced with a single x-ray source mounted opposite to a 64-detector-array in the gantry unit. With gantry rotation times down to 0.33 second for 64-slice

CT (0.375 second for 16-slice CT), temporal resolution for cardiac ECG-gated imaging is again markedly improved. The increased temporal resolution of 64-slice CT has the potential to improve the clinical strength of ECG-gated cardiac examinations at higher heart rates, thereby reducing the number of patients requiring heart rate control. In contrast to previous studies, high diagnostic accuracy has been achieved despite the presence of severely calcified coronary plaques. In addition, using 64-slice CT the scanning time is reduced to less than 15 seconds, allowing a decreased breath hold time, better utilization of contrast medium with fewer enhancements of adjacent structures and a lower dose of applied contrast medium. Improvement of image quality has also been reported in the visualization of all coronary artery branches with high sensitivity and specificity achieved.

The new-generation dual-source MSCT (Somatom Definition FLASH; Siemens Medical Solution, Forchheim, Germany) introduced at the end of 2008 is equipped with two 64-detector row units, each with an alternating focal spot. The 360° gantry rotation time is 280 ms, translating to a temporal resolution of approximately 75 ms when the scanner operates with both x-ray tubes collecting data at the same energy. The vendor has proposed a high-pitch prospectively ECG-triggered scanning acquisition (Achenbach et al. 2006; Flohr, McCollough, et al. 2006). In single-source 64-slice CT, the maximum pitch is roughly 1.5 for gapless image reconstruction. The pitch can be increased up to 3.2 in dual-source systems. For CCTA, the typical phase window required for a diagnostic quality examination regarding motion artefact is 10% of the R-R interval. The pitch required for multiphase acquisition ranges from 0.2 to 0.5, depending on the heart rate (Steigner et al. 2009).

With the high-pitch acquisition mode, only one phase is acquired, which gradually increases with the z-axis table translation. The influence on image quality for different clinical scenarios and heart rates is evaluated with the second generation dual-source CT. Achenbach et al. (2009) have demonstrated the feasibility of this new scanning method using first-generation dual-source CT. However, slow and regular heart rates are the prerequisite for this acquisition protocol that is prospectively triggered by ECG signal and is anticipated to scan the entire heart in 270 ms, with a pitch of up to 3.4 (Achenbach et al. 2009). Another potential advantage of dual-source CT is tissue characterization with both detector systems operating at different tube voltages known as dual-energy CT. Although this has not been extensively studied to date, the two x-ray beams of different energy spectra in theory could better demonstrate varying attenuation characteristics of different tissues (Ruzsics et al. 2008; Rybicki et al. 2008).

1.3.4.5 128- and 256-slice CT

In late 2007, the 128-slice CT (Brilliance iCT; Philips Healthcare, Cleveland, OH) was introduced with a 128 × 0.625-mm detector row system with dual focal spot positions to double the number of slices within the 8-cm (width) z-axis gantry coverage. The iCT has a gantry rotation time of 270 ms, which translates to an approximate temporal resolution of 135 ms. Prospectively ECG-triggered coronary CT angiography typically covers the entire heart in two axial acquisitions over three heartbeats. During the diastole of the first heartbeat, the upper half of the heart is imaged. During the second heartbeat, the X-ray table translates 62.4 mm. Subsequently, the lower half of the heart is acquired during the diastole of the third heartbeat. The scanner is equipped with several radiation reduction capabilities, including a dynamic helical collimator and an adaptive axial collimator to reduce z-over scanning (Hameed et al. 2009; Walker et al. 2009).

Second generation of 128-slice CT was introduced with dual-source which uses two x-ray tubes with opposing 64 detector arrays mounted 90° from each other. The main advantage of this system is that the temporal resolution is effectively halved because each x-ray tube/detector array system only needs to rotate half of the angle that would otherwise be required by a single-source system. The number of detector rows in the longitudinal axis (z-axis) and the number of slices of CT system are not interchangeable terms because multiple systems with an alternating focal spot allow the same z-axis coverage to be sampled twice, and thus the number of image slices generated is double the number of detector rows (Flohr, McCollough, et al. 2006). However, the volume coverage remains the same; for example, a 128-detector row scanner with two alternating z-focal spot positions can be referred to as 256-slice CT. It is important to specify the number of detector rows in z-axis, with or without alternating focal spot positions, and single versus dual source.

1.3.4.6 320-slice CT

This hardware (Aquilion One Dynamic Volume CT; Toshiba Medical System, Tochigi-ken, Japan) currently has the largest z-axis detector coverage. It was released shortly after experiments with a 256-detector row CT prototype (Kido et al. 2007; Mori, Endo, et al. 2005; Mori et al. 2006; Mori, Kondo, et al. 2005). Each detector element is 0.5 mm wide, yielding a maximum of 16-cm z-axis coverage. This configuration allows three-dimensional volumetric entire heart imaging during the diastole of one R-R interval. In 320-detector row CT, the entire heart is imaged with temporal uniformity. Furthermore, if the x-ray beam is turned on for a longer period, the scanner can capture the heart over one or more cardiac cycles. This has been described as four-dimensional CT or volumetric cine imaging (Mori,

Kondo, et al. 2005). The temporal resolution of CT scanner reflects the ability to freeze cardiac motion, thus producing motion-free images. The 320-detector scanner has a standard temporal resolution of approximately 175 ms, one half the gantry rotation times. For patients with higher heart rate (>65 bpm) and contraindications to β-blockers, multi-segment reconstruction can be used at the expense of higher radiation dose. For example, in two-segment reconstruction, data required for image reconstruction are acquired over two cardiac cycles. Therefore, only data from 90° rotation during each of the two cardiac cycles are used, improving the effective temporal resolution by a factor of 2 (Hoe and Toh 2009).

1.3.5 Coronary CT angiography scanning techniques with ECG-gating protocols

Over the last ten years continuing improvements have taken place in the CT technology. The ability to produce images of the coronary artery lumen and wall in order to obtain information on the presence, severity, and characteristics of CAD has made CCTA a reliable non-invasive diagnostic tool in coronary artery imaging. With emergence of the latest technology in CCTA, visualisation of atherosclerotic plaque and luminal stenosis/obstruction has become available for the diagnostic work-up of patients with known or suspected CAD.

The acquisition of the dataset for CCTA consists of three steps including topogram, determination for the adequate contrast enhancement of CCTA and the image acquisition for the entire coronary artery tree. A low-energy topogram is acquired as a first step. This scan permits accurate positioning of the scan volume for subsequent planning on data acquisition inclusive of scan direction, slice thickness and set up of the exposure parameters. In step two, the contrast enhancement setting for the scan can be obtained in two techniques namely bolus tracking technique and the test bolus technique.

The bolus tracking technique uses a series of dynamic low-dose axial scans with an interval of 2 seconds at the level of the carina. This technique allows the operator to track the bolus of contrast material in order to ensure that contrast enhancement is sufficient at the level of the ascending aorta prior to the scan. The CCTA imaging sequence is initiated when the contrast enhancement reaches a predefined value between 100 and 150 Hounsfield units. On the other hand, the test bolus technique requires a small bolus of iodinated contrast agent (10–20 mL) to be injected into the antecubital vein and followed by normal saline (30–50 mL) at a rate of 4–5 mL/s in order to determine the contrast material transit time (Hoffmann, Ferencik, et al. 2006). A non-gated axial image is generated every 2 seconds at the level of the ascending aorta. The time from the start of the injection to the peak contrast enhancement in the ascending aorta determines the time for scan delay after the initial contrast material administration. The test bolus technique is also known as ‘sure start’ technique by some

manufactures. The timing bolus (Achenbach et al. 2005; Hoffmann et al. 2004; Kuettner et al. 2004) and the bolus tracking techniques (Dewey et al. 2004; Hoffmann et al. 2005; Mollet et al. 2004) provide similar results and have been widely used in the current cardiac CT studies.

In the third step, a CT volume dataset for the coronary arteries is acquired; this dataset covers the entire heart from the proximal ascending aorta (approximately 1–2 cm below the carina) to the diaphragmatic surface of the heart. The scan is acquired in a single breath hold during comfortable inspiration and starts with the injection of a contrast agent with a high concentration of iodine (300–400 mg/mL) at a high flow rate (4–6 mL/s). The total volume of contrast agent depends on the scan length, but typically 60–80 mL is injected, followed by a saline flush (40–70 mL at 4–6 mL/s). The actual CT scan starts after the delay is calculated as the contrast material transit time (Hoffmann, Ferencik, et al. 2006).

There are two scanning modes for a CT scan: step-and-shoot CT or sequential and helical or spiral CT. In sequential CT, a cross-sectional image is produced by acquiring a series of axial slices of the body from different angular positions while the X-ray tube and detector rotate 360° around the patient with the table being stationary. The image is then reconstructed from the resulting projection data. However, if the patient moves during the acquisition, the data obtained from the different angular positions are no longer consistent. In fact, the image will be degraded by motion artefacts and may be of limited diagnostic value (Flohr, Bruder, et al. 2006; Flohr et al. 2005).

Spiral CT uses a different scanning principle. Unlike the sequential CT, X-ray the table moves continuously through the gantry in the z-direction while the X-ray tube rotates 360° around the patient. The X-ray traces a spiral path around the patient and produces volume data. The table movement in the z-direction during the data acquisition will generate inconsistent datasets, causing reconstructed images being degraded by the artefacts. Thus, some special reconstruction algorithms such as interpolation techniques are used to generate a planar set of data for each table position producing artefact-free images. Thus it is possible to reconstruct individual slices from a large data volume by overlapping reconstructions as often as required (Flohr, Bruder, et al. 2006; Flohr et al. 2005).

1.3.6 Prospectively ECG-triggered coronary CT angiography

Prospectively ECG-triggered technique uses axial images and an incrementally moving table to cover the heart with minimal overlap of axial slices. Cardiac imaging with electron beam CT also uses prospective data acquisition triggered by ECG. Prospective triggered technique in cardiac CT is not new and it was actually being used by Dr. Godfrey Hounsfeld in early

1980 with conventional single-slice CT (Hounsfield 1980). It was recognized that CT image synchronization with heart diastolic phase was optimal for imaging the heart. However, the findings were not being achieved when the patient heart rate increases.

The prospective triggered technique uses a combined ‘‘step-and-shoot’’ axial data acquisition and an incrementally moving table with adaptive ECG triggering. In this technique, the table is stationary during image acquisition. It then moves to the next position for another scan initiated by the subsequent cardiac cycle. This results in very little overlap between the scans but leads to a significant reduction in radiation dose. In prospective ECG triggering, the tube current is turned off for most of the scan period. The tube current is on only for a short period during diastole which is triggered by the electrocardiogram (Earls 2009).

When a 64-slice system is used, the scan is prescribed by using 3–5 incremental of 64 × 0.625 mm (40 mm) image groups which requires 2–4 incremental table translations of 35 mm. Thus, allow for 5 mm of overlap. The minimum interscan delay is approximately between 0.6 and 1.0 second which normally requires skipping a cardiac cycle between data acquisitions which results in one image acquisition per 2 cardiac R-R cycles (Earls 2009). However, the process will be faster with larger detectors (128-, 256- or 320-slice CT) being used. The detector width determines the number of steps/scans to cover the entire heart and complete an examination. For instance, the dual-source 64-slice CT has a narrower detector array (32 ×2 × 0.6 mm = 38.4 mm per acquisition); thus, it takes more incremental steps (normally 4-5 cardiac cycles) to cover the heart and complete an examination than with the 320-row system (320 × 0.5 mm = 160 mm) which covers the heart in a single acquisition (Hoe and Toh 2009).

Prospectively ECG-triggered technique has a limited number of cardiac phases available for reconstruction. Therefore, mid-diastolic phase (75% of R-R interval) was normally selected for data acquisition for all subjects. In addition, by using add-on ‘padding’ will allow more cardiac phases for reconstruction. Padding technique is described as prolonging the acquisition window in order to allow the reconstruction to adapt with minor heart rate variations and to produce consistent image quality. Padding turns the x-ray tube on before and after the minimum or actual acquisition time (milliseconds) required. Available padding options with current software ranges from 0 to 200 msec (Figure 1-3). No padding is required for patient with stable heart rates with minimal heart rate variability. However, radiation dose also will increase with application of padding window due to expense of radiation exposure on the particular windows phase (Earls 2009; Hausleiter et al. 2006).

Figure 1-3: The use of extra tube-on time to acquire image data during additional cardiac phases. Padding turns tube on prior to minimum half-scan time and leaves it on afterwards. It is recommended in cases when heart rate varies during examination.

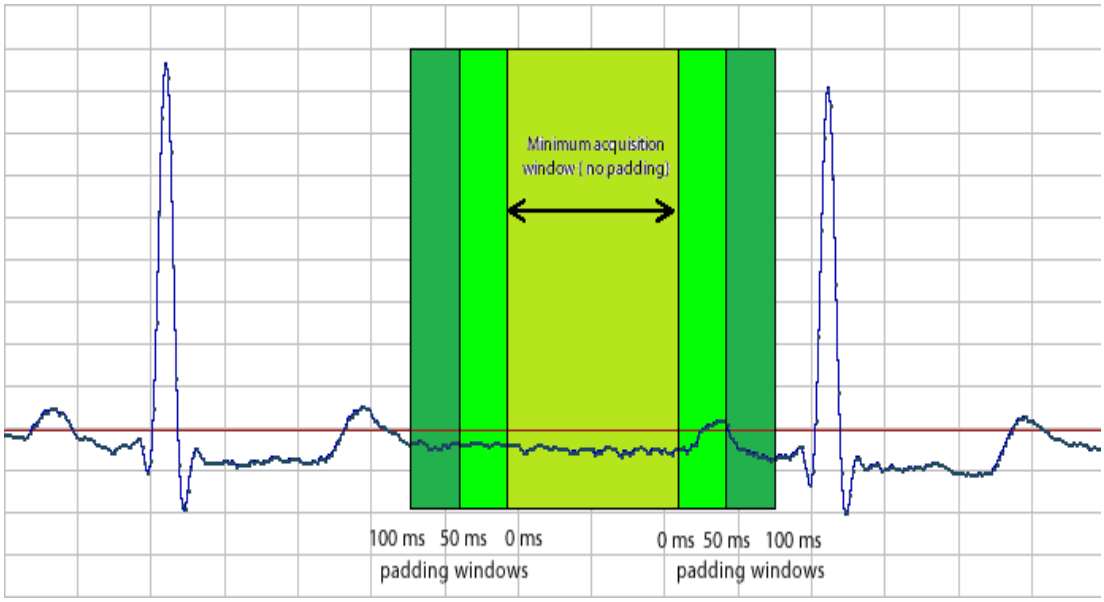

Other than adjusting prospective triggering parameters in order to adapt with high heart rates, application of β-blockade for heart rate control is also commonly used in CCTA to produce better results. However, precautions have to be taken in patients who are contraindicated to β-blockage agent. Alternatively, calcium channel blocker could be used in order to reduce the heart rate. The maximum of 15 mg of intravenous metaprolol (β-blocker) or 40 mg of intravenous *diltiazem* (calcium channel blocker) is recommended prior to the scan in order to control the heart rate (Earls 2009; Pannu, W. Alvarez, and E. K. Fishman 2006).

The major drawback of prospective ECG triggering is that cardiac functional analysis is unavailable. Since prospective technique acquires data during a limited portion of the cardiac cycle, it cannot be used to evaluate cardiac function. Both quantitative and qualitative functions, either global or regional, require images to be reconstructed throughout the entire cardiac cycle. If the clinical scenario or referring physician requires information about cardiac function, then retrospective gating must be undertaken.

Heart rate variability is another limitation for the prospective ECG triggered technique. Heart rate variability of > 5 beat/minute is considered not applicable for prospective triggering. Therefore, the scan has to be reverted into retrospective ECG gating technique if patients' heart rate elevated or heart rate variability does not meet the requirement after β-blocker has been given (Earls 2009).

However, the prospective ECG triggered technique in patients with higher heart rates still produces diagnostic images. CT scanner with higher detector arrays is an alternative to obtain CCTA in patients with high or irregular heart rates. It has been reported that high diagnostic value could be achieved with 320-slice CT angiography in the diagnosis of CAD, with image quality independent of heart rate (Hoe and Toh 2009). The improved temporal resolution (175 ms) and increased coverage scan value (160 mm) of 320-slice CT results in robust image quality within a wide range of heart rates; thus providing the opportunity to image patients with higher heart rates without requiring pre-examination beta-blockage (Hoe and Toh 2009).

1.3.7 Retrospectively ECG-gated coronary CT angiography

Coronary CT angiography is most commonly performed in the spiral acquisition mode with continuous acquisition of data throughout the cardiac cycle. Multiple reconstruction parameters determine the quality of the reconstructed axial images. Images are usually reconstructed with a slice thickness of 0.75 mm, 50% overlap between images (0.4-mm increment), and a pixel matrix of 512 × 512. Although a thinner slice improves the resolution of the 3D dataset and the quality of reconstructed images, it comes at the cost of increased image noise, which can significantly limit the diagnostic assessment of the coronary arteries in patients with body mass index of greater than 30 kg/m^2 (Leschka et al. 2008).

CCTA images are typically reconstructed with a medium smooth reconstruction kernel. Sharper reconstruction kernels can be applied to tailor evaluation of coronary stents. A small field of view (18–20 cm) that encompasses only the heart is used for CCTA evaluation. For the assessment of incidental extra cardiac findings, the raw data are reconstructed with a larger field of view (35 cm) and 3-mm-thick slices. The use of retrospective ECG-gated reconstruction permits the reconstruction of complete datasets collected at different points of the R-R cycle. It has been shown that the optimal reconstruction window in which the coronary arteries can be visualized almost free of motion artefacts lies in mid-diastole (60%–70% of the R-R interval) (Leschka et al. 2009). Exceptions are observed in patients with higher or irregular heart rates, in which a reconstruction window positioned in late systole (25%–35% of the R-R interval) often yields the best image quality. Although the half-scan algorithm (data from 210° and 1 detector are used for a single image) is the default option for all patients with heart rates of less than 70 beats per minute (bpm), sometimes multisector reconstruction algorithms are used in patients with high heart rates to generate diagnostic images (Flohr, McCollough, et al. 2006).

In single-source CT (SSCT), improved temporal resolution is obtained at the expense of limited spiral pitch and correspondingly increased radiation dose to the patient. For a single segment reconstruction, the table has to travel slowly in order to ensure that each z-position of the heart is visualised by a detector slice during each phase of cardiac cycle. Therefore, the patient's heart rate would determine the spiral pitch (if the heart rate goes up, the spiral pitch can be increased). Moreover, if multi-segment reconstructions are applied at higher heart rates to improve temporal resolution, the spiral pitch has to be reduced again. For example, each z-position of the heart has to be visualised by a detector slice during two consecutive heart beats in a 2-segment reconstruction; and three consecutive heart beats for a 3-segment reconstruction; and so on. In general, manufacturers of single-source CT scanners recommend an adaptive approach for ECG-gated cardiac scanning which the pitch of the ECG-gated spiral scan is kept constant at a relatively low value between 0.2 and 0.25. Therefore, more segments are used for image reconstruction at higher heart rates to improve temporal resolution (Dikkers et al. 2009; Wang et al. 2009).

Using a DSCT system, a temporal resolution of a quarter of the gantry rotation time is achieved, independent of the patient's heart rate. Single-segment reconstruction using data from one cardiac cycle for image reconstruction can be applied at all heart rates. Since multi-segment reconstruction will not be required, the spiral pitch can be efficiently adapted to the patient's heart rate and significantly increased at elevated heart rates, compared with single - source CT systems with multi-segment reconstructions required at higher heart rates. Pitch values ranging from 0.25 at lower heart rates up to 0.5 at high heart rates are possible, resulting in coverage of the entire heart volume within 5 to 9 seconds with use of 2 x 32 x 0.6 mm collimation. The increased pitch at higher heart rates not only reduces the examination time, but also reduces the radiation dose to the patient. At a constant tube output and fixed gantry rotation time, higher pitch is directly related to the reduction of patient dose. Using the dedicated DSCT scanner, the patient's heart rate is monitored before the examination with the lowest heart rate being observed during the monitoring phase and an additional safety margin of 10 bpm being subtracted to automatically adjust the pitch values (Flohr, McCollough, et al. 2006; Ketelsen et al. 2010).

Although the opportunity to noninvasively exclude significant CAD provides an attractive rationale for using CCTA in a variety of clinical applications, data on the clinical utility, cost, and cost-effectiveness, prerequisites to justify clinical implementation, are still debatable. Since invasive coronary angiography is associated with a small but not negligible risk of complications (inherent in invasive procedures), inconvenience to patients, and high costs, CCTA may be an effective alternative to invasive coronary angiography, with the

potential of reducing the number of purely diagnostic angiographic procedures. Patients with an intermediate likelihood of CAD (between 30% and 70% probability of having significant CAD, as determined by age, sex, and clinical symptoms) may benefit from CCTA (Gibbons et al. 1997). Other potential applications include preoperative risk assessment, assessment of patency of stents placed in the left main coronary artery, and evaluation of bypass patency. Furthermore, the ability to detect and characterize the extent, distribution, and morphology of coronary atherosclerotic plaque may be useful for improving short- and long-term cardiovascular risk stratification (Achenbach et al. 2004).

1.3.8 Coronary CT angiography-diagnostic accuracy

The diagnostic accuracy of coronary CT angiography has been reported extensively in the literature ranging from the earlier studies using retrospective ECG-gated protocols to the recent reports comparing prospective ECG-triggering and retrospective ECG-gating. In retrospectively ECG-gated CCTA, several studies on different types and generations of MSCT scanners were carried out with overall results showing that CCTA had moderate to high sensitivity of 86-99 % and high specificity of 89-100% in patients with suspected CAD. In particular, a very high negative predictive value (NPV) of over 95% (96-99%) has been reported in these studies indicating that CCTA can be used as a reliable screening tool for CAD (Pontone et al. 2009; Sun and Ng 2012**).** Moreover, multicentre studies were also conducted on 64-slice CT scanner to investigate the diagnostic accuracy of CCTA with different risks of CAD prevalence. The results showed that high sensitivity (94%), specificity (83%) and NPV (99%) was achieved in high risk patients with CAD (68%). Similarly, high diagnostic accuracy was also presented in low risk of CAD with sensitivity, specificity and NPV being 94%, 83% and 99% in 25% of CAD prevalence; 85%,90% and 83% in 56% of CAD prevalence, respectively (Budoff et al. 2008; Meijboom et al. 2008; Miller et al. 2008). A study on the high-pitch mode with 128-slice CT also resulted in high sensitivity, specificity and NPV of 94%, 91% and 97% respectively (Alkadhi et al. 2010).

In recent years, prospective ECG-triggered CCTA is increasingly used in the diagnosis of CAD with promising results reported. The sensitivity (93.7-100%), specificity (82.7-97%) and NPV (95-98%) in the assessment of CAD were reported in multiple studies confirming the feasibility of this fast developing technique (Pontone et al. 2009; Sun and Ng 2012). Several studies on CCTA using DSCT were also conducted to compare the diagnostic accuracy between 64-slice and 128-slice CT. The high sensitivity, specificity and NPV were achieved in 64-slice CT with 100%, 99% and 94% respectively (Scheffel et al. 2006). Similarly, 128-slice DSCT also demonstrated high diagnostic accuracy of 93%, 94% and 97% corresponding to sensitivity, specificity and NPV, respectively (Alkadhi et al. 2010).

However, studies on the diagnostic accuracy of CCTA using the latest CT generations including 256- and 320-slice CT are limited, thus, further research is needed to investigate the diagnostic performance of CCTA with use of these recent models, in particular, the corresponding image quality and radiation dose.

1.4 Radiation dose

1.4.1 Radiation dose effects

Radiation dose could cause deterministic and stochastic effects. Deterministic effect occurs when the radiation dose reaches a threshold dose level. The threshold level in deterministic effect varies in different subjects and the damages are significantly correlated to the amount of dose received. Skin injury, hair fall and cataract are the examples of deterministic effects associated with radiation dose. For example, skin injuries range from skin erythema, moist desquamation, epilation, laceration to necrosis if the skin is exposed to radiation dose beyond the threshold dose at 2 Gy (Bogaert et al. 2009).

On the other hand, stochastic effect can be defined as an effect that occurs without any dose threshold. It happens at all time and the damages are not depending on the amount of dose received. For example, ionising radiation induces cancer and genetic changes. However, previous studies have reported that the increment of radiation dose could increase the chance of developing cancer (Hall 1999).

The assumed risk of cancer estimations are derived from analyses of mortality data based on Japanese atomic bomb survivors exposed to the radiation doses (Brenner et al. 2001; Pierce et al. 1996). This study has reported that there was a strong evidence of an increased cancer risk at equivalent doses greater than 100 mSv, good evidence of an increased risk for doses between 50 and 100 mSv and reasonable evidence for those who had exposed to doses between 10 and 50 mSv.

However, CT contributes to the highest radiation dose of all radiological examinations. Brenner and Hall estimated that approximately between 1.5 and 2% of all cancers in the United States may be caused by radiation exposure from CT examinations (Brenner and Hall 2007). Previous research estimated that CT scans causes 800 cancers in woman and 1300 in man per year in the United Kingdom (Broadhead et al. 1997). Moreover, a study conducted on paediatric CT showed that the percentage increases in the mortality of cancer over the natural background are very low (Brenner et al. 2001). However, in the United States, approximately 500 out of 600,000 children less than 15 years old who are estimated to undergo CT procedure each year will die of cancer (Brenner and Hall 2007).

Thyroid gland is the most radiosensitive organ in human body (UNSCEAR). It was reported that ionizing radiation is the common factor that induces thyroid cancer (Shore 1992). The aetiology of radiation-induced thyroid cancer was derived from the analysis of atomic bomb survivors and radiotherapy patients (Ron et al. 1989; Thompson et al. 1994). Apart from

thyroid cancer, hypothyroidism and single thyroid nodules were found in Nagasaki atomic bomb survivors (Nagataki et al. 1994). However, children are more sensitive and have a higher risk of developing thyroid cancer than adults. With a minimum radiation dose of 10 cGy, it could possibly cause thyroid cancer to develop in children (Ron et al. 1989; Shore 1992). According to the report from the biological effect of ionizing radiation VII (BEIR VII), benign tumour could occur at approximately 50 cGy of radiation exposure (Einstein, Henzlova, and Rajagopalan 2007). This report was supported by other studies that there was a significant relationship between radiation dose and thyroid cancer.

Heart or cardiac organ was known as a radio-resistant organ in early 1900s. However, in 1950s the researcher found that there was evidence of detrimental effects on cardiovascular system on patient who were on radiotherapy treatment for Hodgkin lymphoma and breast cancers, and therefore, cardiac organ is no longer resistant to the radiation (Senkus-Konefka and Jassem 2007). The study showed that the impairment of cardiovascular system was associated with radiation dose threshold of 40 Gy and there was more than 35 Gy of treatment dose that was given to patients for radiotherapy treatment of the Hodgkin lymphoma and breast cancer. The side effects resulting from the radiation exposure was an increase of fibrous tissues in pericardium, myocardium and endocardium layers. Moreover, arteriosclerosis occurred around coronary ostium and proximal coronary arteries due to radiation exposure. In certain cases, other cardiac diseases could develop such as pericarditis and functional valvular defects if a large volume of cardiac region was exposed to the radiation. However, some studies indicated that cardiovascular injury due to radiation was not only caused by radiotherapy, but it can also due to diagnostic radiology examinations and radiation exposure in a working environment (Senkus-Konefka and Jassem 2007).

1.4.2 Radiation dose quantity and measurements

1.4.2.1 CT dose index

The fundamental radiation dose parameter in CT is the computed tomography dose index (CTDI). $CTDI_{100}$ is a measured parameter of radiation exposure which is more convenient than the CTDI and it is regarded as the measurement of choice performed by medical physicists in the clinical setting. It is measured by a 100-mm long pencil-shaped ionization chamber in two different cylindrical acrylic phantoms (16-cm and 32-cm diameter) which was placed at the iso-center of the CT scanner. Most manufacturers use a 16 cm phantom for head and 32 cm phantom for body examinations during CTDI calculation (Wagner, Eifel, and Geise 1994). The $CTDI_w$ is the weighted average of the $CTDI_{100}$ measurements at the center and the peripheral locations of the phantom. This parameter reflects the average

absorbed dose over the two-dimensions (x and y dimensions) of the average radiation dose to a cross-section of a patient's body.

The $CTDI_{vol}$ is different from $CTDI_w$ as the former averages radiation dose over three-dimensions (x, y, and z directions) ($CTDI_w$ represents the average exposure in the x-y plane only). $CTDI_{vol}$ is the weighted CTDI divided by the pitch, or $CTDI_{vol}$= $CTDI_w$ /pitch. The $CTDI_{vol}$ is now the preferred radiation dose parameter in CT dosimetry. $CTDI_{vol}$ is commonly used in clinical practice due to its accessibility to the radiologists and CT operators as it specifies the radiation intensity used to perform a specific CT examination and not to quantify how much radiation that each patient receives from the CT examination (Huda et al. 1997).

1.4.2.2. Dose length product

The dose-length product (DLP) is an indicator of the integrated radiation dose of an entire CT examination. The DLP is an approximation of the total energy a patient absorbs from the scan. It incorporates the number of scans and the scan width, e.g. the total scan length, while in contrast $CTDI_w$ and $CTDI_{vol}$ represent the radiation dose of an individual slice or scan. Therefore, DLP increases with an increase in total scan length or variables that affect the $CTDI_w$ (e.g. tube voltage or tube current) or the $CTDI_{vol}$ (e.g. pitch). Because scan length is expressed in centimeters, the SI unit for DLP is mGy·cm. Similar to $CTDI_{vol}$, DLP is also available on the operator's console.

1.4.2.3 Absorbed dose and equivalent dose

Absorbed dose is an amount of energy that is deposited in a unit of mass of matter (tissue). It is measured in gray (Gy) with 1 Gy equal to 1 joule per kilogram. Each type of ionizing radiation produces different biological effect. For instance, biological effect on tissue which is exposed to 1 Gy alpha radiation is more harmful than 1 Gy of x-rays. This is because alpha particles are more heavily charged and slower than x-rays. Therefore, alpha particles lose much more energy along the travel path before reaching the target (Ng 2003). However, the quantity of equivalent dose is used to compare all types of ionizing radiation equally on the biological effect. Equivalent dose is measured in Sievert (Sv). Equivalent dose is obtained by multiplying the absorbed dose with the radiation weighting factor (Table 1-2).

Table 1-2: Radiation weighting factor for various type and energy range (Ng 2003)

Type and energy range	**Radiation weighting factor, W_R (ICRP-60)**
Photons, all energy	1
Electrons, muons, all energy	1
Neutrons <10 keV	5
10 keV-100 keV	10
>100 keV-2MeV	20
>2 MeV – 20 MeV	10
>20 MeV	5
Protons >2 MeV	5
Alpha particles, fission fragments and heavy nuclei	20

1.4.2.4 Dose area product

Dose area product (DAP) is a product of the irradiated surface area multiplied by the radiation dose at the surface (in grays-centimetre square) ($Gy \cdot cm^2$). DAP is a valuable parameter because radiation-induced biological effects are directly related to both the magnitude of the radiation dose and the total amount of tissue that is irradiated. Similar to the DLP in CT unit, DAP can also be measured directly from fluoroscopy and angiography units with a special ionization chamber at the surface of the x-ray tube collimator. Knowledge of DAP and the location and projection of the x-ray beam allows direct calculation of the effective dose (Nickoloff et al. 2008).

1.4.2.5 Effective dose

The most important parameter in CT imaging is the effective dose (ED), which is valuable in assessing and comparing the potential biological risk of a specific examination. ED is a sum of equivalent doses in organs of the body that are considered radiosensitive. It is a uniform whole-body dose that has the same nominal radiation risk of carcinogenesis and induction of genetic effects as any given non-uniform exposure (Huda, Ogden, and Khorasani 2008). Each organ in human body has different radiosensitivity with some organs more sensitive to the risk of damage than the others. ED can be obtained by multiplying each equivalent dose by a relative organ with the tissue weighting factor related to the risk associated with that

organ and summing over all exposed organ. ICRP publication 103 released in 2007 has recommended values for the tissue weighting factors with major changes different from the previously published ICRP publication 60 (International Commission on Radiological Protection 2003; Huda, Magill, and He 2011) (Table 1-3). The SI unit of estimating ED is the sievert (Sv) or millisievert (mSv). The weighting factors used for individual tissues are based on a statistical analysis of the increase in the long-term incidence and mortality for cancer determined from a life span study of the survivors in Japan during the atomic bomb explosion (Martin 2006; Pierce and Preston 2000; Preston et al. 2003). Usually, tabular data of conversion coefficients are available to estimate ED from entrance skin dose for radiography (Rosenstein 1988; Rosenstein, Beck, and Warner 1979), from dose area product (DAP) for fluoroscopy (Hart, Jones, and Wall 1994b; Le Heron 1992), or from $CTDI_{vol}$ or DLP for CT (European Commission 1999). The goal is to convert the higher radiation doses delivered to a small portion of the body into an equivalent uniform dose to the entire body that carries the same biological risk for causing radiation-induced fatal and nonfatal cancers.

Table 1-3: Tissue weighting factor comparison between ICRP publication-103 and publication-60 (Ng 2003)

Organs	**Tissue weighting factor, W_T**	
	ICRP-103	**ICRP-60**
Colon	0.12	0.12
Lung	0.12	0.12
Red bone marrow	0.12	0.12
Stomach	0.12	0.12
Breast	0.12	0.05
Gonads	0.08	0.20
Bladder	0.04	0.05
Liver/ Oesophagus	0.04	0.05
Thyroid	0.04	0.05
Bone surface/skin	0.01	0.01
Brain	0.01	-
Salivary glands	0.01	-
Remainder tissues	0.12*	0.05[#]

*Remainder tissues in ICRP-103: adrenals, kidneys, muscle, small intestine, pancreas, spleen, thymus, uterus/cervix, prostate, extra-thoracic region, gallbladder, heart, lymphatic nodes and oral mucosa; [#]Remainder tissues in ICRP-60: adrenals, kidney, muscle, small intestine, pancreas, spleen, thymus, uterus, upper large intestine and brain.

1.4.2.6 Background equivalent radiation time

Background equivalent radiation time (BERT) is used to explain the dose to the general public without complicated scientific units, terminology or concepts.. It converts the radiation dose to an equivalent period of natural background radiation in days, weeks, months or years to which the entire population is exposed every day from natural radioactive substance in the air, internal, terrestrial, cosmic and environment. For example, it is more likely for patient to easily understand that "your chest x-ray dose is about equal to 3 days of background radiation" rather than "you have received 0.02 mSv for your chest x-ray examination" (Ng 2003). BERT is not used to provide a high level of diagnostic accuracy, but to relieve anxiety about radiation by giving an understandable and satisfactory answer (Table 1-4) (Nickoloff et al. 2008).

1.4.2.7 Entrance skin dose

Entrance skin dose is an amount of energy imparted per gram of tissue at the entrance surface. It is also known as surface absorbed dose (SAD). 1 Gy is equal to 1 millijoule per gram of energy deposited by the x-rays. Entrance skin dose can be obtained by multiplying the radiation exposure measured in the air at the skin by a factor, f for the tissue. The f factor is a quantity of radiation dose exposure conversion measured in the air (coulomb per kilogram at the standard temperature and pressure) to an equivalent radiation dose absorbed in tissue (grays) at the same location. However, entrance skin dose is not an indicator to measure radiation risks except for skin erythema, but it is useful for organ dose calculation especially in a computer-based program that is involved with Monte Carlo simulations (Rosenstein 1988; Rosenstein, Beck, and Warner 1979).

1.4.2.8 Critical organ dose

Critical organ dose (COD) is more commonly reported in the literature for radiologic examinations. Critical organ dose refers to the energy deposited per unit mass to individual critical organs for which the radiosensitivity and radiation dose are high. Its unit of measurement is usually milligrays, which is equivalent to millijoules per kilogram. COD can be used to assess the risks of irradiation beyond cancer induction for certain organs; for example, other potential biological effects can include skin erythema, cataracts, fetal abnormalities, haematologic effects, vascular damage, and effects on the central nervous system.

Table 1-4: Estimated effective doses for diagnostic medical exposures associated with BERT and lifetime fatal cancer risks from National Radiological Protection Board (NRPB) (Ng 2003).

X-ray examination	**Estimated effective dose (mSv)**	**BERT***	**Fatal cancer risk per examination****
Limbs and joints (exclude hip)	<0.01	<1 days	1 in a few millions
Dental (single bitewing)	<0.01	<1.5 days	1 in a few millions
Dental (panoramic)	0.01	1.5 days	1 in 2 million
Chest (single PA)	0.02	3 days	1 in a million
Skull	0.07	11 days	1 in 300,000
Cervical spine	0.08	2 weeks	1 in 200,000
Thoracic spine	0.7	4 months	1 in 30,000
Lumbar spine	1.3	7 months	1 in 15,000
Abdomen	0.7	4 months	1 in 30,000
Hip	0.3	7 weeks	1 in 67,000
Pelvis	0.7	4 months	1 in 30,000
Intravenous urography	2.5	14 months	1 in 8,000
Barium swallow	1.5	8 months	1 in 13,000
Barium meal	3	16 months	1 in 6,700
Barium follow-through	3	16 months	1 in 6,700
Barium enema	7	3.2 years	1 in 3,000
CT head	2	1 year	1 in 10,000
CT chest	8	3.6 years	1 in 2,500
CT abdomen/pelvis	10	4.5 years	1 in 2,000

*Natural background radiation based on Australia average = 2.4 mSv per year; **Appropriate lifetime risk for patients from 16-69 years old: paediatric=2x; geriatric=5x

Critical organ dose may be determined by other dose descriptors, such as entrance skin dose or dose area product, by using tables or software programs that are based on Monte Carlo calculations for standard patient sizes (Rosenstein 1988; Rosenstein, Beck, and Warner 1979). Also, the critical organ dose values for various organs, along with their corresponding weighting factors, can be used to calculate the effective dose (National Council on Radiation Protection and Measurements 1995; International Commission on Radiological Protection 2003). In clinical practice, knowledge of organ doses and the carcinogenic sensitivity of certain organs can lead to better collimation and patient positioning to reduce the risks from exposure to radiation.

1.4.2.9 Diagnostic acceptable reference level

Diagnostic acceptable reference level is also known as diagnostic reference level (DRL). DRL values are published based on the nationwide evaluation of x-ray trends surveys (Gray et al. 2005; Nickoloff et al. 2008). The data values can be used as a reference point to ensure that all current clinical practice involving radiation in radiological investigations are safe. However, ESD, DAP, or $CTDI_{vol}$ values that are greater than those of DRL may be attributed to the patient's size, the complexity of the clinical case, equipment malfunctions, or suboptimal protocols. Some of the higher values may be unavoidable; however, many of the higher values can be avoided. When patient doses appear to be above those of DRL, especially when they are consistently higher, investigation and assessment are required. If suboptimal protocols or equipment deficiencies are the cause of the higher dose levels, the strategies must be undertaken to reduce the radiation dose.

1.4.2.10 Radiation dosimeter

Radiation dose in clinical practice can be measured accurately by using a dosimeter. There are a plenty of dose measurements tools with different methods being used to measure the radiation dose absorption. The value of absorbed dose is determined indirectly by measuring the radiation effect through ionization of air, fogging of photographic emulsion, thermoluminescence, scintillation and ionization of a semiconductor. However, the most popular method in radiation dosimetry is thermoluminescence dosimeter (TLD) (Ball, Moore, and Turner 2008).

1.4.2.11 Thermoluminescence phenomenon

Thermoluminescence is a condition where the light is emitted from a heated crystalline material which is made up of lithium fluoride (LiF) or calcium fluoride (CaF_2) phosphors. When the crystalline is exposed to the radiation, electrons in the crystal are pulled out from

valence band to the conduction band by a small amount of energy. However, without enough energy, some of the electrons are trapped into one of the isolated levels provided by impurities in the crystal. It will remain immobilized at that state until energy is supplied to release it (usually by heat). Thus, the electrons leave a positive hole in the valance band. By heating the crystal, the trapped electrons will elevate and return to the valence positive hole. A photon of visible light is emitted during the process of returning electrons from the trap to the valence band (Figure 1-4) (Martin 2006). The total light emitted is counted where the measurement for the number of trapped electron indicates the absorbed radiation. Surprisingly, it can be used even after a month of storage.

Figure 1-4: The process of light emission from the radiation exposure in the thermoluminescence phenomenon

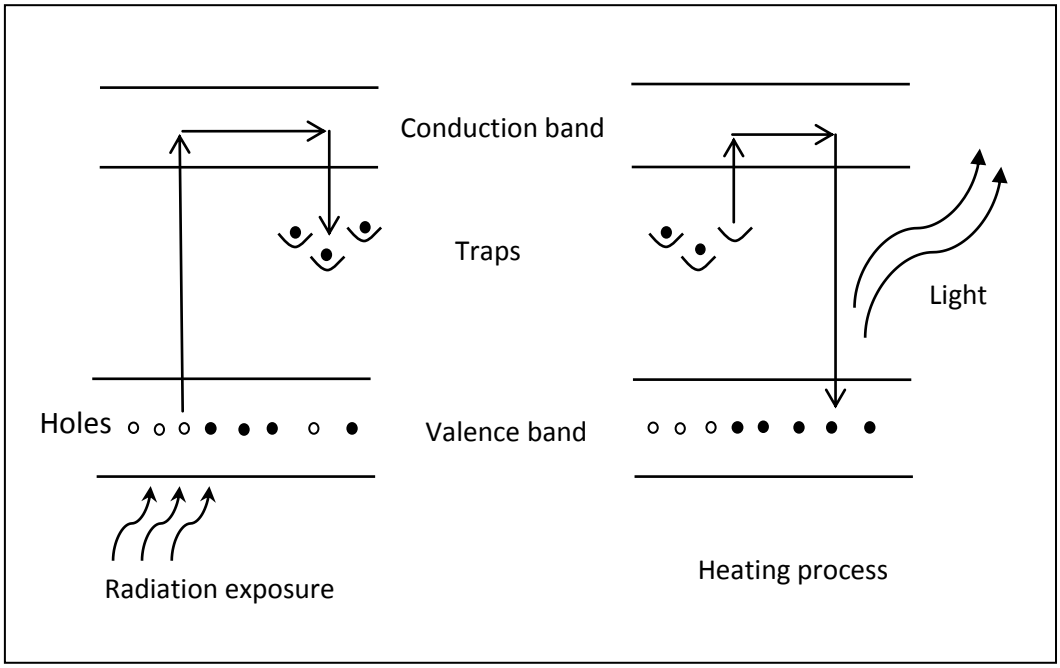

Several types of thermoluminescence dosimeters (TLD) are commercially available for a wide range of applications. For instance, LiF: Mg, $Li_2B_4O_7$, $CaSO_4$: Dy, Al_2O_3, CaF_2: Dy and CaF_2: Mn (Maia and Caldas 2010; Miljanie, Vekie, and Martinieie 1999). In diagnostic radiology, LiF: Mg, Ti or usually known as TLD-100 was chosen for dosimetry purposes in clinical radiation measurement. In fact, it was the first material used in diagnostic radiology and one of the most utilised materials when compared to others (Berni et al. 2002). TLD with LiF: Mg, Ti material is chosen because of the physical shape which is small, light and convenient for local measurement during the radiological examinations. Apart from physical appearance, it is able to measure entrance surface absorbed dose at the reference point at

specific organs without obscuring an image due to the radiolucency specification (Maia and Caldas 2010). Moreover, it has high reproductive capability, thus it can be used repeatedly. The materials are sensitive to detect radiation exposure in a range between 10 μGy and 10 Gy, in addition to having a good linear relationship between thermoluminescence readout value and dose absorption up to 1mrad.

1.4.2.12 CT dose measurement

Effective dose in CT can be easily estimated by a simple calculation through multiplying the DLP with a conversion coefficient factor (E/DLP). Huda, Ogden, and Khorasani (2008) in their study introduced a new approach to determine the ED. They suggested that ED can be calculated from DLP by using ImPACT software package which is based on Monte Carlo simulation performed by the National Radiological Protection Board (1998). Yet, the accuracy of this system is undisputable when Huda, Ogden, and Khorasani (2008) compared those ED calculations with other software packages like CT-expo and ImpactDose. As a result, there were approximately 5% differences between ED/DLP values according to each software package and it was not statistically significant (Huda, Ogden, and Khorasani 2008). CT-Expo is a program run on Monte Carlo dosimetry data while ImpactDose is a personal computer based-program that calculates ED values for arbitrary scanning parameters and anatomic ranges. However, the ED values still can be calculated manually by multiplying the DLP values with the conversion coefficient factor in CT imaging based on individual organs and tissue weighting factors published by the ICRP 103 (Hart, Jones, and Wall 1994a; Huda, Magill, and He 2011; Kalender et al. 1999). Similarly, ED associated with invasive angiography can be estimated by multiplying the DAP values with a conversion coefficient factor (E/DAP).

1.5 Dose reduction strategies in coronary CT angiography

Previous studies have reported that CCTA with use of retrospective ECG-gated technique results in very high radiation dose, which ranged from 13.4 mSv to 31.4 mSv (d'Agostino et al. 2006; Johnson et al. 2006; Poll et al. 2002). This has raised serious concerns in the literature due to the potential risk of radiation-induced malignancy resulting from CCTA. several dose-saving strategies have been introduced to deal with radiation dose issues, and these techniques include anatomy-based tube current modulation (Jung et al. 2003; Starck et al. 2002), ECG-controlled tube current modulation (Abada et al. 2006; Sigal-Cinqualbre et al. 2004; Wintersperger et al. 2005), tube voltage reduction (Geleijns et al. 2006; Hohl et al. 2006), a high-pitch scanning (Achenbach et al. 2010; Achenbach et al. 2009; Coles et al. 2006) and prospective ECG-triggered CCTA (Paul and Abada 2007).

1.5.1 Anatomy-based tube current modulation

Tube current is an important element that is directly related to radiation dose and image quality. With rapid developments of CT technology, implementation of automatic tube current modulation allows significant reduction in radiation dose for CT examinations. In CT examination, automatic tube current modulation can be defined as a series of techniques that enable automatic adjustment of the tube current in x-, y-plane (angular modulation) or z-plane (z-axis modulation), according to the size and attenuation characteristics of the human body. The purpose of these adjustments is to achieve optimum image quality with low radiation dose. The term automatic tube current modulation is similar to automatic exposure-control that is commonly used in conventional radiography (Deetjen et al. 2007; Kalra et al. 2004).

1.5.1.1 Angular modulation (x-y plane)

Since the shape of patients body is not symmetrical (anteroposterior versus lateral), angular-modulation techniques automatically adjust the tube current for each projection angle to the appropriate attenuation according to patient's anatomical structures. Without angular modulation, the tube current is held constant over the 360° rotation, regardless of the patient attenuation profile. The angular-modulation technique reduces tube current as a function of projection angles for low-attenuation projections (anteroposterior versus lateral projections). This technique calculates the modulation function (an objective image quality parameter) from the online attenuation profile of the patient. The modulation function data are processed and sent to the generator control for tube current modulation with a delay of 180° from the x-ray generation angle. In asymmetrical regions being scanned such as the shoulders in chest

CT, the x-ray attenuation is substantially less in the anteroposterior than in the lateral direction. This radiation dose reduction could be achieved up to 90% with application of the angular-modulation technique (Greess et al. 2002). Therefore, the technique of angular modulation helps in improving dose efficiency in the x- and y-axis by reducing radiation exposure in a particular scanning plane.

1.5.1.2 Z-Axis Modulation

The principle of z-axis–modulation technique is different from that of angular modulation (Westerman 2002). Unlike angular modulation, the z-axis modulation technique adjusts the tube current automatically to maintain a user-specified quantum noise level in the image data. It provides a noise index to allow users to select the amount of x-ray noise that will be present in the reconstructed images. Using a localizer radiograph, the scanner computes the tube current required obtaining images with a selected noise level. Hence, z-axis modulation attempts to make all images have a similar noise irrespective of patient size and anatomy. The noise index value is approximately equal to the image noise (standard deviation) in the central region of an image of a uniform phantom. However, the actual noise measured on the image by drawing a region of interest that will differ from the noise index selected for scanning. This is due to the fact that noise index settings only adjust the tube current, whereas the standard deviation is also affected by other parameters, including the reconstruction algorithm, the reconstructed section thickness (if different from the prospective thickness), the use of image space filters, variations in patient anatomy and patient motion, and the presence of beam-hardening artefacts.

A lower minimum tube current may result in reduced exposure to patients, which occasionally increases image noise in smaller patients scanned with a substantially reduced tube current. Generally, larger patients receive higher tube current with z-axis modulation if a fixed-tube-current technique used in order to maintain the selected image noise. In contrast, with automatic tube current modulation, the tube current is inconsistent throughout the scan and thus results in the diagnostic image quality with reduced radiation dose. The main limitation of automatic tube current modulation is the lack of uniformity between techniques developed by different vendors.

The CARE Dose 4D protocol (Siemens, Medical Solutions, Erlangen, Germany) was then introduced in order to adapt the tube current to the patient's individual anatomy and modulate the tube current in the section with the lowest dose levels. Previous studies have shown that 20%–60% dose reduction was achieved, depending on the anatomic region and patient habitus, with improved image quality (Suess and Chen 2002). Another study

combining angular and z-axis modulation (3D Auto mA; GE Yokogowa Medical Systems, Tokyo, Japan) reported significant dose reductions (60%) in abdominal-pelvic CT examinations (Horiuchi 2002). This technique uses a single localizer radiograph to determine patient asymmetry and appropriate angular and z-axis modulation for the patient. The investigators added noise (computer modification of original raw scan data to simulate lower tube current noise levels) to patients' scan data to produce images and calculate the radiation dose reduction.

1.5.2 ECG-controlled tube current modulation

The idea of decreasing radiation doses associated with tube current modulation in CT stimulated manufacturers to improve the CCTA examinations. One of the most recently developed methods, CARE dose 4D by Siemens Medical Solutions), combining the effects of angular and *z*-axis modulation techniques was introduced (Schwartzman, Lacomis, and Wigginton 2003). Virtually all anatomic regions in the thorax, abdomen, and pelvis have benefited from these sophisticated techniques that result in considerable dose reduction (Abada et al. 2006; Hausleiter et al. 2006).

However, the z-axis modulation of CARE dose 4D was not compatible with ECG pulsing. ECG-pulsed tube current modulation is the most significant improvement in minimizing radiation from CT technology and is the only one dedicated to cardiac imaging. ECG pulsing is performed online during cardiac CT examination and allows a decrease in radiation exposure of between 30% and 50% by modulation of tube current output to decrease the dose given during systolic phase (Leber et al. 2005). Therefore, the algorithm for ECG-dependent dose modulation represents a very effective tool for limiting radiation dose in the vast majority of patients undergoing cardiac CT studies.

In ECG-controlled tube current modulation technique, a high tube current with optimal image quality is applied only during the diastolic phase of the cardiac cycle, in which images are most likely to be reconstructed with minimal artefacts, while in the systolic phase, a low tube current (50% of normal tube current) is applied. Image reconstruction during cardiac CT examinations is usually performed in ventricular mid-diastole due to less cardiac motion that caused blurring of cardiac structures. Thus, diagnostic images with high quality are acquired during the diastolic phase (Earls et al. 2008). However, this method totally depends on the patient's heart rate and requires a regular sinus rhythm in order to prevent poor image quality. Unfortunately, the ECG-controlled tube current modulation algorithm is not working in the presence of arrhythmias such as premature extra beats. Thus, this algorithm may not be useful in patients with arrhythmias.

1.5.3 Low tube voltage

Since radiation dose varies with the square of the tube voltage, an application of lower tube voltage during CT data acquisition is another approach for radiation dose reduction. A previous study by Huda et al. (2000) showed that reducing the X-ray tube potential from 140 to 80 kVp at constant tube current decreased the radiation dose by a factor of about 3.4. Image contrast and image noise will increase because there are fewer photons produced (Huda 2002; Huda, Scalzetti, and Levin 2000; Nickoloff and Alderson 2001; Siegel et al. 2004). However, since the contrast-to-noise ratio (CNR) and signal-to-noise ratio (SNR) are the key factor of CT image quality, noise is rather irrelevant if the level of contrast or amount of signals are too high (Huda 2002). The change in image contrast is dependent on the anatomic number (Z) of the structures being investigated. The image structure with high-anatomic-number becomes significantly more prominent than image of low-anatomic-number structures (soft tissue) in the application of low tube voltages (Huda, Scalzetti, and Levin 2000).

It has been confirmed that diagnostic image quality was not affected by lower tube voltages in paediatric CT investigations. Similarly, in a phantom study, Siegel et al. (2004) showed that reduced beam energy in contrast-enhanced paediatric CT decreased radiation dose without affecting image contrast and image noise (Siegel et al. 2004). The interrelationship between beam energy and tube output in terms of image noise has been described by Boone et al. (2003), who characterized image noise for CT techniques using tube voltages of 80–140 kVp and tube currents of 10–300 mA (Boone et al. 2003). Provided the tube current–time product was appropriately adapted, radiation dose was significantly reduced at lower tube voltage while CNR remained at a constant level. Cody et al. (2004) reported that the use of 80-kVp tube voltage resulted in beam-hardening artefacts and thus recommended the use of 100- to 120-kVp settings in paediatric patients. For non-cardiac CT studies with kilovoltage reduction, an increase of the tube current by 50% has been proposed to maintain image quality and to reduce the dose estimates at the same time (Cody et al. 2004). However, a further increase in tube current is limited with the available standard protocols for cardiac CT scanning on the studied CT scanners. Therefore, a trade-off between dose saving and increased image noise has to be considered with current cardiac CT protocols.

A previous study compared the diagnostic quality of the coronary artery segments between good and poor quality in order to detect stenosis in various scan protocols (Herzog et al. 2008). In this qualitative analysis of image quality, no deterioration of diagnostic image quality was detected for scan protocols with the ECG-dose modulation and the 100-kV protocols using 16- and 64-slice CT. The value of this analysis is limited by a potential

selection bias of used scanning protocols. Image obtained with 120-kV scan protocol without ECG modulation (on patients with arrhythmia) are likely to present with more non-diagnostic coronary segments, even when no dose-saving algorithms were applied. However, the impact of dose-saving algorithms on the detection of calcified and non-calcified plaques remains unknown. Therefore, further studies are needed to investigate the balance between dose savings and maintained diagnostic image quality for CCTA investigations.

1.5.4 High pitch value

With the recent advent of second-generation of dual-source, another low-dose technique has been introduced for cardiac CT which is high-pitch scanning mode (Ertel et al. 2009). This technique was successfully tested with dual-source 128-slice CT. In this technique, the data are acquired in a spiral mode while the X-ray table runs with a very high pitch of 3.4 equalling to a table feed of 46 cm/s. When this high-pitch mode is used, the entire heart is scanned within one single cardiac cycle, generally during the diastolic phase (75% R-R interval). The temporal resolution for this system is 75 ms, owing to the gantry rotation time of 280 ms and with regard to quarter rotations for data reconstruction. Early reports on phantom studies have shown that the purpose of this scan mode is to deliver images of diagnostic quality at a low radiation dose. Moreover, two studies have successfully proved that feasibility of this high-pitch mode technique also in patients by using the remodelled first generation, dual-source 64-slice CT scanners with effective dose less than 1 mSv (Achenbach et al. 2009; Hausleiter et al. 2009). Then, several recent studies have reported similar results (Goetti et al. 2010; Lell, Hinkmann, et al. 2009; Lell, Marwan, et al. 2009; Sommer et al. 2010). In addition to low dose aspect, high diagnostic accuracy has been achieved with the high-pitch dual-source CT (Leschka et al. 2009).

In order to apply the high-pitch mode, several requirements must be fulfilled. Firstly, dual-source geometry is necessary in order to obtain the projection data by the second detector for gaps fill-up due to the fast table movement. In this way, the pitch can be increased up to 3.4 while still allowing image reconstruction, although the limited field of view is covered by both detectors. A quarter rotation of data per measurement is used for image reconstruction, and each of the individual axial images has a temporal resolution of a quarter of the rotation time $t_{rot}/4$. At the same time, because of the high pitch, overlapping radiation exposure is avoided, thus reducing the radiation dose to the patient to the minimum level (Alkadhi et al. 2010).

Secondly, a higher temporal resolution is essential to enable single cardiac cycle reconstruction without image distortion due to motion artefacts. Thirdly, patient's heart rate

must be regular and consistent in order to obtain a good image quality. With used of high pitch mode, the examination table is accelerated to the maximum speed during data acquisition which is triggered by the R-peak of the heartbeat. The examination table could not be accelerated in an infinitely small time period; therefore, it has to be set in motion sufficiently earlier prior to scanning acquisition. Inconstant heart rates lead to inaccurate positioning of the data acquisition window, with data being acquired either too early in the (if heart rate decreases) or too late (if heart rate increases) cardiac cycle. Inconsistent heart rates would compromise image quality by stair-step artefacts.

Finally, high pitch mode requires patient with low heart rates (<65 bpm) in order to obtain a motion-free artefact which allowed the acquisition during a single diastolic period (Alkadhi et al. 2010). In patients with high heart rates, a narrow diastolic exposure of R-R interval window may not yield diagnostic image quality of the coronary arteries and therefore, tube current modulation is required for adjustment accordingly (Goetti et al. 2010).

1.5.5 Prospectively ECG-triggered coronary CT angiography

Various strategies have been developed to reduce radiation exposure of patients, and the most important one is prospectively ECG-gated CT coronary angiography, also called step-and-shoot mode. The step-and-shoot mode is characterised by turning on the x-ray tube only at a predefined time point of the cardiac cycle, usually in mid-diastole, while keeping the patient table stationary. The x-ray exposure time of this technique is short, and thus, low radiation doses ranging between 1.2 and 4.3 mSv have been reported using various 64-slice and first-generation, dual-source 64-slice CT (Herzog et al. 2008; Klass et al. 2009; Shuman et al. 2008). Most importantly, this low-dose step-and-shoot method is still able to produce high diagnostic accuracy for the detection of coronary stenosis (Herzog et al. 2008; Scheffel et al. 2008).

Unlike standard retrospective ECG-gating, where the tube output (in mA) is constant throughout the data acquisition during spiral CT which results in high radiation dose, prospective triggering is performed with sequential scans. In prospective triggering, the tube current is turned off for most of the scan period and is triggered by the electrocardiogram to be ‘on’ only for a short period during diastole. Thus, this results in remarkable reduction in radiation dose (Earls 2009). With application of prospective ECG triggering, the radiation dose of CCTA can be reduced by up to 83% when compared to retrospective ECG gating technique (Earls 2009; Lu et al. 2011; Sabarudin, Sun, and Ng 2012; Shuman et al. 2008; Sun et al. 2008; Sun and Ng 2012).

1.5.6 Iterative reconstruction methods

Alternative image reconstruction techniques such as iterative reconstruction have been used mainly in nuclear medicine studies (Knesaurek et al. 1996; Liow et al. 1997). In CCTA, iterative reconstruction (Adaptive Statistical Iterative Reconstruction (ASIR), GE Healthcare) has been introduced as a new reconstruction algorithm (Cheng, Fang, and Tyan 2006; Hara et al. 2009; Liu et al. 2007; Nuyts et al. 1998). Iterative reconstruction is a method to reconstruct 2D and 3D images from measured projections on an object. However, unlike filtered back projection, iterative reconstruction starts with an initial estimate of the object which is subsequently improved in a stepwise fashion by comparing the synthesized image to the one acquired with projection data and improving the previous estimate.

Moreover, iterative reconstruction reduces image noise by iteratively comparing the acquired image to a modeled projection. This reconstruction algorithm is used to help deal with one of the primary issues of dose and tube current reduction for CCTA. Since iterative reconstruction has been consistently associated with image quality improvement, especially improving CNR, it has the possibility of improving spatial resolution (Leipsic et al. 2010; Thibault et al. 2007). With faster computer technologies and adapted techniques, the use of iterative reconstruction for cardiac CT imaging has been increasingly studied and the reconstruction speed now allows its use in clinical practice. Although iterative reconstruction has been shown to reduce noise and improve image quality, enabling reduction in radiation dose in body CT (Nuyts et al. 1998), it has not been systematically studied in CCTA. However, the main limitation to its routine use is the high computational cost, which can be 100–1,000 times higher than for filtered back projection (Wang, Yu, and De Man 2008).

Moreover, iterative reconstruction does not assume that the measured signal is free of noise due to x-ray photon statistics or electronic noise but rather uses more accurate statistical modeling during the reconstruction process (Cheng, Fang, and Tyan 2006). This enables improved noise properties in the reconstructed images, while maintaining spatial resolution and other image quality parameters. The use of iterative reconstruction techniques is expected to increase in CT as computational processing improves and algorithms become more robust and easy to apply. Because more powerful iterative reconstruction algorithms are emerging, the impact of these techniques may show greater noise reduction and thereby permit further reductions in radiation exposure to patients.

1.6 Thesis outline

This research was designed to investigate and compare the radiation dose between retrospective and prospective axial gating in coronary CT angiography. Although some modified parameters were introduced in this research project, the image quality needs to be monitored in order to achieve the acceptable diagnostic quality. The objectives for this research were detailed as follows:

- To seek the satisfaction from the medical imaging specialists and the acceptable diagnostic images in coronary CT angiographic procedures.
- To measure and compare the radiation dose between retrospective and prospective gating in coronary CT angiographic procedures.
- To compare the image quality in both prospective and retrospective ECG-gating coronary CT angiography procedures with aim of determining the clinical feasibility of prospective gating procedure.

The literature review in this chapter has explained the radiation dose arising from a standard CCTA protocol in addition to the implication on the image quality. This thesis contains six papers which are presented from chapter 2 to 7. An overview of all articles is presented in this section which consists of the relevance and the interconnection to the topic. Moreover, all publications included in this study have answered all the issues raised regarding the radiation concern and image quality with an introduction of dose saving protocol of CCTA, namely prospective ECG-triggering CCTA. Basically, the papers cover two main important aspects: radiation dose and image quality associated with CCTA. All aspects are tested with different imaging modalities, protocols and techniques. The overall aim of the thesis is to introduce a latest dose-saving technique in CCTA, namely, prospective ECG triggering. This technique was compared to the standard routine CCTA (retrospective ECG gating) and invasive coronary angiography in terms of radiation dose and image quality.

Paper 1

A systematic review of radiation dose associated with different generations of multidetector CT coronary angiography. *Journal of Medical Imaging and Radiation Oncology* 56 (1): 5-17.

This paper has been published in the Journal of Medical Imaging and Radiation Oncology. Since there were a lot of radiation research ongoing especially associated with CCTA, a meta-analysis on radiation dose was carried out in this paper. The radiation dose results were analysed systematically based on 66 studies published between 1998 and 2011 using

different generations of MSCT scanners ranging from 4-slice to 320-slice CT with use of different dose-saving techniques.

More dose-saving strategies were applied in recent CT generations including prospective ECG-triggered protocols, applications of lower tube voltage and tube current modulation to achieve a significant dose reduction. Prospective ECG triggered protocol was increasingly used in 64-, 125-, 256- and 320-slices with significantly lower radiation dose than that in retrospective ECG-gating technique. This analysis has also shown that dose-saving strategies can substantially reduce the radiation dose in CCTA. The fact that more and more clinicians are opting for dose-saving strategies in CCTA indicates an increased awareness of risks associated with high radiation doses amongst them.

Paper 2

Radiation dose associated with coronary CT angiography and invasive coronary angiography: An experimental study of the effect of dose-saving strategies. *Radiation Protection Dosimetry* 150 (2): 180-187.

This paper has been published in the prestigious journal on radiation dose issue, Radiation Protection Dosimetry. In this paper, a pilot study was conducted on an anthropomorphic human phantom to investigate the effective dose and entrance skin dose in selected radiosensitive organs through invasive and CCTA procedures using different dose-saving techniques. The new protocol in CT angiography, namely prospective ECG triggering was compared with the standard CT protocol for CCTA and the 'gold standard' invasive conventional angiography (ICA). This comparative study was performed to investigate the radiation dose by using different protocols in both CT and ICA. In CCTA, three different protocols were used including prospective ECG triggering, retrospective ECG-gating with and without tube current modulation. On the other hand, invasive coronary angiography was performed with four different magnifications. In this study, the entrance skin dose was measured at the breast and thyroid gland during the procedures. Although ICA produces lower radiation dose than CCTA, application of modified techniques in both CT and invasive coronary angiography is recommended in clinical practice for further reduction in radiation dose.

Paper 3

Coronary CT angiography with prospective ECG-triggering: A systematic review of image quality and radiation dose. *Singapore Medical Journal* 54 (1):15-23

This paper was accepted for publication in the Singapore Medical Journal on June 24, 2012. A systematic review on diagnostic accuracy, image quality and radiation dose of prospective

ECG-triggered CCTA was presented in this paper. The review was performed based on different databases containing 23 studies of CCTA that used prospective ECG triggering associated with diagnostic accuracy, image quality and radiation dose between 2008 and 2011. The effective dose and image quality reported in each study were analysed and compared between the types of multislice CT scanners and scanning protocols. In addition, a formal consensus method, QUADAS (Quality assessment of diagnostic accuracy) for quality assessment of diagnostic accuracy of prospective ECG triggered protocol in the detection of coronary artery disease was also introduced. QUADAS was performed in order to develop and evaluate an evidence based quality of individual studies in terms of potential for bias, lack of applicability and quality of reporting.

Paper 4

Radiation dose in coronary CT angiography associated with prospective ECG-triggering technique: comparisons with different CT generations. *Radiation Protection Dosimetry (Epub ahead of print)* doi:10.1093/rpd/ncs243

This paper was accepted for publication in the journal of Radiation Protection Dosimetry on 21st of August, 2012 and the corrected proof is available online now. In this paper, a retrospective analysis was performed in patients undergoing prospectively ECG-triggered CCTA with single-source 64-slice CT (SSCT), dual-source 64-slice CT (DSCT), dual-source 128-slice CT and 320-slice CT with the aim of comparing radiation dose associated with different CT generations. Several imaging technical parameters were also compared in order to investigate the radiation dose produced during the clinical setting. A total of 164 patients undergoing prospective ECG-triggered CCTA with different types of CT scanners were studied with the mean effective dose estimated 6.8 ± 3.2 mSv, 4.2 ± 1.9 mSv, 4.1 ± 0.6 mSv, and 3.8 ± 1.4 mSv, corresponding to 128-slice DSCT, 64-slice DSCT, 64-slice SSCT and 320-slice CT scanners. A positive relationship was found between effective dose and body mass index (BMI) in this study. Moreover, low radiation dose is achieved in prospective ECG-triggered CCTA, regardless of any CT scanner generation. BMI is identified as the major factor that has a direct impact on the effective dose associated with prospective ECG-triggered CCTA.

Paper 5

A survey study exploring local specialists and radiographers' perceptions of the benefits and challenges in relation to prospective ECG-triggered coronary CT angiography, submitted to *Journal of Medical Imaging and Health Informatics (In press)*

This manuscript was submitted to Asia-Pacific Journal of Public Health and is currently under review. This paper involved investigating and exploring the opinion concerning the benefits and difficulties in performing prospective ECG-triggered CCTA practice in Malaysia among specialists and radiographers. In addition, this study was also conducted in order to determine the levels of preference and the effects of an individual's experience with regard to prospective ECG- triggered CCTA. In this paper, a questionnaire form designed to meet the needs of each respondent group was distributed to 6 national health institutions in Malaysia in which, prospectively ECG-triggered CCTA was performed as a routine cardiac imaging procedure. Respondents were asked to assess their levels of agreement on the benefits and challenges in prospective ECG-triggered CCTA.

Results showed that in total, 53 responses (85%) were received, comprising specialists (21%) and radiographers (79%). Across all the respondents, the main aim of the benefits of prospective ECG-triggered CCTA was considered as: radiation dose reduction, image quality improvement and patients' output increase. Low agreement was achieved on the issue of an increase in the financial incentives to institutions because of prospective ECG-triggered procedures. The issue of heart rate was found to be the main challenge when performing CCTA and this was agreed to by the respondents. However, the remaining challenges listed have been seen to vary according to the groups of respondents and the scanner type.

Paper 6

Coronary CT angiography with single-source and dual-source CT: Comparison of image quality and radiation dose between prospective ECG-triggering and retrospective ECG-gating protocols, *International Journal of Cardiology (Epub ahead of print)*

This paper was accepted for publication in the prestigious cardiology journal, International Journal of Cardiology on September 29, 2012. This prospective study represented the main part of this thesis and it was conducted to investigate and compare image quality and radiation dose between retrospective gating and prospectively ECG-triggered CCTA with use of single-source CT (SSCT) and dual-source CT (DSCT). Different from previous publications, this paper used the latest published conversion coefficient factor (0.026 $mSv \cdot mGy^{-1} \cdot cm^{-1}$) for effective dose calculations. In this study, the image quality was obtained qualitatively assessed by two experienced observers and quantitatively performed by measuring the image noise, SNR and the CNR). Images were obtained from a total of 209 patients who underwent CCTA with suspected CAD scanned with SSCT (n=95) and DSCT (n=114) with prospective ECG triggered and retrospective ECG-gated protocols at two different institutions. Results showed that 793 segments reported missing from a total of 2,880 coronary artery segments was being evaluated. Thus, 2,087 coronary segments were

assessable, with 98.0% classified as of sufficient and 2.0% as of insufficient image quality for clinical diagnosis. DSCT resulted in poor image quality as compared to SSCT for both protocols. However, there was no significant difference in overall image quality between prospective and retrospective gated protocol, regardless of DSCT or SSCT scanners. Prospective ECG triggered protocol was compared in terms of radiation dose calculation between DSCT (6.5 ± 2.9 mSv) and SSCT (6.2 ± 1.0 mSv) scanners and no significant difference was noted (p=0.99). However, the effective dose was significantly lower with DSCT (18.2 ± 8.3 mSv) than with SSCT (28.3 ± 7.0 mSv) in the retrospective gated protocol. Prospective ECG-triggered CCTA reduces radiation dose significantly compared to retrospective ECG-gated CCTA, while maintaining good image quality. CCTA with the use of DSCT resulted in better image quality as compared to SSCT.

In summary, an in-depth analysis of CCTA with regard to the prospectively ECG-triggered and retrospectively ECG-gated protocols was performed in this thesis consisting of these six papers. In addition the diagnostic performance of CCTA was also compared with the 'gold standard' technique, invasive coronary angiography. Clinical value of prospectively ECG-triggered CCTA with regard to dose reduction and image quality based on different generation of multislice CT scanners has been thoroughly investigated in this project, thus, achieving the goal of judiciously utilising this fast growing technique in clinical practice.

1.7 References

Abada, H. T., C. Larchez, B. Daoud, A. Sigal-Cinqualbre, and J. F. Paul. 2006. MDCT of the coronary arteries: feasibility of low-dose CT with ECG-pulsed tube current modulation to reduce radiation dose. *Am J Roentgenol* 186: S387-S390.

Abrams, H. L., and D. F. Adams. 1975. The complications of coronary angiography. *Circulation* 52 (Suppl 2): 27.

Achenbach, S., M. Marwan, D. Ropers, T. Schepis, T. Pflederer, and K. Anders. 2010. Coronary computed tomography angiography with a consistent dose below 1mSv using prospectively electrocardiogram-triggered high-pitch spiral acquisition. *Eur Heart J* 31: 340-346.

Achenbach, S., M. Marwan, T. Schepis, T. Pflederer, H. Bruder, T. Allmendinger, M. Petersilka, K. Anders, M. Lell, A. Kuettner, D. Ropers, W. Daniel, and T. Flohr. 2009. High-pitch spiral acquisition: a new scan mode for coronary CT angiography. *J Cardiovasc Comput Tomogr* 3: 117-121.

Achenbach, S., D. Ropers, U. Hoffmann, B. MacNeill, U. Baum, K. Pohle, T. J. Brady, E. Pomerantsev, J. Ludwig, F. A. Flachskampf, S. Wicky, I. K. Jang, and W. G. Daniel. 2004. Assessment of coronary remodeling in stenotic and nonstenotic coronary atherosclerotic lesions by multidetector spiral computed tomography. *J Am Coll Cardiol* 43: 842-847.

Achenbach, S., D. Ropers, A. Kuettner, T. Flohr, B. Ohnesorge, H. Bruder, H. Theessen, M. Karakaya, W. G. Daniel, W. Bautz, W. A. Kalender, and K. Anders. 2006. Contrast-enhanced coronary artery visualization by dual-source computed tomography-Initial experience. *Eur J Radiol* 57: 331-335.

Achenbach, S., D. Ropers, F. K. Pohle, D. Raaz, J. von Erffa, A. Yilmaz, G. Muschiol, and W. G. Daniel. 2005. Detection of coronary artery stenoses using multi-detector CT with 16 x 0.75 collimation and 375 ms rotation. *Eur Heart J* 26: 1978-1986.

Al Moudi, M., Z. Sun, and N. Lenzo. 2011. Diagnostic value of SPECT, PET and PET/CT in the diagnosis of coronary artery disease: A systematic review. *Biomed Imaging Interv J* 7 (2): e9.

Alkadhi, H., P. Stolzmann, L. Desbiolles, S. Baumueller, R. Goetti, and A. Plass. 2010. Low-dose, 128-slice, dual-source CT coronary angiography: accuracy and radiation dose of the high-pitch and the step-and-shoot mode. *Heart* 96: 933-938.

Angelini, P., J. A. Velasco, and S. Flamm. 2002. Coronary anomalies: incidence, pathophysiology, and clinical relevance. *Circulation* 105: 2449-2454.

Arbab-Zadeh, A., J. Texter, K. M. Ostbye, K. Kitagawa, J. Brinker, R. T. George, J. M. Miller, J. C. Trost, R. A. Lange, J. A. Lima, and A. C. Lardo. 2010. Quantification of lumen stenoses with known dimensions by conventional angiography and computed tomography: implications of using conventional angiography as gold standard. *Heart* 96 (17): 1358-1363.

Ball, J., A. D. Moore, and S. Turner. 2008. *Essential physics for radiographers*. 4th ed. West Sussex: Blackwell Publishing.

Barrett, J., and N. Keat. 2004. Artifacts in CT: recognition and avoidance. *RadioGraphics* 24: 1679-1691.

Bax, J. J., E. E. Van der Wall, and A. De Roos. 2005. *Clinical nuclear cardiology*. Edited by B. l. Zaret and G. A. Beller, *State of the art and future directions*. Philadelphia: Mosby.

Berni, D., C. Gori, B. Lazzari, S. Mazzocchi, F. Rossi, and G. Zatelli. 2002. Use of TLD in evaluating diagnostic reference levels for some radiological examinations. *Radiat Prot Dosim* 101 (1-4): 411-413.

Bi, X., V. Deshpande, O. Simonetti, G. Laub, and D. Li. 2005. Three-dimensional breathhold SSFP coronary MRA: a comparison between 1.5T and 3.0T. *J Magn Reson Imaging* 22 (2): 206-212.

Bogaert, E., K. Bacher, K. Lemmens, M. Carlier, W. Desmet, X. D. Wagter, D. Djian, C. Hanet, G. Heyndrickx, V. Legrand, Y. Taeymans, and H. Thierens. 2009. A large-scale multicentre study of patient skin doses in interventional cardiology: dose-area product action levels and dose reference levels. *Br J Radiol* 82: 303-312.

Boone, J., E. M. Geraghty, J. Seibert, and S. Wootton-Gorges. 2003. Dose reduction in pediatric CT: a rational approach. *Radiology* 228: 352-360.

Botnar, R. M., M. Stuber, P. G. Danias, K. V. Kissinger, and W. J. Manning. 1999. A fast 3D approach for coronary MRA. *J Magn Reson Imaging* 10 (5): 821-825.

Brenner, D. J., C. D. Elliston, E. J. Hall, and W. E. Berdon. 2001. Estimated risks of radiation-induced fatal cancer from pediatric CT. *Am J Roentgenol* 176: 289-296.

Brenner, D. J., and E. J. Hall. 2007. Computed tomography: an increasing source of radiation exposure. *N Engl J Med* 357 (22): 2277-2284.

Broadhead, D. A., C. L. Chapple, K. Faulkner, M. L. Davies, and H. McCallum. 1997. The impact of cardiology on the collective effective dose in the North of England. *Br J Radiol* 70: 492-497.

Budoff, M. J., D. Dowe, J. G. Jollis, M. Gitter, J. Sutherland, E. Halamert, M. Scherer, R. Bellinger, A. Martin, R. Benton, A. Delago, and J. K. Min. 2008. Diagnostic performance of 64-multidetector row coronary computed tomographic angiography for evaluation of coronary artery stenosis in individuals without known coronary artery disease: results from the prospective multicenter ACCURACY (Assessment by Coronary Computed Tomographic Angiography of Individuals Undergoing Invasive Coronary Angiography) trial. *J Am Coll Cardiol* 52: 1724-1732.

Bunce, N. H., and D. J. Pennell. 1999. Coronary MRA: a clinical experience in Europe. *J Magn Reson Imaging* 10: 721-727.

Cerqueira, M., N. Weissman, V. Dilsizian, A. Jacobs, S. Kaul, W. Laskey, D. Pennell, J. Rumberger, T. Ryan, and M. Verani. 2002. Standardized myocardial segmentation and nomenclature for tomographic imaging of the heart. A statement for healthcare professionals from the Cardiac Imaging Committee of the Council on Clinical Cardiology of the American Heart Association. *Circulation* 105: 539-547.

Cheng, L. C. Y., T. Fang, and J. Tyan. 2006. *Proceedings of the IEEE International Conference on Image Processing, Fast iterative adaptive reconstruction in low-dose CT imaging*. New York: IEEE

Ciernak, R. 2011. *X-ray computed tomography in biomedical engineering*. First ed. London: Springer-Verlag.

Cody, D. D., D. M. Moxley, K. T. Krugh, J. C. O'Daniel, L. K. Wagner, and F. Eftekhari. 2004. Strategies for formulating appropriate MDCT techniques when imaging the chest, abdomen, and pelvis in pediatric patients. *Am J Roentgenol* 182: 849-859.

Coles, D. R., M. A. Smail, I. S. Negus, P. Wilde, M. Oberhoff, K. R. Karsch, and A. Baumbach. 2006. Comparison of radiation doses from multislice computed tomography coronary angiography and conventional diagnostic angiography. *J Am Coll Cardiol* 47 (9): 1840-1845.

Costello, P. 1996. Subsecond scanning makes CT even faster. *Diag Imaging* 18: 76-79.

d'Agostino, A. G., M. Remy-Jardin, C. Khalil, V. Delannoy-Deken, T. Flohr, A. Duhamel, and J. Remy. 2006. Low-dose ECG-gated 64-slices helical CT angiography of the chest: evaluation of image quality in 105 patients. *Eur Radiol* 16: 2137-2146.

Danias, P. G. 2004. Coronary magnetic resonance angiography. *Hallenic J Cardiol* 45: 95-99.

Deetjen, A., S. Mollmann, G. Conradi, A. Rolf, A. Schmermund, C. W. Hamm, and T. Dill. 2007. Use of automatic exposure control in multislice computed tomography of the coronaries: comparison of 16-slice and 64-slice scanner data with conventional coronary angiography. *Heart* 93: 1040-1043.

Dewey, M., M. Laule, L. Krug, D. Schnapauff, P. Rogalla, W. Rutsch, B. Hamm, and A. Lembcke. 2004. Multisegment and half-scan reconstruction of 16-slice computed tomography for detection of coronary artery stenoses. *Invest Radiol* 39: 223-229.

Di Carli, M. F., and R. Hachamovitch. 2006. Should PET replace SPECT for evaluating CAD? The end of the beginning. *J Nucl Cardiol* 13: 2-7.

Dikkers, R., M. J. W. Greuter, W. Kristanto, P. M. A. van Ooijen, P. E. Sijens, T. P. Willems, and M. Oudkerk. 2009. Assessment of image quality of 64-row dual source versus single source CT coronary angiography on heart rate: a phantom study. *Eur J Radiol* 70: 61-68.

Dirksen, M. S., J. W. Jukema, J. J. Bax, H. J. Lamb, E. Boersma, J. C. Tuinenburg, J. Geleijns, E. E. van der Wall, and A. de Roos. 2005. Cardiac multidetector-row computed tomography in patients with unstable angina. *Am J Cardiol* 95: 457-461.

Donati, O. F., P. Stolzmann, L. Desbiolles, S. Leschka, S. Kozerke, A. Plass, C. Wyss, V. Falk, B. Marincek, H. Alkadhi, and H. Scheffel. 2011. Coronary artery disease: which degree of coronary artery stenosis is indicative of ischemia? *Eur J Radiol* 80 (1): 120-126.

Earls, J. P. 2009. How to use a prospective gated technique for cardiac CT. *J Cardiovasc Comput Tomogr* 3: 45-51.

Earls, J. P., E. L. Berman, B. A. Urban, C. A. Curry, J. L. Lane, R. S. Jennings, C. C. McCulloch, J. Hsieh, and J. H. Londt. 2008. Prospectively gated transverse coronary CT angiography versus retrospectively gated helical technique: improved image quality and reduced radiation dose. *Radiology* 246: 742-753.

Einstein, A. J., M. J. Henzlova, and S. Rajagopalan. 2007. Radiation dose to the breast and estimated breast cancer risk in women from 64-slice CT coronary angiography: insights from the Biological Effects of Ionizing Radiation (BEIR) VII report. *J Nucl Cardiol* 14 (2): S59.

Elhendy, A., J. J. Bax, and D. Poldermans. 2002. Dobutamine stress myocardial perfusion imaging in coronary artery disease. *J Nuc Med* 43 (12): 1634-1646.

Ertel, D., M. M. Lell, F. Harig, T. Flohr, B. Schmidt, and W. Kalender. 2009. Cardiac spiral dual-source CT with high pitch: a feasibility study. *Eur Radiol* 19: 2357-2362.

European Commission. 1999. *European guidelines on quality criteria for computed tomography: Report EUR 16262*. Brussels European Commission.

Flohr, T. 2003. Image reconstruction and performance evaluation for ECG-gated spiral scanning with a 16-slice CT system. *Med Phys* 30 (10): 2650-2662.

Flohr, T., A. Küttner, H. Bruder, K. Stierstorfer, S. S. Halliburton, S. Schaller, and B. M. Ohnesorge. 2003. Performance evaluation of a multi-slice CT system with 16-slice detector and increased gantry rotation speed for isotropic submillimeter imaging of the heart. *Herz* 28 (1): 7-19

Flohr, T. G., H. Bruder, K. Stierstorfer, and C. McCollough. 2006. Radiation dose with dual source CT. *Med Solutions*, 94-97.

Flohr, T. G., C. H. McCollough, H. Bruder, M. Petersilka, K. Gruber, C. Süβ, M. Grasruck, K. Stierstorfer, B. Krauss, R. Raupach, A. N. Primak, A. Küttner, S. Achenbach, C. Becker, A. Kopp, and B. M. Ohnesorge. 2006. First performance evaluation of a dual-source CT (DSCT) system. *Eur Radiol* 16: 256-268.

Flohr, T. G., S. Schaller, K. Stierstorfer, H. Bruder, B. M. Ohnesorge, and U. J. Schoepf. 2005. Multi-detector row CT systems and image-reconstruction techniques. *Radiology* 235: 756-773.

Flohr, T. G., U. J. Schoepf, A. Kuettner, S. Halliburton, H. Bruder, C. Suess, B. Schmidt, L. Hofmann, E. K. Yucel, S. Schaller, and B. M. Ohnesorge. 2003. Advances in cardiac imaging with 16-section CT systems. *Acad Radiol* 10 (4): 386-401.

Garcia, M. J., J. Lessick, and M. H. K. Hoffmann. 2006. Accuracy of 16-row multidetector computed tomography for the assessment of coronary artery stenosis. *J Am Med Assoc* 296 (4): 403-411.

Geleijns, J., S. M. Artells, W. Veldkamp, L. M. Tortosa, and C. A. Cantera. 2006. Quantitative assessment of selective in-plane shielding of tissues in computed tomography through evaluation of absorbed dose and image quality. *Eur Radiol* 16: 2334-2340.

Gibbons, R. J., G. J. Balady, J. W. Beasley, J. T. Bricker, W. F. Duvernoy, V. F. Froelicher, D. B. Mark, T. H. Marwick, B. D. McCallister, P. D. Thompson, W. L. Winters, F. G. Yanowitz, J. L. Ritchie, M. D. Cheitlin, K. A. Eagle, T. J. Gardner, A. Garson, R. P. Lewis, R. A. O'Rourke, and T. J. Ryan. 1997. ACC/ AHA guidelines for exercise testing: a report of the American College of Cardiology/American Heart Association Task Force on Practice Guidelines (Committee on Exercise Testing). *J Am Coll Cardiol* 30: 260-311.

Giesler, T., U. Baum, D. Ropers, S. Ulzheimer, E. Wenkel, M. Mennicke, W. Bautz, W. A. Kalender, W. G. Daniel, and S. Achenbach. 2002. Noninvasive visualization of coronary arteries using contrast-enhanced multidetector CT: influence of heart rate on image quality and stenosis detection. *Am J Roentgenol* 179: 911-916.

Goetti, R., S. Leschka, S. Baumüller, A. Plass, M. Wieser, and L. Desbiolles. 2010. Low dose high-pitch spiral acquisition 128-slice dual-source computed tomography for

the evaluation of coronary artery bypass graft patency. *Invest Radiol* 45 (6): 324-330.

Goldman, L. W. 2008. Principles of CT: multislice CT. *J Nucl Med Technol* 36 (2): 57-68.

Gray, J. E., B. R. Archer, P. F. Butler, B. B. Hobbs, F. A. Mettler, R. J. Pizzutiello, B. A. Schueler, K. J. Strauss, O. H. Suleiman, and M. J. Yaffe. 2005. Reference values for diagnostic radiology: application and impact. *Radiology* 235 (2): 354-358.

Greess, H., A. Nömayr, H. Wolf, U. Baum, M. Lell, B. Böwing, W. Kalender, and W. Bautz. 2002. Dose reduction in CT examination of children by an attenuation-based on-line modulation of tube current (CARE dose). *Eur Radiol* 12: 1571-1576.

Haberl, R., J. Tittus, E. Böhme, A. Czernik, B. M. Richartz, J. Buck, and P. Steinbigler. 2005. Multislice spiral computed tomographic angiography of coronary arteries in patients with suspected coronary artery disease: An effective filter before catheter angiography? *Am Heart J* 149 (6): 1112-1119.

Hachamovitch, R. 2003. Comparison of the short-term survival benefit associated with revascularization compared with medical therapy in patients with no prior coronary artery disease undergoing stress myocardial perfusion single photon emission computed tomography. *Circulation* 107 (23): 2900-2906.

Hall, E. J. 1999. *Radiobiology for the radiologist*. New York: J.B. Lippincott.

Hameed, T. A., S. D. Teague, M. Vembar, E. Dharaiya, and J. Rydberg. 2009. Low radiation dose ECG-gated chest CT angiography on a 256-slice multidetector CT scanner. *Int J Cardiovasc Imaging* 25: 267-278.

Hara, A. K., R. G. Paden, A. C. Silva, K. L. Kujak, H. J. Lawder, and W. Pavlicek. 2009. Iterative reconstruction technique for reducing body radiation dose at CT: feasibility study. *Am J Roentgenol* 193: 764-771.

Hart, D., D. Jones, and B. Wall. 1994a. *National Radiological Protection Board 1991*. Didcot

Hart, D., D. G. Jones, and B. F. Wall. 1994b. *Estimation of effective dose in diagnostic radiology from entrance surface dose and dose-area product measurements: NRPB-R262.* Oxon: National Radiological Protection Board.

Hausleiter, J., T. Meyer, M. Hadamitzky, E. Huber, M. Zankl, S. Martinoff, A. Kastrati, and A. Schömig. 2006. Radiation dose estimates from cardiac multislice computed tomography in daily practice: impact of different scanning protocols on effective dose estimates. *Circulation* 113: 1305-1310.

Hausleiter, J., T. Meyer, F. Hermann, M. Hadamitzky, M. Krebs, T. C. Gerber, C. McCollough, S. Martinoff, A. Kastrati, A. Schömig, and S. Achenbach. 2009. Estimated radiation dose associated with cardiac CT angiography. *J Am Med Assoc* 301 500-507.

Herzog, B. A., L. Husmann, N. Burkhard, O. Gaemperli, I. Valenta, F. Tatsugami, C. A. Wyss, U. Landmesser, and P. A. Kaufmann. 2008. Accuracy of low-dose computed tomography coronary angiography using prospective electrocardiogram-triggering: first clinical experience. *Eur Heart J* 29: 3037-3042.

Hoe, J., and K. H. Toh. 2009. First experience with 320-row multidetector CT coronary angiography scanning with prospective electrocardiogram gating to reduce radiation dose. *J Cardiovasc Comput Tomogr* 3: 257-261.

Hoffmann, M., J. Lessick, R. Manzke, F. Schmid, E. Gershin, D. Boll, S. Rispler, A. Aschoff, and M. Grass. 2006. Automatic determination of minimal cardiac motion phases for computed tomography imaging: initial experience. *Eur Radiol* 16: 365-373.

Hoffmann, M. H. K., H. Shi, B. L. Schmitz, F. T. Schmid, M. Lieberknecht, R. Schulze, B. Ludwig, U. Kroschel, N. Jahnke, W. Haerer, H.-J. Brambs, and A. J. Aschoff. 2005. Noninvasive coronary angiography with multislice computed tomography. *J Am Med Assoc* 293 (20): 2471-2478.

Hoffmann, U., F. Moselewski, R. C. Cury, M. Ferencik, I. Jang, L. J. Diaz, S. Abbara, T. J. Brady, and S. Achenbach. 2004. Predictive value of 16-slice multidetector spiral computed tomography to detect significant obstructive coronary artery disease in patients at high risk for coronary artery disease patient- versus segment-based analysis. *Circulation* 110: 2638-2643.

Hoffmann, U., M. Ferencik, R. C. Cury, and A. J. Pena. 2006. Coronary CT angiography. *J Nucl Med* 47 (5): 797-806.

Hofman, M. B., S. A. Wickline, and C. H. Lorenz. 1998. Quantification of in-plane motion of the coronary arteries during the cardiac cycle: implications for acquisition window duration for MR flow quantification. *J Magn Reson Imaging* 8: 568-576.

Hohl, C., G. Mühlenbruch, J. Wildberger, C. Leidecker, C. Süss, T. Schmidt, R. Günther, and A. Mahnken. 2006. Estimation of radiation exposure in low-dose multislice computed tomography of the heart and comparison with a calculation program. *Eur Radiol* 16 (8): 1-6.

Hong, C., C. Becker, A. Huber, U. Schoepf, B. Ohnesorge, A. Knez, R. Brüning, and M. Reiser. 2001. ECG-gated reconstructed multi-detector row CT coronary angiography: effect of varying trigger delay on image quality. *Radiology* 220: 712-717.

Horiuchi, T. 2002. Study on 3D modulation auto mA *Jpn Soc Radiol Technol* 78: 166.

Hounsfield, G. N. 1980. Computed medical imaging. *Science* 210: 22-28.

Hsieh, J. 2003. *Computed tomography: principles, design, artifacts, and recent advances*, *Image artifacts: appearances, causes, and corrections*. Bellingham: SPIE Press.

Huda, W. 2002. Dose and image quality in CT. *Pediatr Radiol* 32: 709-713.

Huda, W., J. V. Atherton, D. E. Ware, and W. A. Cumming. 1997. An approach for the estimation of effective radiation dose at CT in pediatric patients. *Radiology* 203: 417-422.

Huda, W., D. Magill, and W. He. 2011. CT effective dose per dose length product using ICRP 103 weighting factors. *Med Phys* 38: 1261-1265.

Huda, W., K. M. Ogden, and M. R. Khorasani. 2008. Converting dose-length product to effective dose at CT. *Radiology* 248: 995-1003.

Huda, W., E. Scalzetti, and G. Levin. 2000. Technique factors and image quality as functions of patient weight at abdominal CT. *Radiology* 217: 430-435.

International Commission on Radiological Protection. 2003. Relative biological effectiveness (RBE), quality factor (Q), and radiation weighting factor (WR). In *ICRP publication 92*. Bethesda,. ICRP.

Janda, S., N. Shahidi, K. Gin, and J. Swiston. 2011. Diagnostic accuracy of echocardiography for pulmonary hypertension: a systematic review and meta-analysis. *Heart* 97 (8): 612-622.

Johnson, T. R., K. Nikolaou, B. J. Wintersperger, A. W. Leber, F. von Ziegler, C. Rist, S. Buhmann, A. Knez, M. F. Reiser, and C. R. Becker. 2006. Dual-source CT cardiac imaging: initial experience. *Eur Radiol* 16: 1409-1415.

Jung, B., A. H. Mahnken, A. Stargardt, J. Simon, T. Flohr, S. Schaller, R. Koos, R. W. Günther, and J. E. Wildberger. 2003. Individually weight-adapted examination protocol in retrospectively ECG-gated MSCT of the heart. *Eur Radiol* 13: 2560-2566.

Kalender, W., W. Seissler, E. Klotz, and P. Vock. 1990. Spiral volumetric CT with single-breath-hold technique, continuous transport, and continuous scanner rotation. *Radiology* 176: 181-183.

Kalender, W. A., B. Schmidt, M. Zankl, and M. Schmidt. 1999. A PC program for estimating organ dose and effective dose values in computed tomography. *Eur Radiol* 9: 555-562.

Kalra, M. K., M. l. M. Maher, T. L. Toth, B. Schmidt, B. L. Westerman, H. T. Morgan, and S. Saini. 2004. Techniques and applications of automatic tube current modulation for CT. *Radiology* 233: 649-657.

Kantarci, M., N. Ceviz, I. Durur, U. Bayraktutan, A. Karaman, F. Alper, O. Onbas, and A. Okur. 2006. Effect of the reconstruction window obtained at isovolumetric relaxation period on the image quality in electrocardiographic-gated 16-multidetector-row computed tomography coronary angiography studies. *J Comput Assist Tomogr* 30: 258-261.

Kennedy, J. W. 1982. Complications associated with cardiac catheterization and angiography. *Cathet Cardiovasc Diagn* 8 (1): 5-11.

Ketelsen, D., C. Thomas, M. Werner, M. H. Luetkhoff, M. Buchgeister, I. Tsiflikas, A. Reimann, C. Burgstahler, H. Brodoefel, A. F. Kopp, C. D. Claussen, and M. Heuschmid. 2010. Dual-source computed tomography: estimation of radiation exposure of ECG-gated and ECG-triggered coronary angiography. *Eur J Radiol* 73 (2): 274-279.10 April 2010).

Khoury, A., F. Aguirre, R. Bach, E. Caracciolo, T. Donohue, T. Wolford, C. Mechem, S. Herrmann, and M. Kern. 1996. Influence of percutaneous transluminal coronary rotational atherectomy with adjunctive percutaneous transluminal coronary angioplasty on coronary blood flow. *Am Heart J* 131 (4): 631-638.

Kido, T., A. Kurata, H. Higashino, Y. Sugawara, H. Okayama, J. Higaki, H. Anno, K. Katada, S. Mori, S. Tanada, M. Endo, and T. Mochizuki. 2007. Cardiac imaging using 256-detector row four-dimensional CT: preliminary clinical report. *Radiat Med* 25: 38-44.

Kim, W. Y., P. G. Danias, M. Stuber, S. D. Flamm, S. Plein, E. Nagel, S. E. Langerak, O. M. Weber, E. M. Pedersen, M. Schmidt, R. M. Botnar, and W. J. Manning. 2001. Coronary magnetic resonance angiography for the detection of coronary stenoses. *N Engl J Med* 345: 1863-1869.

Kim, Y. J., J. S. Seo, B. W. Choi, K. O. Choe, Y. Jang, and Y. G. Ko. 2006. Feasibility and diagnostic accuracy of whole heart coronary MR angiography using free-breathing

3D balanced turbo-field-echo with SENSE and the half-fourier acquisition technique. *Korean J Radiol* 7 (4): 235-242.

Kini, S., K. G. Bis, and L. Weaver. 2007. Normal and variant coronary arterial and venous anatomy on high-resolution CT angiography. *Am J Roentgenol* 88 (6): 1665-1674.

Kisslo, J., B. Firek, T. Ota, D. H. Kang, C. E. Fleishman, G. Stetten, Li, J, C. J. Ohazama, D. Adams, C. Landolfo, T. Ryan, and O. von Ramm. 2000. Real-time volumetric echocardiography: the technology and the possibilities. *Echocardiography* 17 (8): 773-779.

Klass, O., M. Walker, A. Siebach, T. Stuber, S. Feuerlein, M. Juchems, and M. H. K. Hoffmann. 2009. Prospectively gated axial CT coronary angiography: comparison of image quality and effective radiation dose between 64- and 256-slice CT. *Eur Radiol* 20: 1124-1131.

Klingenbeck-Regn, K., S. Schaller, T. Flohr, B. Ohnesorge, A. Kopp, and U. Baum. 1999. Subsecond multi-slice computed tomography: basics and applications. *Eur J Radiol* 31: 110- 124.

Knesaurek, K., J. Machac, S. Vallabhajosula, and M. S. Buchsbaum. 1996. A new iterative reconstruction technique for attenuationcorrection in high-resolution positron emission tomography. *Eur J Nucl Med* 23 (6): 656-661.

Kopp, A. F., S. Schroeder, A. Kuettner, A. Baumbach, C. Georg, R. Kuzo, M. Heuschmid, B. Ohnesorge, K. R. Karsch, and C. D. Claussen. 2002. Non-invasive coronary angiography with high resolution multidetector-row computed tomography. *Eur Heart J* 23 (21): 1714-1725.

Kroft, L. J. M., A. de Roos, and J. Geleijns. 2007. Artifacts in ECG-synchronized MDCT coronary angiography. *Am J Roentgenol* 189: 581-591.

Kuettner, A., T. Beck, and T. Drosch. 2005. Image quality and diagnostic accuracy of non-invasive coronary imaging with 16 detector slice spiral computed tomography with 188 ms temporal resolution. *Heart* 91: 938-941.

Kuettner, A., T. Trabold, S. Schroeder, A. Feyer, T. Beck, A. Brueckner, M. Heuschmid, C. Burgstahler, A. F. Kopp, and C. D. Claussen. 2004. Noninvasive detection of coronary lesions using 16-detector multislice spiral computed tomography technology. *J Am Coll Cardiol* 44 (6): 1230–1237.

Le Heron, J. C. 1992. Estimation of effective dose to the patient during medical x-ray examinations from measurements of the dose-area product. *Phys Med Biol* 37 (11): 2117-2126.

Leber, A. W., A. Knez, F. von Ziegler, A. Becker, K. Nikolaou, S. Paul, B. Wintersperger, M. Reiser, C. R. Becker, G. Steinbeck, and P. Boekstegers. 2005. Quantification of obstructive and non-obstructive coronary lesions by 64-slice computed tomography: a comparative study with quantitative coronary angiography and intravascular ultrasound. *J Am Coll Cardiol* 46 (1): 147-154.

Leipsic, J., T. M. Labounty, B. Heilbron, J. K. Min, G. B. Mancini, F. Y. Lin, C. Taylor, A. Dunning, and J. P. Earls. 2010. Adaptive statistical iterative reconstruction: assessment of image noise and image quality in coronary CT angiography. *Am J Roentgenol* 195 (3): 649-654.

Lell, M., F. Hinkmann, K. Anders, P. Deak, W. Kalender, M. Uder, and S. Achenbach. 2009. High-pitch electrocardiogram-triggered computed tomography of the chest: initial results. *Invest Radiol* 44: 728-733.

Lell, M., M. Marwan, T. Schepis, T. Pflederer, K. Anders, T. Flohr, T. Allmendinger, W. Kalender, D. Ertel, C. Thierfelder, A. Kuettner, D. Ropers, W. G. Daniel, and S. Achenbach. 2009. Prospectively ECG-triggered high-pitch spiral acquisition for coronary CT angiography using dual source CT: technique and initial experience. *Eur Radiol* 19: 2576-2583.

Leschka, S., P. Stolzmann, L. Desbiolles, S. Baumueller, R. Goetti, T. Schertler, H. Scheffel, A. Plass, V. Falk, G. Feuchtner, B. Marincek, and H. Alkadhi. 2009. Diagnostic accuracy of high-pitch dual-source CT for the assessment of coronary stenoses: first experience. *Eur Radiol* 19: 2896-2903.

Leschka, S., P. Stolzmann, F. T. Schmid, H. Scheffel, B. Stinn, B. Marincek, H. Alkadhi, and S. Wildermuth. 2008. Low kilovoltage cardiac dual-source CT: attenuation, noise, and radiation dose. *Eur Radiol* 18: 1809-1817.

Lewis, M., N. Keat, and S. Edyvean. 2006. *16 Slice CT scanner comparison report version 14*. http://www.impactscan.org/reports/Report06012 (accessed 19 June 2010).

Liang, Y., and R. Kruger. 1996. Dual-slice spiral versus single-slice spiral scanning: comparison of the physical performance of two computed tomography scanners. *Med Phys* 23: 205-220.

Liow, J. S., S. C. Strother, K. Rehm, and D. A. Rottenberg. 1997. Improved resolution for PET volume imaging through three-dimensional iterative reconstruction. *J Nucl Med* 38 (10): 1623-1631.

Liu, Y. J., P. P. Zhu, B. Chen, J. Y. Wang, Q. X. Yuan, W. X. Huang, H. Shu, E. R. Li, X. S. Liu, K. Zhang, H. Ming, and Z. Y. Wu. 2007. A new iterative algorithm to reconstruct the refractive index. *Phys Med Biol* 52: L5-L13.

Lu, B., J.-G. Lu, M.-L. Sun, Z.-H. Hou, X.-B. Chen, X. Tang, R.-Z. Wu, L. Johnson, S.-B. Qiao, Y.-J. Yang, and S.-L. Jiang. 2011. Comparison of diagnostic accuracy and radiation dose between prospective triggering and retrospective gated coronary angiography by dual-source computed tomography. *Am J Cardiol* 107: 1278-1284.

Mace, J. D., and N. Kowalczyk. 2004. *Radiographic pathology for technologists*. 4 ed. Missouri: Mosby.

Maia, A. F., and L. V. E. Caldas. 2010. Response of TL materials to diagnostic radiology X radiation beams. *Appl Radiat Isotopes* 68: 780-783.

Manning, W. J., W. Li, and R. R. Edelman. 1993. A preliminary report comparing magnetic resonance coronary angiography with conventional angiography. *N Engl J Med* 328: 828-832.

Martin, J. E. 2006. *Physics for radiation protection*. second ed. Weinheim: Wiley-VCH Verlag GmbH & Co. KGaA.

McCollough, C., and F. Zink. 1999. Performance evaluation of a multi-slice CT system. *Med Phys* 26: 2223-2230.

McKinnon, G. C. 1993. Ultrafast interleaved gradient-echo-planar imaging on a standard scanner. *Magn Reson Med* 30: 609-616.

Meijboom, W. B., M. F. Meijs, J. D. Schuijf, M. J. Cramer, N. R. Mollet, C. A. van Mieghem, K. Nieman, J. M. van Werkhoven, G. Pundziute, A. C. Weustink, A. M. de Vos, F. Pugliese, B. Rensing, J. W. Jukema, J. J. Bax, M. Prokop, P. A. Doevendans, M. G. Hunink, G. P. Krestin, and P. J. de Feyter. 2008. Diagnostic accuracy of 64-slice computed tomography coronary angiography: a prospective, multicenter, multivendor study. *J Am Coll Cardiol* 52: 2135-2144.

Mettler, F. A., and M. J. Guiberteau. 1998. *Essential of nuclear medicine imaging*. 4th ed, *Cardiovascular system*. Pennsylvania: W.B Saunders company.

Miljanie, S., B. Vekie, and R. Martinieie. 1999. Determination of x-ray effective energy and absorbed dose using CaF_2:Mn and LiF:Mg,Ti thermoluminescence dosimeters. *Radiat Prot Dosim* 85 (1-4): 381-384.

Miller, J. M., C. E. Rochitte, M. Dewey, A. Arbab-Zadeh, H. Niinuma, I. Gottlieb, N. Paul, M. E. Clouse, E. P. Shapiro, J. Hoe, A. C. Lardo, D. E. Bush, A. de Roos, C. Cox, J. Brinker, and J. A. Lima. 2008. Diagnostic performance of coronary angiography by 64-row CT. *N Engl J Med* 359: 2324-2336.

Mollet, N. R., F. Cademartiri, K. Nieman, F. Saia, P. A. Lemos, E. P. McFadden, P. M. T. Pattynama, P. W. Serruys, G. P. Krestin, and P. J. de Feyter. 2004. Multislice spiral computed tomography coronary angiography in patients with stable angina pectoris. *J Am Coll Cardiol* 43 (12): 2265-2270.

Mollet, N. R., F. Cademartiri, C. A. G. van Mieghem, G. Runza, E. P. McFadden, T. Baks, P. W. Serruys, G. P. Krestin, and P. J. de Feyter. 2005. High-resolution spiral computed tomography coronary angiography in patients referred for diagnostic conventional coronary angiography. *Circulation* 112: 2318-2323.

Mori, S., M. Endo, T. Obata, K. Murase, H. Fujiwara, K. Susumu, and S. Tanada. 2005. Clinical potentials of the prototype 256-detector row CT-scanner. *Acad Radiol* 12: 148-154.

Mori, S., M. Endo, T. Obata, T. Tsunoo, K. Susumu, and S. Tanada. 2006. Properties of the prototype 256-row (cone beam) CT scanner. *Eur Radiol* 16: 2100-2108.

Mori, S., C. Kondo, N. Suzuki, H. Yamashita, A. Hattori, M. Kusakabe, and M. Endo. 2005. Volumetric cine imaging for cardiovascular circulation using prototype 256-detector row computed tomography scanner (4-dimensional computed tomography): a preliminary study with a porcine model. *J Comput Assist Tomogr* 29: 26-30.

Nagataki, S., Y. Shibata, S. Inoue, N. Yokoyama, M. Izumi, and K. Shimaoka. 1994. Thyroid diseases among atomic bomb survivors in Nagasaki. *J Am Med Assoc* 272: 364-370.

Naghavi, M., E. Falk, H. S. Hecht, M. J. Jamieson, S. Kaul, D. Berman, Z. Fayad, M. J. Budoff, J. Rumberger, T. Z. Naqvi, L. J. Shaw, O. Faergeman, J. Cohn, R. Bahr, W. Koenig, J. Demirovic, D. Arking, V. L. M. Herrera, J. Badimon, J. A. Goldstein, Y. Rudy, J. Airaksinen, R. S. Schwartz, W. A. Riley, R. A. Mendes, P. Douglas, and P. K. Shah. 2006. From vulnerable plaque to vulnerable patient--part III: executive summary of the screening for heart attack prevention and education (SHAPE) task force report. *Am J Cardiol* 98 (2, Supplement 1): 2-15.

National Council on Radiation Protection and Measurements. 1995. Use of personal monitors to estimate effective dose equivalent and effective dose to workers for external exposure to low-LET radiation. In *Report no. 122*. Bethesda. NCRP Publications.p

Ng, K.-H. 2003. Radiation effect and protection in diagnostic radiology. In *The Asian-Oceanian textbook of radiology*, ed. W. C. G. Peh and Y. Hiramatsu, 175. Singapore: TTG Asia Media Pte Ltd.

Nickoloff, E. L., and P. Alderson. 2001. Radiation exposures to patients from CT: reality, public perception and policy. *A J Roentgenol* 177: 285-287.

Nickoloff, E. L., Z. F. Lu, A. K. Dutta, and J. C. So. 2008. Radiation dose descriptors: BERT, COD, DAP, and other strange creatures. *Radiographics* 28 (5): 1439-1450.

Nieman, K., F. Cademartiri, P. A. Lemos, R. Raaijmakers, P. M. T. Pattynama, and P. J. de Feyter. 2002. Reliable noninvasive coronary angiography with fast submillimeter multislice spiral computed tomography. *Circulation* 106 (16): 2051-2054.

Nuyts, J., B. De Man, P. Dupont, M. Defrise, P. Suetens, and L. Mortelmans. 1998. Iterative reconstruction for helical CT: a simulation study. *Phys Med Biol* 43: 729-737.

Pandian, N. G., J. Roelandt, N. C. Nanda, L. Sugeng, Q. L. Cao, J. Azevedo, S. L. Schwartz, M. A. Vannan, A. Ludomirski, G. Marx, and M. Vogel. 1994. Dynamic three-dimensional echocardiography: methods and clinical potential. *Echocardiography* 11 (3): 237-259.

Pandian, N. G., and M. A. Vannan. 1993. Evolving trends and future directions in echocardiograpy. *Int J Card Imag* 2: 81-92.

Pannu, H. K., W. Alvarez, and E. K. Fishman. 2006. β-blockers for cardiac CT: a primer for the radiologist. *Am J Roentgenol* 186: S341-S346.

Paul, J., G. Dambrin, C. Caussin, B. Lancelin, and C. Angel. 2003. Sixteen-slice computed tomography after acute myocardial infarction; from perfusion defect to the culprit lesion. *Circulation* 108: 373 -374.

Paul, J. F., and H. T. Abada. 2007. Strategies for reduction of radiation dose in cardiac multislice CT. *Eur Radiol* 17: 2028-2037.

Pierce, D. A., and D. R. Preston. 2000. Radiation-related cancer risks at low doses among atomic bomb survivors. . *Radiat Res* 154: 178-186.

Pierce, D. A., Y. Shimizu, D. L. Preston, M. Vaeth, and K. Mabuchi. 1996. Studies of the mortality of atomic bomb survivors. Report 12, part I. Cancer: 1950-1990. *Radiat Res* 146: 1-27.

Poll, L., M. Cohnen, S. Brachten, K. Ewen, and U. Modder. 2002. Dose reduction in multi-slice CT of the heart by use of ECG-controlled tube current modulation "ECG pulsing": phantom measurements. *Rofo* 174: 1500-1505.

Pontone, G., D. Andreini, A. L. Bartorelli, S. Cortinovis, S. Mushtaq, E. Bertella, A. Annoni, A. Formenti, E. Nobili, D. Trabattoni, P. Montorsi, G. Ballerini, P. Agostoni, and M. Pepi. 2009. Diagnostic accuracy of coronary computed tomography angiography: a comparison between prospective and retrospective electrocardiogram triggering. *J Am Coll Cardiol* 54: 346-355.

Preston, D. L., Y. Shimizu, D. A. Pierce, A. Suyama, and K. Mabuchi. 2003. Studies of mortality of atomic bomb survivors. Report 13. Solid cancer and non-cancer disease mortality 1950-1957. *Radiat Res* 160: 381-407.

Pugliese, F., N. R. A. Mollet, G. Runza, C. van Mieghem, W. B. Meijboom, P. Malagutti, T. Baks, G. P. Krestin, P. J. de Feyter, and F. Cademartiri. 2006. Diagnostic accuracy

of non-invasive 64-slice CT coronary angiography in patients with stable angina pectoris. *Eur Radiol* 16 (3): 575-582.

Reagan, K., L. M. Boxt, and J. Katz. 1994. Introduction to coronary arteriography. *Radiol Clin North Am* 32: 419-433.

Rees, M. R., F. Zijlstra, J. H. C. Reiber, G. Koning, J. C. Tuinenberg, A. Lansky, G. B. Ligthart, P. J. De Feyter, N. Bruining, R. Hamers, and J. R. Roelandt. 2004. Conventional catheterization. In *Coronary radiology*, ed. A. Baert and K. Sartor, 25-38. Heidelberg: Springer-Verlag.

Ron, E., B. Modan, D. Preston, E. Alfandary, M. Stovall, and J. D. Boice. 1989. Thyroid neoplasia following low-dose radiation in childhood. *Radiat Res* 120: 516-531.

Ropers, D., U. Baum, K. Pohle, K. Anders, S. Ulzheimer, B. Ohnesorge, C. Schlundt, W. Bautz, W. G. Daniel, and S. Achenbach. 2003. Detection of coronary artery stenoses with thin-slice multi-detector row spiral computed tomography and multiplanar reconstruction. . *Circulation* 107: 664 -666.

Rosenstein, M. 1988. *Handbook of selected tissue doses for projections common in diagnostic radiology.*: HHS Publication (FDA). (accessed 2 March 2012).

Rosenstein, M., T. J. Beck, and G. G. Warner. 1979. *Handbook of selected organ doses for projections common in pediatric radiology*. HEW Publication (FDA). (accessed 12 March 2012).

Ross, R. 1999. Atherosclerosis- an inflamatory disease. *N Engl J Med* 340 (2): 115-126.

Ruzsics, B., H. Lee, P. L. Zwerner, M. Gebregziabher, P. Costello, and U. J. Schoepf. 2008. Dual-energy CTof the heart for diagnosing coronary artery stenosis and myocardial ischemia-initial experience. *Eur Radiol* 18: 2414-2424.

Rybicki, F., H. Otero, M. Steigner, G. Vorobiof, L. Nallamshetty, D. Mitsouras, H. Ersoy, R. Mather, P. Judy, T. Cai, K. Coyner, K. Schultz, A. Whitmore, and M. Di Carli. 2008. Initial evaluation of coronary images from 320-detector row computed tomography. *Int J Cardiovasc Imaging* 24 (5): 535-546.

Sabarudin, A., Z. Sun, and K.-H. Ng. 2012. A systematic review of radiation dose associated with different generations of multidetector CT coronary angiography. *J Med Imag Radiat Oncol* 56: 5-17.

Sakuma, H., Y. Ichikawa, N. Suzawa, T. Hirano, K. Makino, N. Koyama, M. Van Cauteren, and K. Takeda. 2005. Assessment of coronary arteries with total study time of less than 30 minutes by using whole-heart coronary MR angiography. *Radiology* 237: 316-321.

Santana, C. A., R. D. Folks, E. V. Garcia, L. Verdes, R. Sanyal, J. Hainer, M. F. Di Carli, and F. P. Esteves. 2007. Quantitative (82) Rb PET/CT: development and validation of myocardial perfusion database. *J Nucl Med* 48 (7): 1122-1128.

Scheffel, H., H. Alkadhi, S. Leschka, A. Plass, L. Desbiolles, I. Guber, T. Krauss, J. Gruenenfelder, M. Genoni, T. Luescher, B. Marincek, and P. Stolzmann. 2008. Low-dose CT coronary angiography in the step-and-shoot mode: diagnostic performance. *Heart* 94: 1132-1137.

Scheffel, H., H. Alkadhi, A. Plass, R. Vachenauer, L. Desbiolles, O. Gaemperli, T. Schepis, T. Frauenfelder, T. Schertler, L. Husmann, J. Grunenfelder, M. Genoni, P. Kaufmann, B. Marincek, and S. Leschka. 2006. Accuracy of dual-source CT

coronary angiography: First experience in a high pre-test probability population without heart rate control. *Eur Radiol* 16 2739-2747.

Schwartzman, D., J. Lacomis, and W. G. Wigginton. 2003. Characterization of left atrium and distal pulmonary vein morphology using multidimensional computed tomography. *J Am Coll Cardiol* 41: 1349 -1357.

Senkus-Konefka, E., and J. Jassem. 2007. Cardiovascular effects of breast cancer radiotherapy. *Cancer Treat Rev* 33 (6): 578-593.

Shore, R. E. 1992. Issues and epidemiological evidence regarding radiation-induced thyroid cancer. *Radiat Res* 131: 98-111.

Shuman, W., K. Branch, J. May, L. Mitsumori, D. Lockhart, T. Dubinski, B. Warren, and J. Caldwell. 2008. Prospective versus retrospective ECG gating for 64-detector CT of the coronary arteries: comparison of image quality and patient radiation dose. *Radiology* 248: 431-437.

Siegel, M. J., B. Schmidt, D. Bradley, C. Suess, and C. Hildebolt. 2004. Radiation dose and image quality in pediatric CT: effect of technical factors and phantom size and shape. *Radiology* 233: 515-522.

Sigal-Cinqualbre, A. B., R. Hennequin, H. Abada, X. Chen, and J. Paul. 2004. Low-kilovoltage multi-detector row chest CT in adults: feasibility and effect on image quality and iodine dose. *Radiology* 231: 169-174.

Slavin, G. S., S. J. Riederer, and R. L. Ehman. 1998. Two-dimensional multishot echo-planar coronary MR angiograph. *Magn Reson Med* 40: 883-889.

Slomka, P. J., L. Le Meunier, S. W. Hayes, W. Acampa, M. Oba, G. G. Haemer, D. S. Berman, and G. Germano. 2008. Comparison of myocardial perfusion ^{82}Rb PET performed with CT and transmission CT-based attenuation correction. *J Nucl Med* 49 (12): 1992-1998.

Sommer, T., M. Hackenbroch, U. Hofer, A. Schmiedel, W. A. Willinek, S. Flacke, J. Gieseke, F. Träber, R. Fimmers, H. Litt, and H. Schild. 2005. Coronary MR angiography at 3.0 T versus that at 1.5 T: initial results in patients suspected of having coronary artery disease. *Radiology* 234: 718-725.

Sommer, W. H., J. C. Schenzle, C. R. Becker, K. Nikolaou, A. Graser, G. Michalski, K. Neumaier, M. F. Reiser, and T. R. Johnson. 2010. Saving dose in triple-rule-out computed tomography examination using a high-pitch dual spiral technique. *Invest Radiol* 45: 64-71.

Starck, G., L. Lonn, A. Cederblad, E. Forssell-Aronsson, L. Sjostrom, and M. Alpsten. 2002. A method to obtain the same levels of CT image noise for patients of various sizes, to minimize radiation dose. *Br J Radiol* 75: 140-150.

Steigner, M., H. Otero, T. Cai, D. Mitsouras, and L. Nallamshetty. 2009. Narrowing the phase window width in prospectively ECG-gated single heart beat 320-detector row coronary CT angiography. *Int J Cardiovasc Imaging* 25 (85-90):

Strauss, H. W., and L. K. Griffeth. 1994. Cardiovascular system. In *Nuclear medicine-technology and technique*, ed. D. R. Bernier, P. E. Christian and J. K. Langan, 271-301. Missouri: Mosby Inc.

Suess, C., and X. Y. Chen. 2002. Dose optimization in pediatric CT: current technology and future innovations. *Pediatr Radiol* 32: 729-734.

Sun, Z., G. H. Choo, and K. H. Ng. 2012 Coronary CT angiography: current status and continuing challenges. *Br J Radiol* 85 (1013): 495-510.

Sun, Z., C. Lin, R. Davidson, C. Dong, and Y. Liao. 2008. Diagnostic value of 64-slice CT angiography in coronary artery disease: a systematic review. *Eur J Radiol* 67: 78-84.

Sun, Z., and K.-H. Ng. 2012. Prospective versus retrospective ECG-gated multislice CT coronary angiography: A systematic review of radiation dose and diagnostic accuracy. *Eur J Radiol* 81: e94-e100.

Taguchi, K., and H. Aradate. 1998. Algorithm for image reconstruction in multi-slice helical CT. *Med.Phys* 25: 550-561.

Taylor, A. M., P. Jhooti, F. Wiesmann, J. Keegan, D. N. Firmin, and D. J. Pennell. 1997. MR navigator-echo monitoring of temporal changes in diaphragm position: implications for MR coronary angiography. *J Magn Reson Imaging* 7: 629-636.

Thibault, J. B., K. D. Sauer, C. A. Bouman, and J. Hsieh. 2007. A three-dimensional statistical approach to improved image quality for multislice helical CT. *Med Phys* 34: 4526-4544.

Thompson, D. E., K. Mabuchi, E. Ron, M. Soda, M. Tokunaga, and S. Ochikubo. 1994. Cancer incidence in atomic bomb survivors. Part II: Solid tumors, 1958-1987. *Radiat Res* 137: S17-S67.

Tsapaki, V., N. A. Ahmed, J. S. AlSuwaidi, A. Beganovic, A. Benider, L. BenOmrane, R. Borisova, S. Economides, L. El-Nachef, D. Faj, A. Hovhannesyan, M. H. Kharita, N. K. Toutaoui, N. Manatrakul, I. Mirsaidov, M. Shaaban, I. Ursulean, J. S. Wambani, A. Zaman, J. Ziliukas, D. Žontar, and M. M. Rehani. 2009. Radiation exposure to patients during interventional procedures in 20 countries: Initial IAEA project results. *Am J Roentgenol* 193: 559-569.

Underwood, S. R., C. Anagnostopoulos, M. Cerqueira, P. J. Ell, E. J. Flint, M. Harbinson, A. D. Kelion, A. Al-Mohammad, E. M. Prvulovich, L. J. Shaw, and A. C. Tweddel. 2004. Myocardial perfusion scintigraphy: the evidence. *Eur J Nucl Med Mol Imaging* 31: 261-291.

van der Vaart, M. G., R. Meerwaldt, R. H. J. A. Slart, G. M. van Dam, R. A. Tio, and C. J. Zeebregts. 2008. Application of PET/SPECT imaging in vascular disease. *Eur J Vasc Endovasc Surg* 35 (5): 507-513.

van Ooijen, P. M. A., J.-L. Sablayrolles, G. Ligabue, and F. Zijlstra. 2004. Coronary anatomy. In *Coronary radiology*, ed. A. Baert and K. Sartor, 1-23. Heidelberg: Springer-Verlag.

Wagner, L. K., P. J. Eifel, and R. A. Geise. 1994. Potential biological effects following high x-ray dose interventional procedures. *J Vasc Interv Radiol* 5: 71-84.

Walker, M. J., M. E. Olszewski, M. Y. Desai, S. S. Halliburton, and S. D. Flamm. 2009. New radiation dose saving technologies for 256-slice cardiac computed tomography angiography. *Int J Cardiovasc Imaging* 25: 189-199.

Wang, G., H. Yu, and B. De Man. 2008 An outlook on x-ray CT research and development. *Med Phys* 35: 1051-1064.

Wang, M., H. Qi, X. Wang, T. Wang, J. Chen, and C. Liu. 2009. Dose performance and image quality: dual source CT versus single source CT in cardiac CT angiography. *Eur J Radiol* 72: 396-400.

Westerman, B. R. 2002. Radiation dose from Toshiba CT scanners. *Pediatr Radiol* 32: 735-737.

Wexler, L., B. Brundage, J. Crouse, R. Detrano, V. Fuster, J. Maddahi, J. Rumberger, W. Stanford, R. White, and K. Taubert. 1996. Coronary artery calcification: pathophysiology, epidemiology, imaging methods, and clinical implications: a statement for health professionals from the American Heart Association *Circulation* 94: 1175-1192.

Wintersperger, B., T. Jakobs, P. Herzog, S. Schaller, K. Nikolaou, C. Suess, C. Weber, M. Reiser, and C. Becker. 2005. Aorto-iliac multidetector-row CT angiography with low kV settings: improved vessel enhancement and simultaneous reduction of radiation dose. *Eur Radiol* 15: 334-341.

CHAPTER 2: A SYSTEMATIC REVIEW OF RADIATION DOSE ASSOCIATED WITH DIFFERENT GENERATIONS OF MULTIDETECTOR CT CORONARY ANGIOGRAPHY

2.1 Introduction

Coronary artery disease (CAD) is a common cardiovascular disease and a leading cause of death amongst people in advanced countries. Early detection and diagnosis play an important role in patient management. Traditionally, this has been achieved with use of invasive coronary angiography; however, this technique is associated with procedure-related complications. Therefore, ever since multi-detector computed tomography angiography (MDCTA) has been introduced as a non-invasive technique in cardiac imaging it has been widely used to detect CAD as a less invasive imaging modality (Brenner and Hall 2007; Naghavi et al. 2006).

Over the last decade MDCT has undergone rapid technical developments, and has demonstrated regular technical improvements starting with the early generation of 4-slice to 16-slice, 64-slice and up till the most recent models of 320-slice scanners (Hein et al. 2009; Rybicki et al. 2008; Stolzmann et al. 2011). Although rapid developments in MDCT technology have led to striking improvements in both image quality and diagnostic value in cardiovascular imaging, MDCT runs the potential risk of high radiation dose (Frush and Yoshizumi 2006; Sun and Ng 2010b, 2010a). Preliminary studies have shown that radiation dose increases with increasing detector rows in CT due to narrow detector collimations and long anatomic coverage (Tsapaki and Rehani 2007). It is generally agreed that CT is an imaging modality with high radiation exposure, as it contributes up to 70 per cent radiation dose of all radiological examinations, although it comprises only 15 per cent of all radiological examinations (Sun, Choo, and Ng 2012). Recent advances and improvements to the spatial and temporal resolution of MDCT have increased its accuracy to diagnose CAD; however, this has resulted in increased radiation dose. The radiation risks associated with cardiac MDCTA have raised serious concerns in the literature (Frush and Yoshizumi 2006; Sun, Choo, and Ng 2012 ; Tsapaki and Rehani 2007). Thus, the questions have to be addressed, which are: Does utilisation of cardiac MDCTA lead to the greatest benefit and is the risk of radiation greater than the benefit expected from the CT examinations? (Budoff and Gupta 2010).

Despite the increased awareness of radiation risk, there are many clinicians and researchers who have not yet realised the amount of radiation exposure associated with coronary CTA, or the possibility of tailoring the scanning protocols to reduce radiation dose. Therefore, the

aim of this study is to carry out a systematic review of radiation dose in coronary CTA performed with different generations of MDCT scanners and various dose-saving techniques based on the available literature. We expect that the research findings of this study will provide valuable information for radiologists and radiographers with regard to optimisation of radiation exposure and judicious use of MDCT in the diagnosis of CAD.

2.2 Materials and methods

The literature search for relevant references was performed by using eight different databases, which included Highwire Press, Ovid, PubMed, ProQuest Health and Medical Complete, Medline, Science Direct, Scopus and Springer Link to cover publications between 1998 (MDCT was first introduced in 1998) and 2011 (last search was done in February 2011). The terms used for identification of references were 'multidetector/multislice CT coronary angiography', 'multidetector/multislice CT coronary angiography', 'radiation dose and effective dose in multidetector CT coronary angiography', and 'dose reduction strategies for CT coronary angiography'. Each of these terms was matched separately with prefix of 4-, 16-, 40-, 64-, 128-, 256-, 320-slice CT. The search was limited to include all the studies that had been published in the English language and were on human subjects. All the retrospective/prospective studies were included in this review as long as the effective radiation dose was provided in studies using MDCTA in the diagnosis of CAD. Exclusion criteria included calcium scoring on coronary CT scans, case reports, phantom studies, and studies with use of electron beam CT. Moreover, all the references were checked manually in order to ensure the precision and originality of the review. Comparisons of effective dose in each CT generation were performed based on multiple variables including demographic characteristics and technical parameters such as exposure factors (kVp, mAs), and scanning protocols (collimation, pitch, ECG-gating).

Data were extracted by two authors (AS and ZS) independently and all disagreements were resolved through consensus. Data extraction was based on the following characteristics in each study: year of publication, number of patients included in each study, age and gender, type of CT scanner, scanning protocols and technique, gantry rotation time, beam collimation, exposure factors (kVp and mA), pitch, method of electrocardiogram (ECG) gating (retrospective or prospective gating), and strategies to reduce radiation dose (adjustment of tube voltage or tube current). Effective dose was recorded in terms of mean value and dose range corresponding to the gender. In addition, $CTDI_{vol}$ and dose length product (DLP) were checked in each study and recorded, wherever available.

2.2.1 Statistical analysis

All data were analyzed and processed using SPSS V 17.0 (SPSS Inc, Chicago, IL). Effective doses are expressed as mean value ± SD. Comparisons were performed using one sample two-sided T test. A *p*-value less than 0.05 was defined as a statistically significant difference.

2.3 Results

The search process and results of obtaining these references are shown in Figure 2-1. Eighty-three citations were identified to be relevant to the cardiac MDCT angiography with reports of radiation dose, and only 66 articles were found to meet the selection requirements for inclusion in this review (Hein et al. 2009; Rybicki et al. 2008; Stolzmann et al. 2011; Achenbach et al. 2000; Becker et al. 2002; Haberl et al. 2005; Jakobs et al. 2002 ; Knez et al. 2001; Kopp et al. 2002; Leber et al. 2003; Roos et al. 2002; Anders et al. 2006; Chiou et al. 2005; Coles et al. 2006; Dill et al. 2008; Garcia, Lessick, and Hoffmann 2006; Hoffmann et al. 2005; Houslay et al. 2007; Kuettner et al. 2004; Leta et al. 2004; Mahnken et al. 2003; Mollet et al. 2004; Park et al. 2009; Schroeder et al. 2001; Yamamoto et al. 2006; Alkadhi et al. 2008; Blankstein et al. 2009; Deetjen et al. 2007; Earls et al. 2008; Feuchtner et al. 2010; Francone et al. 2007; Freeman et al. 2009; Gaspar et al. 2005; Hausleiter, Bischoff, et al. 2009; Hausleiter et al. 2006; Husmann et al. 2010; Leber et al. 2005; Maruyama et al. 2008; Meijboom et al. 2007; Mollet et al. 2005; Nikolaou et al. 2006; Pontone et al. 2009; Pugliese et al. 2006; Rixe et al. 2009; Van Mieghem et al. 2006; Achenbach et al. 2010; Alkadhi et al. 2010; Chao et al. 2010; Chen et al. 2010; Dewey et al. 2009; Efstathopoulos et al. 2009; Graaf et al. 2010; Hoe and Toh 2009; Hunold et al. 2003; Klass et al. 2009; Raff et al. 2005; Ropers et al. 2006; Shuman et al. 2008; Steigner et al. 2009; Walker et al. 2009; Wang et al. 2009; Weigold 2009; Xu et al. 2010; Zhao et al. 2009; Nieman et al. 2001; Nieman et al. 2002), as shown in Figure 2-1. Two studies were reported from the same research group, so one study was excluded from the analysis (Goetti et al. 2010). Twelve studies were performed on 4-slice CT (Achenbach et al. 2000; Becker et al. 2002; Haberl et al. 2005; Hunold et al. 2003; Jakobs et al. 2002 ; Knez et al. 2001; Kopp et al. 2002; Leber et al. 2003; Mahnken et al. 2003; Roos et al. 2002; Schroeder et al. 2001; Nieman et al. 2001), 13 on 16-slice CT (Anders et al. 2006; Chiou et al. 2005; Coles et al. 2006; Dill et al. 2008; Garcia, Lessick, and Hoffmann 2006; Hoffmann et al. 2005; Houslay et al. 2007; Kuettner et al. 2004; Leta et al. 2004; Mollet et al. 2004; Park et al. 2009; Yamamoto et al. 2006; Nieman et al. 2002), 1 on 40-slice CT (Gaspar et al. 2005), 23 on 64-slice CT (Achenbach et al. 2010; Alkadhi et al. 2008; Blankstein et al. 2009; Earls et al. 2008; Feuchtner et al. 2010; Francone et al. 2007; Freeman et al. 2009; Hausleiter, Bischoff, et al. 2009; Husmann et al. 2010; Leber et al. 2005; Maruyama et al. 2008; Meijboom et al. 2007; Mollet et al. 2005; Nikolaou et al. 2006; Pontone et al. 2009; Pugliese et al. 2006; Raff et al. 2005; Ropers et al. 2006; Shuman et al. 2008; Stolzmann et al. 2011; Wang et al. 2009; Xu et al. 2010; Zhao et al.

2009), 1 on 128-slice (Alkadhi et al. 2010), 5 on 256-slice (Chao et al. 2010; Chen et al. 2010; Walker et al. 2009; Weigold 2009; Efstathopoulos et al. 2009), and 6 on 320-slice CT (Dewey et al. 2009; Graaf et al. 2010; Hein et al. 2009; Hoe and Toh 2009; Rybicki et al. 2008; Steigner et al. 2009), respectively, and the remaining five studies consisted of a combination of different generations of MDCT scanners for comparative purposes (Deetjen et al. 2007; Hausleiter et al. 2006; Klass et al. 2009; Rixe et al. 2009; Van Mieghem et al. 2006). Therefore, according to the individual study cases, 12 studies were performed on 4-slice CT, 17 on 16-slice, 1 on 40-slice CT, 28 on 64-slice, 3 on 128-slice, 5 on 256-slice, and 6 on 320-slice CT.

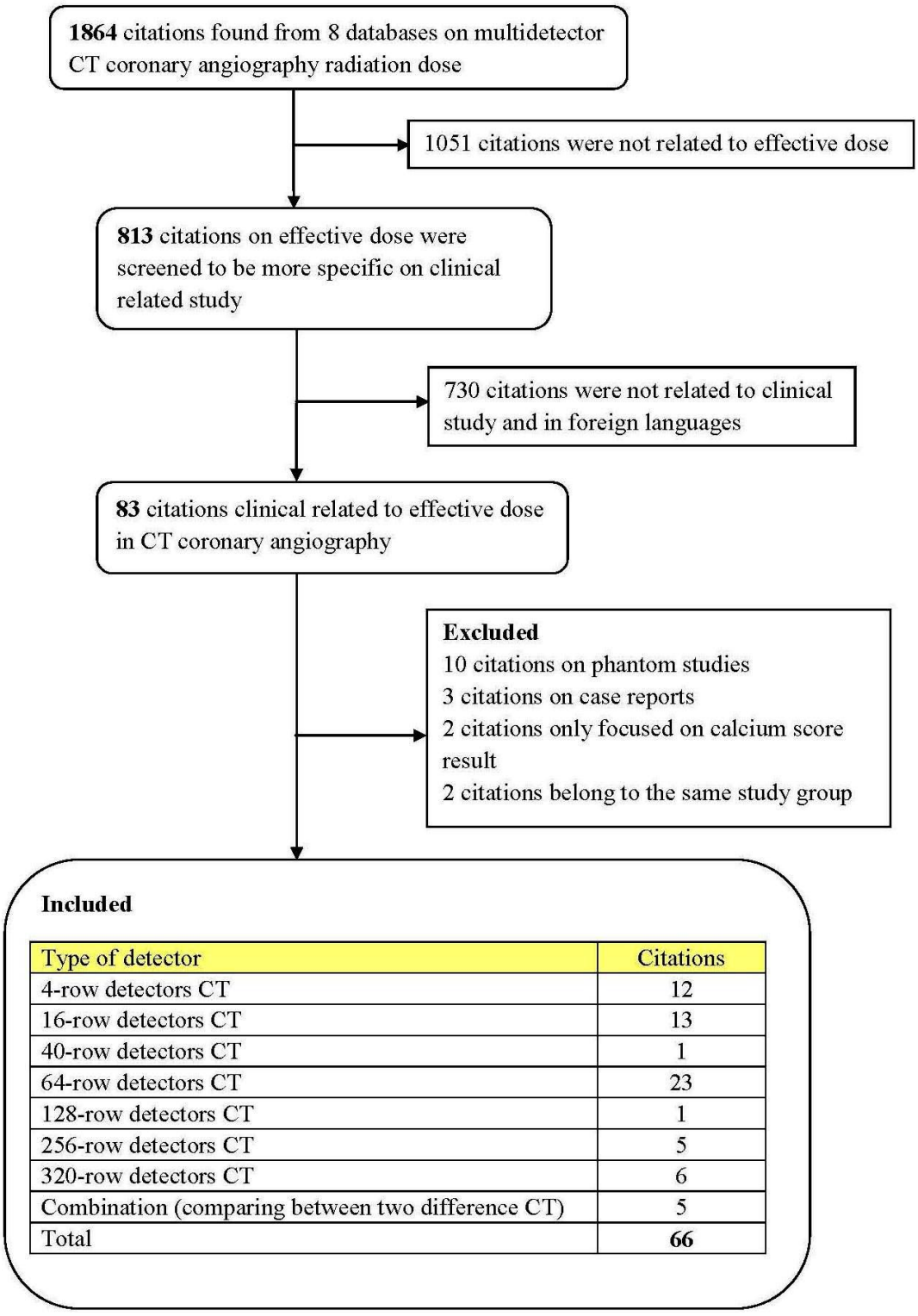

Type of detector	Citations
4-row detectors CT	12
16-row detectors CT	13
40-row detectors CT	1
64-row detectors CT	23
128-row detectors CT	1
256-row detectors CT	5
320-row detectors CT	6
Combination (comparing between two difference CT)	5
Total	**66**

Figure 2-1: Flow chart showing the search strategy of eligible references.

Four different manufacturers of CT scanners were used in the studies with different models. These included Siemens Medical Solution, Philips Medical System, GE Healthcare and Toshiba Corporation Medical System and are shown in Figure 2-2.

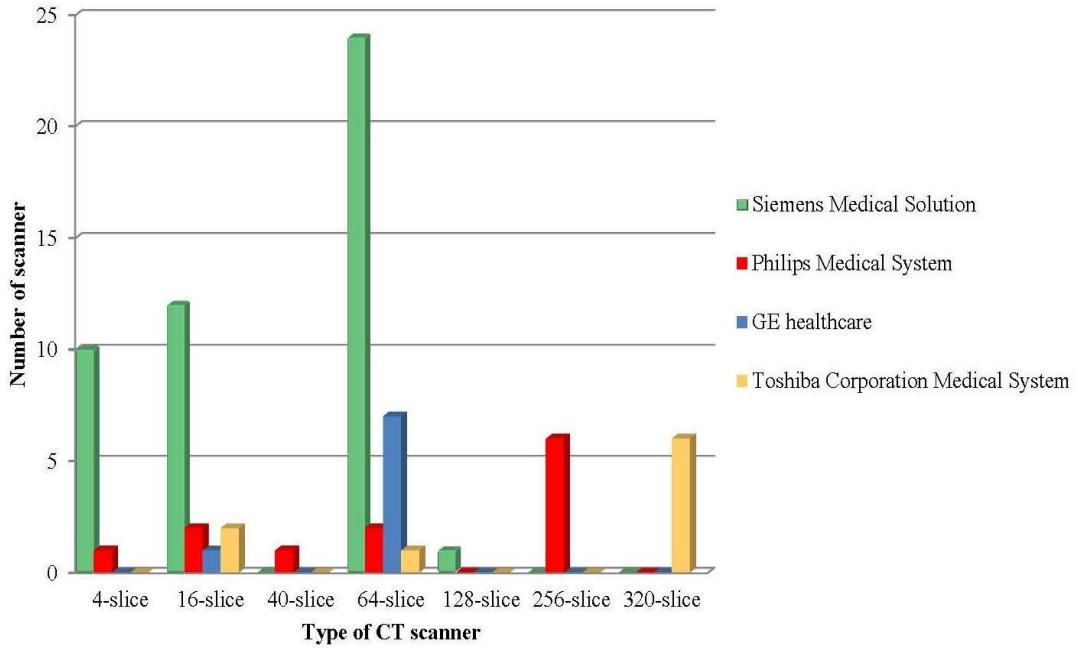

Figure 2-2: Different manufacturers are used in different multidetector CT scanners.

2.3.1 4- and 16-slice CT

Table 2-1 presents the mean effective dose (ED) associated with 4-slice CT coronary angiography in 12 studies, which is 6.0 ± 2.8 mSv. The results were analyzed with different variables such as gender, exposure parameters, and dose saving strategies. In the comparison between genders, the ED was estimated with 4.9 ± 2.5 mSv and 6.6 ± 3.1 mSv in male and female patients, respectively. However, four out of 12 studies did not specify the radiation dose in relation to the patient's gender, since only the mean ED was reported which is 7.0 ± 2.6 mSv (Knez et al. 2001; Leber et al. 2003; Nieman et al. 2001; Roos et al. 2002). Moreover, all studies were performed with retrospective ECG-gating scanning protocols of minimum 120 kVp and a pitch ranging from 0.375 to 2.0. Three out of 12 studies were performed with high pitch corresponding to the heart rate with a pitch of 1.5 used for heart rates below 80 bpm (beats per minute) and pitch 2.0 for heart rates more than 80 bpm (Jakobs et al. 2002 ; Kopp et al. 2002; Nieman et al. 2001).

The mean ED was estimated to be 10.4 ± 4.9 mSv in 16-slice coronary CTA with use of retrospective ECG-gating protocol. A 120 kVp protocol was consistently used in almost 90 per cent of 17 studies performed with 16-slice coronary CTA (Table 2-1), with beam collimation less than 1.0 mm and the mean ED being 9.6 ± 4.3 mSv, which is higher than in 4-slice CTA. A lower dose protocol with 100 kVp was implemented in two studies

(Hausleiter et al. 2006; Park et al. 2009), and the mean ED was 6.4 ± 1.9 mSv, indicating a dose reduction of up to 33 per cent.

Another effective approach for dose reduction called ECG-controlled tube current modulation was applied in six out of 17 studies. This was done to compare it with the conventional retrospective ECG-gating scan without use of tube current modulation. The analysis shows that ED in a scan protocol with application of tube current modulation was significantly lower (6.7 ± 1.8 mSv) than without using tube current modulation (11.6 ± 5.1 mSv) ($p<0.01$). Another aspect that could increase radiation dose is an extension of the scanning region (field of view) with 16-slice CT scanning protocol which may be done in some studies for purposes of reassessment of coronary bypass procedure. The mean ED increased from 9.8 ± 4.3 mSv to 14.8 ± 8.5 mSv if the scan range increased from 100 mm to 149 mm with the normal exposure parameter set at 120 kVp (Anders et al. 2006; Houslay et al. 2007; Yamamoto et al. 2006). Thus, the dose increased considerably with an extended scanning coverage area. However, the radiation dose was not compared between genders in 16-slice CT due to insufficient number of studies that had been conducted. One study was performed with 40-slice CT scanner (Brilliance 40 Philips Medical System) in coronary angiography (Table 2-1). Here the effective radiation dose was reported to be 9.9 ± 2.8 mSv, which is close to the 16-slice CT dose report (10.4 ± 4.9 mSv) (Gaspar et al. 2005).

Table 2-1: Study details of 4-slice, 16-slice and 40-slice CT coronary angiography

Author/Year of publication	No. of patients (male/female)	Mean Age (years)	Effective dose (mSv) (male/female)	Detector collimation (mm)	GRT (ms)	Pitch	Tube voltage (kVp)	Tube current (mA)
Achenbach et al. (2000)	16/9	56	3.9/5.8	4 × 1.0	500	0.375	140	150
Becker et al.(2002)	27/1	64	7.1/9.6	4 × 1.0	500	NS	120	300
Haberl et al.(2005)	83/50	67	5.8-7.4/ 7.6-9.8	4 × 1.0	NS	NS	120	300
Jakobs et al.(2002)	36/14	56.3	1.0/1.4[#]	4 × 2.5	500	1.5	120	100*
	36/14	55.7	1.9/2.5	4 × 2.5	500	1.5	120	100*
Knez et al.(2001)	38/6	60	9.5	4 × 1.0	500	NS	NS	-
Kopp et al.(2002)	79/27	62	5.5/6.5	4 × 1.0	500	1.5-2.0	120	300
Leber et al.(2003)	72/19	61.7	8.2	4 × 1.0	NS	NS	120	300
Mahnken et al.(2003)	27/8	62.3	5.4/7.8	4 × 1.0	500	0.375	120	400*
Nieman et al.(2001)	27/8	59	4.9	4 × 1.0	500	1.5-2.0	140	-
Roos et al.(2002)	20	60	8.85	4 × 1.0	500	0.38-0.75	120	250-400
	20	60	3.65	4 × 2.5	500	1.0	140	150
Schroeder et al.(2003)	13/2	58	6.7-10.9/ 8.1-13	4 × 1.0	500	1.5	140	400*
Anders et al.(2006)	29/3	67	3.4-4.8/ 5.1-7.1	12 × 0.75	420	NS	120	500*
Chiou et al.(2005)	65/7	58	9.0	12/16 × 0.75	420	NS	120	500
Coles et al.(2006)	27/13	60	15.3	16 × 0.75	420	NS	120	550*

	31/20	64	14.2[#]	12 × 0.75	420	NS	120	500*
Deetjen et al.(2007)	39/17	65.96	9.76	16 × 0.75	375	NS	120	550*
	41/10	58.84	5.58[#]	16 × 0.75	375	NS	120	550*
Dill et al. (2008)	49/7	66	9.76	16 × 0.75	375	0.16-0.2	120	550*
Garcia et al. (2006)	162/76	59.8	8.0	16 × 0.75	NS	NS	120-140	400-500
Hausleiter et al. (2006)	27/33	59.1	10.6	16 × 0.75	420	0.18	120	510
	33/33		6.4[#]	16 × 0.75	420	0.18	120	304
	34/34		5	16 × 0.75	420	0.21	100	387
Houslay et al.(2007)	43/7	66	18.5	16 × 1.00	500	0.25	135	250-300
Hoffmann et al.(2005)	57	61.5	8.1	16 × 0.75	420	0.2	120	240
	46		4.9	16 × 0.75	420	-	140	300
Kuettner et al.(2004)	44/16	58.3	5.4[#]	12 × 0.75	NS	NS	120	500
			10.1	12 × 0.75	NS	NS	120	500
Leta et al. (2004)	28/3	66	24.2	NS	NS	NS	120	250-350
Mollet et al. (2004)	113/15	58.9	9.85	16 × 0.75	420	NS	120	400-450
Nieman et al. (2002)	34	58	8-9	12 × 0.75	420	NS	120	400-450
Park et al. (2009)	105	55.9	7.8	16 × 0.75	420	0.2	100	600-630
	80	56.5	10.1	16 × 0.75	420	0.2	120	550-600
Rixe et al. (2009)	49/7	68	9.8	16 × 0.75	NS	0.2-0.24	120	550
Van-Mieghem et al. (2006)	27	61.2	11.8-16.3	16 × 0.75	420	NS	120	400-450
Yamamoto et al. (2006)	36/6	63.6	20.8	16 × 0.625	500/600	0.275	NS	350

Gaspar et al.(2005)	20/20	63.1	9.9	40 × 0.625	420	0.2	120	600-800

GRT= Gantry rotation time;*effective mAs; #Tube current modulation; NS= Not stated

2.3.2 64-slice CT

Twenty-eight studies were carried out using 64-slice CT and a number of comparisons were undertaken between them with different CT models. These are shown in Table 2-2. The comparisons consist of detector technology (single-source and dual-source CT), scanning protocol (prospective and retrospective ECG-gating), and tube voltage (100 and 120 kVp). Overall ED estimation in 64-slice CT was 10.0 ± 6.2 mSv. With conventional retrospective ECG-gating technique, the mean dose of 64-slice CT was 11.8 ± 5.9 mSv compared to prospectively ECG-gating protocol with estimated ED being 4.1 ± 1.7 mSv. The ED was compared between 100 kVp and 120 kVp scanning protocols from five studies (Hausleiter et al. 2006; Kuettner et al. 2004; Alkadhi et al. 2008; Feuchtner et al. 2010; Xu et al. 2010), with a total of 724 patients, with the corresponding mean ED at 5.6 ± 3.0 mSv and 10.7 ± 5.1 mSv, respectively, resulting in a dramatic dose reduction of 48 per cent ($p<0.01$).

Eight out of the 28 studies that were performed with 64-slice CT were scanned with dual-source CT scanners, which were all manufactured by Siemens Medical Solutions. In general, the mean ED in both single source CT (SSCT) and dual-source CT (DSCT) scanners was reported as 11.7 ± 6.3 mSv and 6.7 ± 4.6 mSv, respectively (Figure 2-3). However, the mean ED was differentiated between prospective and retrospective ECG-gating protocols in both scanners with use of DSCT and SSCT. The ED was 9.5 ± 3.9 mSv and 2.8 ± 1.7 mSv in studies performed with retrospective and prospective ECG-gating with DSCT, and 13.4 ± 5.7 mSv and 6.8 ± 5.1 mSv in studies using retrospective and prospective ECG-gating with SSCT, respectively, indicating a significant reduction of ED with prospective gating ($p<0.01$).

The purpose of padding is to provide extra phase information to compensate for variations in heart rate by adding time before and after the centre phase of the acquisition. Padding is described in the range of 0-200 ms and is added to both sides of the centre of the acquisition with padding 0 corresponding to a window of 100 ms scanning time and padding 100 corresponding to a window of 200 ms scanning time (Kalra et al. 2004). Application of padding helps to generate diagnostic images in patients with high heart rate variations; however, this leads to an increase of ED when compared with those without padding (Pontone et al. 2009). The effect of different paddings on radiation dose in prospective ECG-gating protocols was conducted in one study (Pontone et al. 2009), and the results showed that ED was estimated with 5.8 ± 1.8 mSv and 7.4 ± 3.0 mSv with use of 100 ms and 200 ms padding respectively. In contrast, the ED was much lower without padding (Pontone et al. 2009), which is 3.8 ± 1.2 mSv.

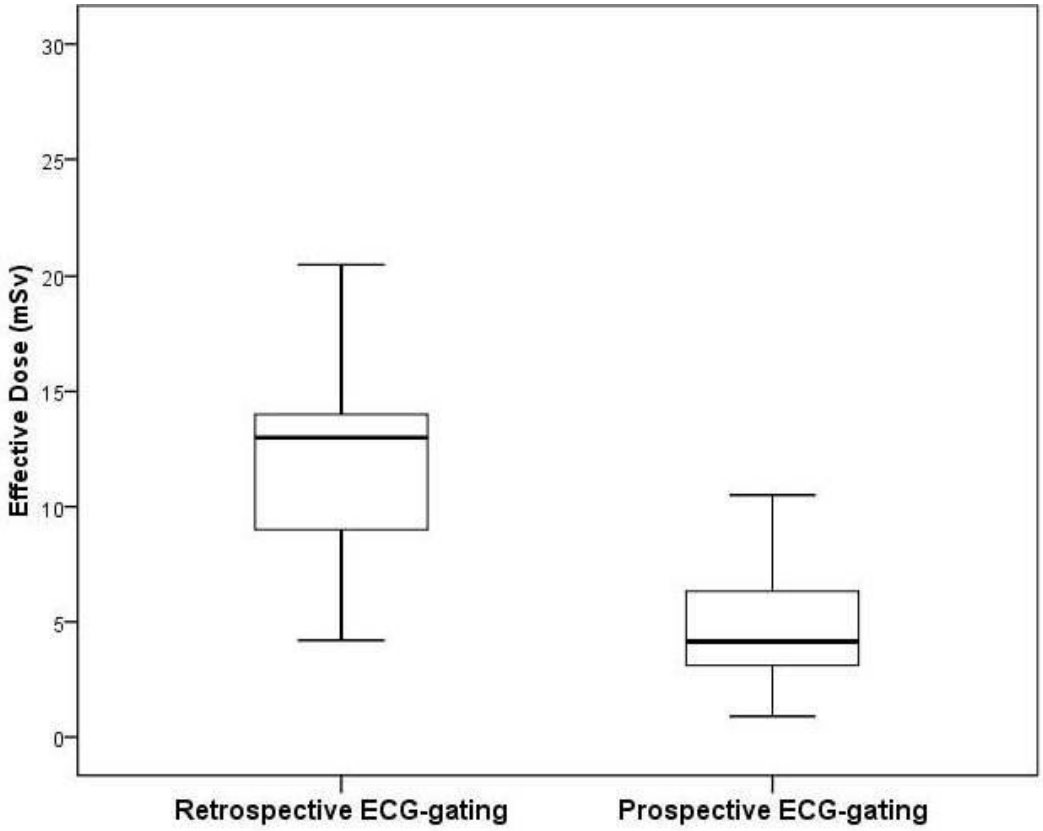

Figure 2-3: Box plot shows the mean effective dose reported in the studies with use of retrospective ECG-gating and prospective ECG-gating. It is obvious that the radiation dose of prospective gating MDCT angiography was significantly lower than that of retrospective gating protocol.

Table 2-2: Study details of 64-slice CT coronary angiography

Author/ Year of publication	No. of patients (male/ female)	Mean Age (years)	Effective Dose (mSv)	Detector collimation (mm)	GRT (ms)	Pitch	Tube voltage (kVp)	Tube current (mA)
Alkadhi et al.(2008)	36/14	57	9.0	2 × 32 × 0.6	330	0.2-0.5	120	330*
	15/13	61.5	2.9^	2 × 32 × 0.6	330	NS	120	330 *
	28/15	59.9	4.2	2 × 32 × 0.6	330	0.2-0.5	100	220*
	26/14	62.9	1.3^	2 × 32 × 0.6	330	NS	100	190*
Achenbach et al.(2010)	50	NS	0.87^	2 × 64 × 0.6	280	3.2-3.4	100	220-290
Blankstein et al.(2009)	114/74	56.5	13.4	2 × 32 × 0.6	330	0.3	80-140	320
	26/16	44.3	3.2^	2 × 32 × 0.6	330	-	80-140	200
Deetjen et al.(2007)	25/22	57.36	13.58	64 × 0.6	330	NS	120	850
Earls et al.(2008)	44/38	55.6	18.4#	64 × 0.625	350	NS	120	647
	71/50	56.7	2.8^	64 × 0.625	350	NS	120	508
Feuchtner et al.(2009)	26	53.1	9.6	32 × 0.6	330	0.2	100	500-800
	26	-	5.3#	32 × 0.6	330	0.2	100	500-800
	25	55.3	18.2	32 × 0.6	330	0.2	120	600-900
	26	-	8.7#	32 × 0.6	330	0.2	120	600-900
Francone et al.(2007)	108/6	63.1	9.5	32 × 2 × 0.6	330	0.2	120	800
Freeman et al.(2009)	157	56	20.3	64 × 0.625	350	NS	NS	NS
	748		3.02^	64 × 0.625	350	NS	NS	NS
	359		6.96^	64 × 0.625	350	NS	NS	NS

Hausleiter et al.(2006)	34/34	59.3	14.8	64 × 0.6	330	0.2	120	870
	36/36		9.4#	64 × 0.6	330	0.2	120	551
	21/49		5.4#	64 × 0.6	330	0.2	100	537
Hausleiter et al.(2009)	384	NS	19	64 × 0.625	NS	NS	100-120	NS
	123	NS	10#	64 × 0.625	NS	NS	120	NS
	380	NS	9#	64 × 0.6	NS	NS	120	NS
	521	NS	11#	2 × 32 × 0.6	NS	NS	100-120	NS
	138	NS	15#	NS	NS	NS	120	NS
Husmann et al.(2010)	28/12	54.9	2.1	64 × 0.625	350	NS	100-120	400-650
Klass et al.(2009)	58/22	58	3.36^	64 × 0.625	420	NS	120-140	150-210
Leber et al.(2005)	59	NS	10-14	64 × 0.6	330	NS	120	550-750
Maruyama et al.(2008)	71/26	69.9	21.1	64 × 0.625	350	NS	120	800
	47/29	69.1	4.3^	64 × 0.625	350	NS	120	800
Meijboom et al.(2007)	279/123	60	13.4-17.0	32 × 2 × 0.6	330	NS	120	850-960
Mollet et al.(2005)	34/18	59.6	15.2-21.4	32 × 2 × 0.6	330	NS	120	900
Nikolaou et al.(2006)	59/13	64	8-10	32 × 2 × 0.6	330	NS	120	850
Pontone et al.(2009)	65/15	64.3	20.5	64 × 0.625	350	NS	120	700
	70/10	64.8	5.7^	64 × 0.625	350	NS	120	700
Pugliese et al.(2006)	35	61	15-20	32 × 2 × 0.6	330	NS	120	900
Raff et al.(2005)	53/17	59	13-18	32 × 0.6	330	NS	120	750-850
Rixe et al.(2009)	22/33	55	8.6	64 × 0.6	330	0.2-0.3	120	850

	95	60	9.6	64 × 0.6	330	0.2-0.5	120	320
	25	60	3.8[#]	64 × 0.6	330	0.2-0.5	100	320
Ropers et al.(2006)	52/32	58	7.5-11.2	64 × 0.6	330	NS	120	750
Shuman et al.(2008)	31/19	47.5	26.7	64 × 0.625	330	0.2-0.3	120	600-790
	33/17	46	6.2[^]	64 × 0.625	330	1.0	100-120	400-500
Stolzmann et al.(2010)	70/30	64.5	8.1	2 × 32 × 0.6	330	0.2-0.4	100-120	330
	58/42	68	2.2[^]	2 × 32 × 0.6	330	0.2-0.4	100-120	190
Van Mieghem et al.(2006)	43	61.2	15.2-21.4	64 × 0.6	330	NS	120	900
Wang et al.(2009)	68/32	53.1	5.9-9.1[#]	2 × 32 × 0.6	NS	0.2-0.4	120	320
	42/18	52.5	9.3	64 × 0.6	NS	0.2	120	770
Xu et al.(2009)	26/24	54.6	7.4[#]	2 × 32 × 0.6	330	0.3-0.4	100	362
	25/25	54.6	3.4[^]	2 × 32 × 0.6	330	NS	100	418
	26/24	56.2	15.5	2 × 32 × 0.6	330	0.3-0.4	120	410
	25/25	56.2	6.5[^]	2 × 32 × 0.6	330	NS	120	506
Zhao et al.(2009)	25/5	58.7	14.6	2 × 32 × 0.6	330	NS	100-120	330-430
	23/7	58.7	2.2[^]	2 × 32 × 0.6	330	NS	100-120	200-260

[#]tube current modulation; *effective mAs; [^]Prospective ECG-triggering CCTA; GRT= gantry tube rotation; NS= Not stated

2.3.3 128-, 256- and 320-slice CT

With latest CT models such as 128-, 256- and 320-slice CT, prospective ECG-gating was found to dominate most scanning protocols, as shown in this analysis. Therefore, the mean ED was estimated for each generation of scanner with 3.6 ± 0.4 mSv, 3.0 ± 1.9 mSv and 7.6 ± 1.6 mSv in 128-, 256- and 320-slice CT respectively. However, some studies were conducted using retrospective ECG-gating in these latest CT generations. The mean estimation of ED was reported with 12.4 ± 1.4 mSv, 11.3 ± 3.8 mSv and 13.5 ± 0.7 mSv in 128-, 256- and 320-slice CT respectively. In the 256-slice CT study, the analysis showed that mean ED in retrospective ECG-gating protocol was even lower with use of tube current modulation (10.3 ± 3.7 mSv) than it was without using tube current modulation (14.1 ± 1.9 mSv) (Achenbach et al. 2000).

Table 2-3 shows studies performed with 320-slice CT, where all studies were conducted with prospective ECG-gating protocol. However, only one study used multiple heartbeats scanning protocol for higher heart rates in order to allow more data reconstruction (Hoe and Toh 2009). A study comparing the radiation dose between single and multiple heartbeat showed that the ED increases from 5.7 ± 1.7 mSv to 16.5 ± 4.2 mSv with use of up to three heartbeat scanning (Hoe and Toh 2009). However, in comparison with the latest generation of MDCT scanners, the ED in 320-slice CT with single-heartbeat scan is still higher than that estimated in 128- (3.6 ± 0.4 mSv) and 256-slice CT (3.0 ± 1.9 mSv).

Figure 2-4 shows the range of mean ED reported in this review based on different CT scanner generations. It is difficult to tell whether or not the increase of CT slices leads to an increase in the radiation dose since various dose saving strategies have been increasingly used in recent generations of MDCT scanners.

Table 2-3: Study details of 128-slice, 256-slice and 320-slice CT coronary angiography

Author/ Year of publication	No. of patients (male/female)	Mean Age	Effective Dose (mSv)	Detector collimation (mm)	GRT (ms)	Pitch	Tube voltage (kVp)	Tube current (mA)
Alkadhi et al.(2010)	38/12	62	1.4	2 × 64 × 0.6	280	0.2-0.5	100	320
	36/14	63	0.9[ψ]	2 × 64 × 0.6	280	3.4	100	320
Chao et al.(2010)	80/24	61.5	14.8[^^]	256 × 0.625	270	NS	120	592
	80/24	61.5	5.1	256 × 0.625	370	NS	120	925
Chen et al.(2010)	5/5	56.3	7.3[^^]	256 × 0.625	270	NS	120	700-900
	3/7	57.9	11.8[^^]	256 × 0.625	270	NS		
	8/2	60	4.7	256 × 0.625	270	NS		
	5/5	54.8	2.7	256 × 0.625	270	NS		
Efstathopoulos et al.(2009)	5/5	55.2	3.2	128 × 0.625	270	NS	120	180-250
	12/3	55.2	13.4[^^]	128 × 0.625	270			800-950
Klass et al.(2009)	58/22	60	3.42	2 ×128 ×0.625	270	NS	120-140	150-250
Walker et al.(2009)	2,811	NS	3.8	2 ×128 ×0.625	270	0.18	120	800
Weigold (2009)	77/12	NS	11.4[^^]	128 × 0.625	270	NS	120	NS
	77/12	NS	4.0	128 × 0.625	270	NS	120	NS
Dewey et al.(2009)	21/9	61	8.1	320 × 0.5	350	NS	120	350-450
Hein et al.(2009)	19/11	63.2	10.5	320 × 0.5	350	NS	120	400
Graaf et al.(2010)	34/30	61	3.9-10.8	320 × 0.5	350	NS	100,120,135	400-580
Hoe and Toh (2009)	109/42	56.3	5.7	320 × 0.5	350	NS	100-120	300-580

	24/12	54.7	13.0[φ]	320 × 0.5	350	NS	120	
	9/3	55.7	17.5[δ]	320 × 0.5	350	NS	120	
Rybicki et al.(2008)	5/1	61.5	14[^^]	320 × 0.5	350	NS	120	400-580
	23/11	52.7	7.2	320 × 0.5	350	NS	120	
Steigner et al.(2009)	28/13	53	6.7	320 × 0.5	350	NS	120	400-580

GRT= Gantry rotation time; [φ] 2-heart beat scan; [δ]3-heart beat scan; [Ψ] High pitch; [^^]Retrospective ECG-gating CCTA; NS= Not stated

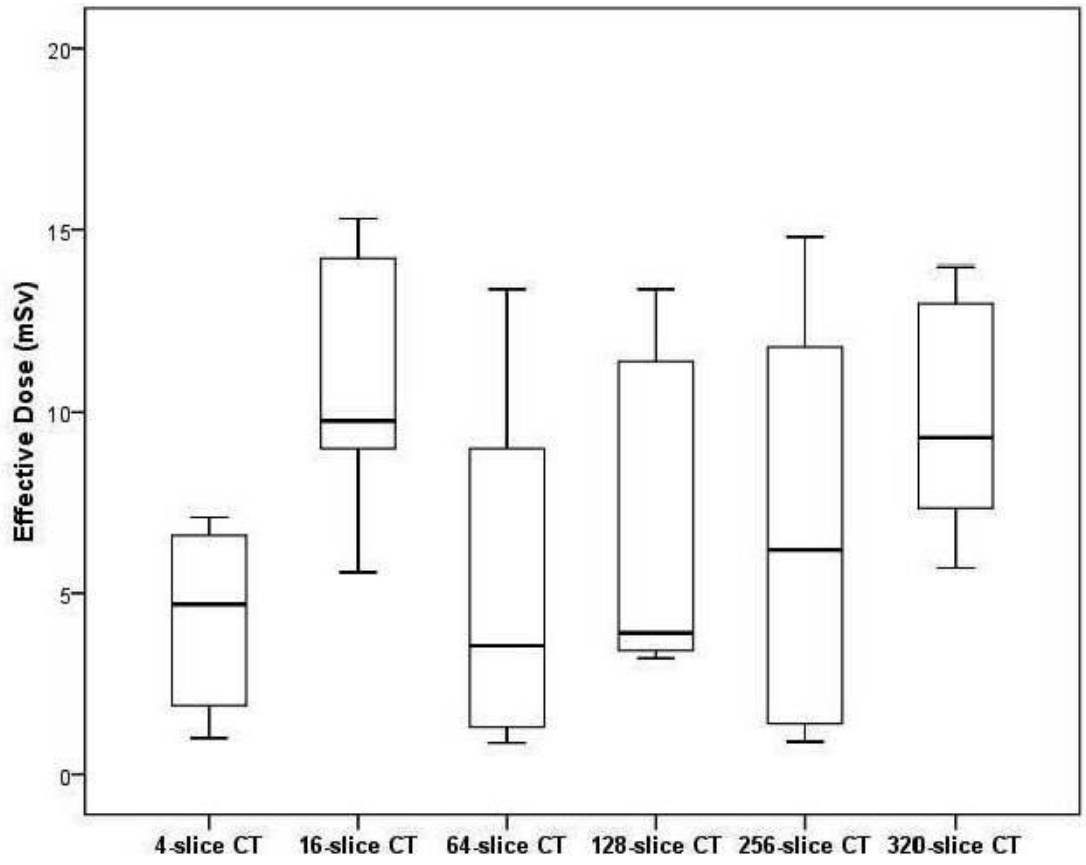

Figure 2-4: Distribution of mean effective dose between 4-, 16-, 64-, 128-, 256- and 320-slice multidetector CT scanners is displayed the box plot. Radiation dose increases with the increase of number of slices; in particular, this is apparent when comparing 4-slice with 16- and 64-slice CT. With latest models such as 128-, 256- and 320-slice CT, radiation dose was reduced to some extent as prospective gating is commonly used.

2.4 Discussion

This review indicates that radiation dose has risen from early generation scanners of 4-slice to 16- and 64-slice CT and will continue to do so if no dose-saving strategies are applied. With increased use of MDCT in coronary imaging due to technological developments the awareness of radiation risk has increased. Thus more and more dose-saving strategies are being employed to reduce the radiation dose while acquiring diagnostic images. This analysis confirms the trend as variable dose-reduction approaches were applied in recent CT scanners, especially 64-slice coronary CTA. This includes the highly effective strategy of ECG-controlled tube current modulation and very effective strategy of prospective ECG-gating, which result in a significant reduction of radiation dose.

Despite promising results of coronary CT angiography, coronary CTA suffers from the disadvantage of high radiation dose, and associated high radiation risks (Brenner and Hall 2007; Hausleiter, Meyer, et al. 2009). Brenner and Hall (2007) estimated that approximately between 1.5 and 2% of all cancers in the United States may be caused by radiation exposure from CT examinations (Brenner and Hall 2007). Davies et al (2011) estimated that in the UK radiation from CT scans causes 800 cancers per year in women and 1,300 in men (Davies, Wathen, and Gleeson 2011). Radiation exposure is especially unsafe for young and female patients as radiation effects are more severe in these groups than in older individuals and in men. Thus, protecting young and female patients from high radiation doses is very important. A recent study reported that one in 270 women aged 40 years who undergoes coronary CT angiography will develop cancer (Smith-Bindman et al. 2009). Therefore, coronary CT angiography should be performed with dose-saving strategies whenever possible so as to reduce the radiation dose to patients.

Several techniques were introduced to reduce the radiation dose in coronary CT imaging in order to accomplish the rule 'as low as reasonably achievable' (ALARA). Variable dose reduction techniques were applied in the studies, which included ECG-controlled tube current modulation, lower x-ray tube voltage, and prospective ECG-gated scanning (Nieman et al. 2001). ECG-controlled tube current modulation technique is regarded as one of the highly effective approaches for dose reduction (Kalra et al. 2004). This approach indicates that tube current can be adjusted in different cardiac phases so that high-quality diagnostic images of coronary arteries during the reconstruction window, and low-quality, higher noise images of the cardiac chamber and cardiac valves during the rest of the cardiac cycle can be achieved. This algorithm restricts the prescribed tube current to a pre-defined time window during the diastolic phase and decreases tube current in the systolic phase of the cardiac cycle, thus achieving significant dose reduction with this method (Coles et al. 2006).

With use of tube current modulation in MDCTA, radiation dose can be reduced between 20 to 50% depending on heart rate (Gies et al. 1999; Hausleiter et al. 2006; Jakobs et al. 2002 ; Walker et al. 2009). This corresponds to our analysis that showed dose reduction between 38 and 51% in 4-, 16-, 64- and 128-slice CT. Another effective approach to reduce radiation dose is to adjust the tube voltage, kVp. Although using a 100-kVp exposure reduces radiation dose between 33 and 48% in 16-slice and 64-slice CT compared to 120 kVp protocols, it should be emphasised that a low tube voltage protocol is only recommended in patients with small body mass index (BMI) or with BMI less than 25 $kg \cdot m^{-2}$ in order to keep the image quality at the diagnostic level (Abada et al. 2006).

Since the time that 64-slice CT was introduced, prospective gating technique has been increasingly used in coronary CT scanning due to its capability to lower radiation doses notably. This is reflected in our findings as the researchers showed increased concerns about the radiation dose associated with coronary CTA in application of variable dose-saving strategies. Prospective ECG-gating method is reported to reduce the ED between 70 and 87% compared to retrospective ECG gating, and results from this review are consistent with other reports (Earls 2009; Husmann et al. 2008; Shuman et al. 2008). According to this analysis, radiation dose was reduced between 66 and 73% with regard to any slice CT generations.

Further dose reduction can be achieved by a combination of prospective ECG gating with high pitch spiral acquisition, which results in a consistent dose below 1 mSv (Achenbach et al. 2010; Alkadhi et al. 2010). This is only achievable with the second generation of dual-source CT scanners with acquisition of 128-slices per gantry rotation, and high temporal resolution of 75 ms (Alkadhi et al. 2010). There is no doubt that prospective gating represents the very effective approach in reducing radiation dose; however, its application is limited to patients with a regular and low heart rate (<65 bpm), and no functional information is available from the scan.

Studies performed with 4-slice and 16-slice CT have shown that the effective radiation dose was estimated in female significantly higher than in male patients due to the different size thickness on the chest region. However, the breast tissue is radiosensitive and keeping the radiation dose to the breast at the minimum level is paramount. This also highlights the importance of reducing radiation dose in young female patients. It is estimated that ED of coronary CTA may reach up to 40 mSv in female patients if no dose-saving strategies are applied and there is associated radiation exposure to breast tissues (Husmann et al. 2008).

There are some limitations in this analysis. First, the searching criteria included only citations on radiation dose in coronary CT angiography from the selected databases. Five per cent of the articles were in non-English languages and were thus excluded from this review. Second, although there were many references especially on earlier types of CT scanners, the reports were limited to diagnostic accuracy, as most of the publications focused on image quality rather than on radiation dose. The development of CT scanners in particular, enabled researchers to improve the scanning technique or diagnostic quality but did nothing to raise awareness of radiation risk. Third, this analysis only looked at the radiation dose and did not assess diagnostic value or image quality related to different types of CT scanners. However, literature on the diagnostic accuracy of MDCT in CAD has been extensively studied and a number of meta-analyses have been published to show the increased accuracy of MDCT

from 4-slice to 64-slice CT (Paul and Abada 2007; Stein et al. 2008; Sun et al. 2008). Moreover, most of the studies on 256- and 320-slice CT were based on phantom experiments, which were excluded from the current analysis. Finally, some studies, especially those using 16-slice CT scanners did not provide detailed information about radiation dose in relation to gender. Thus, it is difficult to perform a comparison with other types of MDCT scanners.

2.5 Conclusion

Diagnostic value of MDCT angiography in the diagnosis of coronary artery disease has improved significantly with technological developments of MDCT technique, leading to increased application of MDCT in cardiac imaging. The amount of radiation dose that is associated with cardiac MDCT remains a major point of deliberation in clinical practice and is reflected in the increased use of dose-saving strategies, as shown in this analysis. With the latest MDCT scanners achieving high diagnostic accuracy, reduction of radiation dose has become a major concern to clinicians and manufacturers. Furthermore, awareness amongst clinicians to reduce radiation doses because of the risks associated with radiation has increased. This is indicated in the fact that more and more dose-saving strategies are being implemented in coronary CT angiography examinations.

2.6 References

Abada, H. T., C. Larchez, B. Daoud, A. Sigal-Cinqualbre, and J. F. Paul. 2006. MDCT of the coronary arteries: feasibility of low-dose CT with ECG-pulsed tube current modulation to reduce radiation dose. *Am J Roentgenol* 186: S387-S390.

Achenbach, S., M. Marwan, D. Ropers, T. Schepis, T. Pflederer, and K. Anders. 2010. Coronary computed tomography angiography with a consistent dose below 1mSv using prospectively electrocardiogram-triggered high-pitch spiral acquisition. *Eur Heart J* 31: 340-346.

Achenbach, S., S. Ulzheimer, U. Baum, M. Kachelrieß, D. Ropers, T. Giesler, W. Bautz, W. G. Daniel, W. A. Kalender, and W. Moshage. 2000. Noninvasive coronary angiography by retrospectively ECG-gated multislice spiral CT. *Circulation* 102: 2823-2828.

Alkadhi, H., P. Stolzmann, L. Desbiolles, S. Baumueller, R. Goetti, and A. Plass. 2010. Low-dose, 128-slice, dual-source CT coronary angiography: accuracy and radiation dose of the high-pitch and the step-and-shoot mode. *Heart* 96: 933-938.

Alkadhi, H., P. Stolzmann, H. Scheffel, L. Desbiolles, S. Baumüller, A. Plass, M. Genoni, B. Marincek, and S. Leschka. 2008. Radiation dose of cardiac dual-source CT: the effect of tailoring the protocol to patient-specific parameters. *Eur J Radiol* 68 (3): 385-391.

Anders, K., U. Baum, M. Schmid, D. Ropers, A. Schmid, K. Pohle, W. G. Daniel, W. Bautz, and S. Achenbach. 2006. Coronary artery bypass graft (CABG) patency: assessment with high-resolution submillimeter 16-slice multidetector-row computed tomography (MDCT) versus coronary angiography. *Eur J Radiol* 57 (3): 336-344.

Becker, C. R., A. Knez, A. Leber, H. Treede, B. Ohnesorge, U. J. Schoepf, and M. F. Reiser. 2002. Detection of coronary artery stenoses with multislice helical CT angiography. *J Comput Assist Tomogr* 26 (5): 750-755.

Blankstein, R., A. Shah, R. Pale, S. Abbara, H. Bezerra, M. Bolen, W. S. Mamuya, U. Hoffmann, T. J. Brady, and R. C. Cury. 2009. Radiation dose and image quality of prospective triggering with dual-source cardiac computed tomography. *Am J Cardiol* 103 (8): 1168-1173.

Brenner, D. J., and E. J. Hall. 2007. Computed tomography: an increasing source of radiation exposure. *N Engl J Med* 357 (22): 2277-2284.

Budoff, M. J., and M. Gupta. 2010. Radiation exposure from cardiac imaging procedures:do the risks outweigh the benefits? *J Am Coll Cardiol* 56 (9): 712-714.

Chao, S.-P., W.-Y. Law, C.-J. Kuo, H.-F. Hung, J.-J. Cheng, H.-M. Lo, and K.-G. Shyu. 2010. The diagnostic accuracy of 256-row computed tomographic angiography compared with invasive coronary angiography in patients with suspected coronary artery disease. *Eur Heart J* 31: 1916-1923.

Chen, L.-K., T.-H. Wu, C.-C. Yang, C.-J. Tsai, and J. J. S. Lee. 2010. Radiation dose to patients and image quality evaluation from coronary 256-slice computed tomographic angiography. *Nucl Instrum Methods Phys Res Sect A* 619: 368-371.

Chiou, K.-R., M.-T. Wu, S.-H. Hsiao, G.-Y. Mar, H.-B. Pan, C.-F. Yang, and C.-P. Liu. 2005. Safety and accuracy of multidetector row computed tomography for early assessment of residual stenosis of the infarct-related artery and the number of diseased vessels after acute myocardial infarction. *Am Heart J* 149 (4): 701-708.

Coles, D. R., M. A. Smail, I. S. Negus, P. Wilde, M. Oberhoff, K. R. Karsch, and A. Baumbach. 2006. Comparison of radiation doses from multislice computed tomography coronary angiography and conventional diagnostic angiography. *J Am Coll Cardiol* 47 (9): 1840-1845.

Davies, H. E., C. G. Wathen, and F. V. Gleeson. 2011. The risks of radiation exposure related to diagnostic imaging and how to minimise them. *Br Med J* 342: d947.

Deetjen, A., S. Mollmann, G. Conradi, A. Rolf, A. Schmermund, C. W. Hamm, and T. Dill. 2007. Use of automatic exposure control in multislice computed tomography of the coronaries: comparison of 16-slice and 64-slice scanner data with conventional coronary angiography. *Heart* 93: 1040-1043.

Dewey, M., E. Zimmermann, F. Deissenrieder, M. Laule, H.-P. Dübel, P. Schlattmann, F. Knebel, W. Rutsch, and B. Hamm. 2009. Noninvasive coronary angiography by 320-row computed tomography with lower radiation exposure and maintained diagnostic accuracy: comparison of results with cardiac catheterization in a head-to-head pilot investigation. *Circulation* 120 (10): 867-875.

Dill, T., A. Deetjen, O. Ekinci, S. Möllmann, G. Conradi, A. Kluge, C. Weber, M. Weber, H. Nef, and C. W. Hamm. 2008. Radiation dose exposure in multislice computed tomography of the coronaries in comparison with conventional coronary angiography. *Int J Cardiol* 124: 307-311.

Earls, J. P. 2009. How to use a prospective gated technique for cardiac CT. *J Cardiovasc Comput Tomogr* 3: 45-51.

Earls, J. P., E. L. Berman, B. A. Urban, C. A. Curry, J. L. Lane, R. S. Jennings, C. C. McCulloch, J. Hsieh, and J. H. Londt. 2008. Prospectively gated transverse coronary CT angiography versus retrospectively gated helical technique: improved image quality and reduced radiation dose. *Radiology* 246: 742-753.

Efstathopoulos, E. P., N. L. Kelekis, I. Pantos, E. Brountzos, S. Argentos, J. Greb´a, D. Ziaka, D. G. Katritsis, and I. Seimenis. 2009. Reduction of the estimated radiation dose and associated patient risk with prospective ECG-gated 256-slice CT coronary angiography. *Phys Med Biol* 54 (17): 5209-5222.

Feuchtner, G. M., D. Jodocy, A. Klauser, B. Haberfellner, I. Aglan, A. Spoeck, S. Hiehs, P. Soegner, and W. Jaschke. 2010. Radiation dose reduction by using 100-kV tube voltage in cardiac 64-slice computed tomography: A comparative study. *Eur J Radiol* 75: e51-e56.

Francone, M., A. Napoli, I. Carbone, M. Cavacece, P. G. Nardis, K. Lanciotti, S. Visconti, L. Bertoletti, E. D. Castro, C. Catalano, and R. Passariello. 2007. Noninvasive imaging of the coronary arteries using a 64-row multidetector CT scanner: initial clinical experience and radiation dose concerns. *Radiologia Medica* 112 (1): 31-46.

Freeman, A. P., R. Comerford, J. Lambros, S. Eggleton, and D. Friedman. 2009. 64 slice CT coronary angiography--marked reduction in radiation dose using prospective gating. *Heart Lung Circ* 18 (Supplement 3): S13-S13.

Frush, D. P., and T. Yoshizumi. 2006. Conventional and CT angiography in children: dosimetry and dose comparisons. *Pediatr Radiol* 36 (2): 154-158.

Garcia, M. J., J. Lessick, and M. H. K. Hoffmann. 2006. Accuracy of 16-row multidetector computed tomography for the assessment of coronary artery stenosis. *J Am Med Assoc* 296 (4): 403-411.

Gaspar, T., D. A. Halon, B. S. Lewis, S. Adawi, J. E. Schliamser, R. Rubinshtein, M. Y. Flugelman, and N. Peled. 2005. Diagnosis of coronary in-stent restenosis with multidetector row spiral computed tomography. *J Am Coll Cardiol* 46 (8): 1573-1579.

Gies, M., W. A. Kalender, H. Wolf, and C. Suess. 1999. Dose reduction in CT by anatomically adapted tube current modulation: simulation studies. *Med Phys* 26: 2235-2247.

Goetti, R., S. Leschka, S. Baumüller, A. Plass, M. Wieser, and L. Desbiolles. 2010. Low dose high-pitch spiral acquisition 128-slice dual-source computed tomography for the evaluation of coronary artery bypass graft patency. *Invest Radiol* 45 (6): 324-330.

Graaf, F. R., J. D. Schuijf, J. E. v. Velzen, L. J. Kroft, A. d. Roos, J. H. C. Reiber, E. Boersma, M. J. Schalij, F. Spano´, J. W. Jukema, E. E. van der Wall, and J. J. Bax. 2010. Diagnostic accuracy of 320-row multidetector computed tomography coronary angiography in the non-invasive evaluation of significant coronary artery disease. *Eur Heart J* 31: 1908-1915.

Haberl, R., J. Tittus, E. Böhme, A. Czernik, B. M. Richartz, J. Buck, and P. Steinbigler. 2005. Multislice spiral computed tomographic angiography of coronary arteries in patients with suspected coronary artery disease: An effective filter before catheter angiography? *Am Heart J* 149 (6): 1112-1119.

Hausleiter, J., B. Bischoff, F. Hein, T. Meyer, M. Hadamitzky, C. Thierfelder, T. Allmendinger, T. G. Flohr, A. Schömig, and S. Martinoff. 2009. Feasibility of dual-source cardiac CT angiography with high-pitch scan protocols. *J Cardiovasc Comput Tomogr* 3: 236-242.

Hausleiter, J., T. Meyer, M. Hadamitzky, E. Huber, M. Zankl, S. Martinoff, A. Kastrati, and A. Schömig. 2006. Radiation dose estimates from cardiac multislice computed tomography in daily practice: impact of different scanning protocols on effective dose estimates. *Circulation* 113: 1305-1310.

Hausleiter, J., T. Meyer, F. Hermann, M. Hadamitzky, M. Krebs, T. C. Gerber, C. McCollough, S. Martinoff, A. Kastrati, A. Schömig, and S. Achenbach. 2009. Estimated radiation dose associated with cardiac CT angiography. *J Am Med Assoc* 301 500-507.

Hein, P. A., V. C. Romano, A. Lembcke, J. May, and P. Rogalla. 2009. Initial experience with a chest pain protocol using 320-slice volume MDCT. *Eur Radiol* 19 (5): 1148-1155.

Hoe, J., and K. H. Toh. 2009. First experience with 320-row multidetector CT coronary angiography scanning with prospective electrocardiogram gating to reduce radiation dose. *J Cardiovasc Comput Tomogr* 3: 257-261.

Hoffmann, M. H. K., H. Shi, B. L. Schmitz, F. T. Schmid, M. Lieberknecht, R. Schulze, B. Ludwig, U. Kroschel, N. Jahnke, W. Haerer, H.-J. Brambs, and A. J. Aschoff. 2005. Noninvasive coronary angiography with multislice computed tomography. *J Am Med Assoc* 293 (20): 2471-2478.

Houslay, E. S., T. Lawton, A. Sengupta, N. G. Uren, G. McKillop, and D. E. Newby. 2007. Non-invasive assessment of coronary artery bypass graft patency using 16-slice computed tomography angiography. *J Cardiothorac Surg* 2: 27-34.

Hunold, P., F. Vogt, A. Schmermund, J. F. Debatin, G. Kerkhoff, T. Budde, R. Erbel, K. Ewen, and J. Barkhausen. 2003. Radiation exposure during cardiac CT: effective doses at multi–detector row CT and electron-beam CT. *Radiology* 226: 145-152.

Husmann, L., B. A. Herzog, I. A. Burger, R. R. Buechel, A. P. Pazhenkottil, P. von Schulthess, C. A. Wyss, O. Gaemperli, U. Landmesser, and P. A. Kaufmann. 2010. Usefulness of additional coronary calcium scoring in low-dose CT coronary angiography with prospective ECG-triggering: impact on total effective radiation dose and diagnostic accuracy. *Acad Radiol* 17 (2): 201-206.

Husmann, L., I. Valenta, O. Gaemperli, O. Adda, V. Treyer, C. A. Wyss, P. Veit-Haibach, F. Tatsugami, G. K. Schulthess, and P. A. Kaufmann. 2008. Feasibility of low-dose coronary CT angiography: first experience with prospective ECG-gating. *Eur Heart J* 29 (2): 191-197.

Jakobs, T. F., C. R. Becker, B. Ohnesorge, T. Flohr, C. Suess, U. J. Schoepf, and F. R. Maximilian. 2002 Multislice helical CT of the heart with retrospective ECG gating: reduction of radiation exposure by ECG-controlled tube current modulation. *Eur Radiol* 12 (5): 1081-1086.

Kalra, M. K., M. l. M. Maher, T. L. Toth, B. Schmidt, B. L. Westerman, H. T. Morgan, and S. Saini. 2004. Techniques and applications of automatic tube current modulation for CT. *Radiology* 233: 649-657.

Klass, O., M. Walker, A. Siebach, T. Stuber, S. Feuerlein, M. Juchems, and M. H. K. Hoffmann. 2009. Prospectively gated axial CT coronary angiography: comparison of image quality and effective radiation dose between 64- and 256-slice CT. *Eur Radiol* 20: 1124-1131.

Knez, A., C. R. Becker, A. Leber, B. Ohnesorge, A. Becker, C. White, R. Haberl, M. F. Reiser, and G. Steinbeck. 2001. Usefulness of multislice spiral computed tomography angiography for determination of coronary artery stenoses. *Am J Cardiol* 88 (10): 1191-1194.

Kopp, A. F., S. Schroeder, A. Kuettner, A. Baumbach, C. Georg, R. Kuzo, M. Heuschmid, B. Ohnesorge, K. R. Karsch, and C. D. Claussen. 2002. Non-invasive coronary angiography with high resolution multidetector-row computed tomography. *Eur Heart J* 23 (21): 1714-1725.

Kuettner, A., T. Trabold, S. Schroeder, A. Feyer, T. Beck, A. Brueckner, M. Heuschmid, C. Burgstahler, A. F. Kopp, and C. D. Claussen. 2004. Noninvasive detection of coronary lesions using 16-detector multislice spiral computed tomography technology. *J Am Coll Cardiol* 44 (6): 1230–1237.

Leber, A. W., A. Knez, C. Becker, A. Becker, C. White, C. Thilo, M. Reiser, R. Haberl, and G. Steinbeck. 2003. Non-invasive intravenous coronary angiography using electron beam tomography and multislice computed tomography. *Heart* 88 (6): 633-639.

Leber, A. W., A. Knez, F. von Ziegler, A. Becker, K. Nikolaou, S. Paul, B. Wintersperger, M. Reiser, C. R. Becker, G. Steinbeck, and P. Boekstegers. 2005. Quantification of obstructive and non-obstructive coronary lesions by 64-slice computed tomography: a comparative study with quantitative coronary angiography and intravascular ultrasound. *J Am Coll Cardiol* 46 (1): 147-154.

Leta, R., F. Carreras, X. Alomar, J. Monell, J. G. Picart, J. M. Augé, A. Salvador, and G. P. Lladó. 2004. Non-invasive coronary angiography with 16 multidetector-row spiral computed tomography: a comparative study with invasive coronary angiography. *Rev Esp Cardiol* 57 (3): 217-224.

Mahnken, A. H., J. E. Wildberger, A. M. Sinha, K. Dedden, S. Stanzel, R. Hoffmann, T. Schmitz-Rode, and R. W. Gunther. 2003. Value of 3D-volume rendering in the assessment of coronary arteries with retrospectively ECG-gated multislice spiral CT. *Acta Radiol* 44: 302-309.

Maruyama, T., M. Takada, T. Hasuike, A. Yoshikawa, E. Namimatsu, and T. Yoshizumi. 2008. Radiation dose reduction and coronary assessability of prospective electrocardiogram-gated computed tomography coronary angiography: comparison with retrospective electrocardiogram-gated helical scan. *J Am Coll Cardiol* 52 (18): 1450-1455.

Meijboom, W. B., A. C. Weustink, F. Pugliese, C. A. G. van Mieghem, N. R. Mollet, N. van Pelt, F. Cademartiri, K. Nieman, E. Vourvouri, E. Regar, G. P. Krestin, and P. J. de Feyter. 2007. Comparison of diagnostic accuracy of 64-slice computed tomography coronary angiography in women versus men with angina pectoris. *Am J Cardiol* 100 (10): 1532-1537.

Mollet, N. R., F. Cademartiri, K. Nieman, F. Saia, P. A. Lemos, E. P. McFadden, P. M. T. Pattynama, P. W. Serruys, G. P. Krestin, and P. J. de Feyter. 2004. Multislice spiral computed tomography coronary angiography in patients with stable angina pectoris. *J Am Coll Cardiol* 43 (12): 2265-2270.

Mollet, N. R., F. Cademartiri, C. A. G. van Mieghem, G. Runza, E. P. McFadden, T. Baks, P. W. Serruys, G. P. Krestin, and P. J. de Feyter. 2005. High-resolution spiral computed tomography coronary angiography in patients referred for diagnostic conventional coronary angiography. *Circulation* 112 (15): 2318-2323.

Naghavi, M., E. Falk, H. S. Hecht, M. J. Jamieson, S. Kaul, D. Berman, Z. Fayad, M. J. Budoff, J. Rumberger, T. Z. Naqvi, L. J. Shaw, O. Faergeman, J. Cohn, R. Bahr, W. Koenig, J. Demirovic, D. Arking, V. L. M. Herrera, J. Badimon, J. A. Goldstein, Y. Rudy, J. Airaksinen, R. S. Schwartz, W. A. Riley, R. A. Mendes, P. Douglas, and P. K. Shah. 2006. From vulnerable plaque to vulnerable patient--part III: executive summary of the screening for heart attack prevention and education (SHAPE) task force report. *Am J Cardiol* 98 (2, Supplement 1): 2-15.

Nieman, K., F. Cademartiri, P. A. Lemos, R. Raaijmakers, P. M. T. Pattynama, and P. J. de Feyter. 2002. Reliable noninvasive coronary angiography with fast submillimeter multislice spiral computed tomography. *Circulation* 106 (16): 2051-2054.

Nieman, K., M. Oudkerk, B. J. Rensing, P. van Ooijen, A. Munne, R.-J. van Geuns, and P. J. de Feyter. 2001. Coronary angiography with multi-slice computed tomography. *Lancet* 357 (9256): 599-603.

Nikolaou, K., A. Knez, C. Rist, B. J. Wintersperger, A. Leber, T. Johnson, M. F. Reiser, and C. R. Becker. 2006. Accuracy of 64-MDCT in the diagnosis of ischemic heart disease. *Am J Roentgenol* 187: 111-117.

Park, E.-A., W. Lee, J.-H. Kang, Y. H. Yin, J. W. Chung, and J. H. Park. 2009. The image quality and radiation dose of 100-kVp versus 120-kVp ECG-gated 16-slice CT coronary angiography. *Korean J Radiol* 10 (3): 235-243.

Paul, J. F., and H. T. Abada. 2007. Strategies for reduction of radiation dose in cardiac multislice CT. *Eur Radiol* 17: 2028-2037.

Pontone, G., D. Andreini, A. L. Bartorelli, S. Cortinovis, S. Mushtaq, E. Bertella, A. Annoni, A. Formenti, E. Nobili, D. Trabattoni, P. Montorsi, G. Ballerini, P. Agostoni, and M. Pepi. 2009. Diagnostic accuracy of coronary computed tomography angiography: a comparison between prospective and retrospective electrocardiogram triggering. *J Am Coll Cardiol* 54: 346-355.

Pugliese, F., N. R. A. Mollet, G. Runza, C. van Mieghem, W. B. Meijboom, P. Malagutti, T. Baks, G. P. Krestin, P. J. de Feyter, and F. Cademartiri. 2006. Diagnostic accuracy of non-invasive 64-slice CT coronary angiography in patients with stable angina pectoris. *Eur Radiol* 16 (3): 575-582.

Raff, G. L., M. J. Gallagher, W. W. O'Neill, and J. A. Goldstein. 2005. Diagnostic accuracy of noninvasive coronary angiography using 64-slice spiral computed tomography. *J Am Coll Cardiol* 46 (3): 552-557.

Rixe, J., G. Conradi, A. Rolf, A. Schmermund, A. Magedanz, D. Erkapic, A. Deetjen, C. W. Hamm, and T. Dill. 2009. Radiation dose exposure of computed tomography coronary angiography: comparison of dual-source,16-slice and 64-slice CT. *Heart* 95: 1337-1342.

Roos, J. E., J. K. Willmann, D. Weishaupt, M. Lachat, B. Marincek, and P. R. Hilfiker. 2002. Thoracic aorta: motion artifact reduction with retrospective and prospective electrocardiography-assisted multi–detector row CT. *Radiology* 222 (1): 271-277.

Ropers, D., J. Rixe, K. Anders, A. Küttner, U. Baum, W. Bautz, W. G. Daniel, and S. Achenbach. 2006. Usefulness of multidetector row spiral computed tomography with 64 × 0.6-mm collimation and 330-ms rotation for the noninvasive detection of significant coronary artery stenoses. *Am J Cardiol* 97 (3): 343-348.

Rybicki, F., H. Otero, M. Steigner, G. Vorobiof, L. Nallamshetty, D. Mitsouras, H. Ersoy, R. Mather, P. Judy, T. Cai, K. Coyner, K. Schultz, A. Whitmore, and M. Di Carli. 2008. Initial evaluation of coronary images from 320-detector row computed tomography. *Int J Cardiovasc Imaging* 24 (5): 535-546.

Schroeder, S., A. F. Kopp, A. Baumbach, A. Kuettner, C. Herdeg, A. Rosenberger, H. K. Selbmann, C. D. Claussen, M. Oberhoff, and K. R. Karsch. 2001. Noninvasive detection of coronary lesions by multislice computed tomography: results of the new age pilot trial. *Catheter Cardiovasc Interv* 53: 352-358.

Shuman, W., K. Branch, J. May, L. Mitsumori, D. Lockhart, T. Dubinski, B. Warren, and J. Caldwell. 2008. Prospective versus retrospective ECG gating for 64-detector CT of the coronary arteries: comparison of image quality and patient radiation dose. *Radiology* 248: 431-437.

Smith-Bindman, R., J. Lipson, R. Marcus, K.-P. Kim, M. Mahesh, R. Gould, A. B. de González, and D. L. Miglioretti. 2009. Radiation dose associated with common computed tomography examinations and the associated lifetime attributable risk of cancer *Arch Intern Med* 169 (22): 2078-2086.

Steigner, M., H. Otero, T. Cai, D. Mitsouras, and L. Nallamshetty. 2009. Narrowing the phase window width in prospectively ECG-gated single heart beat 320-detector row coronary CT angiography. *Int J Cardiovasc Imaging* 25 (85-90):

Stein, P. D., A. Y. Yaekoub, F. Matta, and H. D. Sostman. 2008. 64-slice CT for diagnosis of coronary artery disease: a systematic review. *Am J Med* 121 (8): 715-725.

Stolzmann, P., R. Goetti, S. Baumueller, A. Plass, V. Falk, H. Scheffel, G. Feuchtner, B. Marincek, H. Alkadhi, and S. Leschka. 2011. Prospective and retrospective ECG-gating for CT coronary angiography perform similarly accurate at low heart rates. *Eur J Radiol* 79: 85-91.

Sun, Z., G. H. Choo, and K. H. Ng. 2012 Coronary CT angiography: current status and continuing challenges. *Br J Radiol* 85 (1013): 495-510.

Sun, Z., C. Lin, R. Davidson, C. Dong, and Y. Liao. 2008. Diagnostic value of 64-slice CT angiography in coronary artery disease: a systematic review. *Eur J Radiol* 67: 78-84.

Sun, Z., and K. H. Ng. 2010a. Multislice CT angiography in cardiac imaging-part II: clinical applications in coronary artery disease. *Singapore Med J* 51: 282-289.

Sun, Z., and K. H. Ng. 2010b. Multislice CT angiography in cardiac imaging-part III: radiation risk and dose reduction. *Singapore Med J* 51: 374-380.

Tsapaki, V., and M. Rehani. 2007. Dose management in CT facility. *Biomed Imaging Interv J* 3 (2): e43.

Van Mieghem, C. A. G., F. Cademartiri, N. R. Mollet, P. Malagutti, M. Valgimigli, W. B. Meijboom, F. Pugliese, E. P. McFadden, J. Ligthart, G. Runza, N. Bruining, P. C. Smits, E. Regar, W. J. van der Giessen, G. Sianos, R. Domburg, P. Jaegere, G. P. Krestin, P. W. Serruys, and P. J. de Feyter. 2006. Multislice spiral computed tomography for the evaluation of stent patency after left main coronary artery stenting: a comparison with conventional coronary angiography and intravascular ultrasound. *Circulation* 114: 645-653.

Walker, M. J., M. E. Olszewski, M. Y. Desai, S. S. Halliburton, and S. D. Flamm. 2009. New radiation dose saving technologies for 256-slice cardiac computed tomography angiography. *Int J Cardiovasc Imaging* 25: 189-199.

Wang, M., H. Qi, X. Wang, T. Wang, J. Chen, and C. Liu. 2009. Dose performance and image quality: dual source CT versus single source CT in cardiac CT angiography. *Eur J Radiol* 72: 396-400.

Weigold, W. 2009. Low-dose prospectively gated 256-slice coronary computed tomographic angiography. *Int J Cardiovasc Imaging* 25 (SUPPL. 2): 217-230.

Xu, L., L. Yang, Z. Zhang, Y. Li, Z. Fan, X. Ma, B. Lv, and W. Yu. 2010. Low-dose adaptive sequential scan for dual-source CT coronary angiography in patients with high heart rate: Comparison with retrospective ECG gating. *Eur J Radiol* 76: 183-187.

Yamamoto, M., F. Kimura, H. Niinami, Y. Suda, E. Ueno, and Y. Takeuchi. 2006. Noninvasive assessment of off-pump coronary artery bypass surgery by 16-channel multidetector-row computed tomography. *Ann Thorac Surg* 81: 820-827.

Zhao, L., Z. Zhang, Z. Fan, L. Yang, and J. Du. 2009. Prospective versus retrospective ECG gating for dual source CT of the coronary stent: comparison of image quality, accuracy, and radiation dose. *Eur J Radiol* 77: 436-442.

CHAPTER 3: RADIATION DOSE ASSOCIATED WITH CORONARY CT ANGIOGRAPHY AND INVASIVE CORONARY ANGIOGRAPHY: AN EXPERIMENTAL STUDY OF THE EFFECT OF DOSE-SAVING STRATEGIES

3.1 Introduction

Invasive angiography is regarded as the gold standard technique for diagnostic and therapeutic purposes with regard to vascular diseases (Tan et al. 2007; Tins, Oxtoby, and Patel 2001). Since the emergence of the multislice CT, especially the extensive applications of CT angiography technique, invasive angiography examinations have been replaced by this less-invasive procedure with the aim of reducing procedure-related complications. Nowadays, the multislice CT angiography has become a reliable alternative to conventional angiography in many vascular applications due to its rapid technological developments, which lead to fast scanning and data acquisition with high spatial and temporal resolutions. In the United States, the numbers of CT examinations are estimated to increase gradually over the next ten years since many new applications are being developed for CT procedures to improve the diagnostic accuracy (Measurements 2009). In most clinical centers, multislice CT angiography is being increasingly used to replace conventional angiography as an alternative method in vascular imaging.

One of the main applications of multislice CT angiography is coronary CT angiography, with the diagnostic value having been significantly improved with rapid technical developments from the earlier generation of the 4-slice to the latest model 320-slice CT (Hein et al. 2009; Sun, Choo, and Ng 2012). Despite the high diagnostic value of coronary CT angiography, the radiation dose associated with coronary CT angiography has raised serious concerns in the medical field. In response to this concern, various dose-saving techniques have been introduced to reduce or minimize the radiation dose while acquiring diagnostic quality images. Parameters such as reduced tube voltage, prospective ECG-gating, and tube current modulations including, ECG-controlled and attenuation-dependent modulation have been reported to result in a significant dose reduction in cardiac CT (Sun, Choo, and Ng 2012 ; Sun and Ng 2010). As invasive coronary angiography is still regarded as the gold standard technique in diagnosing coronary artery disease, this procedure is retained with the latest developments in dose-reducing strategies, for instance, spectral shaping filter, pulsed fluoroscopy in cardiac angiography, flat panel detector, continuous half exposure, and the air gap technique in order to increase the accuracy and reduce radiation dose (Lederman et al. 2002; Partridge et al. 2006).

During coronary CT or invasive angiography examinations, it is not unusual for some organs to receive unnecessary exposure to radiation, which leads to the dose level exceeding the acceptable limits. Many radiosensitive organs are at a potential risk of being overexposed since they are located within the radiation exposure coverage, especially the breast tissue and the thyroid gland. It has been shown that the risk of lung or breast cancer development may correlate with radiation exposure from the chest CT scan (Erin Angel et al. 2009; Preston et al. 2003). Therefore, those organs need to be protected and monitored as there is a direct correlation between development of thyroid cancer and radiation exposure. Although many studies suggest that protective shielding results in a significant reduction of radiation dose (McLaughlin and Mooney 2004), it is not feasible to protect all of those organs as it may compromise image quality. It seems impractical to block those organs with designated shielding, which may obscure the regions of interest simultaneously. However, only certain organs are easily protected such as the thyroid gland, eyes (the lens) and the gonad but again, this depends on the type and purpose of the examination. Optimization of the technical parameters is another effective way to protect the radiosensitive organs by reducing radiation dose during CT examinations. The aim of the study was to compare the effective dose estimation (E) and entrance skin dose (ESD) of the selected radiosensitive organs through coronary CT angiography and invasive angiography performed with different protocol settings.

3.2 Materials and methods

3.2.1 Coronary angiography equipments

This study was performed on an anthropomorphic thorax phantom which represents an average male with 175 cm tall and a weight of 74 kg (Pixy, USA) with the use of a 64-slice CT scanner (Brilliance 64, Philips Healthcare, USA) and the Allura Xper FD20 with flat panel detector C-arm (Philips Medical, USA). Three coronary CT angiography protocols were set up for radiation-dose comparisons (E and ESD) including, standard retrospective gating without tube current modulation (routine protocol), retrospective ECG-gating with ECG-controlled tube current modulation (TCM), and prospective axial gating technique (dose-saving protocols). On the other hand, invasive coronary angiography procedure was performed in a series of 11 projections with four different protocols indicated by different magnifications of the flat panel detector of 1.6, 1.8, 2.2, and 2.5 magnification factors.

The ESD was measured using thermoluminescence dosemeter (TLD) rods and the E was determined by calculation from dose length product (DLP) and kerma air product (KAP).

Both doses were recorded during the procedures and compared for both, CT and invasive angiography.

3.2.2 Coronary CT angiography protocols

Since the coronary scan is needed to be triggered by the heart rate, the electrocardiogram leads were attached to a volunteer outside the scanning room for the heart rate readings prior to the scans. No contrast medium was used in this study. Therefore, no image quality assessment was observed throughout the procedures. The coronary CT angiography was performed with a detector collimation of 64 × 0.625 mm, slice thicknesses of 0.8 mm, field of view ranging from 150 mm to 174 mm, tube voltages of 120 kV, and adjustable tube current in the range of 300–500 mA. All the scan protocols were based on the same scout image and using the same volume of coverage in order to obtain the consistency of the study pattern. Specific protocols are detailed in Table 3-1.The protocols were selected and modified according to those applied in the department's routine practice. In addition, it was chosen based on previous studies which were recommended to produce a significant dose reduction as a dose-saving strategy in CT coronary angiography (Kalra et al. 2004; Sun, Choo, and Ng 2012). The DLP from each protocol scanned was recorded.

Table 3-1: Coronary CT angiography protocols

Parameters	**Protocol 1**	**Protocol 2**	**Protocol 3**
Collimation (mm)	64 × 0.625	64 × 0.625	64 × 0.625
Slice thickness (mm)	0.80	0.80	0.80
Increment (mm)	0.40	N/A	0.40
Pitch	0.20	N/A	0.20
Rotation time (s)	0.40	0.40	0.40
Cycle time (s)	N/A	1.90	N/A
FOV (mm)	174.00	150.00	160.00
Tube setting (kVp/mA)	120/381	120/500	120/381
Planned mAs (mAs/slice)	800	N/A	800
current·time (mAs)	800	210	800
Tagging (%)	75	75	75
Cardiac filter	Yes	No	Yes
Adaptive filter	Yes	SP	Yes
*Filter	XCB	XCB	XCB
Scan time (s)	9.98	5.48	9.98
Scan length (mm)	136.0	124.8	136.0
scan angle (°)	N/A	360	N/A
tilt (°)	N/A	0	N/A
Table speed (mm/sec)	19.0	N/A	19.0
Orientation	Feet first	Feet first	Feet first

N/A-not available; *Filter-Xres standard filter for coronary CT (XCB); Protocol 1: Retrospective ECG-gating without tube current modulation (standard); Protocol 2: Prospective ECG-gating; Protocol 3: Retrospective ECG-gating with tube current modulation.

3.2.3 Invasive coronary angiography procedures

Each invasive angiography protocol consisted of 11 projections including left anterior oblique (LAO) 15°/15° caudal, LAO 30°, LAO 30°/30° caudal, LAO 40°/60° caudal, left lateral 90°, anterior-posterior (AP) 30° caudal, AP 20° cranial, AP 40° cranial, right anterior oblique (RAO) 30°/30° cranial, RAO 35°, and RAO 40°/30° caudal. In addition, the dose area product (DAP) reading from each projection was recorded once it was complete. Each projection was obtained at 100–110 cm of source-to-image distance (SID) and at approximately 80 frames of dynamic acquisition. Those projections were suggested in order to cover the entire coronary anatomy during the invasive coronary angiography procedure. The sideways collimation was applied accordingly as in clinical practice to minimize the radiation dose. The exposure filter was selected with 0.10 mmCu/1.00 mmAl and 0.9 mmCu/1.00 mmAl for fluoroscopy filtration from the angiographic system and automatic exposure control was applied. Specific protocols are recorded in Table 3-2.

3.2.4 Radiation dose measurements

ESD was measured by placing the TLD rods securely above the radiosensitive organs on the phantom skin surface. It was paramount to identify the highest point of radiation dose received by organs from the overall dose distribution which includes exposure from either the primary beam or the secondary radiation beams, depending on the location of these organs during coronary CT and invasive angiography procedures. The ESD was then recorded in milligray (mGy) after undergoing a series of procedures including annealing, calibration, radiation dose exposure, and read-out process. The annealing and dose read-out was performed with a Harshaw-5500 reader (Thermo Electron Corp., USA) while calibration was performed with general x-ray machine (Shimadzu, Japan). TLDs calibration was designed to create a graph pattern for radiation dose conversion from nanoculomb (nC) to miligray (mGy) by exposing it to a known dose, which was measured with a digital radiation survey meter (model 660) having an ion-chamber model 660-3 beam measurement probe and a readout/logic unit (model 660-1). These TLDs were interpreted 24 hours after the exposure. The TLD used in this study was micro-rod shaped and sealed in numbered, cylindrical tubing.

Table 3-2: Invasive coronary angiography protocols

Protocols	**Protocol 1 (1.6*)**			**Protocol 2 (1.8*)**			**Protocol 3 (2.2*)**			**Protocol 4 (2.5*)**		
Tube position	kV/mA	time (ms)	Frames	kV/mA	time (ms)	Frames	kV/mA	time (ms)	Frames	kV/mA	time (ms)	Frames
LAO 15°/15°↓	68/470	5	81	68/505	5	79	70/613	5	80	73/653	6	76
LAO 30°/0°	67/455	4	81	67/426	4	82	68/495	5	81	71/628	5	79
LAO 30°/30°↓	70/579	5	83	70/608	5	83	74/660	6	79	75/671	6	79
LAO 60°/40°↓	86/625	7	80	90/596	8	81	99/544	8	77	101/531	8	81
LT Lat 90°/0°	66/391	4	81	66/411	4	81	68/495	5	80	70/593	5	81
AP 0°/30°↓	66/406	4	80	68/505	5	80	70/593	5	82	72/647	5	80
AP 0°/20°↑	65/322	4	80	66/376	4	75	68/480	5	81	69/549	5	80
AP 0°/40°↑	67/436	4	80	68/515	5	78	71/618	5	81	73/656	6	81
RAO 30°/30°↑	64/297	4	80	65/362	4	79	67/436	4	83	69/554	5	82
RAO 35°/0°	65/342	4	79	66/391	4	80	67/455	4	80	68/470	5	80
RAO 40°/30°↓	71/623	5	80	72/650	5	80	74/663	6	84	76/677	6	78

*Magnification factor; LAO- Left anterior oblique; LT-Left; LAT- Lateral; AP- Anterior posterior; RAO-Right anterior oblique

A total of eighteen TLDs were securely taped on the phantom skin surface over the radiosensitive organs for each protocol whereas; three were placed on the bilateral thyroid, breast, and gonad organs in order to measure the dose distribution during the procedures. Four invasive angiography protocols were designed with different flat panel detector magnifications ranging from 19 cm to 31 cm indicating between 1.6 and 2.5 magnification factors. Similar to the coronary CT angiography procedure, 18 different TLDs were used and placed at exactly the same locations in each protocol magnification for dose comparison. The TLD readings of a specific organ were averaged to calculate the dose for this organ.

The E was obtained by straightforward calculation based on a formula. The formula required DLP from CT scans and dose area product (DAP) from invasive angiography. DAP is a quantity known to many interventionalists and it is numerically equal to the KAP which KAP is the quantity recommended by the International Commission on Radiation Units (ICRU) to measure patient doses in interventional radiology (Vano et al. 2009). Both the DAP and the DLP were then multiplied with dose conversion co-efficient factor (DCC) distinctively. The DCC factor was derived from the parts anatomically-specific to the region of the body being scanned in CT while DCC for invasive angiography was derived from a study which met the specific exposure conditions in the coronary angiography procedure (Schultz and Zoetelief 2005). A conversion factor of 0.017 $mSv \cdot mGy^{-1} \cdot cm^{-1}$ was used for the calculation of the E in the chest region (Huda, Ogden, and Khorasani 2008) in coronary CT angiography and 0.2 $mSv \cdot Gy^{-1} \cdot cm^{-2}$ was used to calculate the E in invasive coronary angiography (Broadhead et al. 1997; Schultz and Zoetelief 2005).

3.2.5 Statistical analysis

All data were entered into SPSS V17.0 (SPSS, version 17.0 for Windows, Chicago, Illinois, USA) for statistical analysis. A p-value of <0.05 was considered to indicate statistically significant differences. All of the doses from each protocol were presented in box plot. One-way ANOVA and repeated measures ANOVA were used in ESDs analysis to determine the existing difference in mean ESD of radiosensitive organs (thyroid, breast and gonad) in both CT and invasive coronary angiography of all protocols. With regard to the effective dose, the ANOVA test is perform to determine the significant difference of mean values between the protocols. Moreover, a Duncan multiple range test is used to facilitate statistical comparisons among the mean values in invasive coronary projections.

3.3 Results

3.3.1 Coronary CT angiography

There were no significant differences in ESD measurements between the radiosensitive organs as tested with one-way ANOVA at p=0.32. However, with repeated measures ANOVA, the ESD measured in thyroid, breast and gonad differed significantly within all three protocols (standard retrospective ECG gating, retrospective ECG gating with tube current modulation and prospective ECG gating) at $p<0.05$. Apparently, ESD was found to be the highest at the breast compared to other organs with a mean value of 79.2 ± 1.13 mGy acquired with standard retrospective gating (protocol 1), 34.7 ± 1.9 mGy with prospective ECG-gating technique (protocol 2), and 38.6 ± 0.10 mGy with retrospective with tube current modulation (protocol 3) (Figure 3-1). In fact, the dose received by the breast was six times greater than that by the thyroid during the procedure.

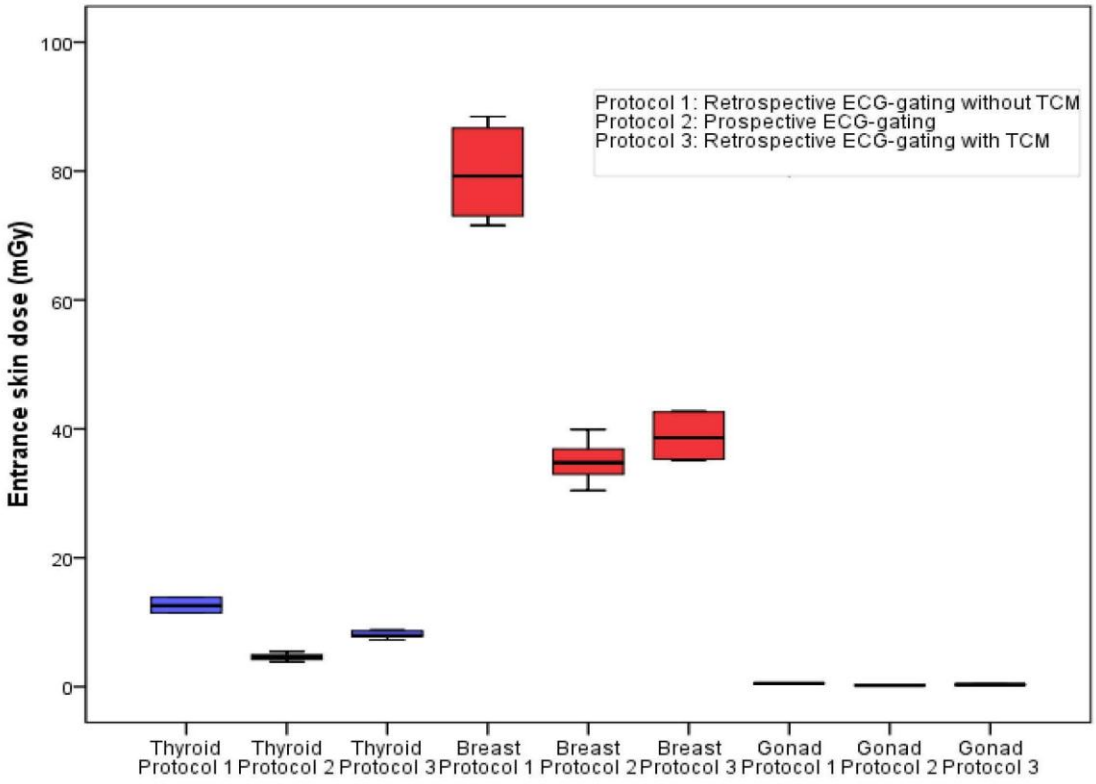

Figure 3-1: Box plot shows the mean ESD of 3 radiosensitive organs (the thyroid, breast, and gonad) in CT coronary angiography. It shows that the breast received the highest dose distribution compared to the thyroid and gonad in prospective gating, retrospective gating with and without tube current modulation.

On the other hand, the DLP was recorded individually for dose comparison among the three protocols (standard retrospective ECG gating, retrospective ECG gating with tube current

modulation and prospective ECG gating) with the inclusion of effective dose estimation. Statistically, there are enormous differences between mean E due to protocols. The p values are reported to be very small ($p<0.001$). The mean effective dose demonstrated that the standard retrospective gating protocol (protocol 1) resulted in the highest dose of 9.6 ± 0.12 mSv, followed by retrospective gating with tube current modulation (protocol 3) (3.3 ± 0.5 mSv), and prospective gating (protocol 2) (2.5 ± 0.8 mSv).

3.3.2 Invasive coronary angiography

Entrance skin dose was measured and recorded for all three radiosensitive organs (the thyroid, the gonads, and the breast) in all four protocols (1.6, 1.8, 2.2, and 2.5 magnification factor). Overall, this study found that ESDs differed insignificantly between radiosensitive organs (thyroid, breast and gonad) as tested with one-way ANOVA at $p=0.26$. However, on further examination with the repeated measures ANOVA, there is a significant difference in ESD within the protocols. In other words, the changes in dose received by organ is significant when the magnification increased or decreased with $p<0.05$. Therefore, thyroid gland returns with higher scores than breast and gonad in all protocols with resultant 3.2 ± 0.7 mGy, 2.0 ± 0.4 mGy, 1.6 ± 0.2 mGy, and 1.4 ± 0.3 mGy corresponding to 1.6 (protocol 1), 1.8 (protocol 2), 2.2 (protocol 3), and 2.5 FD magnifications (protocol 4) (Figure 3-2).

Different magnifications of flat panel detector indicated dose variations among all 11 projections during invasive coronary angiography. The DAP was recorded to determine the radiation dose production in each projection (Table 3-3). The results showed that the LAO 60° with caudal 40° (spider view) projection produced the highest dose which is about 2.3 times higher than the average dose of overall projections significantly as tested with Duncan's multiple comparisons. The effective dose estimation was calculated then from the DAP of total projections at the end of each examination to compare the protocols. The mean effective dose differed significantly across all magnification settings with ANOVA test at $p < 0.05$. Results showed the highest mean of E estimation to be 7.26 ± 0.05 mSv calculated at 1.6 FD magnifications (protocol 1). The effective dose was reduced significantly with 6.35 ± 0.05 mSv, 5.58 ± 0.01mSv, and 4.71 ± 0.07 mSv ($p<0.05$) being achieved and corresponding to the smaller magnifications of 1.8 (protocol 2), 2.2 (protocol 3), and 2.5 (protocol 4), respectively.

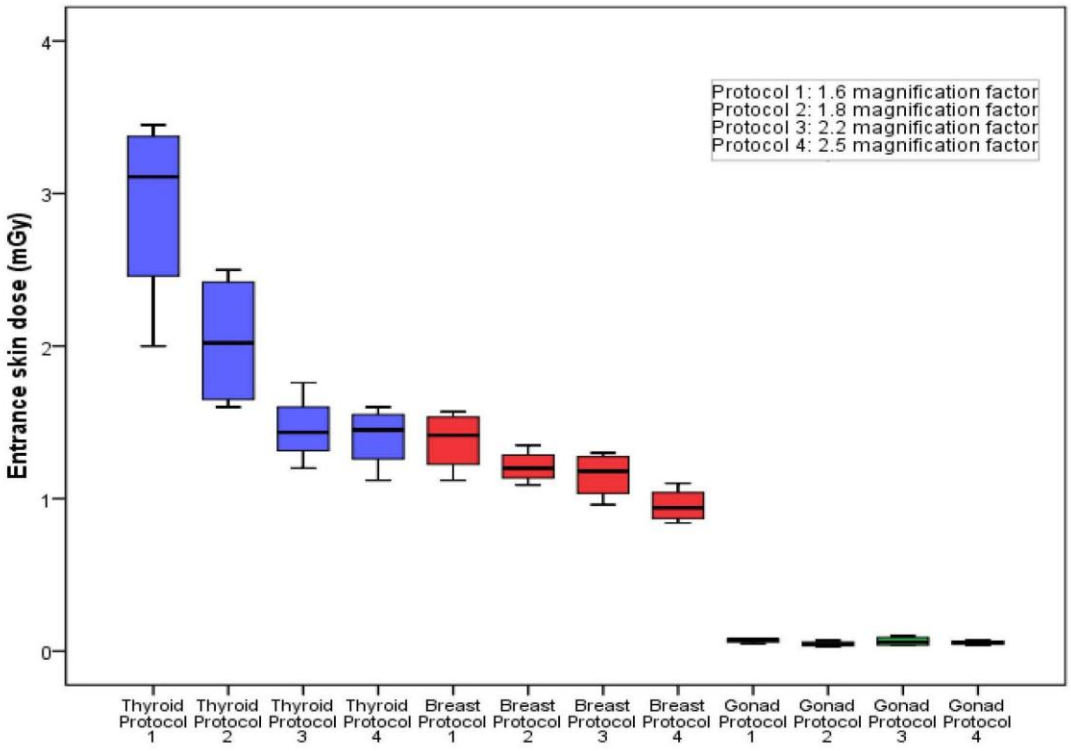

Figure 3-2: Distribution of mean ESD measured at 3 radiosensitive organs (the thyroid, breast, and gonad) in invasive coronary angiography with the use of different magnification factors displayed by the box plot. Apparently, the thyroid gland received the highest radiation dose compared to breast and gonad in all 4 protocols. However, it still remains below 3 mGy which meets the reference dose limit set by European Commission DIMOND III project (2003).

Table 3-3: Dose area product (DAP) results in invasive coronary angiography protocols

Tube position/ Protocols	**Protocol 1 (1.6*) ($mGy \cdot cm^2$)**	**Protocol 2 (1.8*) ($mGy \cdot cm^2$)**	**Protocol 3 (2.2*) ($mGy \cdot cm^2$)**	**Protocol 4 (2.5*) ($mGy \cdot cm^2$)**
LAO 15°/15°↓	2786	2900	2660	2178
LAO 30°/0°	3190	2222	1966	1746
LAO 30°/30°↓	4259	3838	3383	2677
LAO 60°/40°↓ (spider view)	7843	6442	4911	3854
LT LAT 90°/0°	2407	1905	1751	1750
AP 0°/30°↓	2760	2773	2650	2180
AP 0°/20°↑	1913	1693	1794	1578
AP 0°/40°↑	3057	2802	2717	2429
RAO 30°/30°↑	1624	1581	1463	1573
RAO 35°/0°	2012	1792	1540	1160
RAO 40°/30°↓	4472	3681	3076	2415

*Magnification factor; LAO- Left anterior oblique; LT-Left; LAT- Lateral; AP- Anterior posterior; RAO-Right anterior oblique

3.4 Discussion

This study demonstrates four important findings of radiation dose reduction in coronary angiography using CT angiography and the invasive approach. Firstly, coronary CT angiography results in an effective dose that is about 2.5 times higher than that of invasive angiography. Secondly, dose-saving protocols in coronary CT angiography (prospective gating and attenuation dependent tube current modulation) help to reduce the effective dose significantly up to 70% when compared with a standard retrospective gating. Thirdly, effective dose arising from invasive angiography is decreased up to 13% with an increase in magnifications. Finally, invasive angiography leads to a significant reduction in entrance skin dose up to 95% compared to CT coronary angiography at three radiosensitive organs (the thyroid, the breast, and the gonads).

Many studies have reported that the prospective ECG-gating reduces effective dose significantly between 60% and 90% when compared with retrospective ECG-gating (Earls 2009; Freeman et al. 2009). The prospective gating uses a step-and-shoot technique with the radiation beam turned on only at selected cardiac phase, and turned off for the remaining cardiac cycle to keep the dose to a minimum. This is confirmed in our results as the prospective ECG-gating reduces the effective dose by up to 70% compared with retrospective gating.

Radiation dose in CT can be reduced significantly by applying the approach of tube current modulation. Either ECG-controlled or anatomical-dependent tube current modulation results in effective dose reduction significantly between 22% and 52% compared to retrospective ECG-gating without any modifications (Greess et al. 2002; Mayo and Leipsic 2009). In ECG-controlled modulation, the tube current is reduced to the level between 46% and 80% from its maximum at diastole (60–80% of R-R interval) (Mayo and Leipsic 2009). Our findings are consistent with these reports as the results demonstrate a significant reduction of about 65% in effective dose with ECG-controlled tube current modulation when compared with the corresponding retrospective gating.

The entrance skin dose received by each organ varies differently in coronary CT and invasive coronary angiography. This is because of the distance between the x-ray tube and the response organ during the exposure and their locations. For example, in CT coronary angiography, the cardiac phantom was positioned at the center of the x-ray tube so that the breast would receive the maximum dose from the primary radiation beam. However, the thyroid and the gonad only received scattered radiation since they were anatomically situated away from the breast. This was verified by the TLD measurement in our study. In invasive

angiography, the situation was slightly different. The measured thyroid gland dose was the highest compared to that from the breast and the gonad. The caudal tube angulation brings the x-ray tube closer to the thyroid gland and results in increased radiation dose as stated in the inverse square law (Kuon et al. 2004). Moreover, the repetition of caudal tube angulation performed in this study (6 out of 11) explained the fact that the thyroid gland received higher radiation dose than other organs.

Although radiation dose values in both, CT and invasive angiography, such as DAP, air kerma, DLP, and the CT dose index could not be compared directly due to different measurement units, the estimations of effective dose is still measureable and comparable in those angiographic systems. Effective dose represents a general dose quantification of the biological risk in medical exposure where it is not a quantity that can be measured independently. It can only be derived by computation from a model or simulation that has estimated the dose for individual tissues (Martin 2007). Our study estimates the effective dose in all protocols of CT and invasive angiography for comparison. It is essential to provide information and create awareness about radiation dose in angiography among patients, Radiologists, imaging technologists, and the public.

Our study investigates 11 common projections in invasive coronary angiography to cover all the cardiac vessels. The left anterior oblique/caudal (spider view) is shown with 3 times higher dose production compared to other projections. This was reported as being similar to a previous study by Kuon et al. (2004), where the dose was increased up to 2.6 times and 3.7 times higher when the angulation was continuously raised from right to left anterior oblique and cranial to caudal tube angulation, respectively (Kuon et al. 2004). However, the dose was reported to be decreased significantly with every 10° decrement in tube angulations. Since this view is important to optimize the visualization of the left circumflex artery with obtuse marginal, left main artery, bifurcation of left anterior descending and the diagonal artery, therefore, there is no other option but to reduce the dose by eliminating this projection other than limiting the angulation and regulating the time duration of the exposure wisely.

The entrance skin dose was taken into consideration in this study since it predicted the possibility of getting deterministic skin injuries ranging from skin erythema, moist desquamation, epilation, laceration, to necrosis if the skin was exposed beyond the threshold dose at 2 Gy (Bogaert et al. 2009). Deterministic injuries to the skin are associated with overexposure regardless of high radiation exposure setting or increased length of exposure. Therefore, 45 $Gy \cdot cm^2$ was proposed as the diagnostic reference level for coronary angiography by the European Commission DIMOND III project in 2003 in order to prevent the interventionalist from going beyond that dose threshold (Neofotistou et al. 2003).

However, even though the skin received a radiation dose below the dose threshold, it was still at the risk of developing radiation-induced cancer from the stochastic effects.

Our study has its limitations. Although the protocols were developed from previous reports in the literature on CT dose-saving strategies, it is still difficult to measure the accuracy on the protocol guideline since the image quality assessment has not been taken into account. However, this study only used an anthropomorphic phantom to simulate the radiation dose quantification on a standardized patient. No contrast medium was used in any of the angiography protocols. Therefore, there is no way of comparing and assessing image quality, since no contrast enhancement in the coronary arteries could be visualized. Thus, further studies are necessary to verify the accuracy of our results through the administration of a contrast medium and qualitative and quantitative assessment of image quality.

3.5 Conclusion

In conclusion, this study shows that invasive angiography produces significantly lower radiation dose than coronary CT angiography, which is demonstrated by effective dose and entrance skin dose. Modification techniques in coronary CT (dose-saving protocols) and invasive angiography (multi-size magnification) are recommended in daily clinical practice since they produce further dose reduction.

3.6 References

Bogaert, E., K. Bacher, K. Lemmens, M. Carlier, W. Desmet, X. D. Wagter, D. Djian, C. Hanet, G. Heyndrickx, V. Legrand, Y. Taeymans, and H. Thierens. 2009. A large-scale multicentre study of patient skin doses in interventional cardiology: dose-area product action levels and dose reference levels. *Br J Radiol* 82: 303-312.

Broadhead, D. A., C. L. Chapple, K. Faulkner, M. L. Davies, and H. McCallum. 1997. The impact of cardiology on the collective effective dose in the North of England. *Br J Radiol* 70: 492-497.

Earls, J. P. 2009. How to use a prospective gated technique for cardiac CT. *J Cardiovasc Comput Tomogr* 3: 45-51.

Erin Angel, N. Yaghmai, C. M. Jude, J. J. DeMarco, C. H. Cagnon, J. G. Goldin, C. H. McCollough, A. N. Primak, D. D. Cody, D. M. Stevens, and M. F. McNitt-Gray. 2009. Dose to radiosensitive organs during routine chest CT: effects of tube current modulation. *Am J Roentgenol* 193: 1340-1345.

Freeman, A. P., R. Comerford, J. Lambros, S. Eggleton, and D. Friedman. 2009. 64 slice CT coronary angiography--marked reduction in radiation dose using prospective gating. *Heart Lung Circ* 18 (Supplement 3): S13-S13.

Greess, H., A. Nömayr, H. Wolf, U. Baum, M. Lell, B. Böwing, W. Kalender, and W. Bautz. 2002. Dose reduction in CT examination of children by an attenuation-based on-line modulation of tube current (CARE dose). *Eur Radiol* 12: 1571-1576.

Hein, P. A., V. C. Romano, A. Lembcke, J. May, and P. Rogalla. 2009. Initial experience with a chest pain protocol using 320-slice volume MDCT. *Eur Radiol* 19 (5): 1148-1155.

Huda, W., K. M. Ogden, and M. R. Khorasani. 2008. Converting dose-length product to effective dose at CT. *Radiology* 248: 995-1003.

Kalra, M. K., M. l. M. Maher, T. L. Toth, B. Schmidt, B. L. Westerman, H. T. Morgan, and S. Saini. 2004. Techniques and applications of automatic tube current modulation for CT. *Radiology* 233: 649-657.

Kuon, E., J. B. Dahm, K. Empen, D. M. Robinson, G. Reuter, and M. Wucherer. 2004. Identification of less-irradiating tube angulations in invasive cardiology. *J Am Coll Cardiol* 4 (7): 1420-1428.

Lederman, H. M., Z. P. Khademian, M. Felice, and P. J. Hurh. 2002. Dose reduction fluoroscopy in pediatrics. *Pediatr Radiol* 32: 844-848.

Martin, C. J. 2007. Effective dose: how should it be applied to medical exposures? *Br J Radiol* 80: 639-647.

Mayo, J. R., and J. A. Leipsic. 2009. Radiation dose in cardiac CT. *Am J Roentgenol* 192: 646-653.

McLaughlin, D. J., and R. B. Mooney. 2004. Dose reduction to radiosensitive tissues in CT. Do commercially available shields meet the users' needs? *Clin Radiol* 59: 446-450.

Measurements, N. C. o. R. P. a. 2009. *Ionizing radiation exposure of the population of the United States*. Bethesda: National Council on Radiation Protection and Measurements.

Neofotistou, V., E. Vano, R. Padovani, J. Kotre, A. Dowling, M. Toivonen, S. Kottou, V. Tsapaki, S. Willis, G. Bernardi, and K. Faulkner. 2003. Preliminary reference levels in interventional cardiology. *Eur Radiol* 13: 2259-2263.

Partridge, J., G. McGahan, S. Causton, M. Bowers, M. Mason, M. Dalby, and A. Mitchell. 2006. Radiation dose reduction without compromise of image quality in cardiac angiography and intervention with the use of a flat panel detector without an antiscatter grid. *Heart* 92: 507-510.

Preston, D. L., Y. Shimizu, D. A. Pierce, A. Suyama, and K. Mabuchi. 2003. Studies of mortality of atomic bomb survivors. Report 13. Solid cancer and non-cancer disease mortality 1950-1957. *Radiat Res* 160: 381-407.

Schultz, F. W., and J. Zoetelief. 2005. Dose conversion coefficients for interventional procedures. *Radiat Prot Dosim* 117 (1-3): 225-230.

Sun, Z., G. H. Choo, and K. H. Ng. 2012 Coronary CT angiography: current status and continuing challenges. *Br J Radiol* 85 (1013): 495-510.

Sun, Z., and K. H. Ng. 2010. Multislice CT angiography in cardiac imaging-part III: radiation risk and dose reduction. *Singapore Med J* 51: 374-380.

Tan, K., D. Reed, J. Howe, V. Challenor, M. Gibson, and G. McGann. 2007. CT vs conventional angiography in unselected patients with suspected coronary heart disease. *Int J Cardiol* 121 (1): 125-126.

Tins, B., J. Oxtoby, and S. Patel. 2001. Comparison of CT angiography in aortoilliac occlusive disease. *Br J Radiol* 74 (879): 219-225.

Vano, E., R. Sanchez, J. M. Fernandez, J. J. Gallego, J. F. Verdu, M. Gonzalez de Garay, A. Azpiazu, A. Segarra, M. T. Hernandez, M. Canis, F. Diaz, F. Moreno, and J. Palmero. 2009. Patient dose reference levels for interventional radiology: a national approach. *Cardiovasc Intervent Radiol* 32: 19-24.

CHAPTER 4: CORONARY CT ANGIOGRAPHY WITH PROSPECTIVE ECG-TRIGGERING: A SYSTEMATIC REVIEW OF IMAGE QUALITY AND RADIATION DOSE

4.1 Introduction

Coronary computed tomography angiography (CCTA) has been widely used as a useful diagnostic imaging modality for the non-invasive assessment of coronary artery disease (CAD). It has become a reliable and accurate modality to assess the coronary arteries in patient with suspected CAD (Sun et al. 2008). Previous studies have found that retrospective ECG-gated CCTA shows high sensitivities (86-99%) and specificities (89-100%) for coronary artery stenosis and also results in high negative predictive values (NPV) (96-99%) (Pontone et al. 2009; Sun et al. 2008). Prospective ECG-gated CCTA also promises high sensitivity (93.7-100%), specificity (82.7-97%) and NPV (95-98%) in the assessment of CAD (Pontone et al. 2009; Sun and Ng 2012). Although high diagnostic accuracy is achieved with both retrospective and prospective ECG-gating in detecting CAD, the radiation dose associated with these two cardiac examinations is significantly different due to the different approaches used in coronary artery scanning.

It is well-known that CCTA with retrospective ECG-gating leads to high radiation dose up to 31.4 mSv since the volumetric data of the heart is acquired during continuous scans, while only a portion of the data is used for reconstruction (Maruyama et al. 2008; Van Mieghem et al. 2006). In contrast, with exposure taking place at selective phases of cardiac cycle in patients with low and regular heart rate, prospective ECG-triggering is associated with very low radiation dose which indicates a significant reduction in effective dose up to 87% (Efstathopoulos et al. 2009).

A significant dose reduction has been reported in several studies performed with prospective ECG-gated CCTA (Achenbach et al. 2010; De France et al. 2010; Hosch et al. 2011; Klass et al. 2009; Weigold 2009; Zhang et al. 2011). However, diagnostic image quality of prospective triggering in the assessment of coronary arteries or CAD has not been systematically studied. Therefore, the purpose of this article is to investigate the assessments of coronary artery as part of image quality evaluation and radiation dose of CCTA with use of prospective ECG-triggering in the detection of CAD based on a systematic review of the current literature.

4.2 Materials and methods

4.2.1 Literature searching

A search of Medline, SpringerLink, Highwire Press and Science Direct databases of English literature was performed to identify studies performed with prospective ECG-triggering CCTA in patients with suspected or confirmed CAD. The literature search ranged from 2008 to present as prospective ECG-triggering of CCTA was first reported in 2008 (last search was done in October 2011). The following key words were used in searching the relevant articles: CT coronary angiography, prospective ECG gating, multislice CT/multidetector CT with prospective ECG-gating/ECG-triggering, and image quality /diagnostic value of CT coronary angiography.

The eligible articles were identified and selected based on the following criteria: (a) CCTA was performed with use of prospective ECG-gating in the study; (b) information on qualitative and quantitative image quality assessment was provided in each study and (c) the radiation dose associated with CCTA inclusive of effective dose value must be provided. The articles on case reports, review articles, previous treatments (coronary stents or bypass grafts), paediatric cases and phantom studies were excluded from the study.

A formal consensus method, QUADAS" (Quality Assessment of Diagnostic Accuracy Studies) was performed by one author for the quality assessment of diagnostic accuracy in these studies. The QUADAS is regarded as an important tool for quality assessment in systematic reviews as it enables to develop and evaluate an evidence based quality of individual studies in terms of potential for bias, lack of applicability and quality of reporting (Whiting et al. 2003).

4.2.2 Data extraction and analysis

The data were recorded and extracted independently by two authors based on selection criteria (Sabarudin, A and Sun, Z). Disagreements on the final results were resolved by consensus. The data extraction was performed based on each article: year of publication, type of scanner (64-, 128, 256- or 320-slice CT), technical parameters such as beam collimation, gantry rotation time, exposure factors and temporal resolution, patient's demographic data such as number of patients, age, body mass index (BMI) and heart rates were also reported.

Effective dose was recorded from each study as a variable in this review. The estimation of effective does provided in each study was obtained by calculation. It was derived from the original study reports, namely dose-length product (DLP) which was obtained from the CT

scanning protocol of each CCTA study. The DLP was then multiplied with a conversion coefficient factor (CC), which was 0.017 $mSv \cdot mGy^{-1} \cdot cm^{-1}$ based on averaged between male and female anatomical phantoms (Esposito et al. 2011; Huda, Ogden, and Khorasani 2008).

Quantitative and qualitative assessments of diagnostic image quality recorded in each study were analysed. Quantitative image quality was determined by measuring signal-to-noise ratio (SNR) and contrast-to-noise ratio (CNR) for comparisons among the studies. SNR was calculated as the mean Hounsfield unit (HU) of particular region of interest (ROI) divided by image noise. On the other hand, CNR was defined as the difference of attenuation values of the contrast enhancement at two different regions (eg. left ventricular chamber and left ventricular wall) and then divided by image noise. Image noise is a standard deviation, SD of HU measured at selected anatomical region.

Qualitative assessment of image quality was carried out on a per-segment basis by using of three- to five-point Likert ranking scale. The coronary segments were analysed and the results were documented and categorised as percentage of assessable and non-assessable coronary segments. The classification of coronary segment was based on the descriptions of each score in Likert rank-scale. The coronary arteries were characterised into 15-19 segments according to the classification by American Heart Association (AHA) and the extent of stenosis was evaluated in each segment with more than 50% coronary stenosis being defined as significant (Austen et al. 1975). Sensitivity, specificity, positive predictive value (PPV), NPV and diagnostic accuracy for the detection of significant coronary stenosis were also be analysed.

4.2.3 Statistical analysis

All the data were entered into SPSS version 19.0 (SPSS V 19.0, Chicago, ILL) for analysis. Assessment of image quality in each study was extracted and analysed with analysis of variance (ANOVA) for multifactorial mean comparisons. The radiation dose was also compared between the scanner types (dual source vs single source 64-, 128-,256- and 320-slice CT) with use of ANOVA. A p value of <0.05 was considered statistically significant difference.

4.3 Results

A total of 12,670 citations were identified from searching the above-mentioned four different databases. Twenty-three articles met the selection criteria and were included in the analysis (Pontone et al. 2009; Achenbach et al. 2010; Efstathopoulos et al. 2009; Esposito et al. 2011; Hosch et al. 2011; Maruyama et al. 2008; Zhang et al. 2011; Arnoldi et al. 2009; Buechel et al. 2011; Carrascosa et al. 2010; Chen et al. 2010; Duarte et al. 2011; Feng et al. 2010; Gutstein et al. 2008; Hirai et al. 2008; Ko et al. 2010; Lu et al. 2011; Muenzel et al. 2012; Qin et al. 2011; Shuman et al. 2008; Shuman et al. 2009; Stolzmann et al. 2011; Xu et al. 2010). The search process of study attrition diagram is shown in the flow chart (Figure 4-1). In addition, information on image quality assessment was analysed with regard to four different manufactures, namely, Siemens, Philips, Toshiba and GE, and various types of scanners ranging from 64- to 128-, 256- and 320-slice CT. Details of the scanner features are presented in Table 4-1. A total of 2080 patients were included in all 23 studies with a mean age of 59.1 years (95% CI: 45, 70 years). Coronary CT angiography with use of prospective ECG triggering was conducted with an average heart rate of 60.8 beats per minutes (bpm) (95% CI: 54.6, 82.8 bpm) and body mass index of 25.3 kgm^{-2} (95% CI: 22.3, 28 kgm^{-2}). The quality assessment for each study according to QUADAS guideline was presented in Table 4-2.

Figure 4-1: Flow chart showing the search strategy of eligible references.

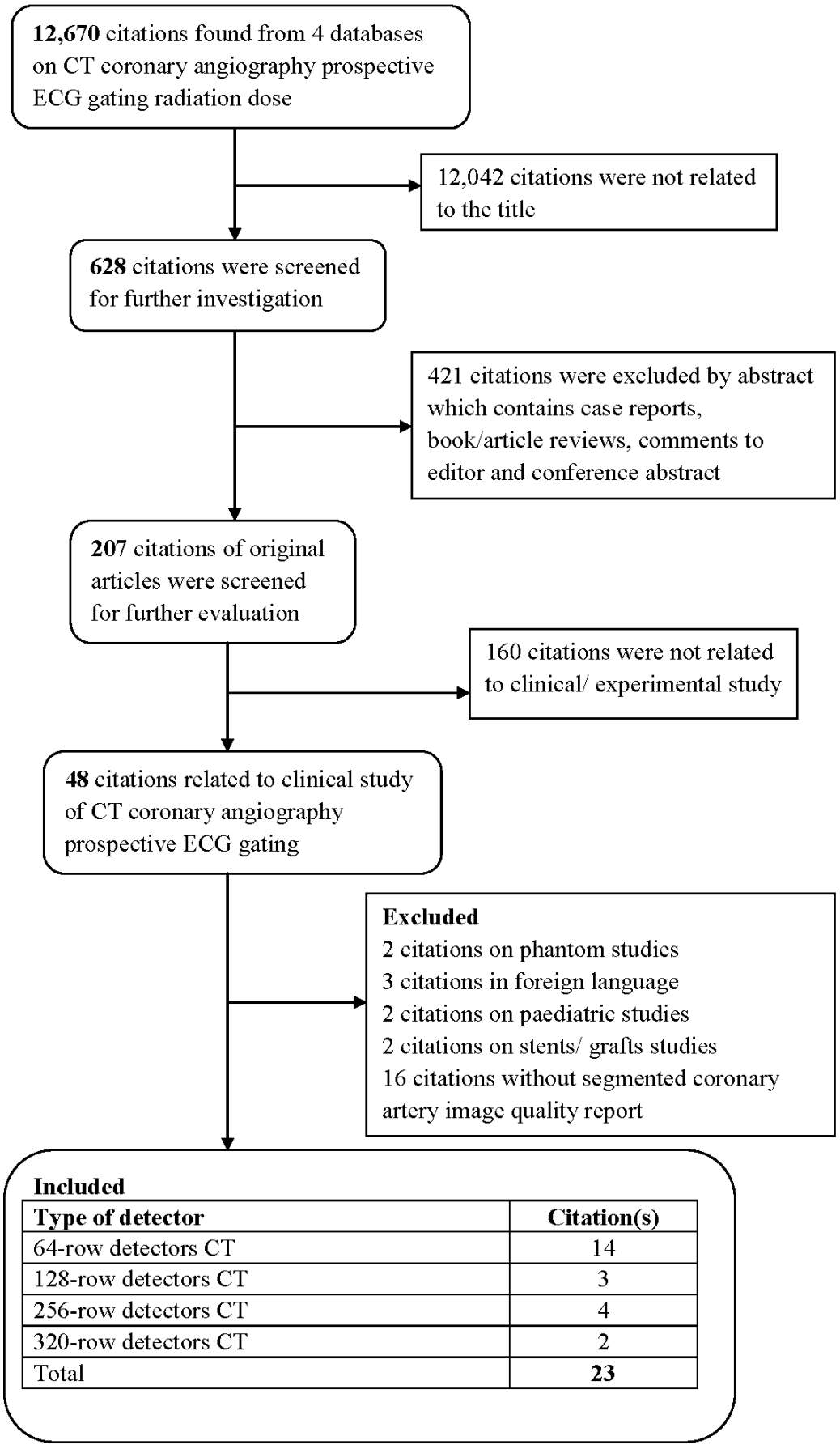

Type of detector	**Citation(s)**
64-row detectors CT	14
128-row detectors CT	3
256-row detectors CT	4
320-row detectors CT	2
Total	**23**

Table 4-1: Study details of prospective ECG-gated CTCA

Studies publication	Detector collimations	No. of patients	Age (years)	HR (b.p.m)	BMI (kg/m^2)	Tube voltage (kVp)	Effective dose (mSv)	Manufacture
Achenbach et.al (2010)	2 × 64 × 0.6	50	n/a	68±9	n/a	100	0.9 ± 0.1	Siemens
Arnoldi et.al (2009)	2 × 32 × 0.6	20	58 ± 10	64±9	23± 4	120	3 ± 1	Siemens
Buechel et.al (2011)	64 × 0.625	612	59 ± 12	62	26±5	100-120	1.8 ± 0.6	GE
Carrascossa et.al (2010)	64 × 0.625	50	62± 13	54.9 ± 6.8	27.7±3.4	120	3.4 ± 0.4	Philips
Chen et.al (2010)	2 ×128 × 0.625	10	60 ± 7	58.7±6.3	23.0±1.5	120	4.7 ± 0.4*	Philips
	2 ×128 × 0.625	10	55± 9	56.6±5.0	23.1±2.1	120	2.77 ± 0.4	Philips
Duarte et.al (2011)	2 × 64 × 0.6	40	62 ± 7	60±5	n/a	100-120	2.1 ± 0.9	Siemens
Efstathopolous et.al (2009)	2 ×128 × 0.625	15	55± 8	57.1 ±7.2	27.8±4.3	120	3.2 ± 0.6	Philips
Esposito et.al (2011)	64 × 0.625	90	61 ± 12	59±7	26±4	100-140	4-5.2	GE
Feng et.al (2010)	2 × 64 × 0.6	31	60 ± 9	67.5 ± 9.7	24.7±3.0	100	2.7 ± 0.7	Siemens
Gutstein et.al (2008)	2 × 32 × 0.6	42	53±12	57.8±4.0	24.9±3.1	100-120	2.2 ± 0.8	Siemens
Hirai et.al (2008)	64 × 0.625	62	65 ± 11	57.1±7.8	n/a	120	4.1 ± 1.8	GE
Hosch et.al (2010)	2 ×128 × 0.625	115	n/a	58±7	n/a	120	3.1±0.4	Philips

Ko et.al (2010)	64 × 0.625	84	56 ± 11	56.5 ± 4.3	23.8±1.5	120	3.43 ± 0.6	GE
Lu et.al (2011)	2 × 32 × 0.6	62	56 ± 10	67.7±10.5	25.3±3.0	120	3.0 ± 1.4	Siemens
Maruyama et.al (2008)	64 × 0.625	76	70 ± 10	54.6 ± 6.9	23.9±4.6	120	4.3 ± 1.3	GE
Muenzel et.al (2011)	2 ×128 × 0.625	29	560	62.5±15.9	25.4±4.0	120	4.8[#]	Philips
	2 ×128 × 0.625	24	65	66.6±14.6	25.2±2.9	120	3.9[##]	Philips
Pontone et.al (2009)	64 × 0.625	80	65 ± 10	54.7 ± 5.2	27.0±3.9	120	5.7 ± 1.5	GE
Qin et.al (2011)	320 × 0.5	240	45 ± 20	56±8	n/a	120	3.3 ± 2.0	Toshiba
Shuman et.al (2008)	64 × 0.625	50	n/a	n/a	n/a	100-120	6.2 ± 2.0	GE
Shuman et.al (2009)	64 × 0.625	31	55 ± 8	59 ± 6	28 ± 5	100-120	9.2 ± 2.2	GE
Stolzman et.al (2011)	2 × 32 × 0.6	100	68 ± 8	58±7	26.3±3.1	100-120	2.2 ± 0.4	Siemens
Xu et.al (2010)	2 × 32 × 0.6	50	55 ± 10	82.8±9.3	n/a	100-120	11.8 ± 4.5	Siemens
Zhang et.al (2011)	320 × 0.5	40	59 ± 10	55.1±5.3	22.3±1.5	100	2.1 ± 0.2	Toshiba
	320 × 0.5	67	56 ± 10	66.2±6.6	27.8±2.7	120	4.6 ± 0.8	Toshiba

n/a=not available;*additional padding windows; [#]FOV>250mm; [##]FOV <250mm; GE=general electric

Table 4-2: Quality Assessment of Diagnostic Accuracy Studies (QUADAS)

Studies publication	Items													
	1	**2**	**3**	**4**	**5**	**6**	**7**	**8**	**9**	**10**	**11**	**12**	**13**	**14**
Achenbach et.al (2010)	Y	Y	Y	U	Y	Y	Y	Y	Y	Y	Y	Y	Y	Y
Arnoldi et.al (2009)	Y	Y	Y	U	Y	Y	Y	Y	Y	Y	Y	Y	Y	Y
Buechel et.al (2011)	Y	Y	Y	Y	Y	Y	Y	Y	Y	Y	Y	Y	Y	Y
Carrascossa et.al (2010)	Y	Y	Y	Y	Y	Y	Y	U	U	Y	Y	Y	Y	Y
Chen et.al (2010)	Y	Y	Y	Y	Y	Y	Y	Y	Y	U	U	Y	Y	Y
Duarte et.al (2011)	Y	Y	Y	Y	Y	Y	Y	U	U	Y	Y	Y	Y	Y
Efstathopolous et.al (2009)	Y	Y	Y	Y	Y	Y	Y	U	U	Y	Y	Y	Y	Y
Esposito et.al (2011)	Y	Y	Y	Y	Y	Y	Y	Y	Y	Y	Y	Y	Y	Y
Feng et.al (2010)	Y	Y	Y	Y	Y	Y	Y	Y	Y	Y	Y	Y	Y	Y
Gutstein et.al (2008)	Y	Y	Y	Y	Y	Y	Y	Y	Y	Y	Y	Y	Y	Y
Hirai et.al (2008)	Y	Y	Y	Y	Y	Y	Y	Y	Y	Y	Y	Y	Y	Y
Hosch et.al (2010)	Y	Y	Y	Y	Y	Y	Y	Y	Y	Y	Y	Y	Y	Y
Ko et.al (2010)	Y	Y	Y	Y	Y	Y	Y	Y	Y	Y	Y	Y	Y	Y

Lu et.al (2011)	Y	Y	Y	Y	Y	Y	Y	Y	Y	U	U	Y	Y	Y
Maruyama et.al (2008)	Y	Y	Y	Y	U	Y	Y	Y	Y	Y	Y	Y	Y	Y
Muenzel et.al (2011)	Y	Y	Y	Y	Y	Y	Y	Y	Y	Y	Y	Y	Y	Y
Pontone et.al (2009)	Y	Y	Y	Y	Y	Y	Y	Y	Y	Y	Y	Y	Y	Y
Qin et.al (2011)	Y	Y	Y	Y	Y	Y	Y	Y	Y	U	U	Y	Y	Y
Shuman et.al (2008)	Y	Y	Y	Y	Y	Y	Y	Y	Y	U	U	Y	Y	Y
Shuman et.al (2009)	Y	Y	Y	Y	Y	Y	Y	Y	Y	Y	Y	Y	Y	Y
Stolzman et.al (2011)	Y	Y	Y	Y	Y	Y	Y	Y	Y	Y	Y	Y	Y	Y
Xu et.al (2010)	Y	Y	Y	Y	Y	Y	Y	Y	Y	Y	Y	Y	Y	Y
Zhang et.al (2011)	Y	Y	Y	Y	Y	Y	Y	Y	Y	Y	Y	Y	Y	Y

Y=yes; U=unclear

Item 1: was the spectrum of patients representative of the patients who will receive the test in practice?

Item 2: was selection criteria clearly described?

Item 3: is the reference standard likely to correctly classify the target condition?

Item 4: is the time period between reference, standard and index test short enough to be reasonably sure that the target condition did not change between the two tests?

Item 5: did the whole sample or a random selection of the sample, receive verification using a reference standard of diagnosis?

Item 6: did patients receive the same reference standard regardless of the index test results?

Item 7: was the reference standard independent of the index test (i.e., the index test did not form part of the reference standard)?

Item 8: was the execution of the index test described in the sufficient detail to permit replication of the test?

Item 9: was the execution of the reference standard described in the sufficient detail to permit its replication?

Item 10: were the index test results interpreted without knowledge of the results of the reference standard?

Item 11: were the reference standard results interpreted without knowledge of the results of the index test?

Item 12: were the same clinical data available when test results were interpreted as would be available when the test is used in practice?

Item 13: were uninterpretable/intermediate test results reported?

Item 14: were withdrawals from the study explained?

4.3.1 Systematic review of image quality associated with prospective ECG-triggering CCTA

Quantitative image assessment was performed in only 4 out of 23 studies (Carrascosa et al. 2010; Feng et al. 2010; Muenzel et al. 2012; Zhang et al. 2011) with mean SNR and CNR of 20.9 (95% CI: 11.7, 28.6) and 18.0 (95% CI: 5.2, 22.2), respectively. There was no significant difference between SNR and CNR groups in these studies. The SNR and CNR was measured at the proximal segment of the right coronary artery and in the left main coronary artery, left ventricular wall and left ventricular chamber (Carrascosa et al. 2010), the root of the ascending aorta (Feng et al. 2010), ascending aorta, pulmonary artery and coronary arteries (Muenzel et al. 2012), ascending aorta and perivascular fatty tissue (Zhang et al. 2011). However, the qualitative image quality could not be analyzed due to the limited number of studies.

Only one study was using single viewer for image quality evaluation (Chen et al. 2010). Of 22 studies, 15 studies (Achenbach et al. 2010; Carrascosa et al. 2010; Feng et al. 2010; Hirai et al. 2008; Hosch et al. 2011; Ko et al. 2010; Lu et al. 2011; Muenzel et al. 2012; Pontone et al. 2009; Qin et al. 2011; Shuman et al. 2008; Shuman et al. 2009; Stolzmann et al. 2011; Xu et al. 2010; Zhang et al. 2011) assessed the inter-observer agreement by using Cohen's kappa statistic with a mean value of 0.79 (95% CI: 0.60, 0.94), indicating excellent agreement between the 2 viewers. Two studies (Duarte et al. 2011; Gutstein et al. 2008) used consensus reading, and that information in the remaining 5 studies was not available (Arnoldi et al. 2009; Buechel et al. 2011; Efstathopoulos et al. 2009; Esposito et al. 2011; Maruyama et al. 2008).

A likert-scale point score system was used in all studies to indicate the evaluability of coronary segment. Two studies were conducted with 3-point scoring system (Arnoldi et al. 2009; Esposito et al. 2011) and another two studies with 5-point scores (Hosch et al. 2011; Muenzel et al. 2012). The 3-point score indicates excellent, moderate and poor image quality (Figure 4-2) while 5-point score was classified distinctively in two studies which one study described the score as excellent, good, moderate, poor and extremely poor image quality (Hosch et al. 2011). In contrast, the other study defined 5-point score as excellent quality, good quality, mild artefacts, severe artefacts and non-evaluable (Figure 4-3) (Muenzel et al. 2012). The remaining 19 studies used 4-point scoring system which consisted of excellent, good, moderate and poor image quality (Figure 4-4). The distribution of each coronary segment was presented in Figure 4-2. However, the coronary segments were only analysed and classified into 2 groups (assessable versus non-assessable segments) based on score description despite using different scoring systems.

A total of 26,620 coronary artery segments were evaluated in these 23 studies with an overall mean value of 96.8% (95% CI: 83,100%) assessable and 3.2% not assessable segments (Table 4-3). There is no statistically significant difference in the mean assessable coronary segments between or within types of scanners (p=0.76). The mean assessable coronary segments in 64-slice scanners (single source versus dual-source CT) were 96.5% (95% CI: 88.2, 99.5%) and 97.5% (95% CI: 92.3, 99.7%) respectively. The mean assessable coronary segments were 97.9% (95% CI: 95.0, 99.5%), 95.6% (95% CI: 83.0, 100%) and 98.9% (95% CI: 98.2, 100%), corresponding to 128-, 256- and 320-slice CT, respectively.

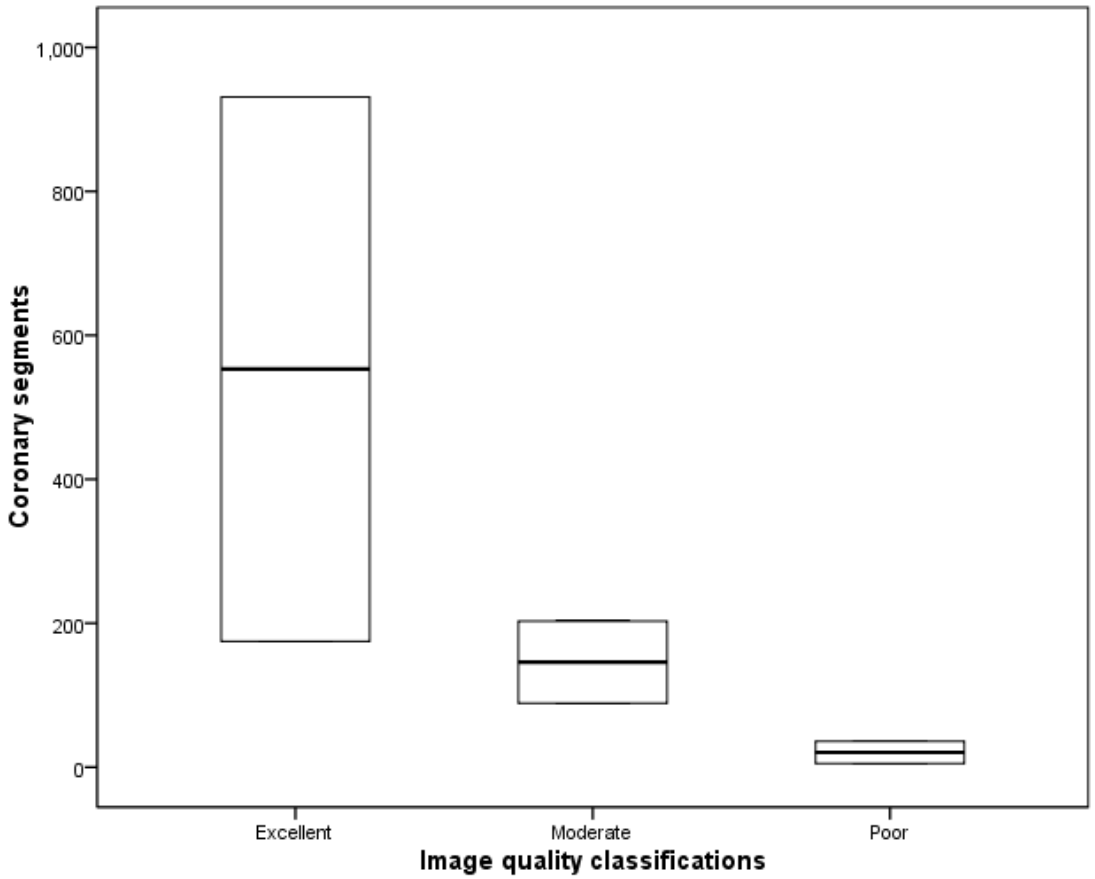

Figure 4-2: Box plot shows the number of coronary segments assessed associated with the image quality classifications with 3-rank scale system in prospective ECG-gating CCTA.

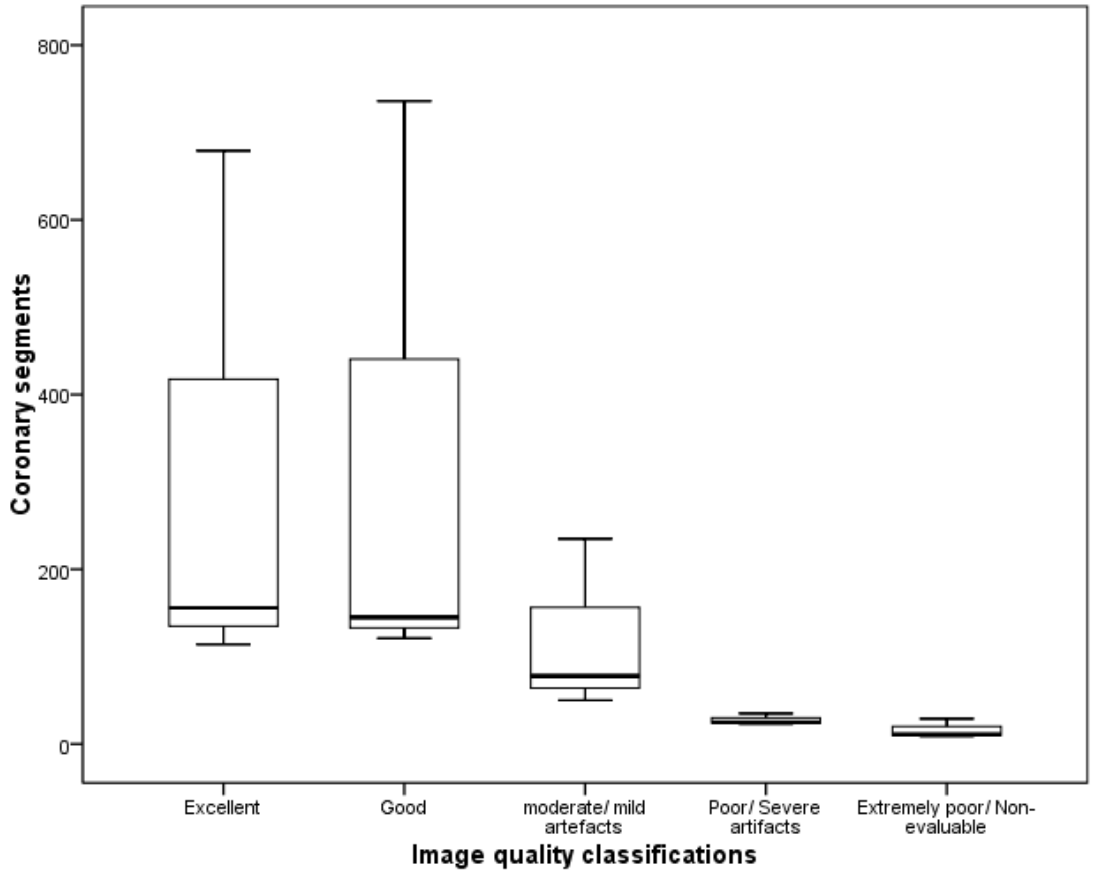

Figure 4-3: Box plot shows the number of coronary segments assessed associated with the image quality classifications with 5-rank scale system in prospective ECG-gating CCTA.

Of 23 studies, evaluation on sensitivity, specificity, PPV, NPV and the accuracy for coronary artery stenosis was available in 5 studies (Carrascosa et al. 2010; Lu et al. 2011; Maruyama et al. 2008; Pontone et al. 2009; Stolzmann et al. 2011). Pooled estimates of sensitivity, specificity, PPV, NPV and accuracy with 95% confidence interval (CI) were 98.3% (95% CI: 96 and 100%), 90.5% (95% CI: 85.7 and 96%), 92.3% (95% CI: 77 and 99%), 90% (95% CI: 75 and 100%) and 96.2% (95% CI: 95 and 98%) for patient-based assessment; 89.8% (95% CI: 76.6 and 98%), 97.2% (95% CI: 95 and 98.5%), 89.8% (95% CI: 85.5 and 96%), 92.8% (95% CI: 83 and 100%) and 95% (95% CI: 93 and 98%) for segment-based assessment; 89.3% (95% CI: 79.6 and 99%), 94.7% (95% CI: 92.3 and 97%), 91.6% (95% CI: 88.2 and 95%), 92.6% (95% CI: 86.2 and 99%) and 92.3% (95% CI: 86.6 and 98%) for vessel-based assessment, respectively.

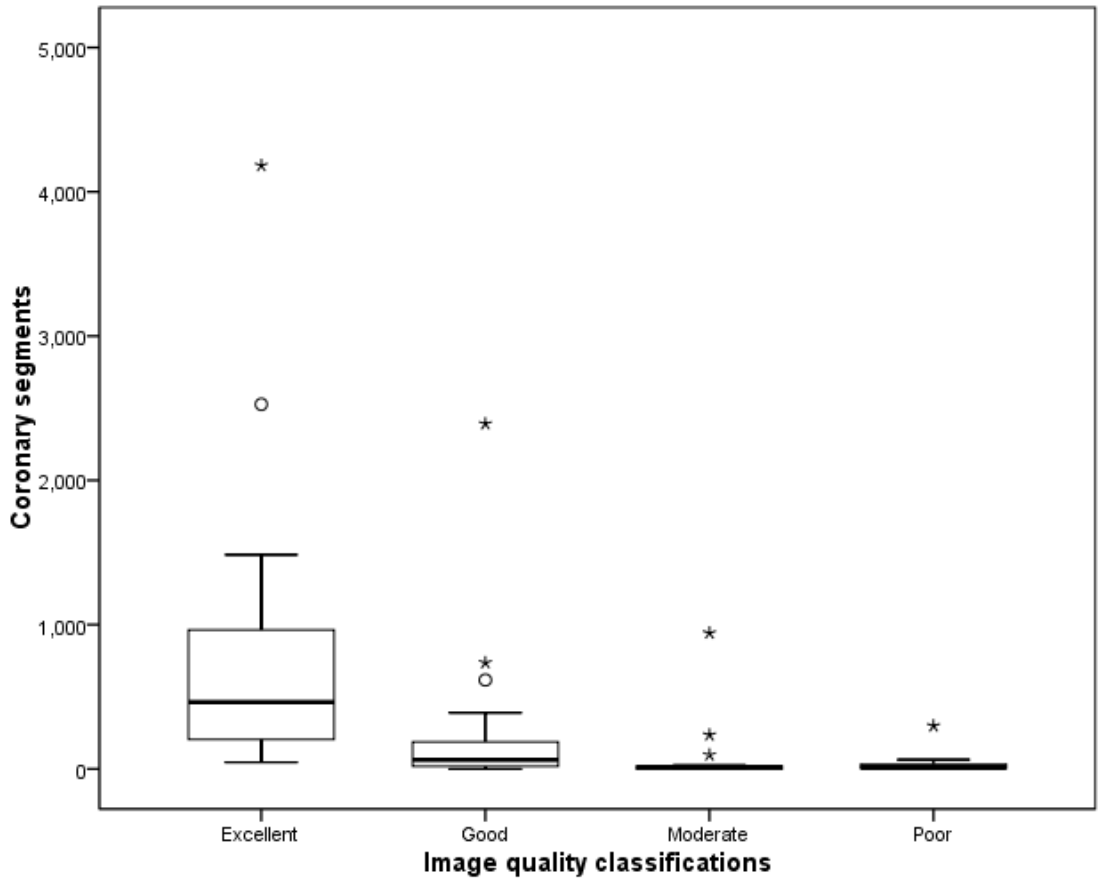

Figure 4-4: Box plot shows the number of coronary segments assessed associated with the image quality classifications with 4-rank scale system in prospective ECG-gating CCTA.

Of 8 studies involving assessment of stenosis, degree of stenosis was investigated in three studies with pooled estimation being 79.1% (95% CI: 55, 94.4%) and 11.2% (95% CI: 5.6, 16%) corresponding to 50-75% stenosis and over 75% occlusion, respectively (Buechel et al. 2011; Carrascosa et al. 2010; Hirai et al. 2008). The remaining five studies focused on the stenosis location and coronary vessels involvement. However, comparison between these data could not be performed due to use of different methods of analysis (Achenbach et al. 2010; Carrascosa et al. 2010; Gutstein et al. 2008; Muenzel et al. 2012; Stolzmann et al. 2011), although the sensitivity in detecting stenosis on vessel-based and segment-based assessment was lower than that on patient-based assessment (89.3% and 89.8% versus 98.3%).

Table 4-3: Analysis of the coronary artery segments in prospective ECG-gated CTCA

Studies publication	Segments classification no.	Total number of segments	Diameter requirement	Assessable segments (%)
Achenbach et.al (2010)	18	742	All segments	99.5
Arnoldi et.al (2009)	15	269	All segments	98.1
Buechel et.al (2011)	16	7814	>1.5 mm	96. 2
Carrascossa et.al (2010)	17	51	>1.5 mm	88.2
Chen et.al (2010)	15	138	n/a*	100
	15	160	n/a	100
Duarte et.al (2011)	16	450	>1.5 mm	99.1
Efstathopolous et.al (2009)	16	224	All segments	83.0
Esposito et.al (2011)	16	1170	All segments	96.9
Feng et.al (2010)	NS	439	n/a	95.0
Gutstein et.al (2008)	15	633	n/a	99.2
Hirai et.al (2008)	17	828	>1.5 mm	98.7
Hosch et.al (2010)	15	1714	All segments	96.3

Ko et.al (2010)	16	1226	>1.5 mm	97.4
Lu et.al (2011)	15	246	All segments	92.3
Maruyama et.al (2008)	15	1089	All segments	96.7
Muenzel et.al (2011)	16	390	>1.0 mm[#]	97.2
	16	294	>1.0 mm[##]	96.9
Pontone et.al (2009)	15	1044	>1.5 mm	95.6
Qin et.al (2011)	15	3240	>1.5 mm	100
Shuman et.al (2008)	19	614	>1.5 mm	98.9
Shuman et.al (2009)	19	394	>1.5 mm	99.5
Stolzman et.al (2011)	16	1508	>1.0 mm	98.4
Xu et.al (2010)	16	610	>1.5 mm	99.7
Zhang et.al (2011)	16	504	>1.5 mm[^]	98.2
	16	829	>1.5 mm[^^]	98.6

n/a=not available; *additional padding windows; [#]FOV>250mm; [##]FOV <250mm; [^]100kVp; [^^]120kVp

4.3.2 Systematic review of radiation dose associated with prospective triggering CCTA

The overall mean effective dose was 3.9 mSv (95% CI: 0.9, 9.2 mSv) in the 23 studies performed with prospective ECG-triggered CCTA. There is no significant difference in the mean effective doses (p=0.47) between 64- (single vs dual source CT), 128-, 256- and 320-slice scanners, with mean effective doses of 4.7 mSv (95% CI: 1.8, 9.2 mSv), 4.4 mSv (95% CI: 2.2, 11.8 mSv), 1.8 mSv (95% CI: 0.9, 2.7 mSv), 3.5 mSv (95% CI: 2.1, 4.8 mSv) and 3.3 mSv (95% CI: 2.1, 4.6 mSv) respectively, corresponding to these different types of scanners. There were several techniques introduced in some studies in order to produce further reduction in radiation dose. One study was conducted with high pitch value resulting in the effective dose of less than 1.0 mSv (Achenbach et al. 2010). In addition, applying with high field of view (FOV) and lowering tube voltage (100 kVp) also led to radiation dose reduction with 4.8 vs 3.9 mSv (FOV>250 mm vs FOV<250 mm) (Muenzel et al. 2012) and 2.1 vs 4.6 mSv (100 vs 120 kVp) (Zhang et al. 2011).

4.4 Discussion

This analysis highlights two findings that are considerably important for clinical applications in coronary CT angiography with use of prospective ECG-gating protocol. Firstly, this review shows that high percentage of assessable coronary segments was achieved with a mean value of 96.8% regardless of any type of scanners. Secondly, prospective ECG-gating CCTA has demonstrated high sensitivity, specificity, NPV, PPV and accuracy in detecting CAD with significantly lower radiation dose.

In this review, 96.8% of coronary segments were found to be assessable in the evaluation throughout the subjective image quality assessment, with a very small number of non-assessable segments reported in this prospective ECG-gating technique. Targeting patients with appropriate heart rate might reduce the coronary segments rejection depending on the scanner type and scanning technique. Beta-blockage is routinely recommended as a prerequisite prior to the scan to lower the heart rate with aim of achieving diagnostic image quality (Pannu, W. Alvarez, and E. K. Fishman 2006), since heart rate is the key factor in determining image quality. A recent study showed that the percentage of non-assessable coronary images was increased significantly with heart rate over 57 bpm and with heart rate variability more than 6 bpm (Ko et al. 2010). However, it has been reported that image quality acquired in dual-source CT (DSCT) using prospective ECG-gating was diagnostic in patients with heart rate more than 65 bpm (Xu et al. 2010). Assessable segments in DSCT coronary angiography were found to be slightly higher than those in single-source CT coronary angiography according to this review, although there is no significant difference.

Further studies comparing DSCT with single-slice CT coronary angiography using prospective ECG-gating are required to confirm the diagnostic accuracy.

In response to the concern of high radiation dose in CT, various dose-saving strategies were introduced in the literature with the aim of reducing the radiation dose associated with CCTA, while still preserving diagnostic value in CAD (Pontone et al. 2009). Of several dose saving strategies, prospective ECG-triggering represents the most recently developed approach with a significant reduction of radiation dose when compared to conventional retrospective ECG-gating (Sun 2010; Sun and Ng 2012). Although we did not focus on the retrospective ECG-gating CCTA in this review, radiation dose results from previous studies confirmed that the effective dose was reduced significantly in prospective ECG-gating (3.9 mSv) compared to retrospective ECG-gating (18-24 mSv) (Earls et al. 2008; Hirai et al. 2008). This is also supported by several studies conducted on radiation dose indicating that prospective ECG-gated CCTA leads to a dose reduction by up to 83% when compared to retrospective ECG-gating (Lu et al. 2011; Shuman et al. 2008; Earls 2009; Sabarudin, Z. Sun, and K-H. Ng 2012). This analysis shows that the effective dose in CCTA with prospective ECG gating was even lower than that in invasive coronary angiography as reported in the previous study (5.6 mSv) (Coles et al. 2006). Application of high pitch and lower tube voltage in prospective ECG-gating can result in further radiation dose reduction with less than 1 mSv (Alkadhi et al. 2010; Achenbach et al. 2010).

The principle of prospective ECG-triggering is that data acquisition only takes place in the selected cardiac phase by selectively only turning on the x-ray tube when triggered by the ECG signal, and turning it off or dramatically lowering it during the rest of the R-R cycle. This technique is limited to heart rate less than 70 or 65 beats per minute (bpm). In addition, ECG-triggered sequential scan is usually restricted to scanning with non-overlapping adjacent slices, or slice increments with only small overlap. The scan time to cover the heart volume is thus directly proportional to the slice increment. Consequently, prospective ECG-triggering puts high demand on the z-axis coverage, therefore, it is normally performed with 64-slice or more slice scanners. Presence of misalignment due to acquisition of images in 4-5 heart beats to cover the entire heart with 64-slice CT is an example of this limitation. This can be overcome with the latest 320-slice CT scanner, which enables coverage of the cardiac volume in a single heartbeat (Hoe and Toh 2009). This is confirmed by this analysis, since prospective ECG-triggering CCTA with 320-slice CT shows lower dose than the other generations of CT scanners, although no significant difference was reached.

Some limitations exist in this review. Firstly, there is lack of objective assessment reported in all studies. Only 17% (4 out of 23) of the studies provided details on quantitative

assessment of image quality. In contrast, the subjective image analysis was reported in all of the studies. Each study must provide a subjective image quality assessment as a requirement limits the number of studies included in this review. Moreover, image quality evaluation by single viewer might lead to bias results in scoring the coronary artery segments. However, the majority of studies (96%) obtaining their image quality assessment by 2 viewers with good inter-observer agreement. Secondly, limited information on diagnostic image accuracy was in this review. Investigation of diagnostic value of prospective ECG-triggering should be conducted in more studies with a large cohort of patients. Finally, the publication bias may affect the results with the exclusion of non-English language publications.

4.5 Conclusion

In conclusion, this systematic review shows that prospective ECG-triggered coronary CT angiography results in high diagnostic image quality with high diagnostic accuracy in detecting coronary artery stenosis. Prospective ECG-triggering protocol produces a significantly lower radiation dose compared to retrospective ECG-gating CCTA.

4.6 References

Achenbach, S., M. Marwan, D. Ropers, T. Schepis, T. Pflederer, and K. Anders. 2010. Coronary computed tomography angiography with a consistent dose below 1mSv using prospectively electrocardiogram-triggered high-pitch spiral acquisition. *Eur Heart J* 31: 340-346.

Alkadhi, H., P. Stolzmann, L. Desbiolles, S. Baumueller, R. Goetti, and A. Plass. 2010. Low-dose, 128-slice, dual-source CT coronary angiography: accuracy and radiation dose of the high-pitch and the step-and-shoot mode. *Heart* 96: 933-938.

Arnoldi, E., T. R. Johnson, C. Rist, B. J. Wintersperger, W. H. Sommer, A. Becker, C. R. Becker, M. F. Reiser, and K. Nikolaou. 2009. Adequate image quality with reduced radiation dose in prospectively triggered coronary CTA compared with retrospective techniques. *Eur Radiol* 19: 2147-2155.

Austen, W. G., J. E. Edwards, R. L. Frye, G. G. Gensini, V. L. Gott, L. S. C. Griffith, D. C. McGoon, M. L. Murphy, and B. B. Roe. 1975. *Report of the ad hoc committee for grading of coronary artery disease*. American Heart Association.

Buechel, R. R., L. Husmann, B. A. Herzog, A. P. Pazhenkottil, R. Nkoulou, J. R. Ghadri, V. Treyer, P-V Schulthess, and P. A. Kaufmann. 2011. Low-dose computed tomography coronary angiography with prospective electrocardiogram triggering. *J Am Coll Cardiol* 57 (3): 332-336.

Carrascosa, P., C. Capunay, A. Deviggiano, A. Goldsmit, C.Tajer, M. Bettinotti, J. Carrascosa, T. B.Ivanc, A. Fallahi, and M. J.Garcı´a. 2010. Accuracy of low-dose prospectively gated axial coronary CT angiography for the assessment of coronary artery stenosis in patients with stable heart rate. *J Cardiovasc Comput Tomogr* 4: 197-205.

Chen, L.-K., T.-H. Wu, C.-C. Yang, C.-J. Tsai, and J. J. S. Lee. 2010. Radiation dose to patients and image quality evaluation from coronary 256-slice computed tomographic angiography. *Nucl Instrum Methods Phys Res Sect A* 619: 368-371.

Coles, D. R., M. A. Smail, I. S. Negus, P. Wilde, M. Oberhoff, K. R. Karsch, and A. Baumbach. 2006. Comparison of radiation doses from multislice computed tomography coronary angiography and conventional diagnostic angiography. *J Am Coll Cardiol* 47 (9): 1840-1845.

De France, T., E. Dubois, D. Gebow, A. Ramirez, F. Wolf, and G. M. Feuchtner. 2010. Helical prospective ECG-gating in cardiac computed tomography: radiation dose and image quality. *Int J Cardiovasc Imaging* 26: 99-110.

Duarte, R., G. Fernandez, D. Castellon, and J. C. Costa. 2011. Prospective coronary CT angiography 128-MDCT versus retrospective 64-MDCT: improved image quality and reduced radiation dose. *Heart, Lung Circ* 20: 119-125.

Earls, J. P. 2009. How to use a prospective gated technique for cardiac CT. *J Cardiovasc Comput Tomogr* 3: 45-51.

Earls, J. P., E. L. Berman, B. A. Urban, C. A. Curry, J. L. Lane, R. S. Jennings, C. C. McCulloch, J. Hsieh, and J. H. Londt. 2008. Prospectively gated transverse coronary CT angiography versus retrospectively gated helical technique: improved image quality and reduced radiation dose. *Radiology* 246: 742-753.

Efstathopoulos, E. P., N. L. Kelekis, I. Pantos, E. Brountzos, S. Argentos, J. Greb´a, D. Ziaka, D. G. Katritsis, and I. Seimenis. 2009. Reduction of the estimated radiation dose and associated patient risk with prospective ECG-gated 256-slice CT coronary angiography. *Phys Med Biol* 54 (17): 5209-5222.

Esposito, A., F. De Cobelli, C. Colantoni, G. Perseghin, A. del Vecchio, T. Canu, R. Calandrino, and A. D. Maschio. 2011. Gender influence on dose saving allowed by prospective-triggered 64-slice multidetector computed tomography coronary angiography as compared with retrospective-gated mode. *Int J Cardiol* 158 (2): 253-259.

Feng, Q., Y. Yin, X. Hua, R. Zhu, J. Hua, and J. Xu. 2010. Prospective ECG triggering versus low-dose retrospective ECG-gated 128-channel CT coronary angiography: comparison of image quality and radiation dose. *Clinical Radiol* 65: 809-814.

Gutstein, A., A. Wolak, C. Lee, D. Dey, M. Ohba, Y. Suzuki, V. Cheng, H. Gransar, S. Suzuki, J. Friedman, L. E. Thomson, S. Hayes, R. Pimentel, W. Paz, P. Slomka, and D. S. Berman. 2008. Predicting success of prospective and retrospective gating with dual-source coronary computed tomography angiography: development of selection criteria and initial experience. *J Cardiovasc Comput Tomogr* 2: 81-90.

Hirai, N., J. Horiguchi, C. Fujioka, M. Kiguchi, H. Yamamoto, N. Matsuura, T. Kitagawa, H. Teragawa, N. Kohno, and K. Ito. 2008. Prospective versus retrospective ECG-gated 64-detector coronary CT angiography: assessment of image quality, stenosis, and radiation dose. *Radiology* 248: 424-430.

Hoe, J., and K. H. Toh. 2009. First experience with 320-row multidetector CT coronary angiography scanning with prospective electrocardiogram gating to reduce radiation dose. *J Cardiovasc Comput Tomogr* 3: 257-261.

Hosch, W., T. Heye, F. Schulz, S. Lehrke, M. Schlieter, E. Giannitsis, H-U. Kauczor, H. A. Katus, and G. Korosoglou. 2011. Image quality and radiation dose in 256-slice cardiac computed tomography: Comparison of prospective versus retrospective image acquisition protocols. *Eur J Radiol* 80 (1): 127-135.

Huda, W., K. M. Ogden, and M. R. Khorasani. 2008. Converting dose-length product to effective dose at CT. *Radiology* 248: 995-1003.

Klass, O., M. Walker, A. Siebach, T. Stuber, S. Feuerlein, M. Juchems, and M. H. K. Hoffmann. 2009. Prospectively gated axial CT coronary angiography: comparison of image quality and effective radiation dose between 64- and 256-slice CT. *Eur Radiol* 20: 1124-1131.

Ko, S. M., N. R. Kim, D. H. Kim, M. G. Song, and J. H. Kim. 2010. Assessment of image quality and radiation dose in prospective ECG-triggered coronary CT angiography compared with retrospective ECG-gated coronary CT angiography. *Int J Cardiovasc Imaging* 26: 93-101.

Lu, B., J.-G. Lu, M.-L. Sun, Z.-H. Hou, X.-B. Chen, X. Tang, R.-Z. Wu, L. Johnson, S.-B. Qiao, Y.-J. Yang, and S.-L. Jiang. 2011. Comparison of diagnostic accuracy and radiation dose between prospective triggering and retrospective gated coronary angiography by dual-source computed tomography. *Am J Cardiol* 107: 1278-1284.

Maruyama, T., M. Takada, T. Hasuike, A. Yoshikawa, E. Namimatsu, and T. Yoshizumi. 2008. Radiation dose reduction and coronary assessability of prospective

electrocardiogram-gated computed tomography coronary angiography: comparison with retrospective electrocardiogram-gated helical scan. *J Am Coll Cardiol* 52 (18): 1450-1455.

Muenzel, D., P. B. Noel, F. Dorn, M. Dobritz, E. J. Rummeny, and A. Huber. 2012. Coronary CT angiography in step-and-shoot technique with 256-slice CT: impact of the field of view on image quality, craniocaudal coverage, and radiation exposure. *Eur J Radiol* 81: 1562-1568.

Pannu, H. K., W. Alvarez, and E. K. Fishman. 2006. β-blockers for cardiac CT: a primer for the radiologist. *Am J Roentgenol* 186: S341-S346.

Pontone, G., D. Andreini, A. L. Bartorelli, S. Cortinovis, S. Mushtaq, E. Bertella, A. Annoni, A. Formenti, E. Nobili, D. Trabattoni, P. Montorsi, G. Ballerini, P. Agostoni, and M. Pepi. 2009. Diagnostic accuracy of coronary computed tomography angiography: a comparison between prospective and retrospective electrocardiogram triggering. *J Am Coll Cardiol* 54: 346-355.

Qin, J., L-Y Liu, X-C Meng, J-S Zhang, Y-X Dong, Y. Fang, and H. Shan. 2011. Prospective versus retrospective ECG gating for 320-detector CT of the coronary arteries: comparison of image quality and patient radiation dose. *Clinical Imaging* 35: 193-197.

Sabarudin, A., Z. Sun, and K-H. Ng. 2012. Radiation dose associated with coronary CT angiography and invasive coronary angiography: An experimental study of the effect of dose-saving strategies. *Radiat Prot Dosim* 150 (2): 180-187.

Shuman, W., K. Branch, J. May, L. Mitsumori, D. Lockhart, T. Dubinski, B. Warren, and J. Caldwell. 2008. Prospective versus retrospective ECG gating for 64-detector CT of the coronary arteries: comparison of image quality and patient radiation dose. *Radiology* 248: 431-437.

Shuman, W. P., K. R. Branch, J. M. May, L. M. Mitsumori, J. N. Strote, B. H. Warren, T. J. Dubinsky, D. W. Lockhart, and J. H. Caldwell. 2009. Whole-chest 64-MDCT of emergency department patients with nonspecific chest pain: radiation dose and coronary artery image quality with prospective ECG triggering versus retrospective ECG gating. *Am J Roentgenol* 192: 1662-1667.

Stolzmann, P., R. Goetti, S. Baumueller, A. Plass, V. Falk, H. Scheffel, G. Feuchtner, B. Marincek, H. Alkadhi, and S. Leschka. 2011. Prospective and retrospective ECG-gating for CT coronary angiography perform similarly accurate at low heart rates. *Eur J Radiol* 79: 85-91.

Sun, Z. 2010. Multislice CT angiography in cardiac imaging: prospective ECG-gating or retrospective ECG-gating? . *Biomed Imaging Interv J* 6 (1): e4.

Sun, Z., C. Lin, R. Davidson, C. Dong, and Y. Liao. 2008. Diagnostic value of 64-slice CT angiography in coronary artery disease: a systematic review. *Eur J Radiol* 67: 78-84.

Sun, Z., and K.-H. Ng. 2012. Prospective versus retrospective ECG-gated multislice CT coronary angiography: A systematic review of radiation dose and diagnostic accuracy. *Eur J Radiol* 81: e94-e100.

Van Mieghem, C. A. G., F. Cademartiri, N. R. Mollet, P. Malagutti, M. Valgimigli, W. B. Meijboom, F. Pugliese, E. P. McFadden, J. Ligthart, G. Runza, N. Bruining, P. C. Smits, E. Regar, W. J. van der Giessen, G. Sianos, R. Domburg, P. Jaegere, G. P. Krestin, P. W. Serruys, and P. J. de Feyter. 2006. Multislice spiral computed tomography for the evaluation of stent patency after left main coronary artery stenting: a comparison with conventional coronary angiography and intravascular ultrasound. *Circulation* 114: 645-653.

Weigold, W. 2009. Low-dose prospectively gated 256-slice coronary computed tomographic angiography. *Int J Cardiovasc Imaging* 25 (SUPPL. 2): 217-230.

Whiting, P., A. W. Rutjes, J. B. Reitsma, P. M. Bossuyt, and J. Kleijnen. 2003. The development of QUADAS: a tool for the quality assessment of studies of diagnostic accuracy included in systematic reviews. *BMC Med Res Methodol* 3: 25. http://www.biomedcentral.com/1471-2288/3/25 (accessed November 11, 2011.).

Xu, L., L. Yang, Z. Zhang, Y. Li, Z. Fan, X. Ma, B. Lv, and W. Yu. 2010. Low-dose adaptive sequential scan for dual-source CT coronary angiography in patients with high heart rate: Comparison with retrospective ECG gating. *Eur J Radiol* 76: 183-187.

Zhang, C., Z. Zhang, Z. Yan, L. Xu, W. Yu, and R. Wang. 2011. 320-row CT coronary angiography: effect of 100-kV tube voltages on image quality, contrast volume, and radiation dose. *Int J Cardiovasc Imaging* 27 (7): 1059-1068.

CHAPTER 5: RADIATION DOSE IN CORONARY CT ANGIOGRAPHY ASSOCIATED WITH PROSPECTIVE ECG-TRIGGERING TECHNIQUE: COMPARISONS WITH DIFFERENT CT GENERATIONS

5.1 Introduction

Coronary computed tomography angiography (CCTA) has been increasingly used in the diagnosis of coronary artery disease (CAD), thanks to its non-invasiveness, rapid acquisition of high resolution images and high diagnostic accuracy (Mollet et al. 2005; Raff et al. 2005). With rapid improvements in spatial and temporal resolution, CCTA not only visualises coronary anatomy and characterises plaque components, but also allows for quantitative analysis of coronary stenosis (Achenbach et al. 2006; Budoff et al. 2006; Earls et al. 2008; Hein et al. 2009; Rybicki et al. 2008). The rapidly increasing multidetector CT (MDCT) scanners have led to the increase of CCTA examinations worldwide (Efstathopoulos et al. 2009). However, high-radiation dose resulting from CCTA raises a major concern, as radiation-induced cancer is not negligible (Budoff et al. 2006; Coles et al. 2006; Efstathopoulos et al. 2009).

Previous studies have reported that CCTA with use of retrospective ECG-gating technique results in very high effective dose, which ranged from 13.4 mSv to 31.4 mSv (Earls et al. 2008; Einstein, Henzlova, and Rajagopalan 2007; Hirai et al. 2008; Maruyama et al. 2008). However, several dose-saving strategies have been introduced in the retrospective ECG-gated CCTA to deal with radiation dose issues, and these techniques include anatomy-based tube current modulation (Deetjen et al. 2007; Kalra et al. 2004), ECG-controlled tube current modulation (Abada et al. 2006; Gutstein et al. 2008; Hausleiter et al. 2006), tube voltage reduction (Francone et al. 2008; Herzog et al. 2008) and high-pitch scanning (Achenbach et al. 2010; Alkadhi et al. 2010).

Apart from these dose-saving strategies, prospective ECG-triggering technique was recently introduced in CCTA examination with resultant very low dose when compared to conventional retrospective ECG-triggering protocol (Earls et al. 2008; Hoe and Toh 2009; Maruyama et al. 2008). In prospective ECG-triggering (also called step-and-shoot mode), exposure is triggered by ECG signal and x-ray tube is only turned on at the selected cardiac phase (diastolic), and turned off during the rest of the cardiac cycle. Consequently, this results in a significant reduction of radiation dose during prospective ECG-triggering CCTA. In contrast, in retrospective gating technique, the x-ray tube remains turned on throughout the entire cardiac cycle, leading to higher radiation dose than the prospective triggering protocol (Earls 2009).

Because of the promising low-dose results, many studies have been conducted with recent CT models ranging from 64-slice to 320-slice scanners to compare prospective triggering and retrospective ECG-gating protocols with regard to the dose reduction, image quality and diagnostic value in CCTA (De France et al. 2010; Hoe and Toh 2009; Rybicki et al. 2008; Zhang et al. 2011). Despite satisfactory results in prospective ECG-triggered protocol, very few studies have been conducted to compare the radiation dose between different CT generations with use of prospective triggering (Efstathopoulos et al. 2012; Klass et al. 2009). Therefore, the aim of study was to compare the radiation dose associated with different multislice CT generations that is done using prospective ECG-triggering technique, based on a retrospective analysis of the patients undergoing CCTA.

5.2 Materials and methods

Three hospitals in Klang Valley, Malaysia and one major public hospital in Perth, Western Australia were selected for this study to determine radiation dose exposure to patients in routine CCTA procedures over 6 months (July 2011-January 2012). A retrospective data analysis was performed in all patients undergoing prospective ECG-triggered CCTA with different generations of MDCT scanners. All patients were referred for CCTA due to suspected or known CAD. Patients scanned with retrospective ECG-gated protocol, for other cardiovascular diseases such as pulmonary embolism or coronary artery bypass grafts were excluded from this study. The data were collected and recorded from each hospital independently.

5.2.1 Coronary CT angiography protocols

The study patients were divided into four groups based on CT scanner generations used. There were four different CT scanners from various manufacturers used in the study, namely single-source 64-slice CT (SSCT) (Brilliance 64, Philips Healthcare, USA), dual-source 64-slice CT (DSCT) (Somatom Definition, Siemens Healthcare, Germany), dual-source 128-slice CT (Somatom Definition Flash, Siemens Healthcare, Germany) and 320-slice CT (Aquilion ONE, Toshiba Medical System, Japan). Table 5-1 lists the details of CCTA scanning protocols corresponding to different generations of CT scanners, and patient characteristics. The tube current (mA) was selected manually depending on the availability of the scanner system (Table 5-1). Therefore, no tube current modulation was used in this study.

Table 5-1: Details of CCTA protocols and patients demographic

Manufacturer	Philips	Siemens	Siemens	Toshiba
Model	Briliance CT	Somatom Definition	Somatom Definition Flash	Aquillion ONE
No. of patients	43	50	31	40
Age (years)	49.3 ± 13.2	53.4 ± 9.6	49.0 ± 11.0	52.8 ± 9.3
Male (%)	51	58	55	75
BMI (kg/m^2)	25.7 ± 2.3	26.3 ± 3.8	25.5 ± 4.4	26.4 ± 4.2
$CTDI_{vol}$ (mGy)	15.7 ± 1.9	17.4 ± 7.8	28.4 ± 12.9	19.0 ± 6.8
Effective dose (mSv)	4.1 ± 0.6	4.2 ± 1.9	6.8 ± 3.2	3.8 ± 1.4
Exposure windows in R-R interval (%)	75	70-75	70, 10-90	70, 30-90
Tube voltage (kVp)	120	100-120	100-120	100-120
Tube current (mA)	150-210	320	320	300-580
No. of detector (mm)	64 × 0.625	32 × 2 × 0.625	64 × 2 × 0.625	320 × 0.5
Gantry rotation (ms)	420	330	280	350

All scan protocols covered from the level of tracheal bifurcation to the diaphragm and a non-ionic contrast media between 60 and 85 ml was administered with a flow rate from 4.5 to 6.0 ml/s in all study groups. A bolus tracking technique was used in all studies to ensure optimal coronary enhancement. The parameters of CT volume dose index ($CTDI_{vol}$) and dose length product (DLP) values were obtained from the scans. Effective dose was derived from the product of DLP and a conversion coefficient of 0.017 $mSv \cdot mGy^{-1} \cdot cm^{-1}$ was used for the chest region (Huda, Ogden, and Khorasani 2008).

5.2.2 Statistical analysis

Descriptive data were presented as mean ± standard deviation. Data analysis was performed by using SPSS version 19.0 (SPSS V19.0, Chicago, USA). A p value of less than 0.05 was considered statistical significance. Pearson correlation was used to test the relation between radiation dose and BMI in each group. Analysis of variance (ANOVA) test was also used for multifactorial mean comparisons.

5.3 Results

A total of 164 patients (98 males, 66 females) undergoing a prospective ECG-triggered CCTA procedure were included in the analysis. Demographic data of the study and radiation dose information are presented in Table 5-1.

The mean effective doses for each CT scanner group are presented in Figure 5-1. The results show that the highest effective dose was estimated at 6.8 ± 3.2 mSv in patients scanned with 128-slice DSCT, followed by 4.2 ± 1.9 mSv with 64-slice DSCT and 4.1 ± 0.6 mSv with 64-slice SSCT. Effective dose estimated in 320-slice CT was 3.8 ± 1.4 mSv, which is the lowest among the groups. There was a significant difference in the mean effective dose in patients scanned with 128-slice DSCT when compared to the other groups ($p<0.05$). However, no significant differences were found in the mean effective doses between 64-slice (SSCT and DSCT) and 320-slice CT groups ($p=0.71$).

The effective dose in males was slightly higher than that in females for 64-slice SSCT (4.1 mSv versus 4.0 mSv), 64-slice DSCT (4.4 mSv versus 4.1 mSv), 128-slice DSCT (6.9 mSv versus 6.6 mSv) and 320-slice CT (3.8 mSv versus 3.7 mSv). However, there was no significant difference in effective dose between males and females in all study groups ($p=$ 0.07, 0.27, 0.38 and 0.19 corresponding to 64-slice SSCT, 64-slice DSCT, 128-slice DSCT and 320 slice CT group, respectively).

Analysis of the relation between effective dose and BMI shows a significantly positive relationship (Figures 5-2,5-3, 5-4 and 5-5) in all groups with a Pearson correlation factor at $r=0.6$, $r= 0.8$, $r= 0.4$ and $r=0.7$, corresponding to 64-slice SSCT, 64-slice DSCT, 128-slice DSCT and 320-slice CT groups, respectively.

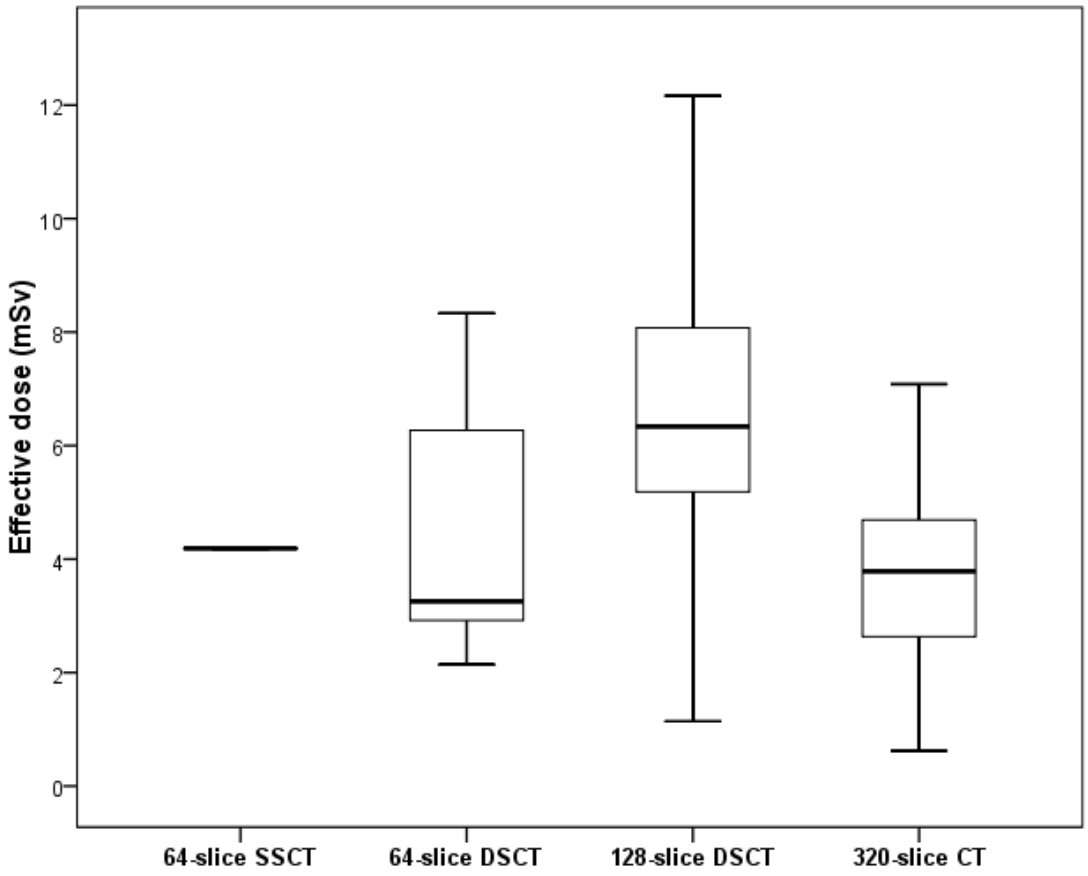

Figure 5-1: Box plot shows the mean effective dose reported in the studies with use of 64-slice SSCT, 64-slice DSCT, 128-slice DSCT and 320-slice CT. It shows that effective dose in 128-slice DSCT is the highest amongst all of four groups. Also, there is a very small range of dose distribution in 64-slice SSCT group. The box indicates the first to third quartiles, the line in the box indicates median quartile, and whiskers indicate the minimum and maximum values.

The effective dose was also compared between 100 kVp and 120 kVp protocols in three groups using 64-slice DSCT, 128-slice DSCT and 320-slice CT. The results show that the differences in effective dose between 100 kVp and 120 kVp protocols are significant in all groups. The mean effective doses were estimated with 3.0 ± 0.5 mSv and 6.6 ± 1.1 mSv in 64-slice DSCT; 5.3 ± 2.1 mSv and 8.0 ± 3.4 mSv in 128-slice DSCT; and 2.8 ± 1.0 mSv and 4.5 ± 1.2 mSv in 320-slice CT corresponding to 100 and 120 kVp respectively. However, the comparison was not performed in 64-slice SSCT group since 100 kVp was not available in the system.

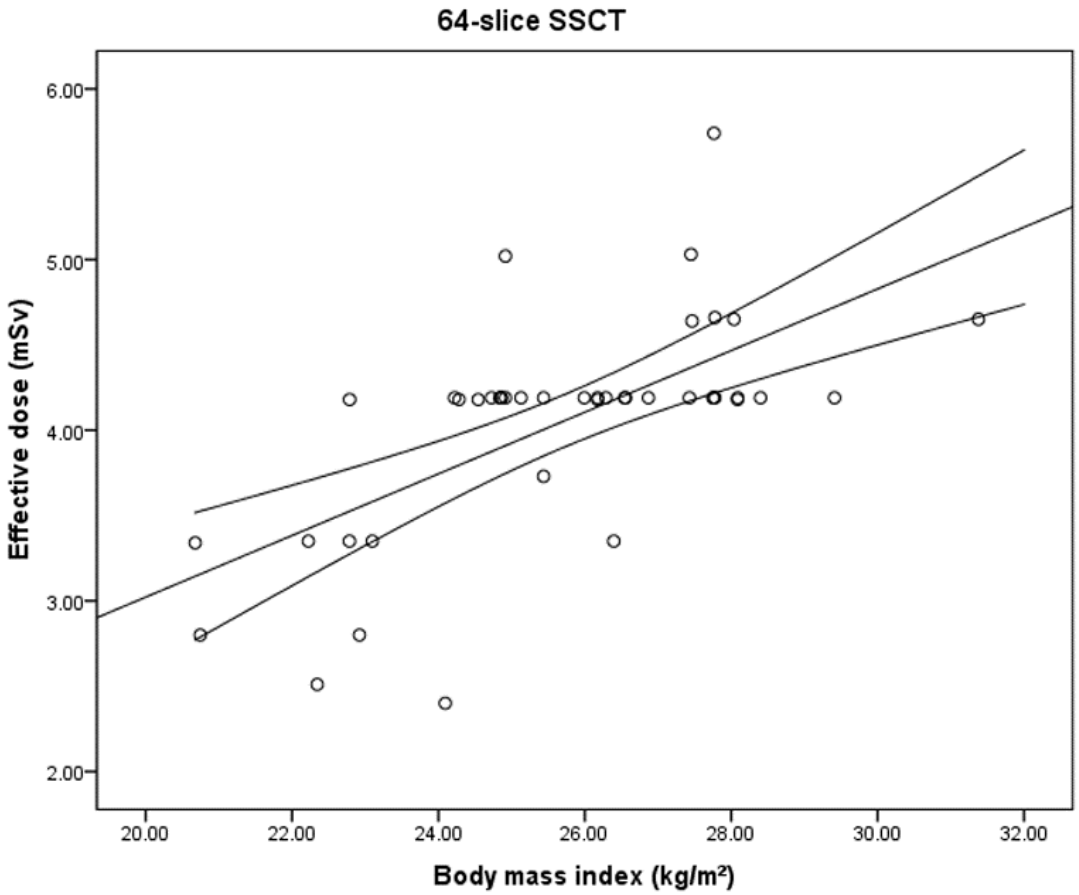

Figure 5-2: Correlation graph analysis of effective dose depending on body mass index (BMI) for 64-slice SSCT; r = 0.6.

5.4 Discussion

This study highlights two important findings in radiation dose associated with prospective ECG-triggered CCTA. First, low-radiation dose can be achieved in CCTA between different generations of CT scanners with the application of prospective ECG-triggering protocol. Second, BMI affects the radiation dose significantly. Patients with large BMI are most likely to receive higher radiation dose when undergoing prospective ECG-triggered CCTA.

This comparative study was performed at four different clinical centres where coronary CT angiography was performed using different types of MDCT scanners. Since this study was performed with prospective ECG-triggering, the scan acquisition was made in sequential (axial) mode rather than spiral (helical) mode. BMI is another main factor that needs to be considered during CCTA as it is closely related to the selection of kVp and mA values, thus, it has a direct impact on radiation dose and image quality due to the wide ranges of kVp or mA selections. Despite different clinical sites were included, the same scanning protocol was used among these centres, thus enabling a comparative analysis of radiation dose from

different generations of MDCT scanners. Selection of tube voltage was based on patients' BMI. Patients with BMI < 25 kg/m^2 was scanned with 100 kVp protocol, while a patient with BMI > 25 kg/m^2, a tube voltage of 120 kVp was applied. Although the 100 kVp protocol was not available with the 64-slice SSCT, the results were not significantly affected due to a small number of patients (n=11) having BMI less than 25 kg/m^2 in this cohort. Previous studies have reported that effective dose in 100 kVp was significantly lower than that in 120 kVp which patients were classified into these two groups (100- and 120-kVp) based on their BMI (Feuchtner, Jodocy, et al. 2010; Park et al. 2009; Zhang et al. 2011).

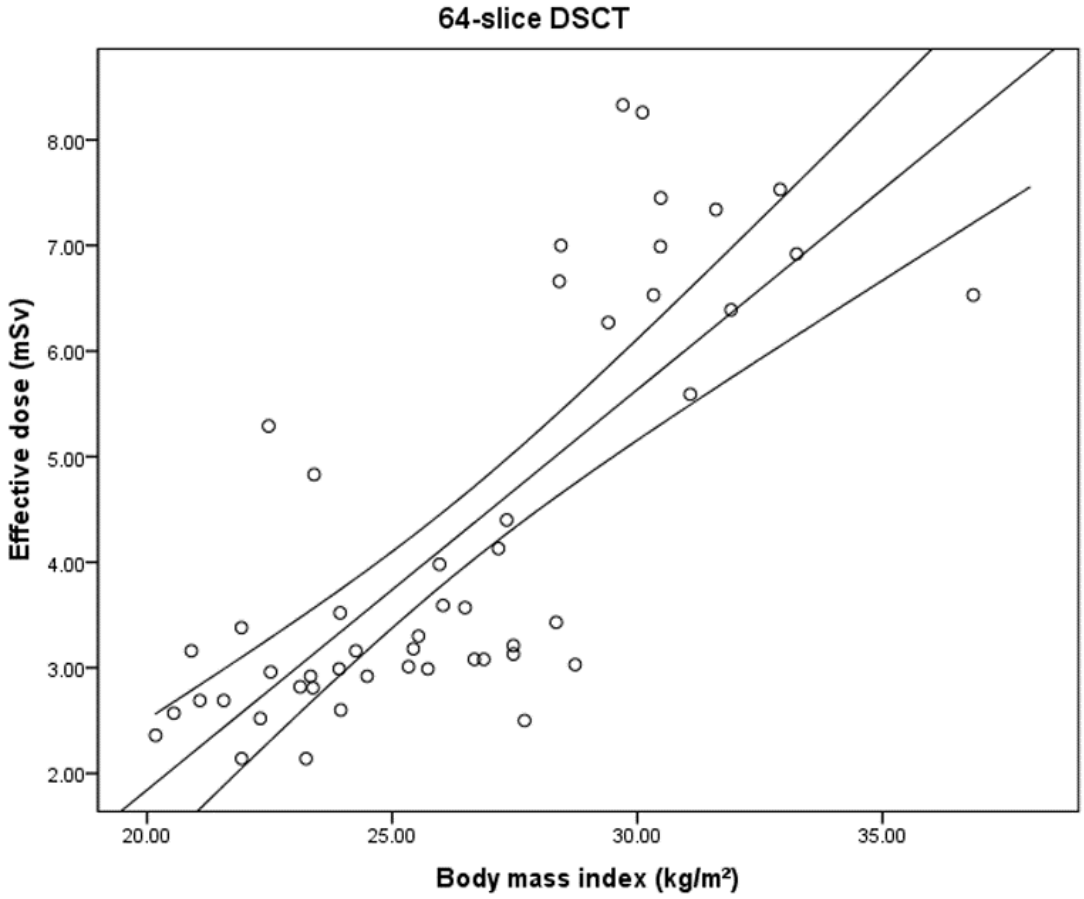

Figure 5-3: Correlation graph analysis of effective dose depending on body mass index (BMI) for 64-slice DSCT; r = 0.8.

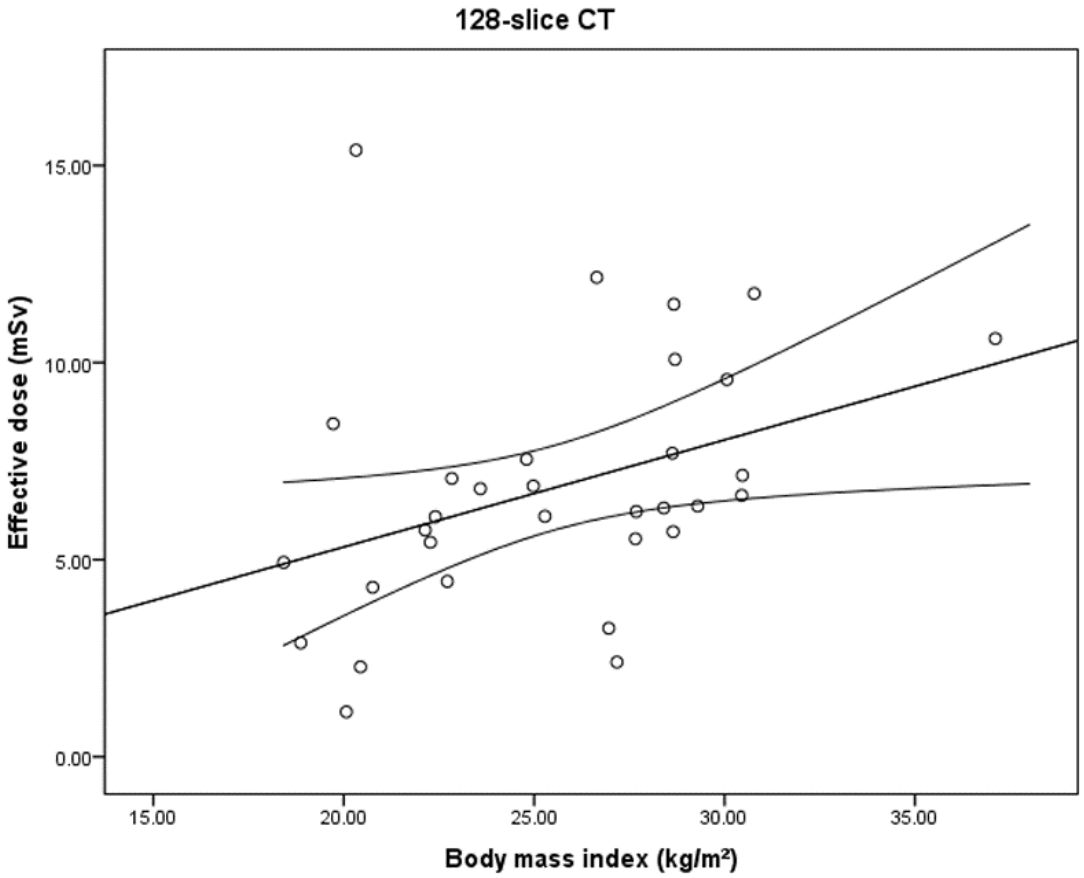

Figure 5-4: Correlation graph analysis of effective dose depending on body mass index (BMI) for 128-slice DSCT; r = 0.4.

It has been widely reported that prospective ECG-triggering protocol reduces radiation dose significantly compared to the conventional retrospective ECG-gating technique, with a dose reduction ranging from 76% to 83% (Earls et al. 2008; Hirai et al. 2008; Maruyama et al. 2008). Our results are in line with previous reports. The effective dose of prospective ECG-triggered CCTA was estimated between 3.8 mSv and 6.8 mSv, which correspond to dose reduction between 63% and 82% when compared to effective dose in retrospective ECG-gating from previous studies (Earls et al. 2008; Hirai et al. 2008; Maruyama et al. 2008). In addition, low-radiation dose recorded in our study was found to be similar to that of invasive coronary angiography, which ranges from 3.1 mSv to 10.6 mSv (Betsou et al. 1998; Karpinner et al. 1995; Leung and Martin 1996).

Our study showed that mean effective dose estimated from 64-slice CT scanners (DSCT with 4.2 mSv and SSCT with 4.1 mSv) was consistent with previous results, in which effective dose in DSCT ranged from 2.2 to 6.5 mSv (Alkadhi et al. 2010; Blankstein et al. 2009; Stolzmann et al. 2011; Xu et al. 2010; Zhao et al. 2009) and in SSCT ranged from 2.8 to 5.7 mSv (Earls et al. 2008; Freeman et al. 2009; Klass et al. 2009; Maruyama et al. 2008;

Pontone et al. 2009). Current data also show that there was no significant difference in effective dose between 64-slice DSCT and SSCT (p=0.97) with prospective ECG-triggered protocol since sequential mode data acquisition (step-and-shoot) was used in the study.

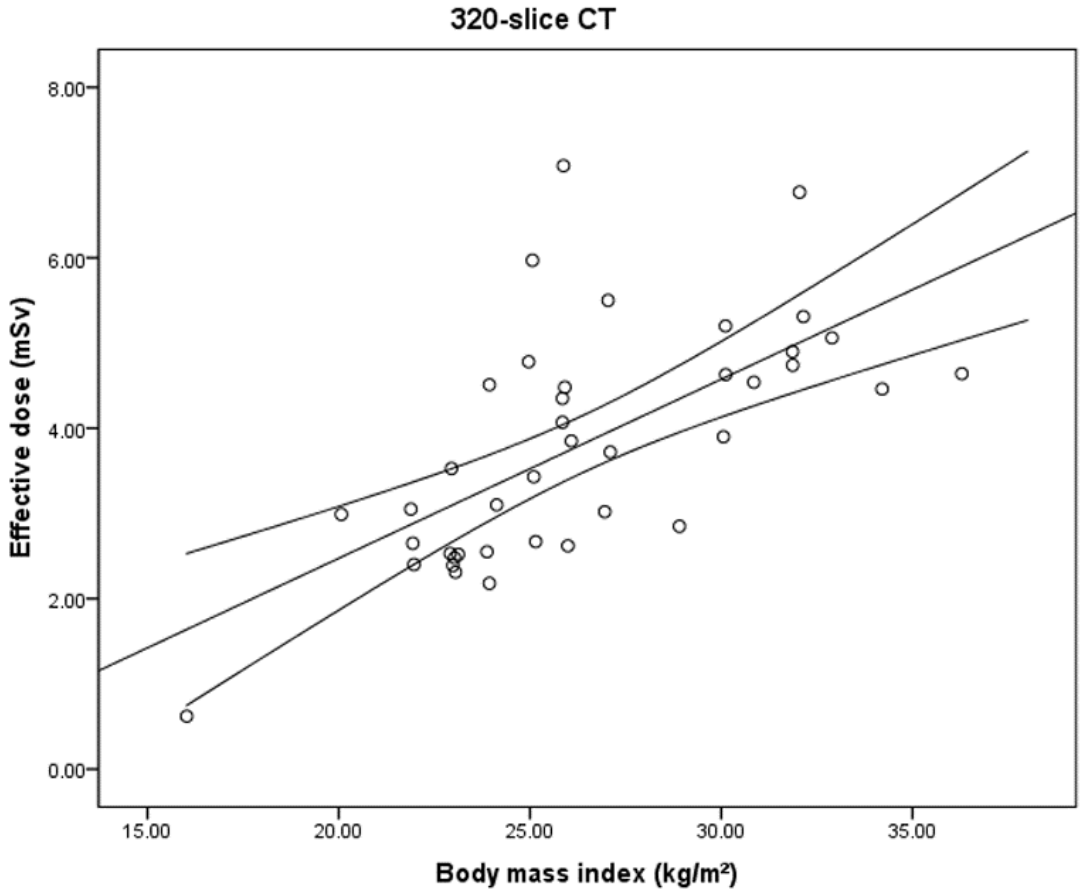

Figure 5-5: Correlation graph analysis of effective dose depending on body mass index (BMI) for 320-slice CT; r = 0.7.

However, studies on 64-slice CT with the application of retrospective ECG-gated CCTA reported that DSCT produces significantly lower radiation dose compared to SSCT in patients with higher heart rate (>70 bpm) due to interchangable pitch mode corresponding to patients' heart rate (Sabarudin, Sun, and Ng 2012; Wang et al. 2009).

The 128-slice DSCT using prospective ECG-triggering technique is associated with a wide range of effective dose. In comparison with other reports using 128-slice DSCT prospective ECG-triggering technique, the average effective dose in our data is significantly lower than that reported in other studies, which ranges from 1.7 to 14 mSv (Anders et al. 2009; Feuchtner, Götti, et al. 2010). However, the wide range in 128-slice CT effective dose might be caused by the scanning protocol variations such as adding 'padding' windows for patients

with high heart rate variability. Padding technique is described as prolonging the acquisition window in order to compensate for minor heart rate variations and to produce consistent image quality. However, the average effective dose (6.8 mSv) in our study was found to be higher than that acquired with the high-pitch spiral mode reported in some recent studies using 128-slice CT with estimated effective dose of less than 1 mSv (Achenbach et al. 2010; Alkadhi et al. 2010). This emphasises the importance of using high-pitch model in cardiac imaging.

Our study shows that there is no significant difference in effective dose between male and female patients. This is different from the previous literature data, since higher effective dose was reported in females (ranges from 16.3 mSv to 18 mSv) than males (ranges from 12 mSv to 15 mSv) when CCTA was performed with retrospective ECG-gating protocol (Esposito et al. 2012; Mollet et al. 2005; Raff et al. 2005). However, a study conducted on radiation dose comparison reported that breast dose could be reduced up to 76% with the application of prospective ECG-triggered protocol with use of 70-80% exposure window (Abadi et al. 2011). This is because there is only a small amount of radiation dose absorbed in the breast tissue during prospective ECG-triggered protocol, which leads to a minimal contribution to the total radiation dose.

There are some limitations in this study. For example, image quality assessment was not included since this study focused on the dose comparison between different generations of CT scanners, rather than image quality assessment. Another limitation is a small number of cases being included in each study group due to the strict heart rate control applied to all patients undergoing prospective ECG-gating protocol, thus, excluding a large number of patients. Further studies in patients undergoing prospective ECG-triggered CCTA with inclusion of different heart rates should be conducted to explore the resultant radiation dose.

5.5 Conclusion

In conclusion, low radiation dose can be achieved in low and regular heart rate with prospective ECG-triggering protocol, regardless of the CT scanner generation. Although there is no significant difference in effective dose between genders, BMI is identified as the main factor that significantly affects the radiation dose in prospective ECG-triggered CCTA in our study.

5.6 References

Abada, H. T., C. Larchez, B. Daoud, A. Sigal-Cinqualbre, and J. F. Paul. 2006. MDCT of the coronary arteries: feasibility of low-dose CT with ECG-pulsed tube current modulation to reduce radiation dose. *Am J Roentgenol* 186: S387-S390.

Abadi, S., H. Mehrez, A. Ursani, M. Parker, and N. Paul. 2011. Direct quantification of breast dose during coronary CT angiography and evaluation of dose reduction strategies. *Am J Roentgenol* 196: W152-W158.

Achenbach, S., M. Marwan, D. Ropers, T. Schepis, T. Pflederer, and K. Anders. 2010. Coronary computed tomography angiography with a consistent dose below 1mSv using prospectively electrocardiogram-triggered high-pitch spiral acquisition. *Eur Heart J* 31: 340-346.

Achenbach, S., D. Ropers, A. Kuettner, T. Flohr, B. Ohnesorge, H. Bruder, H. Theessen, M. Karakaya, W. G. Daniel, W. Bautz, W. A. Kalender, and K. Anders. 2006. Contrast-enhanced coronary artery visualization by dual-source computed tomography-Initial experience. *Eur J Radiol* 57: 331-335.

Alkadhi, H., P. Stolzmann, L. Desbiolles, S. Baumueller, R. Goetti, and A. Plass. 2010. Low-dose, 128-slice, dual-source CT coronary angiography: accuracy and radiation dose of the high-pitch and the step-and-shoot mode. *Heart* 96: 933-938.

Anders, K., U. Baum, S. Gauss, M. A. Kuefner, S. Achenbach, A. Kuettner, W. G. Daniel, M. Uder, and D. Ropers. 2009. Initial experience with prospectively triggered, sequential CT coronary angiography on a 128-slice scanner. *Rofo* 181: 332-338.

Betsou, S., E. P. Efstathopoulos, D. Katritsis, K. Faulkner, and G. Panayiotakis. 1998. Patient radiation doses during cardiac catheterization procedures. *Br J Radiol* 71: 634-639.

Blankstein, R., A. Shah, R. Pale, S. Abbara, H. Bezerra, M. Bolen, W. S. Mamuya, U. Hoffmann, T. J. Brady, and R. C. Cury. 2009. Radiation dose and image quality of prospective triggering with dual-source cardiac computed tomography. *Am J Cardiol* 103 (8): 1168-1173.

Budoff, M. J., S. Achenbach, R. S. Blumenthal, J. J. Carr, J. G. Goldin, P. Greenland, A. D. Guerci, J. A.C. Lima, D. J. Rader, G. D. Rubin, L. J. Shaw, and S. E. Wiegers. 2006. Assessment of coronary artery disease by cardiac computed tomography-a scientific statement from the American Heart Association Committee on Cardiovascular Imaging and Intervention, Council on Cardiovascular Radiology and Intervention and Committee on Cardiac Imaging, Council on Clinical Cardiology. *Circulation* 114 (16): 1761-1791.

Coles, D. R., M. A. Smail, I. S. Negus, P. Wilde, M. Oberhoff, K. R. Karsch, and A. Baumbach. 2006. Comparison of radiation doses from multislice computed tomography coronary angiography and conventional diagnostic angiography. *J Am Coll Cardiol* 47 (9): 1840-1845.

De France, T., E. Dubois, D. Gebow, A. Ramirez, F. Wolf, and G. M. Feuchtner. 2010. Helical prospective ECG-gating in cardiac computed tomography: radiation dose and image quality. *Int J Cardiovasc Imaging* 26: 99-110.

Deetjen, A., S. Mollmann, G. Conradi, A. Rolf, A. Schmermund, C. W. Hamm, and T. Dill. 2007. Use of automatic exposure control in multislice computed tomography of the coronaries: comparison of 16-slice and 64-slice scanner data with conventional coronary angiography. *Heart* 93: 1040-1043.

Earls, J. P. 2009. How to use a prospective gated technique for cardiac CT. *J Cardiovasc Comput Tomogr* 3: 45-51.

Earls, J. P., E. L. Berman, B. A. Urban, C. A. Curry, J. L. Lane, R. S. Jennings, C. C. McCulloch, J. Hsieh, and J. H. Londt. 2008. Prospectively gated transverse coronary CT angiography versus retrospectively gated helical technique: improved image quality and reduced radiation dose. *Radiology* 246: 742-753.

Efstathopoulos, E. P., N. L. Kelekis, I. Pantos, E. Brountzos, S. Argentos, J. Greb´a, D. Ziaka, D. G. Katritsis, and I. Seimenis. 2009. Reduction of the estimated radiation dose and associated patient risk with prospective ECG-gated 256-slice CT coronary angiography. *Phys Med Biol* 54 (17): 5209-5222.

Efstathopoulos, E. P., I. Pantos, S. Thalassinou, S. Argentos, N. L. Kelekis, T. Zografos, G. Panayiotakis, and D. G. Katritsis. 2012. Patient radiation doses in cardiac computed tomography:comparison of published results with prospective and retrospective acquisition. *Radiat Prot Dosim* 148: 83-91.

Einstein, A. J., M. J. Henzlova, and S. Rajagopalan. 2007. Estimating risk of cancer associated with radiation exposure from 64-slice computed tomography coronary angiography. *J Am Med Assoc* 298 (3): 317-323.

Esposito, A., F. De Cobelli, C. Colantoni, G. Perseghin, A. del Vecchio, T. Canu, R. Calandrino, and A. D. Maschio. 2012. Gender influence on dose saving allowed by prospective-triggered 64-slice multidetector computed tomography coronary angiography as compared with retrospective-gated mode. *Int J Cardiol* 158 (2): 253-259.

Feuchtner, G., R. Götti, A. Plass, S. Baumueller, P. Stolzmann, H. Scheffel, M. Wieser, B. Marincek, H. Alkadhi, and S. Leschka. 2010. Dual-step prospective ECG-triggered 128-slice dual-source CT for evaluation of coronary arteries and cardiac function without heart rate control: a technical note. *Eur Radiol* 20 (9): 2092-2099.

Feuchtner, G. M., D. Jodocy, A. Klauser, B. Haberfellner, I. Aglan, A. Spoeck, S. Hiehs, P. Soegner, and W. Jaschke. 2010. Radiation dose reduction by using 100-kV tube voltage in cardiac 64-slice computed tomography: A comparative study. *Eur J Radiol* 75: e51-e56.

Francone, M., E. DiCastro, A. Napoli, C. Bolzan, I. Carbone, L. Bertoletti, L. Iuliano, C. Catalano, and R. Passariello. 2008. Dose reduction and image quality assessment in 64-detector row computed tomography of the coronary arteries using an automatic exposure control system. *J Comput Assist Tomogr* 32: 668-678.

Freeman, A. P., R. Comerford, J. Lambros, S. Eggleton, and D. Friedman. 2009. 64 slice CT coronary angiography--marked reduction in radiation dose using prospective gating. *Heart Lung Circ* 18 (Supplement 3): S13-S13.

Gutstein, A., A. Wolak, C. Lee, D. Dey, M. Ohba, Y. Suzuki, V. Cheng, H. Gransar, S. Suzuki, J. Friedman, L. E. Thomson, S. Hayes, R. Pimentel, W. Paz, P. Slomka, and D. S. Berman. 2008. Predicting success of prospective and retrospective gating with

dual-source coronary computed tomography angiography: development of selection criteria and initial experience. *J Cardiovasc Comput Tomogr* 2: 81-90.

Hausleiter, J., T. Meyer, M. Hadamitzky, E. Huber, M. Zankl, S. Martinoff, A. Kastrati, and A. Schömig. 2006. Radiation dose estimates from cardiac multislice computed tomography in daily practice: impact of different scanning protocols on effective dose estimates. *Circulation* 113: 1305-1310.

Hein, P. A., V. C. Romano, A. Lembcke, J. May, and P. Rogalla. 2009. Initial experience with a chest pain protocol using 320-slice volume MDCT. *Eur Radiol* 19 (5): 1148-1155.

Herzog, C., D. M. Mulvihill, S. A. Nguyen, G. Savino, B. Schmidt, P. Costello, T. J. Vogl, and U. J. Schoepf. 2008. Pediatric cardiovascular CT angiography: radiation dose reduction using automatic anatomic tube current modulation. *Am J Roentgenol* 190: 1232-1240.

Hirai, N., J. Horiguchi, C. Fujioka, M. Kiguchi, H. Yamamoto, N. Matsuura, T. Kitagawa, H. Teragawa, N. Kohno, and K. Ito. 2008. Prospective versus retrospective ECG-gated 64-detector coronary CT angiography: assessment of image quality, stenosis, and radiation dose. *Radiology* 248: 424-430.

Hoe, J., and K. H. Toh. 2009. First experience with 320-row multidetector CT coronary angiography scanning with prospective electrocardiogram gating to reduce radiation dose. *J Cardiovasc Comput Tomogr* 3: 257-261.

Huda, W., K. M. Ogden, and M. R. Khorasani. 2008. Converting dose-length product to effective dose at CT. *Radiology* 248: 995-1003.

Kalra, M. K., M. l. M. Maher, T. L. Toth, B. Schmidt, B. L. Westerman, H. T. Morgan, and S. Saini. 2004. Techniques and applications of automatic tube current modulation for CT. *Radiology* 233: 649-657.

Karpinner, J., T. Parviainen, A. Servomaa, and T. Komppa. 1995. Radiation risk and exposure of radiologists and patients during coronary angiography and percutaneous transluminar coronary angioplasty (PTCA). *Radiat Prot Dosim* 57: 481-485.

Klass, O., M. Walker, A. Siebach, T. Stuber, S. Feuerlein, M. Juchems, and M. H. K. Hoffmann. 2009. Prospectively gated axial CT coronary angiography: comparison of image quality and effective radiation dose between 64- and 256-slice CT. *Eur Radiol* 20: 1124-1131.

Leung, K. C., and C. J. Martin. 1996. Effective doses for coronary angiography. *Br J Radiol* 69: 426-431.

Maruyama, T., M. Takada, T. Hasuike, A. Yoshikawa, E. Namimatsu, and T. Yoshizumi. 2008. Radiation dose reduction and coronary assessability of prospective electrocardiogram-gated computed tomography coronary angiography: comparison with retrospective electrocardiogram-gated helical scan. *J Am Coll Cardiol* 52 (18): 1450-1455.

Mollet, N. R., F. Cademartiri, C. A. G. van Mieghem, G. Runza, E. P. McFadden, T. Baks, P. W. Serruys, G. P. Krestin, and P. J. de Feyter. 2005. High-resolution spiral computed tomography coronary angiography in patients referred for diagnostic conventional coronary angiography. *Circulation* 112 (15): 2318-2323.

Park, E.-A., W. Lee, J.-H. Kang, Y. H. Yin, J. W. Chung, and J. H. Park. 2009. The image quality and radiation dose of 100-kVp versus 120-kVp ECG-gated 16-slice CT coronary angiography. *Korean J Radiol* 10 (3): 235-243.

Pontone, G., D. Andreini, A. L. Bartorelli, S. Cortinovis, S. Mushtaq, E. Bertella, A. Annoni, A. Formenti, E. Nobili, D. Trabattoni, P. Montorsi, G. Ballerini, P. Agostoni, and M. Pepi. 2009. Diagnostic accuracy of coronary computed tomography angiography: a comparison between prospective and retrospective electrocardiogram triggering. *J Am Coll Cardiol* 54: 346-355.

Raff, G. L., M. J. Gallagher, W. W. O'Neill, and J. A. Goldstein. 2005. Diagnostic accuracy of noninvasive coronary angiography using 64-slice spiral computed tomography. *J Am Coll Cardiol* 46 (3): 552-557.

Rybicki, F., H. Otero, M. Steigner, G. Vorobiof, L. Nallamshetty, D. Mitsouras, H. Ersoy, R. Mather, P. Judy, T. Cai, K. Coyner, K. Schultz, A. Whitmore, and M. Di Carli. 2008. Initial evaluation of coronary images from 320-detector row computed tomography. *Int J Cardiovasc Imaging* 24 (5): 535-546.

Sabarudin, A., Z. Sun, and K.-H. Ng. 2012. A systematic review of radiation dose associated with different generations of multidetector CT coronary angiography. *J Med Imag Radiat Oncol* 56: 5-17.

Stolzmann, P., R. Goetti, S. Baumueller, A. Plass, V. Falk, H. Scheffel, G. Feuchtner, B. Marincek, H. Alkadhi, and S. Leschka. 2011. Prospective and retrospective ECG-gating for CT coronary angiography perform similarly accurate at low heart rates. *Eur J Radiol* 79: 85-91.

Wang, M., H. Qi, X. Wang, T. Wang, J. Chen, and C. Liu. 2009. Dose performance and image quality: dual source CT versus single source CT in cardiac CT angiography. *Eur J Radiol* 72: 396-400.

Xu, L., L. Yang, Z. Zhang, Y. Li, Z. Fan, X. Ma, B. Lv, and W. Yu. 2010. Low-dose adaptive sequential scan for dual-source CT coronary angiography in patients with high heart rate: Comparison with retrospective ECG gating. *Eur J Radiol* 76: 183-187.

Zhang, C., Z. Zhang, Z. Yan, L. Xu, W. Yu, and R. Wang. 2011. 320-row CT coronary angiography: effect of 100-kV tube voltages on image quality, contrast volume, and radiation dose. *Int J Cardiovasc Imaging* 27 (7): 1059-1068.

Zhao, L., Z. Zhang, Z. Fan, L. Yang, and J. Du. 2009. Prospective versus retrospective ECG gating for dual source CT of the coronary stent: comparison of image quality, accuracy, and radiation dose. *Eur J Radiol* 77: 436-442.

CHAPTER 6: A SURVEY STUDY EXPLORING LOCAL CARDIOLOGISTS AND RADIOGRAPHERS' PERCEPTIONS OF THE BENEFITS AND CHALLENGES IN RELATION TO PROSPECTIVE ECG-GATED CORONARY CT ANGIOGRAPHY

6.1 Introduction

Coronary CT Angiography (CCTA) has been increasingly used in the diagnosis of coronary artery disease due to improved spatial and temporal resolution since 64- or more slice-CT was introduced into clinical practice (Earls et al. 2008; Efstathopoulos et al. 2009; Hamon, Morello, and Riddell 2007; Hein et al. 2009; Kalender 2000; Sun 2010). However, high radiation doses associated with CCTA has raised serious concerns in the field of medicine and literature, as radiation-induced malignancy is non-negligible. In response to these concerns, several dose-saving strategies have been introduced, such as electrocardiogram (ECG)-controlled tube current modulation (Abada et al. 2006; Hausleiter et al. 2006), lowering the tube voltage (Francone et al. 2008; Herzog et al. 2008), high pitch values (Achenbach et al. 2010) and prospective ECG-triggering techniques (Bischoff et al. 2010; Pontone et al. 2009; Shuman et al. 2008) with the aim of achieving minimal dose with diagnostic image quality.

Of these dose-saving approaches, prospective ECG-triggering CCTA has proved to be a very effective approach for dose reduction when compared to other dose-saving strategies (Earls et al. 2008; Sabarudin, Sun, and Ng 2012). Prospective ECG-triggered data acquisition was initially used in coronary calcium scoring with electron-beam CT (Hounsfield 1980; Sun 2010). Currently, prospective ECG-triggering technique has been widely used in clinical practice for Coronary CT Angiography due to the very low radiation dose involved.

Despite all these advantages, there are some challenges that exist when performing prospective ECG-triggering technique in order to achieve satisfactory diagnostic results. It is generally agreed, that prospective ECG-triggering is applicable to patients with a low and regular heart rate (Earls et al. 2008; Herzog et al. 2008; Ko et al. 2010) albeit with high diagnostic accuracy (>90%). Image quality and diagnostic accuracy of CCTA will be compromised due to the artefacts in patients with high (>65 bpm) or irregular heart rate (heart rate variation >6bpm) (Ko et al. 2010; Pontone et al. 2009). It has been reported that the diagnostic accuracy of prospective ECG-triggering was inferior to that received from retrospective ECG-gating, given the presence of artefacts due to high heart rate variability in prospective ECG-triggered scans, which resulted in the reduction of diagnostic sensitivity and specificity (Pontone et al. 2009). The number of non-assessable coronary arteries was increased in patients with a heart rate more than 75 bpm when prospective ECG-triggering was used (Ko et al. 2010). Therefore, prospective ECG-triggered CCTA has inherent

limitations that present some potential challenges for clinicians to deal with, before this technique is widely recommended in clinical practice. Although more studies using prospective ECG-triggered CCTA are being performed at many clinical centres, there is little information available in the literature with regard to the perceptions or opinions of clinicians towards the application of prospective triggering techniques. In order to provide some insights into this area, a structured survey was conducted among clinical and imaging practitioners consisting of cardiologists, radiologists and radiographers who were experienced in using prospective ECG-triggering CCTA in their practice in Malaysia. This survey has been designed to explore their opinions concerning the benefits and difficulties in performing prospective ECG-gating CCTA, and determined the levels of preference and effects of an individual's experience when undergoing prospective ECG-gating CCTA.

6.2 Materials and methods

6.2.1 Survey design and setting

The survey process commenced with an in-depth consultation with cardiologists from the National Heart Institute at Kuala Lumpur, Malaysia. This enabled the identification of the benefits of performing prospective ECG-gating CCTA and the challenges in pursuing the procedure (Table 6-1) in all 3 sections of the questionnaires (Appendix B). This study was approved by the local institutional ethics committee.

This study was a cross-sectional study conducted in 6 health institutions in the Klang Valley, Malaysia and included public and private hospitals where prospective ECG-gating CCTA was routinely performed for the diagnosis of coronary artery disease between November 2011 and January 2012. The recruitment of subjects was undertaken through convenience sampling among radiologists, cardiologists and radiographers who were experienced in performing prospective ECG-gated CTCA. Radiographers and specialists who had no experience in coronary CT examinations/reports were excluded from the study. All potential subjects were screened and only those meeting the selection criteria were given the survey form. All respondents were required to return the survey form on the same day.

Respondents were asked a few profile questions including their demographic details, work experience and organizational background as shown in section 1. The main part of the questionnaire was presented in sections 2 and 3. These two sections dealt with the potential benefits and the difficulties in performing prospective ECG-triggering CCTA based on the respondents' clinical experiences. The respondents were asked about their degree of agreement with regard to the benefits and difficulties in performing prospective ECG-

triggering CCTA. The response options included: 'strongly agree', 'agree', 'do not know', 'disagree' and 'strongly disagree'.

Table 6-1: Respondents were asked to state their level of agreement for each statement which leads to the benefits and limitations of prospective ECG-triggered coronary CT angiography (strongly agree, agree, do not know, disagree and strongly disagree).

Benefits of prospective ECG-triggered CCTA	**Difficulties in performing prospective ECG-triggered CCTA**
Reduce radiation dose	Heart rate issues
Improve diagnostic image quality	Difficulty in obtaining cardiac functional assessments
Increase number of patients or cases (patient's output)	Image quality concerns
Increase financial incentives	Diagnostic accuracy concerns
-	Data processing management issues

6.2.2 Statistical analysis

All data were analysed using the SPSS version 19.0 (SPSS V 19.0, Chicago, ILL). Descriptive statistics were expressed as mean value ± standard deviation. One sample t-test and analysis of variance (ANOVA) was performed to determine if there was any significant difference between the respondents from different institutions (specialists versus radiographers, public hospitals versus private practice) and the types of scanners used (64-, 128-, 256- and 320-slice CT) respectively.

6.3 Results

6.3.1 Respondents' backgrounds

In total, 53 out of 62 respondents returned the questionnaires (response rate of 85%) in this survey (Table 6-2). Eleven out of 16 specialists responded and these specialists consisted of 9 cardiologists and 2 radiologists who were actively (reporting/conducting) involved in prospective ECG-gating CCTA. Nine specialists were male and the 2 remaining were female. All specialists had at least 6 years of working experience with Coronary CT Angiography, with 36.4% of the specialists having more than 20 years' experience in cardiac CT imaging. More than half of them were consultants in private practice institutions (n=9).

Table 6-2: Respondent's distribution

Subgroup	**Number of respondents**	**Male**	**Private hospitals**	**Year of experience (>6 years)**
Cardiologists	9 (17%)	9 (17%)	7 (13%)	9 (17%)
Radiologists	2 (4%)	0 (0%)	2 (4%)	2 (4%)
Radiographers	42 (79%)	21 (40%)	33 (62%)	12 (23%)
Total	**53 (100%)**	**30 (57%)**	**42 (79%)**	**23 (44%)**

Of 46 radiographers who received the questionnaires, 42 responded displaying an equal ratio between the male and female respondents. Most of the radiographers (71%) who participated in this study had less than 6 years of experience in performing Coronary CT Angiography examinations. However, 7 radiographers were found to have more than 10 years' experiences with CCTA imaging. In addition, more than half of responding radiographers had worked in private hospitals (n=33) compared to the small number of radiographers working in the public health institutions (n=9).

6.3.2 Benefits and challenges in performing prospective ECG-gating CCTA

There was no significant difference in the perceptions or opinions between the specialists and radiographers with regard to the benefits and difficulties in performing prospective ECG-gating CCTA (p-= 0.43-0.44). A comparison between specialists and radiographers' opinions on both, the benefits and challenges in performing prospective ECG-gating CCTA is displayed in Table 6-3. All specialists indicated that reduction in radiation doses was the main benefit of using prospective ECG-gating technique, while 93% radiographers showed similar opinions.

Table 6-3: Percentage of agreement (strongly agree and agree) with regard to benefits and difficulties when performing prospective ECG-triggered CCTA between two groups of respondents.

Items	Specialists			Radiographers		
	Number of agreement (n)	**%**	**X^2, *p*-value**	**Number of agreement (n)**	**%**	**X^2, *p*-value**
Reduce radiation dose	11	100.0	-	39	92.9	30.86 (0.000)
Improve diagnostic image quality	9	81.8	4.45 (0.035)	33	78.6	13.71 (0.000)
Increase number of patients or cases (patient's output)	8	72.7	2.27 (0.132)	28	66.7	4.67 (0.031)
Increase financial incentives	2	18.2	4.45 (0.035)	18	42.9	0.86 (0.355)
Heart rate issues	11	100.0	-	32	76.2	11.52 (0.001)
Difficulty in obtaining cardiac functional assessments	9	81.8	4.45 (0.035)	22	52.4	0.095 (0.758)
Image quality concerns	10	90.9	7.36 (0.007)	30	71.4	7.71 (0.005)
Diagnostic accuracy concerns	8	72.7	2.27 (0.132)	27	64.3	3.43 (0.064)
Data processing management issues	7	63.6	0.82 (0.366)	24	57.1	0.86 (0.355)

More than 65% of each respondent groups agreed that with the use of prospective ECG-gating CCTA technique, there would be an increase in the acquisition of diagnostic quality images and the number of cases (patients' output). However, there was little agreement among respondent groups with regard to the factor that prospective ECG-gating techniques would not result in any profits accruing to the institutions. Further, more than half of specialists (63.6%) did not know how the scanning technique correlated with the institutional economy benefits. With regard to the prospective ECG-gating technique and whether it could improve image quality, both, the specialists and radiographers displayed strong agreement at 82% and 79% respectively, although this did not result in a significant difference.

All the specialists agreed that heart rate issues were the major obstacles when performing prospective ECG-gating techniques. This was also supported by the radiographers of whom, 76.2% agreed that heart rate issue was an obstacle when performing the CCTA. More than 55% respondents agreed that the cardiac functional analysis, data processing, image quality and diagnostic accuracy were more likely to affect the performance of prospective ECG-gating CCTA. However, there were significant disagreements between both, the specialists (36%) and radiographers' (33%) groups in terms of data processing management compared to other factors that influenced the performance of prospective ECG-gating techniques. In addition, about 41% radiographers did not know that cardiac functional analysis could not be assessed with prospective ECG-gating CCTA.

6.3.3 Perceived benefits and challenges in performing prospective ECG-gating CCTA among CT scanners

Respondents who were experienced in the use of all types of CT scanners agreed that radiation doses in Coronary CT Angiography could be reduced significantly with prospective-ECG gating (Table 6-4). A 100% consensus was achieved in that prospective ECG-gating techniques associated with radiation dose reduction in 64-, 256- and 320-slice CT could be acquired, although less than 80% respondents from each scanner type chose the 'strongly agreed' option. However, 11% of respondents did not know that prospective ECG-gating with 128-slice CT could reduce radiation dose.

There was a good agreement achieved in the case of the 256- and 320-slice CT with regard to the increase in the numbers of patients in prospective ECG-gating CCTA compared to what was seen in the cases of the 64- and 128-slice CT (>80% versus <60%).

Table 6-4: Percentage of agreement (strongly agree and agree) with regard to benefits and difficulties when performing prospective ECG-triggered CCTA according to different types of CT scanners.

Items	**64-slice CT**		**128-slice CT**		**256-slice CT**		**320-slice CT**	
	Number of agreement	**%**	**Number of agreement**	**%**	**Number of agreement**	**%**	**Number of agreement**	**%**
Benefits								
Reduce radiation dose	9	100.0	24	88.9	12	100.0	5	100.0
Improve diagnostic image quality	2	22.2	25	92.6	12	100.0	3	60.0
Increase number of patients or cases (patient's output)	5	55.6	16	59.3	11	91.7	4	80.0
Increase financial incentives	2	22.2	7	25.9	9	75.0	2	40.0
Obstacles								
Heart rate issues	9	100.0	25	92.6	4	33.3	5	100.0
Difficulty in obtaining cardiac functional assessments	6	66.7	20	74.1	2	16.7	3	60.0
Image quality concerns	8	88.9	24	88.9	3	25.0	5	100.0
Diagnostic accuracy concerns	6	66.7	21	77.8	3	25.0	5	100.0
Data processing management issues	5	55.6	19	70.4	3	25.0	4	80.0

In contrast, there was some disagreement among about 40% of the respondents with regard to the use of the 64- and 128-slice CT indicating that prospective ECG-gating would increase the numbers of patients. Prospective ECG-gating CCTA that could increase financial incentives for institution was agreed to with regard to the 256-slice CT (75%). However, those respondents who worked in the hospital with 64-, 128 and 320-slice CT scanners did not know that prospective ECG-gating could also be beneficial to the institutional economy.

There was a consensus reached by respondents when discussing all types of CT scanners that the heart rate issue was a major challenge in prospective ECG-gating CCTA except in the 256-slice CT, since about 67% of the 256-slice CT users did not agree that the heart rate was an issue in prospective ECG-gating. Similarly, the remaining challenges in prospective ECG-gating including image quality and diagnostic accuracy concerns, data processing and the inability to perform cardiac functional analysis were achieved with good agreement with reference to all types of CT scanners, excluding the 256-slice CT. Seventy-five per cent of the 256-slice CT users were likely to disagree on the data processing issue, image quality and diagnostic accuracy concern. In addition, 75% of the 256-slice CT respondents did not know that cardiac functional analysis could not be performed with prospective ECG-gating CCTA.

6.4 Discussion

This analysis emphasises two major findings that are considered clinically important to measure the degree of satisfaction of CT users with regard to the use of prospective ECG-gating protocols in Malaysia. Firstly, this survey shows that prospective ECG-gating is associated with a significantly lower radiation dose, which was agreed to by all the users regardless of any groups and types of scanners (94%). Secondly, the majority of the respondents (>70%) agreed that the heart rate was a main concern in achieving good image quality for prospective ECG-gating CCTA.

It is well-known that prospective ECG-gating CCTA is regarded as the most effective technique to reduce radiation doses and associated with a less invasive modality in the diagnosis of coronary artery disease. Previous studies have shown that prospective ECG-gating significantly reduces radiation dose by more than 80% compared to retrospective ECG-gating methods (Earls 2009; Efstathopoulos et al. 2009; Gutstein et al. 2008; Hirai et al. 2008; Husmann et al. 2008; Rybicki et al. 2008). Therefore, the use of prospective gating methods is increasingly recommended in imaging centres, especially in the developing countries.

Our survey shows that there is a reasonable level of consensus among specialists and radiographers' groups regarding the benefits of prospective ECG-gating protocol, especially in radiation dose reduction and image quality improvement. Since the specialists are not really exposed to the medical bills, this explains the results of the high percentage of people unaware of the 'increasing financial incentives' factor, which is beneficial to prospective ECG-gating CCTA.

Although cardiac functional assessment was unlikely to be achieved in prospective ECG-gating protocol, it was not a major concern in coronary artery disease assessment as reported by researchers (Earls 2009). However, if the cardiac functional assessment did prove necessary for clinical diagnosis, it was advised that retrospective ECG-gating technique should be performed. Prospective ECG-gating technique was introduced in Malaysia a few years ago, with the installation of the 128-, 256- and 320-slice CT scanners. However, this technique was introduced for Coronary CT imaging in the National Heart Institution with 64-slice and dual-source CT in late 2011. Therefore, it is necessary to identify whether prospective ECG-triggered CCTA has been introduced into the cardiac imaging, and whether it has been accepted as a valuable technique by local specialists. This survey shows that the specialists and radiographers' responses were consistent with existent literature as to the attractive benefits of prospective gating (Sun 2010; Muenzel et al. 2012). Several studies related to prospective ECG-gating CCTA have been published in literature with a focus on radiation dose, image quality and diagnostic accuracy (Bischoff et al. 2010; Earls et al. 2008; Hirai et al. 2008; Husmann et al. 2008; Muenzel et al. 2012; Hoe and Toh 2009). Satisfactory results have been achieved according to these studies, with a significant reduction in radiation dose with the use of prospective ECG-gating CCTA. However, the users' perceptions' regarding satisfaction of prospective ECG-triggering techniques has not been studied, to the best of our knowledge.

Several studies on radiation dose awareness among clinicians and health professionals were published in the previous literatures (Chun-sing et al. 2012; Correia et al. 2005; Shiralkar et al. 2003; Soye and Paterson 2008; Thomas et al. 2006). The results showed that radiologists are best equipped with the relevant knowledge pertaining to radiation exposure related to radiological imaging as compared to other physicians (Chun-sing et al. 2012). Although the information given was limited to general radiological examinations, including chest x-ray and CT scan, it is still applicable to other radiological imaging procedures. Therefore, the result of this study is aligned with previous studies and points to the fact that prospective ECG-gating is beneficial in reducing radiation dose (Earls et al. 2008; Efstathopoulos et al. 2009; Ko et al. 2010; Shuman et al. 2008; Husmann et al. 2008).

We believe that it is important for CT practitioners' teams to make current information regarding CT radiation dose widely available since there are debatable issues about the potential risk of radiation-induced cancer (Brenner and Hall 2007). Moreover, current information regarding the radiation dose related to the latest technological advancements in CT imaging should be made available to the public. Thus, it is necessary that healthcare providers, healthcare professionals and patients be aware of the radiation risks associated with CT, so as to accurately weigh the risks and benefits associated with prospective ECG-gating CCTA (Thomas and Lindell 2001). Thus, results from this study are considered valuable for current clinical practice with regard to the implementation of prospective gating techniques.

The cohort of sample respondents was probably skewed to those specialists who were involved with coronary CT reports and radiographers who were working with the latest CT scanners. In terms of professional backgrounds, it was skewed towards the private hospitals since there was a huge competition among individuals engaged in private practice in convincing patients to adopt the latest technology which was fast, safe and convenient.

The answer scale for sections 2 and 3, which asked respondents to choose their levels of agreement on the benefits and the difficulties in performing prospective ECG-gating Coronary CT Angiography, did not include a 'neither agree nor disagree' option. This was because our study did not force respondents to choose the levels of agreement if they did not feel that their option was strong enough to be worth selecting. Therefore, the 'don't know' option allowed respondents to state that they had no opinion or had not thought about any particular issue.

6.5 Conclusion

In conclusion, although there is a reasonable level of consensus with regard to the benefits and challenges in prospective ECG-gating CCTA, regardless of the respondents group or scanner type users, the reduction in radiation dose seems to be the most agreed benefit while the heart rate issue is the most likely challenge in prospective ECG-gating CCTA. Our study is the first-scale survey of the views of specialists and radiographers responding to the prospective ECG-gating Coronary CT Angiography protocol in Malaysia. It was designed to stimulate discussion after the prospective ECG-gating technique was introduced in Malaysian health institutions a few years ago. The results of this unique survey provide an insight into the current perceptions on the usefulness of prospective ECG-gating techniques in CCTA.

6.6 References

Abada, H. T., C. Larchez, B. Daoud, A. Sigal-Cinqualbre, and J. F. Paul. 2006. MDCT of the coronary arteries: feasibility of low-dose CT with ECG-pulsed tube current modulation to reduce radiation dose. *Am J Roentgenol* 186: S387-S390.

Achenbach, S., M. Marwan, D. Ropers, T. Schepis, T. Pflederer, and K. Anders. 2010. Coronary computed tomography angiography with a consistent dose below 1mSv using prospectively electrocardiogram-triggered high-pitch spiral acquisition. *Eur Heart J* 31: 340-346.

Bischoff, B., F. Hein, T. Meyer, M. Krebs, M. Hadamitzky, S. Martinoff, A. Schömig, and J. Hausleiter. 2010. Comparison of sequential and helical scanning for radiation dose and image quality: results of the prospective multicenter study on radiation dose estimates of cardiac CT angiography (PROTECTION) I study. *Am J Roentgenol* 194: 1495-1499.

Brenner, D. J., and E. J. Hall. 2007. Computed tomography: an increasing source of radiation exposure. *N Engl J Med* 357 (22): 2277-2284.

Chun-sing, W., H. Bingsheng, S. Ho-kwan, W. Wai-lam, Y. Ka-ling, and C. Y. C. Tiffany. 2012. A questionnaire study assessing local physicians, radiologists and interns' knowledge and practice pertaining to radiation exposure related to radiological imaging. *Eur J Radiol* 81 (3): e264-e268.

Correia, M. J., A. Hellies, M. G. Andreassi, B. Chelarducci, and E. Picano. 2005. Lack of radiological awareness among physicians working in a tertiary care cardiological centre. *Int J Cardiol* 103: 307-11.

Earls, J. P. 2009. How to use a prospective gated technique for cardiac CT. *J Cardiovasc Comput Tomogr* 3: 45-51.

Earls, J. P., E. L. Berman, B. A. Urban, C. A. Curry, J. L. Lane, R. S. Jennings, C. C. McCulloch, J. Hsieh, and J. H. Londt. 2008. Prospectively gated transverse coronary CT angiography versus retrospectively gated helical technique: improved image quality and reduced radiation dose. *Radiology* 246: 742-753.

Efstathopoulos, E. P., N. L. Kelekis, I. Pantos, E. Brountzos, S. Argentos, J. Greb´a, D. Ziaka, D. G. Katritsis, and I. Seimenis. 2009. Reduction of the estimated radiation dose and associated patient risk with prospective ECG-gated 256-slice CT coronary angiography. *Phys Med Biol* 54 (17): 5209-5222.

Francone, M., E. DiCastro, A. Napoli, C. Bolzan, I. Carbone, L. Bertoletti, L. Iuliano, C. Catalano, and R. Passariello. 2008. Dose reduction and image quality assessment in 64-detector row computed tomography of the coronary arteries using an automatic exposure control system. *J Comput Assist Tomogr* 32: 668-678.

Gutstein, A., A. Wolak, C. Lee, D. Dey, M. Ohba, Y. Suzuki, V. Cheng, H. Gransar, S. Suzuki, J. Friedman, L. E. Thomson, S. Hayes, R. Pimentel, W. Paz, P. Slomka, and D. S. Berman. 2008. Predicting success of prospective and retrospective gating with dual-source coronary computed tomography angiography: development of selection criteria and initial experience. *J Cardiovasc Comput Tomogr* 2: 81-90.

Hamon, M., R. Morello, and J. W. Riddell. 2007. Coronary arteries: diagnostic performance of 16- versus 64-section spiral CT compared with invasive coronary angiography: meta-analysis. *Radiology* 245: 720 -731.

Hausleiter, J., T. Meyer, M. Hadamitzky, E. Huber, M. Zankl, S. Martinoff, A. Kastrati, and A. Schömig. 2006. Radiation dose estimates from cardiac multislice computed tomography in daily practice: impact of different scanning protocols on effective dose estimates. *Circulation* 113: 1305-1310.

Hein, P. A., V. C. Romano, A. Lembcke, J. May, and P. Rogalla. 2009. Initial experience with a chest pain protocol using 320-slice volume MDCT. *Eur Radiol* 19 (5): 1148-1155.

Herzog, C., D. M. Mulvihill, S. A. Nguyen, G. Savino, B. Schmidt, P. Costello, T. J. Vogl, and U. J. Schoepf. 2008. Pediatric cardiovascular CT angiography: radiation dose reduction using automatic anatomic tube current modulation. *Am J Roentgenol* 190: 1232-1240.

Hirai, N., J. Horiguchi, C. Fujioka, M. Kiguchi, H. Yamamoto, N. Matsuura, T. Kitagawa, H. Teragawa, N. Kohno, and K. Ito. 2008. Prospective versus retrospective ECG-gated 64-detector coronary CT angiography: assessment of image quality, stenosis, and radiation dose. *Radiology* 248: 424-430.

Hoe, J., and K. H. Toh. 2009. First experience with 320-row multidetector CT coronary angiography scanning with prospective electrocardiogram gating to reduce radiation dose. *J Cardiovasc Comput Tomogr* 3: 257-261.

Hounsfield, G. N. 1980. Computed medical imaging. *Science* 210: 22-28.

Husmann, L., I. Valenta, O. Gaemperli, O. Adda, V. Treyer, C. A. Wyss, P. Veit-Haibach, F. Tatsugami, G. K. Schulthess, and P. A. Kaufmann. 2008. Feasibility of low-dose coronary CT angiography: first experience with prospective ECG-gating. *Eur Heart J* 29 (2): 191-197.

Kalender, W. A. 2000. *Computed tomography: fundamentals, system technology, image quality, applications*. Munich: MCD Verlag.

Ko, S. M., N. R. Kim, D. H. Kim, M. G. Song, and J. H. Kim. 2010. Assessment of image quality and radiation dose in prospective ECG-triggered coronary CT angiography compared with retrospective ECG-gated coronary CT angiography. *Int J Cardiovasc Imaging* 26: 93-101.

Muenzel, D., P. B. Noel, F. Dorn, M. Dobritz, E. J. Rummeny, and A. Huber. 2012. Coronary CT angiography in step-and-shoot technique with 256-slice CT: impact of the field of view on image quality, craniocaudal coverage, and radiation exposure. *Eur J Radiol* 81: 1562-1568.

Pontone, G., D. Andreini, A. L. Bartorelli, S. Cortinovis, S. Mushtaq, E. Bertella, A. Annoni, A. Formenti, E. Nobili, D. Trabattoni, P. Montorsi, G. Ballerini, P. Agostoni, and M. Pepi. 2009. Diagnostic accuracy of coronary computed tomography angiography: a comparison between prospective and retrospective electrocardiogram triggering. *J Am Coll Cardiol* 54: 346-355.

Rybicki, F., H. Otero, M. Steigner, G. Vorobiof, L. Nallamshetty, D. Mitsouras, H. Ersoy, R. Mather, P. Judy, T. Cai, K. Coyner, K. Schultz, A. Whitmore, and M. Di Carli. 2008.

Initial evaluation of coronary images from 320-detector row computed tomography. *Int J Cardiovasc Imaging* 24 (5): 535-546.

Sabarudin, A., Z. Sun, and K.-H. Ng. 2012. A systematic review of radiation dose associated with different generations of multidetector CT coronary angiography. *J Med Imag Radiat Oncol* 56: 5-17.

Shiralkar, S., A. Rennie, M. Snow, R. B. Galland, M. H. Lewis, and K. Gower-Thomas. 2003. Doctors' knowledge of radiation exposure: questionnaire study. *Br Med J* 327: 371-372.

Shuman, W., K. Branch, J. May, L. Mitsumori, D. Lockhart, T. Dubinski, B. Warren, and J. Caldwell. 2008. Prospective versus retrospective ECG gating for 64-detector CT of the coronary arteries: comparison of image quality and patient radiation dose. *Radiology* 248: 431-437.

Soye, J. A., and A. Paterson. 2008. A survey of awareness of radiation dose among health professionals in Northern Ireland. *Br J Radiol* 81: 725-729.

Sun, Z. 2010. Multislice CT angiography in cardiac imaging: prospective ECG-gating or retrospective ECG-gating? . *Biomed Imaging Interv J* 6 (1): e4.

Thomas, K. E., J. E. Parnell-Parmley, R. Moineddin, E. Charkot, G. BenDavid, C. Krajewski, and S. Haidar. 2006. Assessment of radiation dose awareness among pediatricians. *Pediatr Radiol* 36: 823-832.

Thomas, R. H., and B. Lindell. 2001. In radiological protection, the protection quantities should be expressed in terms of measurable physical quantities. *Radiat Prot Dosimetry* 94: 287-292.

CHAPTER 7: CORONARY CT ANGIOGRAPHY WITH SINGLE-SOURCE AND DUAL-SOURCE CT: COMPARISON OF IMAGE QUALITY AND RADIATION DOSE BETWEEN PROSPECTIVE ECG-TRIGGERED AND RETROSPECTIVE ECG-GATED PROTOCOLS

7.1 Introduction

Coronary CT angiography (CCTA) has gained a leading role in the diagnosis of coronary artery disease (CAD) due to its high diagnostic value, in particular, a very high negative predictive value (95–99%) (Budoff et al. 2006; Sun et al. 2008). With 64- or more slice CT, non-invasive CCTA has become a reliable alternative to invasive coronary angiography in the diagnosis of patients with suspected CAD (Sun et al. 2008).

Traditionally, CCTA was performed using retrospective ECG gating, which enables acquisition of volume data, but at the expense of high radiation dose, since data is acquired during a spiral CT protocol (Efstathopoulos et al. 2012). High radiation dose associated with retrospective ECG-gated CCTA raised major concerns in the literature; thus, strategies for reducing radiation dose in retrospective ECG gating have been developed and widely introduced in present-day clinical centres. These strategies include tube current modulation that is either attenuation-based (Deetjen et al. 2007; Kalra et al. 2004) or ECG-control-based (Abada et al. 2006; Gutstein et al. 2008), lower tube voltage (Hausleiter et al. 2006; Leschka et al. 2008), high-pitch scanning (Achenbach et al. 2010; Alkadhi et al. 2010), and prospective ECG triggering (Earls 2009; Efstathopoulos et al. 2012; Hoe and Toh 2009). Of these strategies, prospective ECG triggering represents the most effective approach with a significant dose reduction when compared to the conventional retrospective ECG-gated protocol, but with high diagnostic image quality.

Unlike the principle of retrospective ECG gating, the principle of prospective ECG triggering is that data acquisition takes place only in the selected cardiac phase by selectively turning on the X-ray tube when triggered by the ECG signal, and turning it off or dramatically lowering it during the rest of the R–R cycle (Efstathopoulos et al. 2012).

Radiation dose and image quality with prospective ECG triggering are increasingly being studied and compared with retrospective ECG gating in the literature (Ko et al. 2010; Lu et al. 2011; Shuman et al. 2008; Sun and Ng 2012). Despite the promising results that have been achieved in dose reduction and image quality, there is a concern about the accuracy of effective dose calculation. Moreover, to our knowledge there is a lack of systematic investigation on image quality comparison between different types of scanners (single-source vs. dual-source CT) with prospective and retrospective ECG-gated CCTA techniques.

Therefore, the aim of this study was to investigate and compare image quality and radiation dose between prospective ECG-triggered and retrospective ECG-gated CCTA protocols, using different types of 64-slice CT scanners.

7.2 Materials and methods

7.2.1 Study population

This is a cross-sectional study comparing radiation dose and image quality between prospective triggered and retrospective ECG-gated CCTA in two major public hospitals, Royal Perth Hospital, Perth, Australia, and National Heart Institute, Kuala Lumpur, Malaysia. The study was approved by both the institutional ethical review boards. The first part of the study was conducted retrospectively between January and July 2011 in the Royal Perth Hospital with 95 patients with suspected CAD who underwent CCTA with single-source CT (SSCT). The second part of the study was conducted prospectively with 114 consecutive patients who underwent CCTA between August 2011 and January 2012 with dual-source CT (DSCT) in the National Heart Institute. Written informed consent was obtained from all patients. The data including demographic information (i.e. age, gender, body mass index and heart rate) and scan parameters (i.e. scan duration, longitudinal scan range, tube voltage and pitch) were collected from each patient. Heart rate which was defined as the average heart rate during image acquisition was also recorded for each patient. All patients had sinus heart rhythm. Patients with renal insufficiency presenting with elevated serum creatinine levels (> 1.5 mg/dL), documented hypersensitivity to iodinated contrast materials and any indications related to heart surgery, that is, post-coronary artery bypass graft assessments, heart valve and pacemaker placement and patients with obvious coronary wall calcifications (calcium score >1000) were excluded from the study.

7.2.2 SSCT scanning protocols

The CCTA protocol was divided into prospective triggering (n=43) and retrospective ECG gating (n=52), both of which were performed with a 64-slice scanner (Brilliance 64, Philips Healthcare, USA). The CCTA was performed with detector collimation of 64 × 0.625 mm, slice thicknesses of 0.8 mm, field of view ranging from 150 to 170 mm and adjustable tube current in the range of 300–500 mA with a tube voltage of 120 kV. A pitch of 0.2 and an ECG-pulsing window of 30–80% of the R–R interval were used in retrospective ECG-gating protocol.

7.2.3 DSCT scanning protocols

The CCTA protocol was divided into prospective triggering (*n*=50) and retrospective ECG gating (*n*=64), both of which were performed with a 64-slice CT scanner (Somatom Definition, Siemens Medical Solutions, Germany). CCTA protocol was performed with beam collimation of 2 × 32 × 0.6 mm, slice acquisition of 2 × 64 × 0.6 mm with z-flying focal spot and 320 mAs per rotation and tube voltage of 120 kV. For retrospective ECG-gating protocol, the ECG-pulsing window was set at 30–80% of the R–R interval with pitch of 0.2–0.43, which was automatically adapted to the heart rate.

7.2.4 Contrast medium administration

A minimum of 65 mL contrast agent (*Iomeron* 350 mgI/mL) was administered intravenously at a flow rate of 5.0–5.5 mL/s followed by 50 mL saline flush at 5 mL/s. The amount of contrast medium required for coronary CT examination was calculated according to the following formula: $V = IR \cdot ST$, where V is volume in millilitres, IR is the injection rate (mL/s) and ST is the scanning time in seconds (Hirai et al. 2008). Bolus was tracked by using an automated bolus triggering technique at the region of interest, that is, at the ascending aorta, with a baseline threshold of 120 HU (Hounsfield units).

Details about the use of beta-blockers are presented in Figure 7-1. However, in retrospective ECG-gated protocol, beta-blockers were given only to patients with heart rate > 70 bpm (beats per minute) in the SSCT group and > 100 bpm in the DSCT group.

Figure 7-1: Flow chart showing the administration of beta-blocker

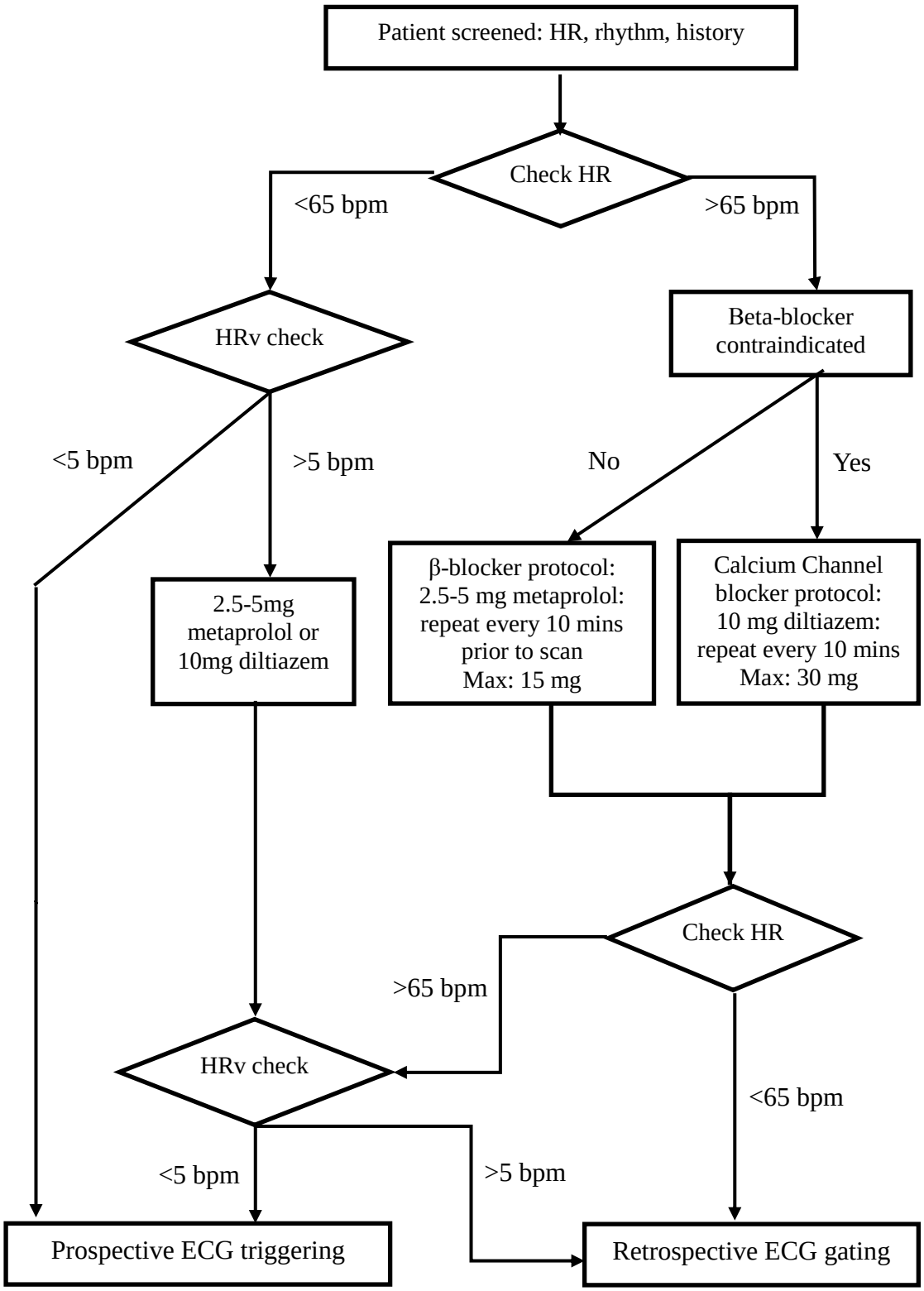

*HR-Heart rate; HRv-Heart rate variability

7.2.5 Analysis of image quality

Assessment of image quality was determined by two experienced viewers with at least 5 years of experience in cardiac CT imaging who were blinded to the acquisition parameters and protocols. Each image was scored subjectively with a 4-point grading scale. Details of the grading scale are presented in Table 7-1. Each coronary segment was evaluated according to the 16-segment model based on the American Heart Association's (AHA) guidelines (Austen et al. 1975; Scanlon et al. 1999).

Table 7-1: Image quality score descriptions

Image quality score	Quality level	Description
1	Excellent	All vessels had continuous course which surrounded by low-attenuation fat with good and uniform contrast enhancement and no artifacts
2	Good	Presence of discrete blurring of vessel margin in any planar orientation with minor motion artifacts, increased image noise, low contrast enhancement without stair-step artifact. However, evaluations of the vessel lumen and plaque characteristics are possible and satisfactory.
3	Moderate	Noticeably blurred vessel/plaque margins and distinctly broader motion artifacts extending less than 5 mm from the vessel center. Reduced image quality due to any combination of motion, slice miss-registration, increased image noise, poor contrast enhancement or presence of extensive coronary calcification, making interpretation difficult. However, the image quality was sufficient to assess the patency of the artery.
4	Poor	Inadequate delineation between vessel and surrounding tissue with presence of streak artifacts extending at least 5 mm from center of the vessel and stair-step artifacts of > 25% of the vessel diameter. Non-assessable the artery patency due to impaired image quality.

The right coronary artery (RCA) included segments 1-4, the left main coronary artery and left anterior descending coronary artery (LAD) included segments 5-10, and the left circumflex coronary artery (LCx) included segments 11-15. If present, the intermediate artery was designated as segment 16. Coronary artery analysis was performed in all vessels with at least a 1.0-mm luminal diameter at their origin. If the segment was not present due to anatomical variants, image quality was recorded as missing. Sufficient quality (score 1, 2 and 3) was defined as excellent, good and moderate, respectively, which was considered to be evaluable for diagnosis. Insufficient image quality was ranked with a score of 4 which was described as poor or of no diagnostic value.

The image quality was also measured quantitatively with a commercially available software Analyze 7.0 (Analyze, version 7.0 for Windows, Kansas, USA). The objective parameters of image quality included CT attenuation, image noise, signal-to-noise ratio (SNR) and contrast-to-noise ratio (CNR). CT attenuation was measured in HU and defined as the mean value while image noise was measured in terms of standard deviation (SD). Both CT attenuation and image noise were measured at three different regions of interest (ROI) with a circular ROI of 200, 7, and 3–5 mm^2 placed at the ascending aorta, perivascular fatty tissue and coronary artery (left main and proximal right coronary artery), respectively (Figure 7-2). The SNR was determined by dividing CT attenuation with image noise, while CNR was calculated by dividing contrast enhancement (CT attenuation at the aorta minus CT attenuation at the fat) with image noise, that is, $CNR_{aorta} = Mean_{aorta} – Mean_{fat}/SD_{aorta}$ (Muenzel et al. 2012).

7.2.6 Estimation of effective dose

The effective dose (*E*) was estimated by multiplying the dose-length product (DLP) with a conversion coefficient factor (*E*/DLP), *k* ($mSv \cdot mGy^{-1} \cdot cm^{-1}$). The DLP value is available on the scanner console and the *k* factor of 0.026 $mSv \cdot mGy^{-1} \cdot cm^{-1}$ was used for the cardiac region instead of chest CT (0.014 or 0.017 $mSv \cdot mGy^{-1} \cdot cm^{-1}$) based on International Commission on Radiological Protection (ICRP-103) publication (Huda, Magill, and He 2011; Huda et al. 2010). Since the conversion coefficient factor of 0.017 $mSv \cdot mGy^{-1} \cdot cm^{-1}$ is widely used in the literature (Huda, Ogden, and Khorasani 2008), the results of effective dose were also provided by using a conversion coefficient factor of 0.017 $mSv \cdot mGy^{-1} \cdot cm^{-1}$ for comparison.

Figure 7-2: The quantitative measurement was obtained by locating the ROI at the root of the ascending aorta (a), perivascular fatty tissue (b), left main artery (c) and proximal RCA (d). If image quality scores were 2 or more, ROI was put at the area where artefacts were least severe.

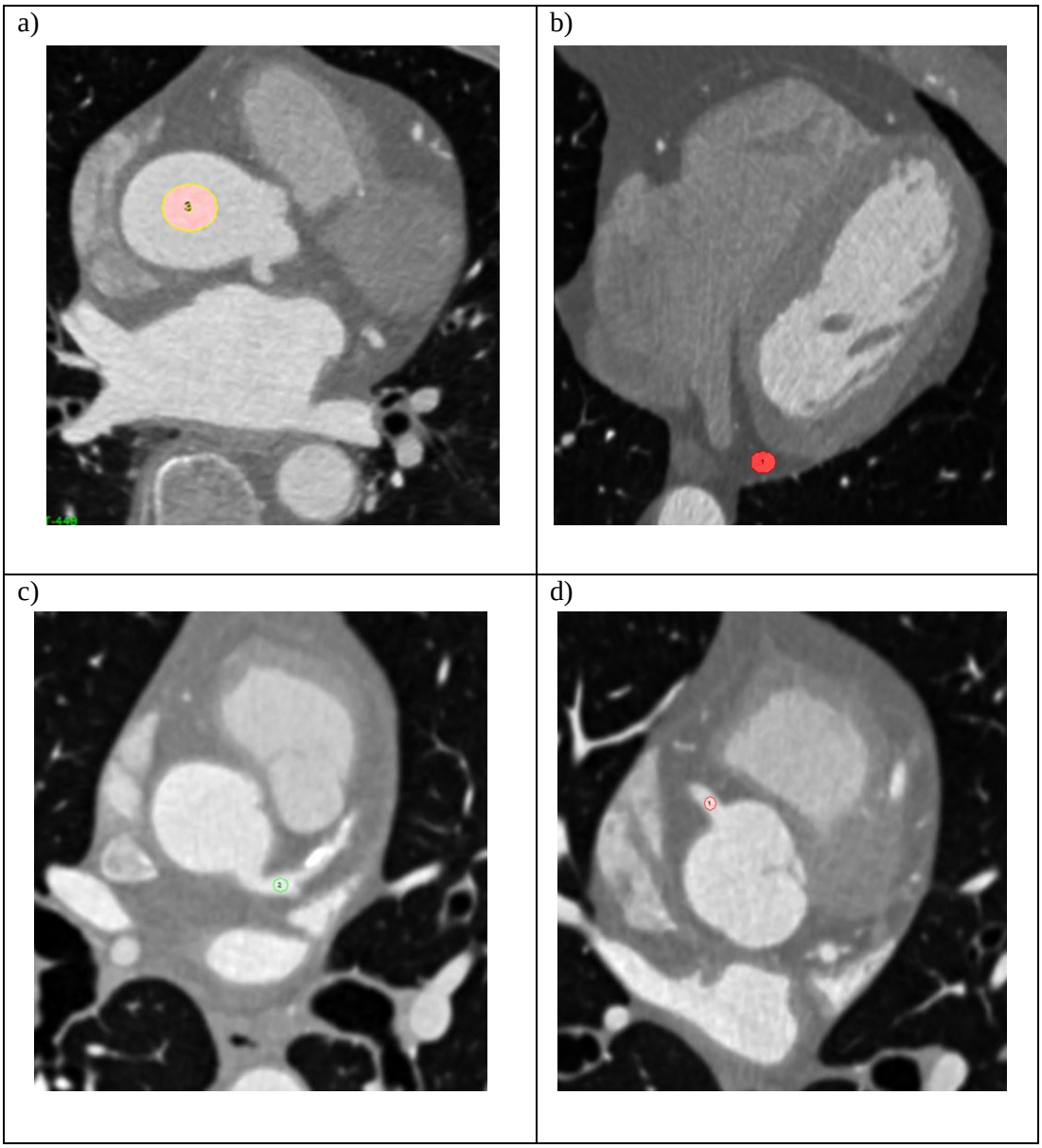

7.2.7 Statistical analysis

All data were entered into SPSS V17.0 (SPSS, version 17.0 for Windows, Chicago, Illinois, USA) for statistical analysis. A *p* value of <0.05 was considered to indicate a statistically significant difference. The values were normally distributed in all prospective and retrospective ECG-gated groups with inclusion of DSCT and SSCT. Those values were compared with one-way analysis of variance (ANOVA) for multi-factor interaction analysis. The doses from each protocol were presented in box plots while the correlation between *E*

and body mass index (BMI) was analysed with Pearson's correlation in both prospective triggered and retrospective ECG-gated groups between DSCT and SSCT. For image quality parameter, inter-observer agreement for image analysis was estimated by kappa statistics and classified as follows: poor ($\kappa < 0.20$); fair ($\kappa = 0.21–0.40$); moderate ($\kappa = 0.41–0.60$); good ($\kappa = 0.61–0.80$) and excellent agreement ($\kappa = 0.81–1.00$). Kruskal–Wallis test was conducted for further statistical non-parametric analysis in image quality assessment. Quantitative image analysis such as CT attenuation, image noise, SNR and CNR were compared using the Student's *t*-test.

7.3 Results

Details on patient demographics, CAD risk factor and beta-blocker usage are presented in Table 7-2. A total of 2,880 coronary artery segments were evaluated. However, 793 segments (mainly posterior lateral branch, second diagonal artery, second obtuse marginal branch and ramus intermedius segment) were not considered because of anatomical variants. Therefore, 2,087 segments were assessable of which 2,046 (98.0%) segments were ranked as of sufficient image quality (score 1 to 3), while only 41 segments (2.0%) were classified as of insufficient image quality (score 4) regardless of prospective or retrospective ECG-gated CCTA protocols.

7.3.1 Diagnostic performance of image quality

The image quality of coronary artery segments was assessed by two readers with a kappa score of 0.65 and 0.62 for both prospective and retrospective ECG-gated group respectively, indicating good inter-observer agreement. In the retrospective ECG-gated group, evaluation was undertaken with reconstructions at the mid-diastolic phase in 70% of the patients (81/116), resulting in better image quality, while for the remaining 30% of patients, reconstruction was selected at the end-systolic phase.

Table 7-2: Patients demographic data, CAD risk factor and percentage of beta-blockers administration

Characteristics		**Dual source 64-slice CT**		**Single source 64-slice CT**	
		PPG	**RPG**	**PPG**	**RPG**
Demographics	Number of patients	50	64	43	52
	Mean age (years)	53 ± 10	53 ± 9	49 ± 13	55 ± 15
	Mean BMI (kg/m^2)	26.3 ± 3.8	27.7 ± 5.2	25.7 ± 2.3	25.6 ± 2.8
	Male (%)	58	55	51	50
	Heart rate (b.p.m)	56.3 ± 6.4	67.9 ± 9.6	56.3 ± 6.0	72.4 ± 7.3
Risk factor (%)	Diabetes	16	23	26	23
	Hyperlipidaemia	20	22	19	21
	Hypertension	54	66	53	56
	Obesity	42	52	51	54
	Family history	30	23	42	40
	Smoking	52	48	65	67
IV β-blocker usage (%)	None	46	n/a	69.7	n/a
	2.5 mg	26		30.3	
	5 mg	22			
	10 mg	6			
	>10 mg	0			

*PPG=Prospective ECG-triggering; RPG=Retrospective ECG-gating

Image quality was rated as excellent (image quality score 1) in 182/528 (34.5%) and 120/504 (23.8%) for the retrospective ECG-gated group, 152/504 (30.2%) and 244/551 (44.3%) for the prospective ECG-triggered group with DSCT and SSCT, respectively. Moreover, sufficient image quality with scores of 2 and 3 was found in 342/528 (64.8%) and 375/504 (74.4%) coronary segments with protocols using retrospective ECG-gated DSCT and SSCT groups, whereas this was found in 343/504 (68.0%) and 288/551 (52.3%) coronary segments in the prospective ECG-triggered DSCT and SSCT groups. Insufficient image quality (score 4) was found in 4/528 (0.8%) and 9/504 (1.8%) coronary segments for the retrospective gated group and in 9/504 (1.8%) and 19/551 (3.4%) coronary segments for the prospective triggered group, corresponding to DSCT and SSCT, respectively. Although DSCT led to fewer instances of insufficient image quality, there were no significant differences in the mean quality scores between prospective triggered and retrospective ECG-gated protocols ($p>0.05$) as shown in Table 7-3.

All quantitative measurements of image quality are given in Table 7-3. For the analysis of image quality, most of the measurements did not show significant differences in terms of CT attenuation, image noise, SNR and CNR between different anatomical locations, regardless of CT scanners and CCTA protocols ($p>0.05$). Only image noise measurements in DSCT with use of retrospective ECG-gated protocol were significantly different between aorta versus RCA (25.6 HU vs. 38.3 HU) and aorta versus LCA (25.6 HU vs. 35.6 HU) ($p<0.05$).

Table 7-3: Results of image quality (objective and subjective analysis)

Quantitative image quality parameters		**Dual source 64-slice CT (DSCT)**		**Single source 64-slice CT (SSCT)**	
		PPG	**RPG**	**PPG**	**RPG**
CT attenuation (HU)	Aorta	448.40 ± 64.57	442.89 ± 109.65	425.63 ± 98.81	434.52 ± 123.53
	RCA	467.46 ± 120.97	469.32 ± 121.98	459.56 ± 111.29	472.62 ± 116.63
	LCA	466.38 ± 91.96	462.33 ± 122.64	450.70 ± 108.22	465.36 ± 113.94
	Perivascular fat	-116.22 ± 17.81	-103.62 ± 22.71	-111.51 ± 37.51	-104.69 ± 46.23
Image noise (HU)	Aorta	25.53 ± 7.13	25.58 ± 7.95	23.83 ± 7.22	19.65 ± 9.02
	RCA	23.88 ± 9.28	38.32 ± 16.29	21.09 ± 5.99	21.42 ± 7.53
	LCA	24.59 ± 8.07	35.63 ± 14.78	21.76 ± 7.58	22.01 ± 9.49
	Perivascular fat	29.41 ± 7.64	21.94 ± 6.96	25.41 ± 7.07	20.71 ± 7.71
SNR	Aorta	19.33 ± 7.48	18.84 ± 7.17	19.74 ± 8.22	26.62 ± 15.06
	RCA	22.74 ± 10.26	15.22 ± 10.92	23.40 ± 8.54	24.42 ± 9.46

	LCA	21.17 ± 8.39	15.62 ± 8.38	23.11 ± 9.04	25.62 ± 14.56
CNR	Aorta	24.39 ± 9.50	23.30 ± 8.78	24.93 ± 10.44	33.19 ± 17.91
	RCA	28.33 ± 12.16	18.45 ± 12.65	29.24 ± 10.75	29.97 ± 11.60
	LCA	26.47 ± 10.18	19.14 ± 10.07	29.07 ± 11.85	31.44 ± 17.23
Qualitative image average score (subjective analysis)		**1.87 ± 0.71**	**1.80 ± 0.68**	**1.79 ± 0.84**	**2.00 ± 0.72**

*PPG=Prospective ECG-triggering; RPG=Retrospective ECG-gating

7.3.2 Radiation dose comparison

In prospective ECG-triggered groups using DSCT and SSCT protocols, the mean DLP was 249.3 ± 109.7 mGy·cm and 238.3 ± 37.9 mGy·cm corresponding to an effective dose estimation of 6.5 ± 2.9 mSv and 6.2 ± 1.0 mSv, respectively, with no significant difference between these two protocols (p=0.99). Whereas in the retrospective ECG-gated groups using DSCT and SSCT protocols, the mean DLP was 699.5 ± 318.9 mGy·cm and 1088.5 ± 269.8 mGy·cm corresponding to an effective dose estimation of 18.2 ± 8.3 mSv and 28.3 ± 7.0 mSv, respectively, resulting in significant difference between these two protocols (Figure 7-3). However, estimation of effective doses was lower by 35% with application of 0.017 $mSv \cdot mGy^{-1} \cdot cm^{-1}$ conversion coefficient factor when compared to that with use of 0.026 $mSv \cdot mGy^{-1} \cdot cm^{-1}$ (Table 7-4). With regard to effective dose comparison in genders, none of the results were significantly different between males and females (Figure 7-4). In the prospective ECG-triggered group, the effective dose was slightly higher in males than in females with the use of DSCT (6.7 ± 3.0 mSv vs. 6.2 ± 2.7 mSv) (p=0.28) and SSCT scanners (6.3 ± 0.8 mSv vs. 6.1 ± 1.2 mSv) (p=0.07). In the retrospective ECG-gated group, the effective dose was similarly higher in males than in females with the use of SSCT (29.4 ± 7.5 mSv vs. 27.2 ± 6.4 mSv) (p=0.22). On the other hand, the effective dose estimation in females was greater than in males with the use of DSCT scanner (20.4 ± 9.2 mSv vs. 16.3 ± 7.1 mSv) (p=0.16), despite no significant difference being reached.

The correlation between effective doses and patients' BMI was tested with Pearson correlation and this resulted in a strong positive linear correlation for SSCT with prospective ECG triggering (r=0.64), SSCT with retrospective ECG gating (r=0.65) and DSCT with retrospective ECG gating (r= 0.62). However, the prospective ECG-triggered group with DSCT showed weak positive linear correlation (r=0.11). All these correlations are presented in Figure 7-5.

Figure 7-3: Box plot shows the mean effective dose estimation reported in the studies with use of 64-slice single-source CT (SSCT) and 64-slice dual-source CT (DSCT) with prospective and retrospective ECG-gated CCTA. Effective dose estimated in SSCT with retrospective ECG-gated CCTA is the highest amongst all of the four groups. The box indicates the first to third quartiles, with the line in the box indicating median quartile, and whiskers indicate the minimum and maximum values. The estimation of effective dose was calculated based on 0.026 $mSv \cdot mGy^{-1} \cdot cm^{-1}$ conversion coefficient factor.

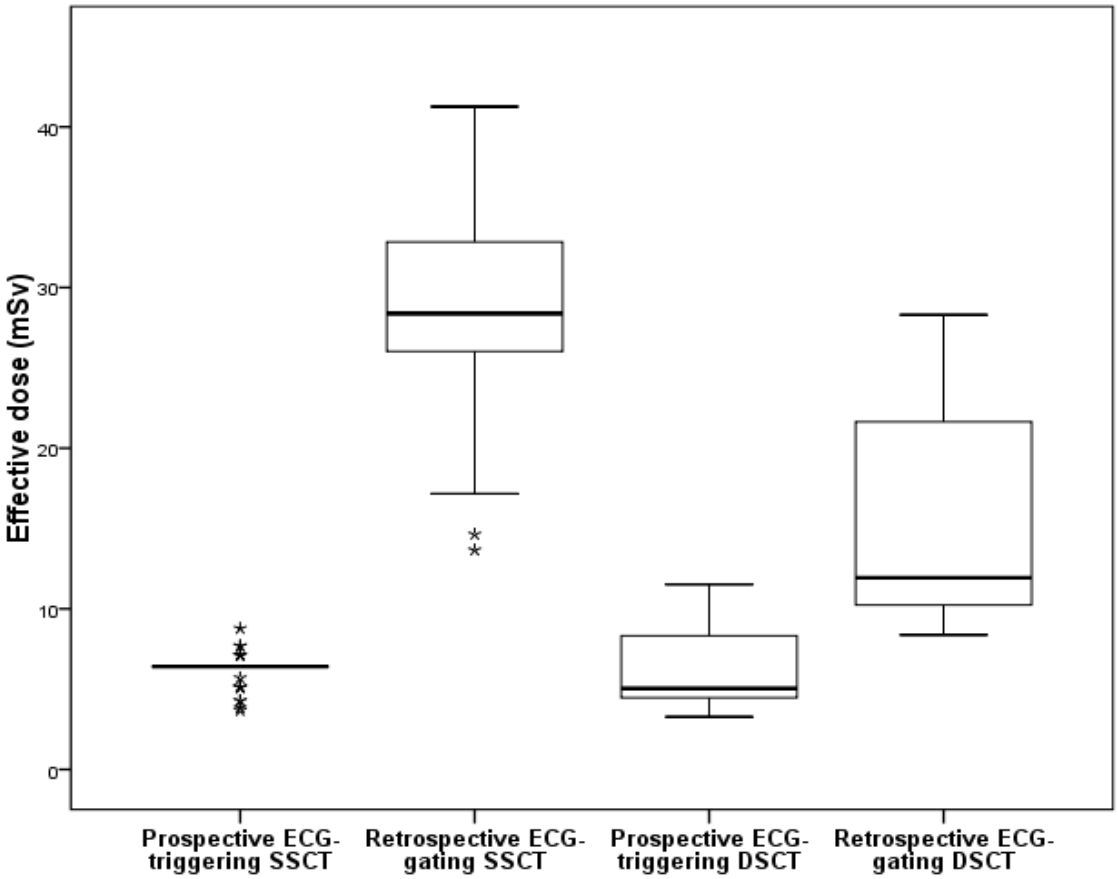

Table 7-4: Estimation of effective dose based on two different conversion coefficient factors.

Protocol	**Prospective ECG-gating CCTA**				**Retrospective ECG-gating CCTA**			
Scanner type	**DSCT**		**SSCT**		**DSCT**		**SSCT**	
***k* (mSv·mGy^{-1}·cm^{-1})**	**0.017**	**0.026**	**0.017**	**0.026**	**0.017**	**0.026**	**0.017**	**0.026**
Overall	4.2 ± 1.9	6.5 ± 2.9	4.1 ± 0.6	6.2 ± 1.0	11.9 ± 5.4	18.2 ± 8.3	18.5 ± 4.6	28.3 ± 7.0
Male	4.4 ± 2.0	6.7 ± 3.0	4.1 ± 0.5	6.3 ± 0.8	10.7 ± 4.6	16.3 ± 7.1	19.3 ± 4.9	29.4 ± 7.5
Female	4.0 ± 1.8	6.2 ± 2.7	4.0 ± 0.8	6.1 ± 1.2	13.4 ± 6.0	20.4 ± 9.2	17.8 ± 4.2	27.2 ± 6.4

Figure 7-4: Box plot shows the mean estimation of effective dose comparison between genders in SSCT and DSCT with prospective and retrospective ECG-gated CCTA. The box indicates the first to third quartiles, with the line in the box indicating the median quartile, and whiskers indicate the minimum and maximum values. The estimation of effective dose was calculated based on 0.026 $mSv \cdot mGy^{-1} \cdot cm^{-1}$ conversion coefficient factor.

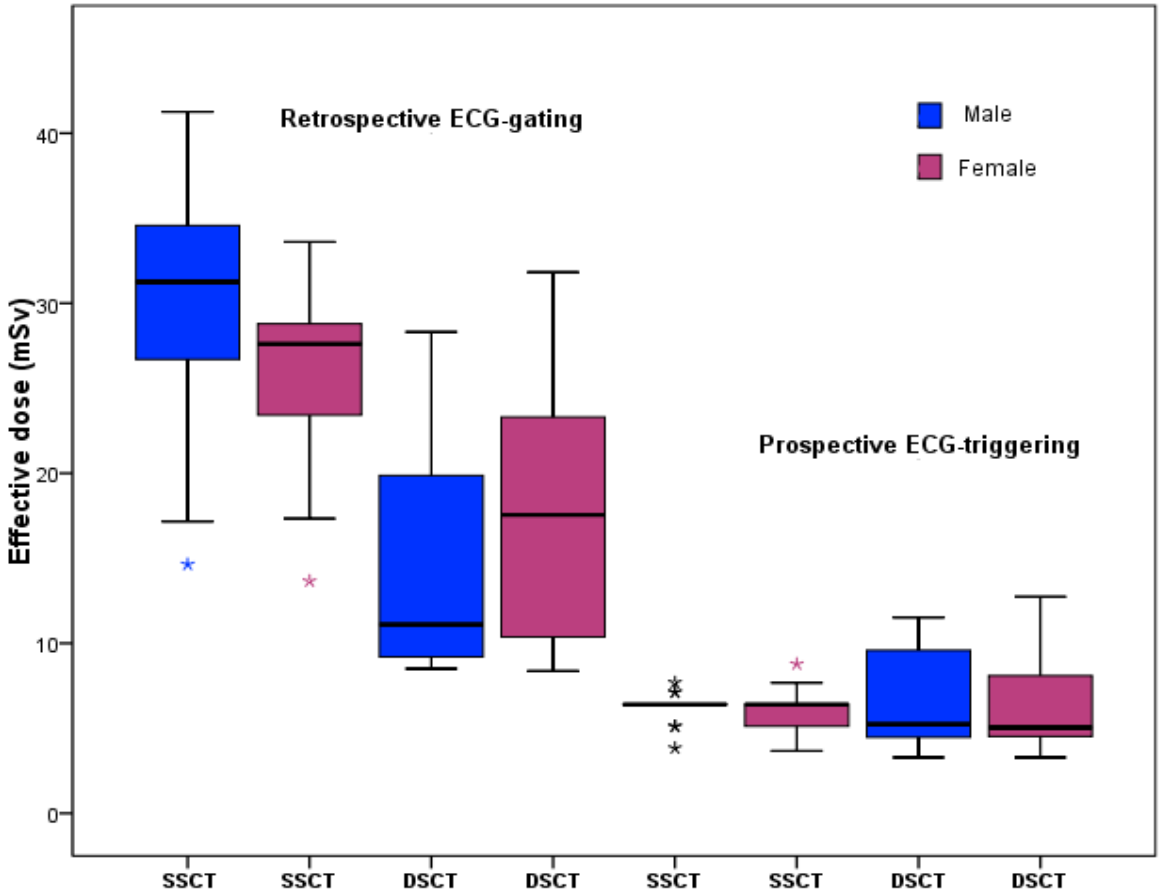

Figure 7-5: Graph shows correlation analysis of effective dose estimation depending on body mass index (BMI) for prospective (a) and retrospective (b) ECG-gated CCTA groups. In prospective gating, a strong positive correlation was shown only in SSCT (r=0.64) while in DSCT this resulted in a weak positive correlation (r = 0.11). However, in the retrospective ECG gating, both SSCT and DSCT showed a strong positive correlation with r=0.65 and r=0.62, respectively. The estimation of effective dose was calculated based on 0.026 $mSv \cdot mGy^{-1} \cdot cm^{-1}$ conversion coefficient factor.

Figure 7-5(a)

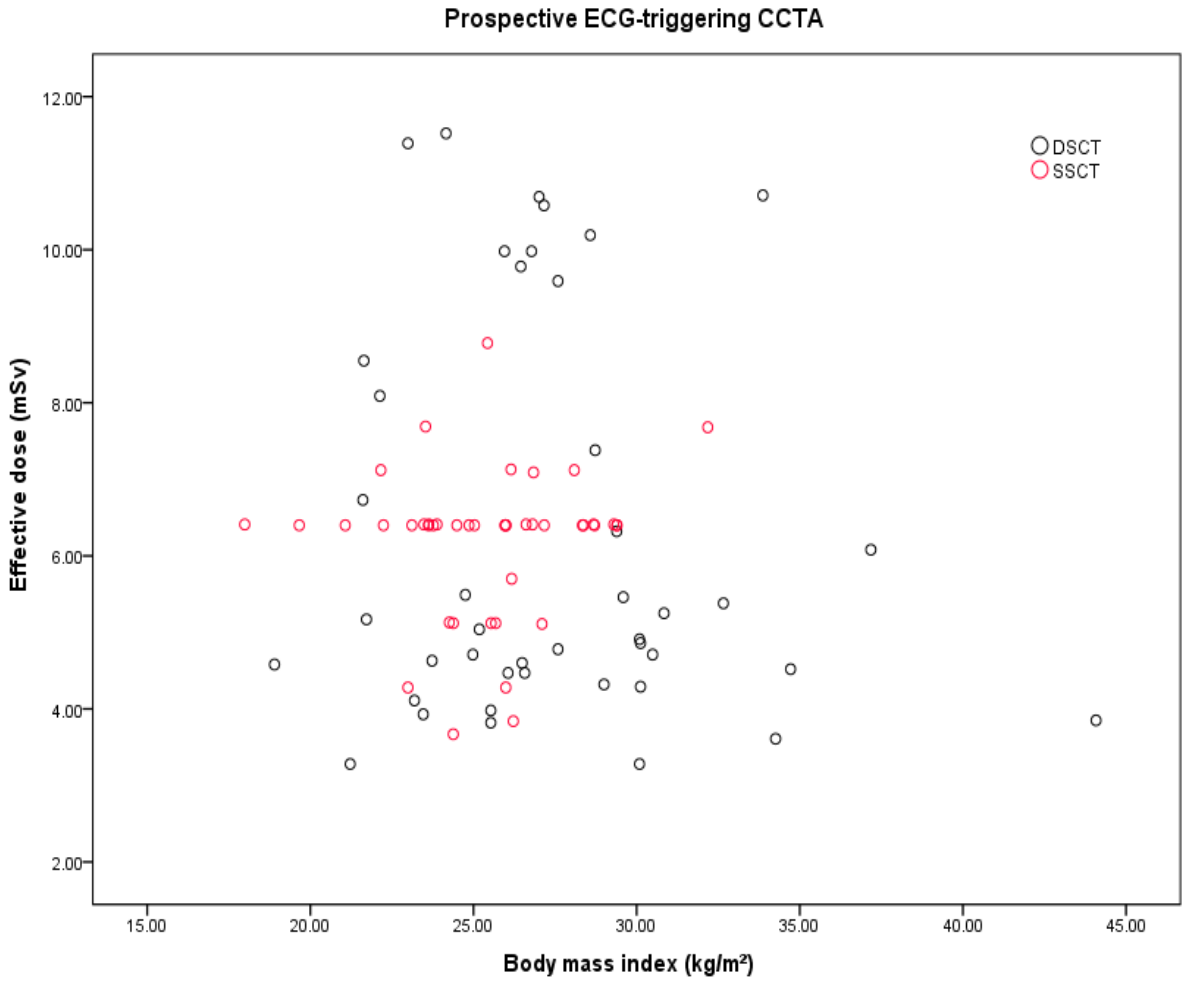

Figure 7-5 (b)

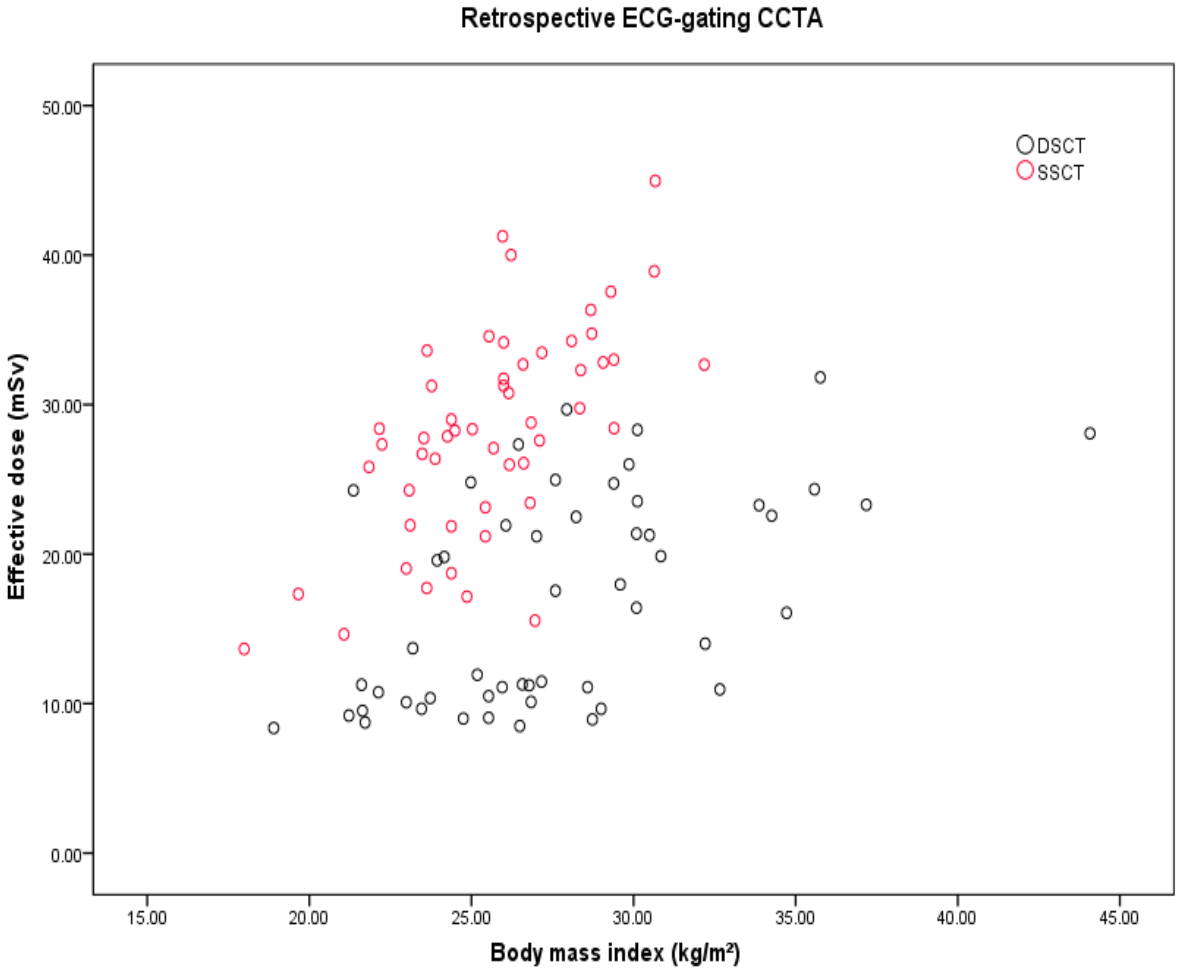

7.4 Discussion

This study demonstrates two main findings which are useful for clinical study. Firstly, there was no significant difference in image quality between prospective ECG-triggered and retrospective ECG-gated CCTA regardless of the use of SSCT or DSCT scanner. All images were presented with sufficient quality in more than 96% of the coronary segments. Secondly, prospective ECG-triggered CCTA leads to a significant lower radiation dose compared to with a retrospective ECG-gated technique performed with both DSCT and SSCT techniques.

Prospective ECG-triggered CCTA has been widely used in the diagnosis of CAD since it provides a lower radiation dose. This method has since been evaluated for image quality of the coronary arteries and for diagnostic accuracy as well as effective radiation dose in several studies (Hirai et al. 2008; Ko et al. 2010; Lu et al. 2011; Shuman et al. 2008; Sun and

Ng 2012). Studies comparing prospective triggering with retrospective gating have shown that prospective triggering resulted in high image quality with lower percentage of suboptimal images (Earls et al. 2008; Shuman et al. 2008). Earl et al. (2008) conducted a comparative study of 121 patients using prospective triggered CCTA examinations with 82 patients on retrospective ECG-gated CCTA. They found out that image quality was significantly improved with prospective triggering with low percentage of non-evaluable segments (1.4% for prospective and 2.1% for retrospective gated CCTA). Shuman et al. (2008) also showed similar results that the coronary segments with unadjusted chest size were likely to have a better image quality score in prospective triggering than in retrospective gating (p=0.03). However, when adjusted by comparing patients with the same chest size, the score of image quality was not significantly different between prospective triggering and retrospective ECG gating, but 77% lower patient dose was achieved with prospective triggering when compared with that of retrospective gating. Although prospective ECG-triggered CCTA with SSCT in our study resulted in the highest score of excellent image quality (44.3%), the percentage of insufficient image quality was still high (3.4%) compared to retrospective gating (1.8%). Similar findings were noted with prospective triggering (1.8%) compared to retrospective gating using DSCT (0.8%). This is because the heart rate was elevated unexpectedly during data acquisition in some cases using prospective ECG-triggered protocol. The presence of inadequate ECG synchronization caused severe stair-step artefacts which led to poor image quality. Our results are similar to those of a previous study (Ko et al. 2010), where the non-assessable coronary segments were higher in the prospective triggering (2.6%) than in the retrospective ECG gating (0.9%).

It has been reported that prospective ECG triggering using single-source 64-slice CT scanners substantially reduced radiation doses with sufficient image quality of the coronary arteries (Arnoldi et al. 2009; Earls et al. 2008; Hirai et al. 2008). The major disadvantage of the prospectively triggered method is the limited predefined interval for data acquisition (normally in the mid-diastole phase). Therefore, only reconstructed images from a single phase of the cardiac cycle are available for diagnostic interpretation to represent the entire coronary artery segments. In patients with higher heart rate (>70 bpm), image reconstruction is set in the systolic phase to ensure diagnostic image quality. In our study, beta-blockers were used in patients with higher heart rate (>65 bpm) in order to minimize risk of non-diagnostic image quality for prospective ECG triggering. Apart from beta-blockers, ivabradine can also be used as an alternative to reduce heart rate. Oral ivabradine has been reported to be a safe and effective heart rate lowering agent when compared to the beta-blockers, according to a recent study (Guaricci et al. 2012). However, if the heart rate cannot be controlled after administration of heart rate lowering drugs, the scan is reverted to

retrospective gated protocol. This is because small heart rate irregularities might lead to stair-step artefacts. Previous studies have found a significant correlation between average heart rate and cardiac motion artefact and also between heart rate variability and stair-step artefacts (Ko et al. 2010; Stolzmann et al. 2008). Less heart rate variability has been reported in CCTA using contrast agents with lower osmolarity compared to higher osmolarity contrast agents (Choi et al. 2012). Other than heart rate restriction, prospective ECG-triggered technique could not provide information on ventricular or valvular function. Again, a retrospective ECG-gated procedure should be obtained to meet the purpose.

In comparison with SSCT, DSCT is advantageous because CCTA can be undertaken in patients with higher or even irregular heart rates such as atrial fibrillation. This is due to the improvement of temporal resolution at 83 ms in DSCT, which allows the pitch to increase by up to 0.5 at increased heart rates ranging from 70 to 100 bpm without affecting image quality (Dikkers et al. 2009). Another advantage of DSCT is that it produces lower radiation dose than SSCT in retrospective gated protocol (Rixe et al. 2009). This was confirmed in our study as the effective dose recorded with DSCT (18.2 mSv) was significantly lower than with SSCT (28.3 mSv).

The available data have shown that effective dose in females was significantly higher than in males in retrospective ECG-gated CCTA (Mollet et al. 2005; Raff et al. 2005), however, the impact of sex on dose reduction associated with prospective ECG-triggered compared to retrospective ECG-gated CCTA between DSCT and SSCT has not been addressed. Results of this study indicate that radiation dose did not differ significantly between genders in prospective ECG-triggered CCTA. The dose difference between males and females was observed in retrospective ECG-gated CCTA, which is consistent with a recent report by Esposito et al (2012).

The latest conversion coefficient factor (E/DLP) was used in this study to accurately estimate the effective dose for CCTA examination, which represents a unique aspect of this study. The E/DLP value that is specific for coronary CT examinations has not been widely used in the literature (Huda, Magill, and He 2011). The current practices assume that the *E*/DLP used in coronary CT were similar to that used for chest CT examinations (0.014 or 0.017 $mSv \cdot mGy^{-1} \cdot cm^{-1}$) (Commission 1999; Hausleiter et al. 2009; Huda et al. 2010). However, this is considered inadequate as the estimation does not reflect the measurement at the cardiac region. Therefore, the *E*/DLP value of 0.026 $mSv \cdot mGy^{-1} \cdot cm^{-1}$ was applied in this study since this value was likely to be more accurate for estimation of radiation dose associated with cardiac CT compared to the chest CT (Huda, Magill, and He 2011). The reason for the update is because the cardiac region is likely to be more radiosensitive than

the chest, which results in *E*/DLP ratios. Moreover, the tissue weighting factor in the breast has been reported in ICRP-103 and it changed significantly from 0.05 to 0.12 (Huda, Magill, and He 2011; Huda et al. 2010). These changes have led to an increase in effective dose of about 35% compared to the *E*/DLP value for averaged chest CT examinations. We admit that the estimation of effective dose calculation for CCTA based on the new conversion coefficient factor value is much higher than that calculated with the current approach, but it is of paramount importance to apply the timely relevant factor according to the latest publication of the ICRP tissue weighting factor.

Although our analysis of radiation dose reduction using the above-described strategies is reasonable and sufficient since it combines both qualitative and quantitative methods, we acknowledge several limitations in our work. Firstly, our comparative study used two different CT scanners from different manufacturers. Therefore, certain features might vary significantly in both types of scanners such as power output availability and technical parameters setting. Secondly, we did not investigate the diagnostic accuracy in the detection of CAD in both prospective and retrospective ECG-gating groups, neither in SSCT nor in DSCT because most patients did not undergo invasive coronary angiography examinations for further assessments. Lastly, although low tube voltage (100 kV) was applied in some subgroups (prospective ECG-triggered and retrospective ECG-gated CCTA with use of DSCT) for dose comparison, results were not presented in the present study due to inhomogeneity of patients group.

7.5 Conclusion

In conclusion, prospective ECG-triggered CCTA reduces radiation dose significantly compared to retrospective ECG-gated CCTA, while maintaining good image quality. Although prospective ECG triggering provides no significant difference in radiation dose between both types of scanners, DSCT is advantageous since it results in lower percentage of insufficient image quality as compared to SSCT. Taking into account the advantages and disadvantages of the different techniques, the following guidelines for the selection of different CCTA protocols are recommended: in patients with slow and regular heart rate a protocol with prospective ECG triggering should be chosen, whereas in patients with higher or irregular heart rate retrospective ECG gating should be considered.

7.6 References

Abada, H. T., C. Larchez, B. Daoud, A. Sigal-Cinqualbre, and J. F. Paul. 2006. MDCT of the coronary arteries: feasibility of low-dose CT with ECG-pulsed tube current modulation to reduce radiation dose. *Am J Roentgenol* 186: S387-S390.

Achenbach, S., M. Marwan, D. Ropers, T. Schepis, T. Pflederer, and K. Anders. 2010. Coronary computed tomography angiography with a consistent dose below 1mSv using prospectively electrocardiogram-triggered high-pitch spiral acquisition. *Eur Heart J* 31: 340-346.

Alkadhi, H., P. Stolzmann, L. Desbiolles, S. Baumueller, R. Goetti, and A. Plass. 2010. Low-dose, 128-slice, dual-source CT coronary angiography: accuracy and radiation dose of the high-pitch and the step-and-shoot mode. *Heart* 96: 933-938.

Arnoldi, E., T. R. Johnson, C. Rist, B. J. Wintersperger, W. H. Sommer, A. Becker, C. R. Becker, M. F. Reiser, and K. Nikolaou. 2009. Adequate image quality with reduced radiation dose in prospectively triggered coronary CTA compared with retrospective techniques. *Eur Radiol* 19: 2147-2155.

Austen, W. G., J. E. Edwards, R. L. Frye, G. G. Gensini, V. L. Gott, L. S. C. Griffith, D. C. McGoon, M. L. Murphy, and B. B. Roe. 1975. *Report of the ad hoc committee for grading of coronary artery disease*. American Heart Association.

Budoff, M. J., S. Achenbach, R. S. Blumenthal, J. J. Carr, J. G. Goldin, P. Greenland, A. D. Guerci, J. A. C. Lima, D. J. Rader, G. D. Rubin, L. J. Shaw, and S. E. Wiegers. 2006. AHA scientific statement: assessment of coronary artery disease by cardiac computed tomography-a scientific statement from the American Heart Association Committee on Cardiovascular Imaging and Intervention, Council on Cardiovascular Radiology and Intervention, and Committee on Cardiac Imaging, Council on Clinical Cardiology. *Circulation* 114: 1761-1791.

Choi, T.-Y., V. Woo, M. Gupta, S. Sourayanezhad, D. Li, S. S. Mao, and M. Budoff. 2012. Comparison of iodixanol 320 and iohexol 350 in image quality during 64-slice multidetector computed tomography: Prospective randomized study. *Int J Cardiol* 158: 134-138.

Deetjen, A., S. Mollmann, G. Conradi, A. Rolf, A. Schmermund, C. W. Hamm, and T. Dill. 2007. Use of automatic exposure control in multislice computed tomography of the coronaries: comparison of 16-slice and 64-slice scanner data with conventional coronary angiography. *Heart* 93: 1040-1043.

Dikkers, R., M. J. W. Greuter, W. Kristanto, P. M. A. van Ooijen, P. E. Sijens, T. P. Willems, and M. Oudkerk. 2009. Assessment of image quality of 64-row dual source versus single source CT coronary angiography on heart rate: a phantom study. *Eur J Radiol* 70: 61-68.

Earls, J. P. 2009. How to use a prospective gated technique for cardiac CT. *J Cardiovasc Comput Tomogr* 3: 45-51.

Earls, J. P., E. L. Berman, B. A. Urban, C. A. Curry, J. L. Lane, R. S. Jennings, C. C. McCulloch, J. Hsieh, and J. H. Londt. 2008. Prospectively gated transverse coronary CT angiography versus retrospectively gated helical technique: improved image quality and reduced radiation dose. *Radiology* 246: 742-753.

Efstathopoulos, E. P., I. Pantos, S. Thalassinou, S. Argentos, N. L. Kelekis, T. Zografos, G. Panayiotakis, and D. G. Katritsis. 2012. Patient radiation doses in cardiac computed tomography:comparison of published results with prospective and retrospective acquisition. *Radiat Prot Dosim* 148: 83-91.

Esposito, A., F. De Cobelli, C. Colantoni, G. Perseghin, A. del Vecchio, T. Canu, R. Calandrino, and A. D. Maschio. 2012. Gender influence on dose saving allowed by prospective-triggered 64-slice multidetector computed tomography coronary angiography as compared with retrospective-gated mode. *Int J Cardiol* 158: 253-259.

European Commission 1999. *European guidelines on quality criteria for computed tomography: Report EUR 16262*. Brussels European Commission.

Guaricci, A. I., J. D. Schuijf, F. Cademartiri, N. D. Brunetti, D. Montrone, E. Maffei, C. Tedeschi, R. Ieva, L. Di Biase, M. Midiri, L. Macarini, and M. Di Biase. 2012. Incremental value and safety of oral ivabradine for heart rate reduction in computed tomography coronary angiography. *Int J Cardiol* 156: 28-33.

Gutstein, A., A. Wolak, C. Lee, D. Dey, M. Ohba, Y. Suzuki, V. Cheng, H. Gransar, S. Suzuki, J. Friedman, L. E. Thomson, S. Hayes, R. Pimentel, W. Paz, P. Slomka, and D. S. Berman. 2008. Predicting success of prospective and retrospective gating with dual-source coronary computed tomography angiography: development of selection criteria and initial experience. *J Cardiovasc Comput Tomogr* 2: 81-90.

Hausleiter, J., T. Meyer, M. Hadamitzky, E. Huber, M. Zankl, S. Martinoff, A. Kastrati, and A. Schömig. 2006. Radiation dose estimates from cardiac multislice computed tomography in daily practice: impact of different scanning protocols on effective dose estimates. *Circulation* 113: 1305-1310.

Hausleiter, J., T. Meyer, F. Hermann, M. Hadamitzky, M. Krebs, T. C. Gerber, C. McCollough, S. Martinoff, A. Kastrati, A. Schömig, and S. Achenbach. 2009. Estimated radiation dose associated with cardiac CT angiography. *J Am Med Assoc* 301 500-507.

Hirai, N., J. Horiguchi, C. Fujioka, M. Kiguchi, H. Yamamoto, N. Matsuura, T. Kitagawa, H. Teragawa, N. Kohno, and K. Ito. 2008. Prospective versus retrospective ECG-gated 64-detector coronary CT angiography: assessment of image quality, stenosis, and radiation dose. *Radiology* 248: 424-430.

Hoe, J., and K. H. Toh. 2009. First experience with 320-row multidetector CT coronary angiography scanning with prospective electrocardiogram gating to reduce radiation dose. *J Cardiovasc Comput Tomogr* 3: 257-261.

Huda, W., D. Magill, and W. He. 2011. CT effective dose per dose length product using ICRP 103 weighting factors. *Med Phys* 38: 1261-1265.

Huda, W., K. M. Ogden, and M. R. Khorasani. 2008. Converting dose-length product to effective dose at CT. *Radiology* 248: 995-1003.

Huda, W., S. Tipnis, A. Sterzik, and U. J. Schoepf. 2010. Computing effective dose in cardiac CT. *Phys. Med. Biol.* 55: 3675-3684.

Kalra, M. K., M. l. M. Maher, T. L. Toth, B. Schmidt, B. L. Westerman, H. T. Morgan, and S. Saini. 2004. Techniques and applications of automatic tube current modulation for CT. *Radiology* 233: 649-657.

Ko, S. M., N. R. Kim, D. H. Kim, M. G. Song, and J. H. Kim. 2010. Assessment of image quality and radiation dose in prospective ECG-triggered coronary CT angiography compared with retrospective ECG-gated coronary CT angiography. *Int J Cardiovasc Imaging* 26: 93-101.

Leschka, S., P. Stolzmann, F. T. Schmid, H. Scheffel, B. Stinn, B. Marincek, H. Alkadhi, and S. Wildermuth. 2008. Low kilovoltage cardiac dual-source CT: attenuation, noise, and radiation dose. *Eur Radiol* 18: 1809-1817.

Lu, B., J.-G. Lu, M.-L. Sun, Z.-H. Hou, X.-B. Chen, X. Tang, R.-Z. Wu, L. Johnson, S.-B. Qiao, Y.-J. Yang, and S.-L. Jiang. 2011. Comparison of diagnostic accuracy and radiation dose between prospective triggering and retrospective gated coronary angiography by dual-source computed tomography. *Am J Cardiol* 107: 1278-1284.

Mollet, N. R., F. Cademartiri, C. A. G. van Mieghem, G. Runza, E. P. McFadden, T. Baks, P. W. Serruys, G. P. Krestin, and P. J. de Feyter. 2005. High-resolution spiral computed tomography coronary angiography in patients referred for diagnostic conventional coronary angiography. *Circulation* 112: 2318-2323.

Muenzel, D., P. B. Noel, F. Dorn, M. Dobritz, E. J. Rummeny, and A. Huber. 2012. Coronary CT angiography in step-and-shoot technique with 256-slice CT: impact of the field of view on image quality, craniocaudal coverage, and radiation exposure. *Eur J Radiol* 81: 1562-1568.

Raff, G. L., M. J. Gallagher, W. W. O'Neill, and J. A. Goldstein. 2005. Diagnostic accuracy of noninvasive coronary angiography using 64-slice spiral computed tomography. *J Am Coll Cardiol* 46: 552-557.

Rixe, J., G. Conradi, A. Rolf, A. Schmermund, A. Magedanz, D. Erkapic, A. Deetjen, C. W. Hamm, and T. Dill. 2009. Radiation dose exposure of computed tomography coronary angiography: comparison of dual-source,16-slice and 64-slice CT. *Heart* 95: 1337-1342.

Scanlon, P. J., D. P. Faxon, A. M. Audet, B. Carabello, G. J. Dehmer, K. A. Eagle, R. D. Legako, D. F. Leon, J. A. Murray, S. E. Nissen, C. J. Pepine, and R. M. Watson. 1999. ACC/AHA guidelines for coronary angiography. A report of the American College of Cardiology/ American Heart Association Task Force on practice guidelines (Committee on Coronary Angiography). Developed in collaboration with the Society for Cardiac Angiography and Interventions. *J Am Coll Cardiol* 33: 1756-1824.

Shuman, W., K. Branch, J. May, L. Mitsumori, D. Lockhart, T. Dubinski, B. Warren, and J. Caldwell. 2008. Prospective versus retrospective ECG gating for 64-detector CT of the coronary arteries: comparison of image quality and patient radiation dose. *Radiology* 248: 431-437.

Stolzmann, P., S. Leschka, H. Scheffel, T. Krauss, L. Desbiolles, A. Plass, M. Genoni, T. G. Flohr, S. Wildermuth, B. Marincek, and H. Alkadhi. 2008. Dual source CT in step-and-shoot mode: noninvasive coronary angiography with low radiation dose. *Radiology* 249: 71-80.

Sun, Z., C. Lin, R. Davidson, C. Dong, and Y. Liao. 2008. Diagnostic value of 64-slice CT angiography in coronary artery disease: a systematic review. *Eur J Radiol* 67: 78-84.

Sun, Z., and K.-H. Ng. 2012. Prospective versus retrospective ECG-gated multislice CT coronary angiography: A systematic review of radiation dose and diagnostic accuracy. *Eur J Radiol* 81: e94-e100.

CHAPTER 8: CONCLUSIONS AND FUTURE DIRECTIONS

8.1 Conclusions

In this thesis, the research has investigated the diagnostic performance and radiation dose associated with prospective ECG-triggered coronary CT angiography when compared to the conventional retrospective ECG-gated coronary CT angiography and invasive coronary angiography. This research has used an anthropomorphic model to test different cardiac CT protocols for dose reduction strategies.

A systematic comparison of different CT generations with use of prospective ECG-triggered technique and a well-designed questionnaire of investigating the local specialists and radiographers' perceptions of prospective ECG-triggered coronary CT angiography has demonstrated the usefulness and clinical acceptance of this rapidly developed technique. The results in this section also addressed one of the objectives of this study which is about seeking satisfaction in terms of the acceptable diagnostic images among the users including radiologists, cardiologists and radiographers.

Prospective ECG-triggered coronary CT angiography has been shown to significantly reduce radiation dose compared to retrospective ECG-gated protocol, while maintaining diagnostic image quality. The research outcomes are summarised as follows:

- Coronary CT angiography with prospective ECG-triggered technique produced significantly lower radiation dose than that standard retrospective ECG-gated protocol. Although this has been confirmed in the literature, this study further validates the statement of low-dose protocol with use of prospective ECG-triggering by comparing different generation of multislice CT scanners, and through both qualitatively and quantitative assessments.

- Although the radiation dose was found higher in retrospective gated protocol, the radiation dose differed significantly between dual-source and single-source CT scanners with the radiation dose being lower in dual-source CT compared to single-source CT scanner.

- In prospective ECG-triggered protocol, there is no significant difference in radiation dose between different generations of CT scanners.

- Radiation dose does not differ significantly between genders regardless of coronary CT angiography protocols.

- The low radiation dose in prospective triggered coronary CT angiography can only be achieved in patients with low and regular heart rate.

The low radiation dose in prospective ECG-triggered coronary CT angiography is similar to or even lower than that in the invasive coronary angiography. This further confirms the feasibility of prospective ECG-triggered coronary CT angiography in the diagnosis of coronary artery disease.

8.2 Future directions

This study improves our understanding of the clinical applications of prospective ECG-triggered coronary CT angiography with regard to image quality and radiation dose. Moreover, these research findings highlight the effectiveness of low dose protocol with use of prospective triggering. However, there are few suggestions for the future research, which are detailed as follows:

- Studies focusing on the a combination of multiple dose-reduction strategies such as combining prospective triggering with low tube voltage or high pitch spiral CT acquisition to achieve even lower radiation dose with acceptable diagnostic images;

- Research focusing on the diagnostic performance of prospective ECG-triggered coronary CT angiography in patients with high or irregular heart rates using dual-source CT or 320-slice CT so that this technique will be applicable to more patients;

- Research investigating the prognostic value of prospective ECG-triggered coronary angiography for prediction of major adverse cardiac events, as there are very limited reports available in the literature;

- Studies based on a large population and multicentres with inclusion of diagnostic accuracy of prospective triggering should be performed to verify our results.

Appendix A

Dual source CT coronary angiography: effectiveness of radiation dose reduction with low tube voltage.

Radiation Protection Dosimetry (2013), Vol. 153, No. 4, pp. 441–447 doi:10.1093/rpd/ncs127
Advance Access publication 17 July 2012

DUAL-SOURCE CT CORONARY ANGIOGRAPHY: EFFECTIVENESS OF RADIATION DOSE REDUCTION WITH LOWER TUBE VOLTAGE

Akmal Sabarudin[1,2,*], Ahmad Khairuddin Md Yusof[3], May Fang Tay[1], Kwan-Hoong Ng[4] and Zhonghua Sun[2]
[1]Diagnostic Imaging & Radiotherapy Programme, Faculty of Health Sciences, Universiti Kebangsaan Malaysia, 50300 Kuala Lumpur, Malaysia
[2]Discipline of Medical Imaging, Department of Imaging and Applied Physics, Curtin University, GPO Box U1987, Perth, Western Australia 6845, Australia
[3]Department of Cardiology, National Heart Institute, 50300 Kuala Lumpur, Malaysia
[4]Department of Biomedical Imaging, University of Malaya, Kuala Lumpur 50603, Malaysia

*Corresponding author: akmal.sabarudin@postgrad.curtin.edu.au

Received February 27 2012, revised May 29 2012, accepted June 21 2012

This study was conducted to investigate the effectiveness of dose-saving protocols in dual-source computed tomography (CT) coronary angiography compared with invasive coronary angiography (ICA). On 50 patients who underwent coronary CT angiography was performed dual-source CT (DSCT) and compared with ICA procedures. Entrance skin dose (ESD), which was measured at the thyroid gland, and effective dose (E) were assessed for both imaging modalities. The mean ESD measured at the thyroid gland was the highest at 120 kVp, followed by the 100 kVp DSCT and the ICA protocols with 4.0 ± 1.8, 2.7 ± 1.0 and 1.1 ± 1.2 mGy, respectively. The mean E was estimated to be 10.3 ± 2.1, 6.2 ± 2.3 and 5.3 ± 3.4 mSv corresponding to the 120-kVp, 100-kVp DSCT and ICA protocols, respectively. The application of 100 kVp in DSCT coronary angiography is feasible only in patients with a low body mass index of <25 kg m^{-2}, which leads to a significant dose reduction with the radiation dose being equivalent to that of ICA.

INTRODUCTION

Since 1998, multi-detector computed tomography (CT) has undergone rapid development from 4-slice to 320-slice. The technologies in CT have been developed to make CT angiography a reliable non-invasive diagnostic method for cardiovascular disease, especially coronary CT angiography. Many studies of CT coronary angiography associated with radiation dose and image quality have been conducted to evaluate and improve the performance in clinical practice[1–4]. Although it is well-known that invasive angiography is the gold standard technique for cardiovascular imaging with radiation dose lower than that of coronary CT angiography[5, 6], recent developments in CT techniques, especially application of dose-saving strategies in coronary CT angiography, are towards the most efficient technique in cardiovascular imaging with less invasive, less radiation and high accuracy in the diagnosis of coronary artery disease[3, 7]. In fact, improved diagnostic value of coronary CT angiography with an advantage of its being a less invasive modality has been demonstrated in some studies[1, 8].

Despite all of these advances and technical improvements in CT technology such as increased use of dual-source CT (DSCT), the radiation dose associated with CT in cardiac imaging is still high, ranging from 4.9 to 31.4 mSv[3, 4], depending on the type of CT scanners and scanning protocols used. This has raised serious concern, as the risk of radiation-induced malignancy is not negligible[9, 10]. Therefore, various dose-saving strategies have been explored to reduce the CT-associated radiation dose so that it can be used as a reliable imaging modality in the diagnosis of cardiovascular disease. Of these strategies, lowering the tube voltage and adjustment of tube current (Electrocardiography (ECG)-controlled tube current modulation) are the most effective approaches that are commonly used in clinical practice[8, 11].

It was reported that by lowering the tube voltage to 100 kVp in coronary CT angiography, the radiation dose could be reduced between 25 and 35 % compared with that in the standard 120-kVp tube protocol[11, 12]. However, lowering the 100 kVp setting should be carefully applied in patients with a large body mass index (BMI) as the possible increase in image noise resulting from a lower kVp setting could interfere with diagnostic image quality[8]. Therefore, the purpose of this study was to measure and compare the effective dose estimate (E) and entrance skin dose (ESD) at the radiosensitive organ

(thyroid gland) in coronary angiography procedures between conventional invasive and DSCT with different protocol settings.

MATERIALS AND METHODS

Patients

This study investigated radiation doses on a representative group of the Malaysian population that underwent coronary angiography procedures at the National Heart Institute, Kuala Lumpur, during a 6-month period. This study was approved by the local hospital ethics committee. Written consent was obtained from all the patients. The patients' demographic data with the 100-kVp CT protocol ($n=25$) were compared with those scanned with 120 kVp ($n=25$) and all the patients had obtained invasive coronary angiography (ICA) procedure ($n=50$) as shown in Table 1. All the patients had stable sinus rhythm and were older than 18 y. Patients with elevated serum creatinine levels >1.5 mg dl^{-1}, or allergic reactions to iodinated contrast medium or previous history of undergoing coronary bypass grafting or coronary stent placement were excluded from this study.

Coronary CT angiography scanning protocols

Coronary CT angiography was performed with Somatom Definition 64 (Siemens Medical Solution, Germany) with $2 \times 32 \times 0.6$ mm collimation, a *z*-flying focal spot, a pitch ranging from 0.2 to 0.44 depending on the heart rate and 320 mAs per rotation with two different tube voltages depending on the patient's BMI, being 100 kVp (<25 kg m^{-2}) and 120 kVp (>25 kg m^{-2}). In addition, an ECG-pulsing window with 70–70, 40–70 and 35–70 % of the R–R interval was used respectively, with consistent, low (50–60 bpm), high (60–90 bpm) and extremely high (>90 bpm) heart rates. All patients were given 0.5 mg of sublingual *Nitroglycerine* prior to the scan. Patients with irregular heart rate and higher than 80 bpm were given a 5-mg dose of *Metaprolol* (beta-blockers), whereas patients who were contraindicated to beta-blockers were given 5 mg of *Verapamil*.

A contrast agent (*Iomeron* 350 mgI ml^{-1}) with a minimum of 60 ml was administered intravenously at a flow rate of 5.0–5.5 ml s^{-1} followed by 50 ml of saline flush at 5 ml s^{-1}. The amount of contrast medium required for coronary CT examination was calculated according to the following formula:

V=IR·ST, where V is volume in millilitres, IR is injection rate (ml s^{-1}) and ST is scanning time in seconds[13]. Bolus timing was achieved by using an automated bolus triggering technique at the region of interest i.e. at the ascending aorta, with a threshold detection of 120 HU. Scanning was undertaken in the cranio-caudal direction with simultaneous ECG-signal reading from the patient for image reconstruction purposes on the retrospective ECG-gating. Each scan was acquired from the midlevel of the ascending aorta to the diaphragm. The image series were reconstructed with a slice thickness of 0.75 mm and an increment of 0.5 mm, using a medium-soft convolution kernel (B26f)[14].

ICA scanning protocols

ICA was performed with Integris H5000C single-plane (Philips Medical, USA) ceiling suspension with a high output X-ray tube, 100-kW OPTIMUS-CP generator, image intensification between 5 and 9 inches and a full-field image display with a high-resolution dynamic acquisition. The investigation followed a standard protocol of 11 projections (8 left coronary artery, 3 right coronary artery with left anterior oblique, right anterior oblique and lateral and anterior–posterior projections). Percutaneous coronary intervention procedures were excluded from this study.

Radiation dose measurements and estimation of effective dose

Two types of dose measurements were performed in this study: ESD and effective dose (E). ESD was

Table 1. Demographic data of the study.

Parameters	DSCT coronary angiography		ICA
	100 kVp	120 kVp	
Age (range) [years]	58.2 ± 10.2 (41–80)	57.1 ± 9.1 (39–77)	57.6 ± 9.6 (39–80)
Gender: male (% male)	18/25 (72 %)	17/25 (68 %)	35/50 (70 %)
BMI (range) [kg m^{-2}]	22.4 ± 1.8 (16.7–24.8)	29.1 ± 3.2 (25.8–40.1)	25.7 ± 4.3 (16.7–40.1)
HR (range) [bpm]	73.5 ± 9.9 (62–91)	72.9 ± 8.8 (60–89)	n/a

DSCT, dual-source CT; ICA, invasive coronary angiography; BMI, body mass index; HR, heart rate.

measured by using thermoluminescence dosemeter (TLD) chips. The ESD was obtained in milligrays with a series of procedures consisting of annealing, calibration, radiation exposure and read-out process. The annealing and dose read-out was performed with a Harshaw-5500 reader (Thermo Electron Corp., USA), while calibration was performed with a general X-ray system (GE healthcare, USA). A series of known radiation exposures were obtained during TLD calibration to create a graph pattern for radiation dose conversion from nanoculomb to milligray. The doses were then measured with a digital radiation survey meter (model 660) with an ion-chamber (model 660-3) beam measurement probe and a readout/logic unit (model 660-1). These TLDs were interpreted 24 h after the exposure. The TLD used in this study was thin micro-square shaped and sealed with numbers for identification[15]. Those TLD chips were placed on top of the skin surface at the thyroid gland (radiosensitive organ) before the exposure began in both CT and ICA procedures. The thyroid glands are located at 3 cm below the thyroid cartilage. The thyroid cartilage is prominent and easy to identify physically at the level of fifth cervical spine. At the completion of this procedure, the doses from TLD chips were read to acquire the dose distribution on that particular area. The ESD is expressed in milligrays. The second method of dose measurement, E, reflects the non-uniform radiation absorption of individual body organs relative to a whole-body radiation dose. Therefore, it is calculated on the basis of radiation exposure to individual organs and the relative risk to each organ tissue, and is expressed in millisieverts. The E calculation in DSCT was performed by multiplying the dose-length product (DLP) by a conversion factor, k (mSv mGy^{-1} cm^{-1}). The DLP read-out is available on the CT console after each scan. The conversion factor is derived anatomically and is specific to the body region being scanned[16]. For the chest region, a k-value of 0.017 mSv mGy^{-1} cm^{-1} was used. Similar to the DSCT, E in ICA was calculated from dose-area product which was multiplied by a conversion factor, k (with units of $mSvGy^{-1}$ cm^{-2}). A k-value of 0.20 mSv Gy^{-1} cm^{-2} was used in this study, which meets the condition of the scanning parameter with inclusion of Cu filtration of 0.10 mmCu/1.00 mmAl[17, 18].

Statistical analyses

All the data were entered into SPSS V17.0 (SPSS, version 17.0 for Windows, Chicago, IL, USA) for statistical analysis. A p-value of <0.05 was considered to indicate a statistically significant difference. The doses from the 100-kVp and the 120-kVp protocols were presented in box plots. The student t-test and one-way analysis of variance were used to analyse the multi-factor interaction.

RESULTS

Both CT and ICA were successfully performed in this study without any complications. The mean estimates of the effective doses for the DSCT 100-kVp, 120-kVp and ICA protocols are presented in Figure 1. The mean E estimates in the DSCT 100 and 120-kVp protocols were 6.2 ± 2.3 and 10.3 ± 2.1 mSv, respectively ($p < 0.05$), whereas the mean E in ICA was estimated to be 5.3 ± 3.4 mSv, which is significantly lower than that measured in DSCT with the 120-kVp protocol ($p < 0.05$), but the difference in E between invasive angiography and the 100-kVp protocol (DSCT) was not statistically significant ($p=0.31$).

The results of the ESD measured at the thyroid gland are presented in Figure 2. The mean ESD measured in the DSCT of 120-kVp protocol was 4.0 ± 1.8 mGy, which is the highest, followed by the 100-kVp protocol and invasive angiography, which were 2.7 ± 1.0 and 1.1 ± 1.2 mGy, respectively. All mean ESDs were significantly different among these three groups ($p < 0.05$).

In DSCT, the effective dose differed significantly ($p < 0.05$) between patients with higher (>75 bpm) and lower (<75 bpm) heart rate in both the 100 and 120-kVp protocols. The mean E corresponding to patients with higher and lower heart rate was measured as 4.2 ± 0.3 and 7.7 ± 1.9 mSv (100-kVp

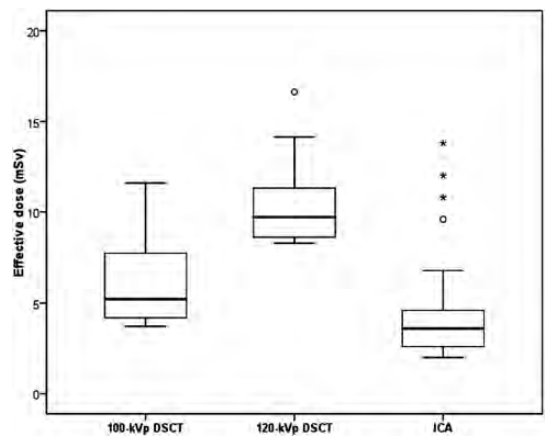

Figure 1. Box plot shows the mean effective dose reported in the studies with use of 120 kVp, 100 kVp (DSCT) and ICA. It is obvious that effective dose at 120 kVp was the highest among the other protocols. The box indicates the first to third quartiles, the line in the box indicates median quartile, the circle indicates outliers and whiskers indicate the minimum and maximum values.

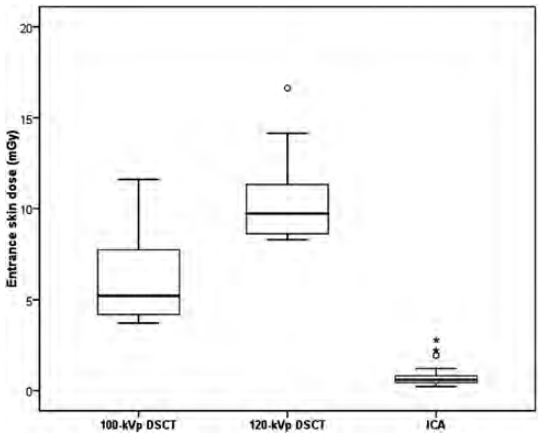

Figure 2. Box plot shows the mean ESD measured at thyroid gland in DSCT (100 and 120 kVp) protocols and ICA. It shows that ICA received the lowest dose to the thyroid compared with DSCT.

protocol) and 8.5 ± 0.2 and 11.5 ± 2.0 mSv (120-kVp protocol). The mean effective dose and ESD were also compared between genders. Both E and ESD estimated in ICA and DSCT between males and females differed insignificantly. The dose estimated in males was higher than females for the ICA procedure. The mean E and ESD were estimated to be 6.0 ± 3.4 and 3.6 ± 3.0 mSv ($p=0.06$) and 1.2 ± 1.2 and 0.9 ± 1.1 mGy ($p=0.42$) among males and females for ICA, respectively. In contrast, the dose calculated in females was higher than that for males for the DSCT procedure. The mean doses corresponding to males and females were measured as 8.2 ± 3.2 and 8.4 ± 2.6 mSv ($p=0.36$) (E) and 3.2 ± 1.7 and 3.6 ± 1.2 mGy ($p=0.81$) (ESD).

DISCUSSION

This study reported three important findings of radiation dose in coronary angiography study using the CT angiography and the invasive approach. Firstly, DSCT with a 100-kVp setting shows a significant reduction in effective dose by 40 % compared with 120 kVp in DSCT. Secondly, the entrance skin dose measured at the thyroid gland also results in a significant reduction in CT with the application of 100-kVp tube voltage at 33% but the dose still cannot be as low as that measured in the invasive coronary procedure. Finally, DSCT demonstrates that effective dose can be reduced further with higher heart rates and the doses recorded in females was higher than in males despite having an insignificant difference either in E or in ESD.

It has been demonstrated that DSCT has the potential to reduce radiation doses[2, 11]. With a dedicated dose reduction algorithm in DSCT, the radiation dose can be significantly reduced, and it is even lower than that of single-source CT (SSCT). Comparison of effective dose between DSCT and SSCT angiography procedures has been performed in previous studies[8, 11, 12]. These results show that SSCT produces an E between 12.7 and 22.7 mSv, whereas DSCT produces an E between 8.9 and 10.4 msV. However, those results are shown with a 120-kVp retrospective ECG-gating of coronary CT angiography. Lowering kVp from 120 to 100 may lead to further dose reduction in coronary CT angiography.

Although 120 kVp is routinely used for CT imaging, including cardiac scans, lower tube voltage is increasingly applied to further reduce the radiation dose. Moreover, ECG-controlled tube current modulation is another approach for dose reduction. In this study, a 100-kVp scanning protocol was used in 25 patients with a BMI of <25 kg m^{-2} and the estimated E value was decreased even further by 40 %. This is in agreement with the results reported in previous literature[6, 19, 20], which stated that the dose could be reduced between 30 and 53 % with the application of a lower tube voltage (100 kVp) either in SSCT or in DSCT. However, the lowering of tube voltage results in an increase in image noise, which may compromise diagnostic image quality, and this is especially apparent in overweight patients or patients having high coronary calcium scores[8]. Therefore, a low-tube voltage protocol is feasible only in patients with a low BMI of <25 kg m^{-2}[11].

Another advantage of DSCT is that it can be performed on patients with higher and regular heart rates. This is because the improvement of temporal resolution at 83 ms in DSCT allows an increase of the pitch by 0.5 at elevated heart rates. In DSCT, the pitch is dependent on heart rates and ranges from 0.25 to 0.50[21]. The pitch is interchangeable corresponding to the heart rates with higher pitch being applied to patients with higher heart rates. Thus, this allows DSCT coronary angiography to be performed on patients with various ranges of consistent heart rates from 70 to 100 bpm without affecting image quality[6]. The use of higher pitch in DSCT scanning results in a significant dose reduction. Previous studies confirmed that the mean E estimate was between 10.1 and 19.7 mSv for patients with a lower heart rate (50–60 bpm) and between 7.8 and 13.2 mSv for patients with a high heart rate (70–110 bpm)[12, 21].

In addition to the assessment of E between different kVp ranges, which has been conducted in previous studies[8, 11, 12], this study also evaluated the ESD, using TLD measurements among three different population groups undergoing both the CT and ICA procedures. The values obtained by the TLDs represent the dose at thyroid skin level in all the patients. Our results showed that the highest ESD was found at DSCT with 120 kVp (4.0 mGy), which is much lower than the recommended threshold

range (beyond 2 Gy)[22–24]. The ESD can be estimated accurately at any specific location in order to measure the amount of dose received after the body region has been exposed to the radiation. TLD-100 is the most suitable type for diagnostic radiology dose study as it has many advantages: it is easy to handle and since the size is small, it is very useful for local dose measurement on the patient[25].

This research focused on the thyroid gland because of its anatomical location and distance from the heart, which could lead to exposure to higher amounts of radiation compared with other radiosensitive organs such as the gonads, bladder and intestines during coronary angiography examinations. In 2008, the estimated age-standardised thyroid cancer incidence rates were 4.7 and 1.5 per 100 000 women and men, respectively[26]. According to these rates, thyroid cancer accounted for 2.7 % of all incident cancer among women worldwide and 0.7 % of cancer diagnosed among men[26]. However, overall mortality rates for thyroid cancer were low for women than men with 0.6 and 0.3 out of 100 000 incident respectively, although thyroid cancer is generally associated with greater mortality at older ages. A review on medical exposure to radiation and thyroid cancer has estimated that about 1000 future thyroid cancers could be related to CT scans conducted in the USA in 2007[27, 28]. In addition, although most studies of thyroid cancer have demonstrated that risks following acute thyroid doses from 0.5 Gy to several Gy, a few have evaluated that the effect of thyroid doses as low as 0.1 Gy[29–31] occurred.

Generally, it is not necessary to shield all other organs (testicles, ovaries, bladder and colon) located away from the heart while performing coronary angiography, since the amount of radiation received by those organs is relatively small with a mean value of <0.13 mGy[32]. Although the breasts and lungs absorb the maximum amount of radiation from the primary beam in CT coronary angiography, it is difficult to shield the breast and lung because these organs are located within the scanning field. Although bismuth breast shielding was introduced as radiation protection device, it is not recommended to be applied because of their impact on image noise, which could compromise diagnostic image quality[33]. Previous studies have demonstrated that bismuth breast shielding was only applied on the right breast while the left breast was left unshielded for comparison purposes. Therefore, the image quality on shielded coronary artery was still inconclusive[34–36].

Studies conducted with DSCT have shown that the effective radiation dose estimated in females is significantly higher than in male patients because of the size thickness on the chest region. However, the breast tissue is radiosensitive and keeping the radiation dose to the breast at the minimum level is of paramount importance. Similar to this, some studies also reported that higher dose was estimated in women than men for coronary CT angiography. For instance, Raff *et al.* [7] reported that an effective dose was 13 mSv for men and 18 mSv for women. In addition, Mollet *et al.* [3] also supported this finding with higher dose reported in women (21 mSv) than in men (15 mSv) in a 64-slice DSCT.

Some limitations exist in the study. We did not include image quality assessment, since this study focuses on the dose comparison between CCTA and ICA, rather than image quality assessment. However, all the CT images in this study were reported completely by consultant cardiologist with sufficient diagnostic image quality and further assessments on image quality are not required. Another limitation of this study is that the dose distribution (ESD) on the other radiosensitive organs such as the eyes, breast and the gonads was not assessed. Although the breasts are anatomically located in the scanned region, application of radio-protection device seems to be not recommended during the scan because of image quality concerns[33].

CONCLUSION

The radiation dose can be reduced with the use of low-tube voltage in patients with high heart rates undergoing DSCT coronary angiography. A 100-kVp DSCT protocol is feasible only in patients with a low BMI of <25 kg m^{-2}, which leads to a significant dose reduction with the effective dose being almost similar to that of ICA. Further studies with inclusion of assessment of image quality and diagnostic value are required to verify the preliminary results of this study.

ACKNOWLEDGEMENTS

The authors thank all the cardiologists, CT radiographers and interventional radiologists in the National Heart Institute, Kuala Lumpur, for their assistance in conducting the study.

REFERENCES

1. Earls, J. P., Berman, E. L., Urban, B. A., Curry, C. A., Lane, J. L., Jennings, R. S., McCulloch, C. C., Hsieh, J. and Londt, J. H. *Prospectively gated transverse coronary CT angiography versus retrospectively gated helical technique: improved image quality and reduced radiation dose.* Radiology **246**, 742–753 (2008).
2. Flohr, T. G. *et al. First performance evaluation of a dual-source CT (DSCT) system*. Eur. Radiol. **16**, 256–268 (2006).
3. Mollet, N. R., Cademartiri, F., van Mieghem, C. A. G., Runza, G., McFadden, E. P., Baks, T., Serruys, P. W.,

Krestin, G. P. and de Feyter, P. J. *High-resolution spiral computed tomography coronary angiography in patients referred for diagnostic conventional coronary angiography.* Circulation **112**, 2318–2323 (2005).
4. Nieman, K., Oudkerk, M., Rensing, B. J., van Ooijen, P., Munne, A., van Geuns, R.-J. and de Feyter, P. J. *Coronary angiography with multi-slice computed tomography.* Lancet **357**, 599–603 (2001).
5. Deetjen, A., Mollmann, S., Conradi, G., Rolf, A., Schmermund, A., Hamm, C. W. and Dill, T. *Use of automatic exposure control in multislice computed tomography of the coronaries: comparison of 16-slice and 64-slice scanner data with conventional coronary angiography.* Heart **93**, 1040–1043 (2007).
6. Dill, T., Deetjen, A., Ekinci, O., Möllmann, S., Conradi, G., Kluge, A., Weber, C., Weber, M., Nef, H. and Hamm, C. W. *Radiation dose exposure in multislice computed tomography of the coronaries in comparison with conventional coronary angiography.* Int. J. Cardiol. **124**, 307–311 (2008).
7. Raff, G. L., Gallagher, M. J., O'Neill, W. W. and Goldstein, J. A. *Diagnostic accuracy of noninvasive coronary angiography using 64-slice spiral computed tomography.* J. Am. Coll. Cardiol. **46**, 552–557 (2005).
8. Feuchtner, G. M., Jodocy, D., Klauser, A., Haberfellner, B., Aglan, I., Spoeck, A., Hiehs, S., Soegner, P. and Jaschke, W. *Radiation dose reduction by using 100-kV tube voltage in cardiac 64-slice computed tomography: a comparative study.* Eur. J. Radiol. **75**, e51–e56 (2010).
9. Brenner, D. J., Elliston, C. D., Hall, E. J. and Berdon, W. E. *Estimated risks of radiation-induced fatal cancer from pediatric CT.* Am. J. Roentgenol. **176**, 289–296 (2001).
10. Linet, M. S., Kim, K. P. and Rajaraman, P. *Children's exposure to diagnostic medical radiation and cancer risk: epidemiologic and dosimetric considerations.* Pediatr. Radiol. **39**, S4–S26 (2009).
11. Leschka, S., Stolzmann, P., Schmid, F. T., Scheffel, H., Stinn, B., Marincek, B., Alkadhi, H. and Wildermuth, S. *Low kilovoltage cardiac dual-source CT: attenuation, noise, and radiation dose.* Eur. Radiol. **18**, 1809–1817 (2008).
12. Rixe, J., Conradi, G., Rolf, A., Schmermund, A., Magedanz, A., Erkapic, D., Deetjen, A., Hamm, C. W. and Dill, T. *Radiation dose exposure of computed tomography coronary angiography: comparison of dual-source,16-slice and 64-slice CT.* Heart **95**, 1337–1342 (2009).
13. Hirai, N., Horiguchi, J., Fujioka, C., Kiguchi, M., Yamamoto, H., Matsuura, N., Kitagawa, T., Teragawa, H., Kohno, N. and Ito, K. *Prospective versus retrospective ECG-gated 64-detector coronary CT angiography: assessment of image quality, stenosis, and radiation dose.* Radiology **248**, 424–430 (2008).
14. Becker, R., Nikolaou, K. and Glazer, G. *Multislice CT*, third edn. Springer-Verlag (2008) ISBN 978-3-540-33124-7.
15. Sabarudin, A., Sun, Z. and Ng, K.-H. *Ng, radiation dose associated with coronary CT angiography and invasive coronary angiography: an experimental study of the effect of dose-saving strategies.* Radiat. Prot. Dosim. **150**, 180–187 (2011).
16. Huda, W., Ogden, K. M. and Khorasani, M. R. *Converting dose-length product to effective dose at CT.* Radiology **248**, 995–1003 (2008).
17. Broadhead, D. A., Chapple, C. L., Faulkner, K., Davies, M. L. and McCallum, H. *The impact of cardiology on the collective effective dose in the North of England*. Br. J. Radiol. **70**, 492–497 (1997).
18. Schultz, F. W. and Zoetelief, J. *Dose conversion coefficients for interventional procedures.* Radiat. Prot. Dosim. **117**, 225–230 (2005).
19. Freeman, A. P., Comerford, R., Lambros, J., Eggleton, S. and Friedman, D. *64 slice CT coronary angiography-marked reduction in radiation dose using prospective gating*. Heart Lung Circ. **18**, S13 (2009).
20. Xu, L., Yang, L., Zhang, Z., Li, Y., Fan, Z., Ma, X., Lv, B. and Yu, W. *Low-dose adaptive sequential scan for dual-source CT coronary angiography in patients with high heart rate: comparison with retrospective ECG gating*. Eur. J. Radiol. **76**, 183–187 (2010).
21. Dikkers, R., Greuter, M. J. W., Kristanto, W., van Ooijen, P. M. A., Sijens, P. E., Willems, T. P. and Oudkerk, M. *Assessment of image quality of 64-row dual source versus single source CT coronary angiography on heart rate: a phantom study.* Eur. J. Radiol. **70**, 61–68 (2009).
22. National Council on Radiation Protection and Measurements. *Radiation dose management for fluoroscopically-guided interventional medical procedures.* NRCP Report No. 168. National Council on Radiation Protection and Measurements (2010). www.ncrponline.org.
23. Dauer, L. T., Thornton, R., Erdi, Y., Ching, H., Hamacher, K., Boylan, D. C., Williamson, M. J., Balter, S. and St. Germain, J. *Estimating radiation doses to the skin from interventional radiology procedures for a patient population with cancer.* J. Vasc. Interv. Radiol. **20**, 782–788 (2009).
24. Bogaert, E. *et al. A large-scale multicentre study of patient skin doses in interventional cardiology: dose-area product action levels and dose reference levels.* Br. J. Radiol. **82**, 303–312 (2009).
25. Maia, A. F. and Caldas, L. V. E. *Response of TL materials to diagnostic radiology X radiation beams.* Appl. Radiat. Isot. **68**, 780–783 (2010).
26. Ferlay, J., Shin, H., Bray, F., Forman, D., Mathers, C. and Parkin, D. *Estimates of worldwide burden of cancer in 2008: GLOBOCAN 2008*. Int. J. Cancer **127**, 2893–2917 (2010).
27. Berrington de Gonzalez, A., Mahesh, M., Kim, K., Bhargavan, M., Lewis, R., Mettler, F. and Land, C. *Projected cancer risks from computed tomographic scans performed in the United States in 2007*. Arch. Intern. Med. **169**, 2071–2077 (2009).
28. Schonfeld, S. J., Lee, C. and Berrington de Gonzalez, A. *Medical exposure to radiation and thyroid cancer*. Clin. Oncol. **23**, 244–250 (2011).
29. Pottern, L. M., Kaplan, M. M., Reed Larsen, P., Enrique Silva, J., Koenig, R. J., Lubin, J. H., Stovall, M. and Boice, J. D Jr *Thyroid nodularity after childhood irradiation for lymphoid hyperplasia: a comparison of questionnaire and clinical findings.* J. Clin. Epidemiol. **43**, 449–460 (1990).
30. Fürst, C. J., Lundell, M., Holm, L.-E. and Silfversward, C. *Cancer incidence after radiotherapy for*

skin hemangioma: a retrospective cohort study in Sweden. J. Natl. Cancer Inst. **80**, 1387–1392 (1988).
31. Ron, E., Lubin, J. H., Shore, R. E., Mabuchi, K., Modan, B., Pottern, L. M., Schneider, A. B., Tucker, M. A. and Boice, J. D. Jr *Thyroid cancer after exposure to external radiation: a pooled analysis of seven studies.* Radiat. Res. **141**, 259–277 (1995).
32. Goetti, R., Leschka, S., Boschung, M., Mayer, S., Wyss, C., Stolzmann, P. and Frauenfelder, T. *Radiation doses from phantom measurements at high-pitch dual-source computed tomography coronary angiography.* Eur. J. Radiol. **81**, 773–779 (2011).
33. Vollmar, S. P. and Kalender, W. A. *Reduction of dose to the female breast as a result of spectral optimisation for high-contrast thoracic CT imaging: a phantom study.* Br. J. Radiol. **82**, 920–929 (2009).
34. Yilmaz, M. H., Yaşar, D., Albayram, S., Adaletli, İ., Özer, H., Ozbayrak, M., Mihmanli, I. and Akman, C. *Coronary calcium scoring with MDCT: the radiation dose to the breast and the effectiveness of bismuth breast shield.* Eur. J. Radiol. **61**, 139–143 (2007).
35. Hohl, C., Wildberger, J. E., Süß, C., Thomas, C., Mühlenbruch, G., Schmidt, T., Honnef, D., Günther, R. W. and Mahnken, A. H. *Radiation dose reduction to breast and thyroid during MDCT: effectiveness of an in-plane bismuth shield.* Acta Radiol. **47**, 562–567 (2006).
36. Yilmaz, M. H., Albayram, S., Yaşar, D., Özer, H., Adaletli, İ., Selçuk, D., Akman, C. and Altuğ, A. *Female breast radiation exposure during thorax multidetector computed tomography and the effectiveness of bismuth breast shield to reduce breast radiation dose.* J. Comput. Assist. Tomogr. **31**, 138–142 (2007).

Appendix B

Survey for radiographers regarding prospective ECG-triggering coronary CT angiography

Section 1

Please complete the information below:

1) Are you:

☐ Male ☐ Female

2) Years in practice:

☐ 1-3 years ☐ 4-6 years ☐ 7-10 years ☐ over 10 years

3) Which area do you currently work?

☐ Government hospital ☐ Private hospital

☐ Other health institutions, please specify: _____

Section 2

We are interested to know your opinion on the **benefits** of prospective ECG-gated coronary CT angiography. Below is a list of the potential benefits from prospective ECG-gating coronary CT angiography which are referenced from the previous studies reported in the literature. Please give your response to the statements below in order to reflect your personal views on prospective ECG-gating coronary CT angiography.

a. Reduces radiation dose

☐ Strongly agree ☐ Agree ☐ Don't know ☐ Disagree ☐ Strongly disagree

b. Improves diagnostic image quality

☐ Strongly agree ☐ Agree ☐ Don't know ☐ Disagree ☐ Strongly disagree

c. Increases number of patients/cases (patient's output)

☐ Strongly agree ☐ Agree ☐ Don't know ☐ Disagree ☐ Strongly disagree

d. Increases financial incentives

☐ Strongly agree ☐ Agree ☐ Don't know ☐ Disagree ☐ Strongly disagree

Section 3

We are interested to know your concern on the **challenges/ obstacles** in performing prospective ECG-gating coronary CT angiography. Listed below are the major problems that might influence the efficiency of performing the prospective ECG-gating coronary CT angiography. Please give your response to the statements below in order to reflect your personal thought on the challenges in prospective ECG-gating coronary CT angiography.

a. Heart rate issues

☐ Strongly agree ☐ Agree ☐ Don't know ☐ Disagree ☐ Strongly disagree

b. Difficulty in obtaining cardiac functional assessments

☐ Strongly agree ☐ Agree ☐ Don't know ☐ Disagree ☐ Strongly disagree

c. Image quality concerns

☐ Strongly agree ☐ Agree ☐ Don't know ☐ Disagree ☐ Strongly disagree

d. Diagnostic accuracy concerns

☐ Strongly agree ☐ Agree ☐ Don't know ☐ Disagree ☐ Strongly disagree

e. Data processing management (pre-/post-processing)

☐ Strongly agree ☐ Agree ☐ Don't know ☐ Disagree ☐ Strongly disagree

Thank you

Survey for clinical specialists (cardiologists and radiologists) regarding prospective ECG-triggering coronary CT angiography

Section 1

Please complete the information below:

4) Are you:

☐ Male ☐ Female

5) Are you:

☐ Radiologist ☐ Cardiologist

6) Years in practice:

☐ 1-5 years ☐ 6-10 years ☐ 11-20 years ☐ over 20 years

7) Which area do you currently work?

☐ Government hospital ☐ Private hospital

☐ Other health institutions, please specify: _____

Section 2

We are interested to know your opinion on the **benefits** of prospective ECG-gated coronary CT angiography. Below is a list of the potential benefits from prospective ECG-gating coronary CT angiography which are referenced from the previous studies reported in the literature. Please give your response to the statements below in order to reflect your personal views on prospective ECG-gating coronary CT angiography.

e. Reduces radiation dose

☐ Strongly agree ☐ Agree ☐ Don't know ☐ Disagree ☐ Strongly disagree

f. Improves diagnostic image quality

☐ Strongly agree ☐ Agree ☐ Don't know ☐ Disagree ☐ Strongly disagree

g. Increases number of patients/cases (patient's output)

☐ Strongly agree ☐ Agree ☐ Don't know ☐ Disagree ☐ Strongly disagree

h. Increases financial incentives

☐ Strongly agree ☐ Agree ☐ Don't know ☐ Disagree ☐ Strongly disagree

Section 3

We are interested to know your concern on the **challenges/ obstacles** in performing prospective ECG-gating coronary CT angiography. Listed below are the major problems that might influence the efficiency of performing the prospective ECG-gating coronary CT angiography. Please give your response to the statements below in order to reflect your personal thought on the challenges in prospective ECG-gating coronary CT angiography.

f. Heart rate issues

☐ Strongly agree ☐ Agree ☐ Don't know ☐ Disagree ☐ Strongly disagree

g. Difficulty in obtaining cardiac functional assessments

☐ Strongly agree ☐ Agree ☐ Don't know ☐ Disagree ☐ Strongly disagree

h. Image quality concerns

☐ Strongly agree ☐ Agree ☐ Don't know ☐ Disagree ☐ Strongly disagree

i. Diagnostic accuracy concerns

☐ Strongly agree ☐ Agree ☐ Don't know ☐ Disagree ☐ Strongly disagree

j. Data processing management (pre-/post-processing)

☐ Strongly agree ☐ Agree ☐ Don't know ☐ Disagree ☐ Strongly disagree

Thank you